7 Integrated demonstrations

The purpose of this chapter is a demonstration of monitoring, modelling, and assessment methods that were introduced and described in the preceding Chapters 2, 3, 4, 5, and 6. The methods are applied to the three target areas that were investigated in the ALPNAP project (see Fig. 1.2 in Chapter 1).

Brennero/Brenner corridor:	Lower Inn valley	Section 7.1
Brennero/Brenner corridor:	Adige/Etsch valley	Section 7.2
Fréjus corridor:	Susa and Maurienne valley	Section 7.3

In the Brennero/Brenner corridor target areas it was possible to perform special measurement campaigns. With the help of the data gained it is possible to demonstrate the chain from the base and emission data (Chapter 2), via meteorological analyses (Chapter 3), transport of air pollutants (Chapter 4), and propagation of noise (Chapter 5), to the impact assessments of the strains of air pollution and noise with respect to health and socio-economic costs (Chapter 6). Measurements and model simulations are used in combination. In the Lower Inn valley it was possible to analyse the synchronous recordings of air pollution and noise. The impact assessments focus on the effects of noise (Lower Inn valley) and air pollution (Adige/Etsch valley).

In the Fréjus corridor supplementary investigations are presented. These include the simulation of high pollution episodes, the treatment of tunnels and viaducts in air pollution modelling, and extended noise mapping.

Finally, in Section 7.4 the assessment of scenarios is shown. In the Brennero/Brenner corridor the air quality situation of the year 2005 was compared with possible future situations according to two different assumptions about the change in traffic. In the Fréjus area a future air pollution scenario is presented. In addition, the exposure effects of an assumed modal shift from road to rail is shown with the aid of air pollution indices, noise pollution indices, and combines air pollution and noise Exposure Indices.

7.1 Brenner Corridor: Lower Inn valley

7.1.1 General information

Within the ALPNAP project a measurement campaign in combination with a health survey was performed in the Lower Inn valley. The meteorological measurements served as an essential basis to understand the governing processes in air pollution and noise dispersion. Measurement and modelling results and their strategy are described in the following paragraphs. Selected results of the two EUFAR research projects INNAP (Boundary layer structure in the Inn valley during high air pollution) and INNOX (NO_x-structure in the Inn Valley during high air pollution) are incorporated as well.

The air quality experiment was designed to determine the spatial variation and distribution of air pollution induced by inner Alpine traffic. The field data were also used for the set-up and validation of numerical simulations of air quality.

The campaign was performed between November 2005 and January 2006. The target area as shown in Fig. 7.1 was centred around Schwaz and Vomp (47°20’ N / 11° 41 E / 540 m ASL),

where exceedances of nitrogen dioxide (NO_2) and PM10 are continuously recorded by the routine monitoring network.

A two-way approach was taken during the field phase rounding off the existing routine monitoring network including e.g. monitoring stations of regional and national authorities (Landesumweltamt Tirol – LT) for air pollution and temperature profiling along a slope. The first step realized permanent air pollution and meteorological instrumentation including a sodar (vertical profiles of wind, turbulence and acoustic backscatter intensity), a ceilometer (vertical profiles of optical backscatter intensity), an open-path DOAS (Differential Optical Absorption Spectroscopy, long-path air pollution information in different directions), three automated weather stations (AWS) and 10 passive samplers for NO_2 which provide an extended view of the spatial and temporal development throughout the winter. The position of the instruments is shown in Figs. 7.2 and 7.3, selected images of the devices are shown in Fig. 7.4.

Secondly, during high air pollution episodes additional measurements were performed. These include profiling with a tethered balloon at the base station to determine the vertical structure of dust particles, temperature, humidity and wind, mobile car traverses yielding PM10 and meteorological information and sampling of volatile organic compounds (VOCs) at selected locations.

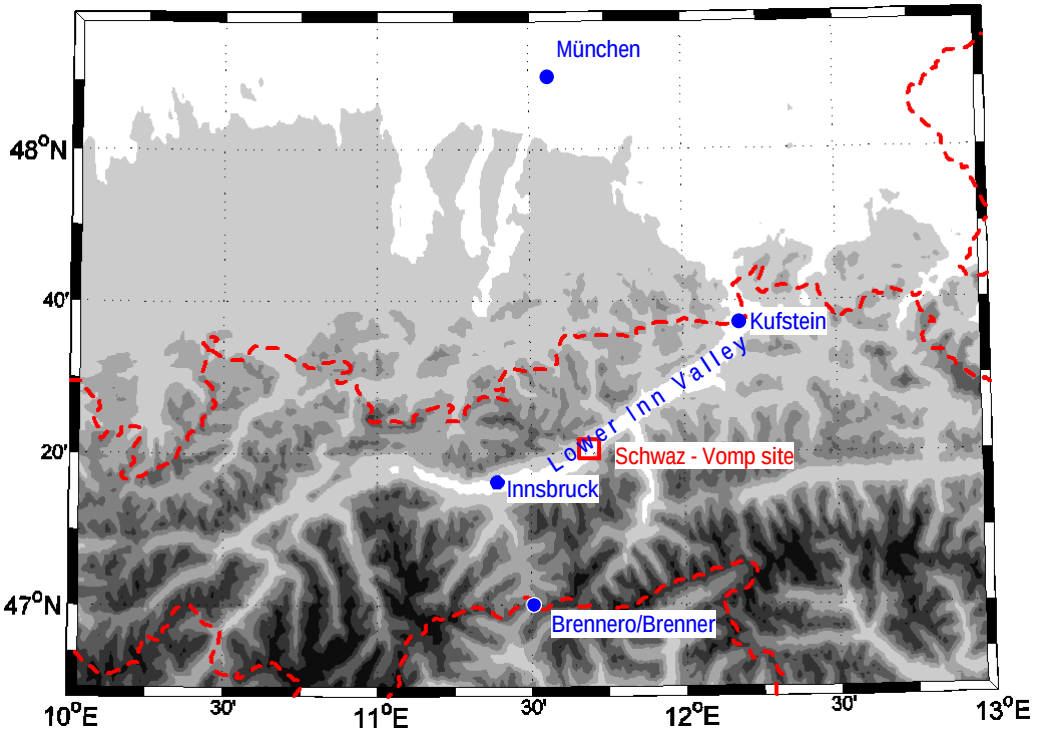

Fig. 7.1 Orographic map showing the location of the Lower Inn valley target area (rectangle). Topography with 30" resolution and shaded contours every 200 m starting from 600 m ASL.

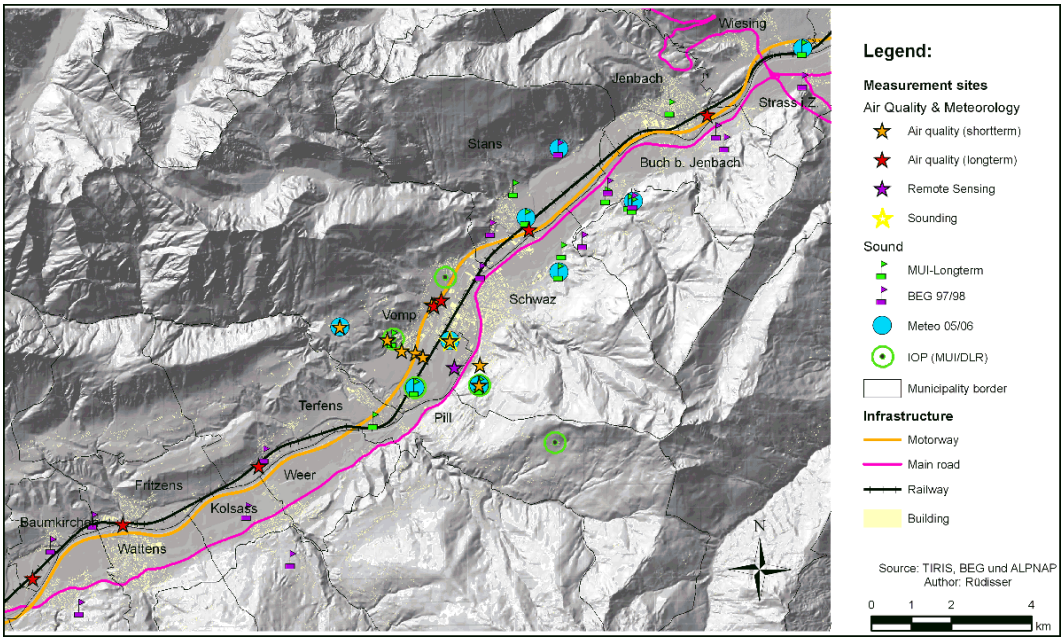

Fig. 7.2 Overview map of the Lower Inn valley target area between Innsbruck and Rosenheim. The map shows the 25 km long valley segment between Wattens and Jenbach. The symbols show the location of the measurement sites during the ALPNAP campaign 2005/2006.

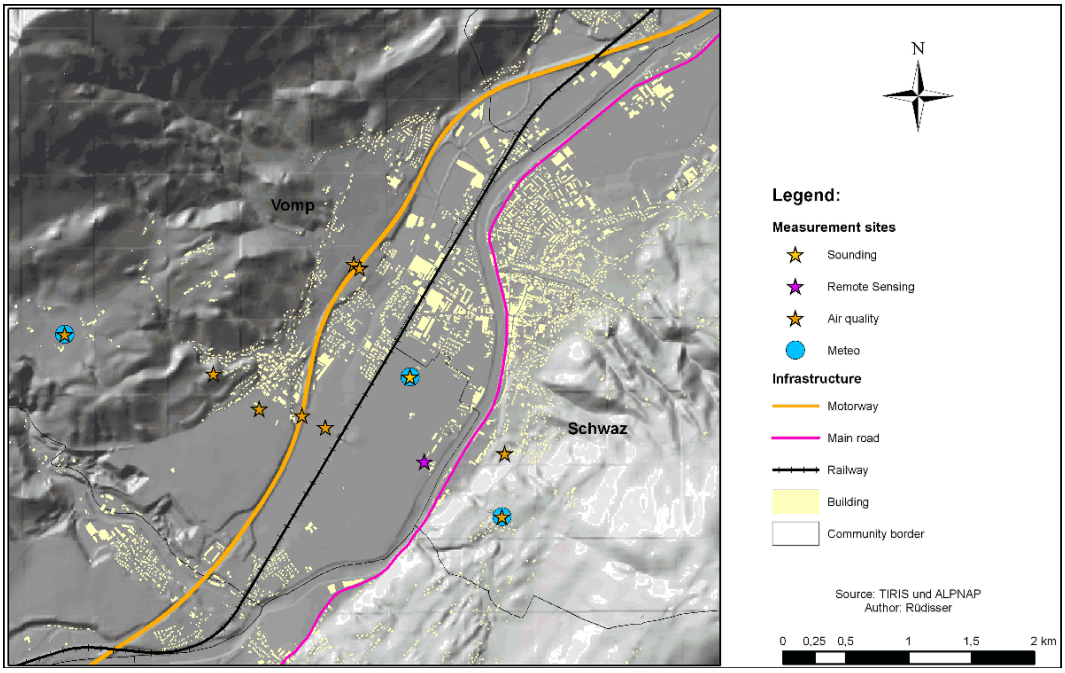

Fig. 7.3 Close-up of the area around Schwaz/Tyrol where measurements were concentrated during the Intensive Observation Periods (IOP) of the ALPNAP campaign 2005/2006. The symbols show the location of the measurement sites.

(a)

(b)

(c)

(d)

(e)

(f)

(g)

(h)

Fig. 7.4: Selected images of the measurement devices: (a) Tethersonde balloon and meteorological sonde; (b) Sodar; (c) Ceilometer; (d) Automatic Weather Station (AWS) at Arzberg; (e) AWS at basic station Schwaz (10 m mast); (f) air pollution measurement van and separate (g) PM10 unit (left) and mobile car platform (right); (h) Differential Optical Absorption Spectrometer (DOAS) looking across the motorway

Characteristic monthly mean values in the target area are summarised in Tab. 7.1. From a meteorological point of view the winter 2005/ 06 was characterised by an early and permanent snow pack beginning mid November and persistent synoptically undisturbed high pressure regimes with intermittent disruptions especially in January. This led to unusually cold temperatures in January, namely in the target area 4.4 °C below the average from 1993 – 2002 (-1.0 °C). From an air pollution point of view November and December 2005 can be seen as typical months. In January 2006 on the other hand the dominant stable periods led to particularly high pollution burden. NO_x (PM10) was 35.7 % (53.8 %) above the average from 2000 – 2004. A shift towards a higher share of NO_2 was observed. All thresholds have been exceeded more often than in previous years. The frequent exceedance of the half hourly mean NO_2 threshold of 200 µg/m^3 has not been observed in previous winters.

Tab. 7.1 Mean monthly values in the target area for winter 2005 / 2006. Air quality data are taken from the permanent Land Tirol station Vomp Raststätte.

Parameter / Month	Nov 2005	Dec 2006	Jan 2006
Mean Temperature (°C)	2.9	-1.9	-5.4
Days with snow deck	12	31	31
Precipitation (mm)	35	120	59
Mean NO_2 (µg/m^3)	71	88	126
Mean NO (µg/m^3)	222	225	322
Mean PM_{10} (µg/m^3)	35	43	66

7.1.2 Emissions

Road traffic emissions were calculated for three different road types: the motorway A12, class “A” roads (federal highways) and class “B” roads (state roads), based on traffic data from traffic count stations within the Lower Inn valley. The input data are described in the following paragraphs followed by the results from emission modelling.

7.1.2.1 Traffic data:

Data were used from the counting stations Vomp located at the A12, Pill at the A-road B171 and Stans at the B-road L215. Average Daily Traffic Volumes (ADTV) data from Weer, Vomp Ost, Schwaz Ost (all B171) and Wiesing (L215) were assigned to the respective road sections. These traffic count data were processed to obtain one year ADTV and diurnal and monthly cycles to be used in the air quality modelling studies, see Fig. 7.5. The aim was to model emissions for the base year and future scenarios (in kg km^{-1}·h^{-1}) for each average hour of the year using the following approach for each pollutant:

$$Emission\ (VC) = Annual\ Mean\ Emission\ (VC) \cdot f_{diurn,VC} \cdot f_{week,VC} \cdot f_{month,VC}$$

Fig. 7.6 and Fig. 7.7 show the results for the non-dimensional factors $f_{diurn,\ vc}$, $f_{week,\ vc}$, $f_{month,vc}$ derived from the traffic count station Vomp at the A12. These factors describe the diurnal, weekday or monthly cycle, i.e. temporal weight per vehicle class (VC). In addition values for Pill at the A-road B171 are presented in Fig. 7.5. Fig. 7.5 (left) shows clearly the impact of the night time driving ban for heavy goods vehicles > 7.5 tons on the motorway. During night there is a low traffic flow of heavy duty vehicles (HDV) and after 05 CET. the number of heavy duty vehicles (HDV) increases rapidely. In contrast, passenger car motorway traffic shows a continuous cycle with the

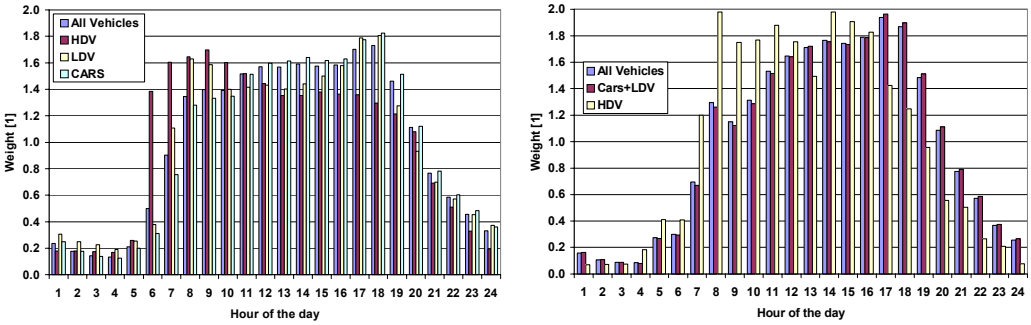

Fig. 7.5 Normalized diurnal cycles calculated from automatic count data at Vomp (A12; left panel) and Pill (B171; right panel). The automatic traffic count data for Pill did not enable a separation between "Cars" and "LDV".

maximum number of cars in the late evening. Here, the interference of emissions with meteorological conditions is of special interest in the view point of measures like night time driving bans or temporal speed limits in order to reduce the exposure concentrations. On the A- and B-roads the diurnal cycles of the car traffic volume are roughly similar to the motorway. The traffic volume of HDV is more related to business hours with a strong increase in the morning hours. The seasonal cycle for cars seems affected by holidays and road conditions (see Fig. 7.6). The maximum traffic volume is found during the summer months on all three different roads. There is reduced HDV traffic activity on all three road types in winter, but less pronounced on the motorway and more HDV traffic activity in summer. The seasonal variation is about ± 20 %. The weekday cycle is quite balanced for all vehicles and passenger cars (see Fig. 7.6). However, HDV traffic is by ~ 40 % reduced at Saturday and by 82 % on Sunday due to a driving ban. Light Duty Vehicle (LDV) traffic is reduced to a lesser extent at the weekends, about 20 % at Saturday and about 33 % on Sunday.

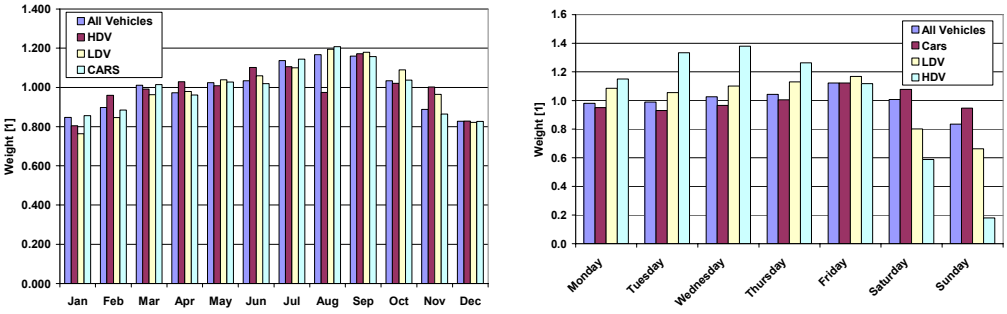

Fig. 7.6 Normalized seasonal (left) and week day cycles (right) calculated from automatic count data at Vomp (A12).

Emission modelling results for the Unterinntal target area domain:

In this work, traffic emission data were calculated using the road Network Emission model NEMO, domestic heating emission data from Tyrol and industrial emission data from the EMEP (Co-operative programme for monitoring and evaluation of the long-range transmission of air pollutants in Europe) emission inventory were processed.

Road traffic emission modelling was carried out for three road types within the model domain of the Lower Inn valley east of Innsbruck around Schwaz (see Fig. 7.3). The motorway (A12), the federal highways B171, B181 and B169) and the state roads were digitalized within the model domain. For each of these three road types the traffic was classified into "Cars" and "HDV", resulting in six different traffic emission sources. Tab. 7.2 provides detailed information about important traffic emission modelling input parameters used for the motorway A12. Slopes for A-roads and B-roads as well as the height of road embankments were not available. The slopes for these roads have been obtained by slicing the Digital Terrain Model (DTM) data with the location of these street networks and filtering these data. Note, due to the assigned driving situations and slopes the emissions are different on the respective road sections, in particular for HDV. Emissions for class "B" roads comprise only "Landesstraßen", i.e. the other traffic on minor streets or in towns and villages was not considered.

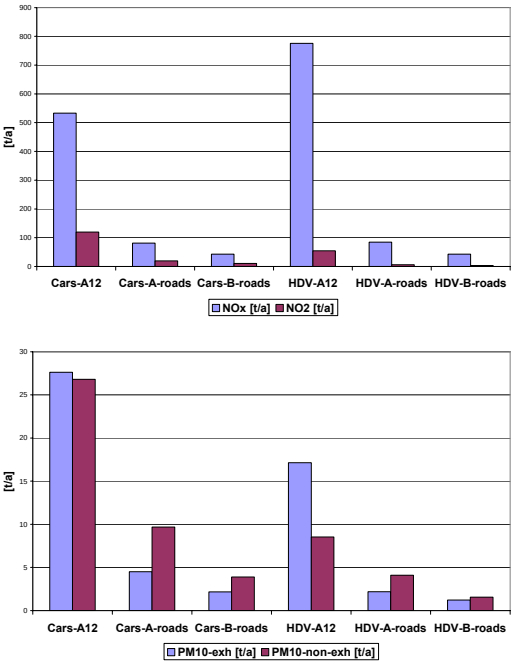

Fig. 7.7 Top: total annual NO_x and NO_2 emissions on three different road types within the modelling domain. Cars includes LDV, HDV includes coaches, trucks without trailer and tractor trailer. Bottom: total annual PM10 exhaust and PM10 non-exhaust emissions on three different road types within the modelling domain.

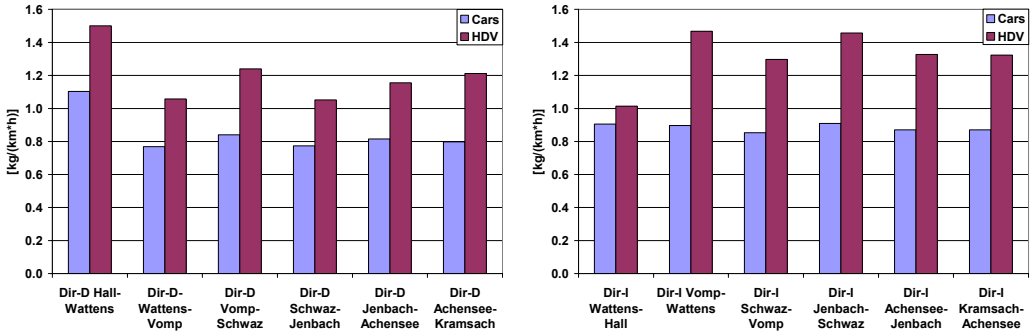

Fig. 7.8 A12-motorway section averaged NO_x emissions. Dir-D denotes the direction towards Rosenheim (left) and Dir-I the direction towards Innsbruck (right).

Tab. 7.2 Modelled daily traffic volume (annual mean) values and average slope of the motorway sections. Dir-I denotes the driving direction towards Innsbruck and Italy and Dir-D denotes the driving direction towards Germany.

Sections on A12	Slope	ADTV-Cars	ADTV-HDV
Dir-D Hall-Wattens	0.42	25879	4556
Dir-D-Wattens-Vomp	-0.34	21547	4546
Dir-D Vomp-Schwaz	-0.03	21849	4534
Dir-D Schwaz-Jenbach	-0.34	21707	4500
Dir-D Jenbach-Achensee	-0.14	21742	4458
Dir-D Achensee-Kramsach	0.08	20203	4197
Dir-I Wattens-Hall	-0.42	25880	4556
Dir-I Vomp-Wattens	0.34	21424	4572
Dir-I Schwaz-Vomp	0.03	21849	4588
Dir-I Jenbach-Schwaz	0.34	21707	4500
Dir-I Achensee-Jenbach	0.14	21742	4458
Dir-I Kramsach-Achensee	0.14	21742	4458

Fig. 7.7 (top) shows the domain integrated NO_x and primary NO_2 emissions for class "Cars" and class "HDV" for the three different road networks. The results for PM10 are shown in Fig. 7.7 (bottom) correspondingly. The motorway is clearly the major source of NO_x and primary emitted NO_2 when emissions from both classes are considered. Same holds for PM10. Noteworthy is the large share of primary emitted NO_2 (~22 %) from car motorway traffic. Although the motorway share of HDV is on average 16 %, HDV are the major NO_x emitters. Even on A-roads HDV is the main source for NOx emissions. On B-roads the emissions of Cars and HDV are on the same level. For PM10 the situation is different. Cars are the main emission source for PM10 exhaust and non-exhaust. PM10 non-exhaust emissions are due to abrasion (e.g. tire wear) or fragmentation processes (e.g. road dust). Notable are the large contributions of A- and B-roads PM10-non-exhaust emissions. It should be noted, that the effect of slope on PM10 non-exhaust emissions is not known yet (presumably higher fragmentation) and the impact of winter sanding and de-icing is not considered. That means, the given total annual PM10 non-exhaust emissions are certainly underestimated.

Six motorway sections in each direction between Hall and Kramsach were selected in order to investigate the spatial variability of emissions. NO_x and PM10 non-exhaust emissions vary up to a factor of 1.5 due to the different traffic volume, different HDV share and different slope ranging only between ± 0.42 on each direction (see Fig. 7.8**)**. HC emissions varied up to a factor of 1.3.

The emission modelling results indicate that NO_x motorway emissions are mainly attributable to HDV traffic. However, PM10 exhaust, PM10 non-exhaust and HC emissions are generally larger from car traffic. Similar results can be found for the A-roads in case the HDV share is high. Due to the significantly reduced traffic volume the emissions on A-roads are significantly smaller compared to the motorway emissions.

Domestic heating emissions on a community level were obtained from the Tyrolean provincial government and together with cadastral / GIS data assigned to localized sources, i.e. individual households. Currently, work on an emission inventory for Tyrol is in progress. However, these data were not available yet. Without emission inventory data the data base for PM10 is very sparse. Therefore, as a remedy industrial NO_x and PM10 emissions were used from the EMEP emission inventory and aggregated to industrial facilities within the Unterinntal target area. It must be noted, that especially the PM10 emissions were certainly strongly underestimated, since impor-

tant PM10 sources such as construction industry or agriculture could not be considered. Moreover, the ratio of overall NO_x/PM10 domestic heating emissions is 5. In contrast, the ratio for the urban area of Graz is about 5, in Klagenfurt it is about 2.5 and in the rural Lavanttal in Austria it is about 1.6 (Sturm et al., 2007). This ratio depends strongly on the domestic fuels used. Here, it should be noted that in the Lavanttal and most likely in Tyrol there is a large share of wood burning. The emission factors for wood burning have a large uncertainty and are subject of intense research (e.g. Gaegauf, 2005). Due to the lack of further major PM10 emission sources and possibly underestimated domestic heating a large background value for PM10 results. Fig. 7.9 shows the share of different emission groups based on input data from traffic count stations, data from LT (domestic heating) and EMEP (industry), and the data processing and modelling work of TU Graz.

Fig.: 7.9 Total NO_x and PM10 Emissions as used in the Unterinntal target area simulations. The PM10 Emissions are to a large extent incomplete or unknown, see text for details.

In summary, the emission data base within target area for NO_x is sound; major deficiencies are missing detailed information about the class "B" road network, urban traffic and industrial emissions. The emission data base for PM10 is sparse because an emission inventory was not available yet.

7.1.3 Measurement results

7.1.3.1 Data quality management

Extensive calibration and intercomparison work was performed before and after the ALPNAP field measurements in order to ensure high quality data and comparability between different measurement devices. This concerned meteorological as well as air pollution instrumentation. The basic calibrations were performed in accredited laboratories using approved standards.

However, proper laboratory calibration is not sufficient to fully characterize the final performance of the instruments. This is mainly due to disturbing factors during exposure of the instruments in the field. For instance there is a need to protect thermometers from radia-

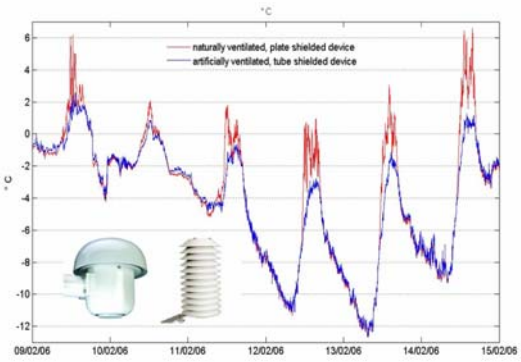

Fig. 7.10 Time series of temperature measurements using laboratory calibrated sensors mounted in different thermometer screens (ALPNAP-intercomparison measurement, Arzberg, 09 – 15 Feb 2006).

tion by a screen or shield, and to shelter it from precipitation or mechanical damage. The individual performance of such devices strongly depends on their construction and the measurement conditions. Fig. 7.10 demonstrates that during high solar insolation the naturally ventilated and plate shielded device yields air temperatures that are several centigrades in excess of measurements employing artificially ventilated screens. The effect is diminishing during night and overcast conditions which are mainly due to the combined effect of correspondingly reduced solar radiation and higher wind speeds.

Unfortunately, such effects are often neglected despite the fact they are known in principle and despite existing official recommendations on this topic as well (WMO, 2000). On the other hand, there are some real world limitations due to constraints of power supply. Thus intercomparison measurements are inevitable measures to at least quantify the inherent uncertainties. Preferably, these types of measurements should be performed before and after the field measurements themselves, which also helps to assess potential effects of further disturbances e.g. due to drifting sensor calibrations. Finally, the field data are to be quality-controlled with respect to outliers, values out of (physical) range and special conditions (e.g. icing).

7.1.3.2 Energy balance investigation

The comprehensive ALPNAP field provided exemplary results on the interaction of meteorology, air pollution and noise in complex terrain. In this context, the evolution of snow played an important role, influencing the strength and persistence of inversions via the surface energy balance.

The evaluation of the surface energy balance is based on mast profile measurements at the bottom of the Inn valley. The available data were used to drive a physically based model (Aschauer et al., 2007). The seasonal evolution of the basic snow physical parameters (which are difficult if not impossible to measure directly) and the mass and energy balance were calculated. The evaluation of the resultant fluxes was verified by independent data such as surface snow temperature and direct measurements of the turbulent heat flux.

The calculations demonstrate the isolating effect of snow on the underlying ground (Fig. 7.11 a), which has important feed backs on the atmospheric boundary layer (strong surface cooling). The resulting temperature inversion is associated with diminishing turbulent heat fluxes (Fig. 7.11 b). It is notable however, that there are intermittent periods in which the sensible heat flux directed from the surface to the atmosphere (unstable conditions and negative Richardson numbers, respectively). These cases are mainly associated with surface heating during periods of strong solar insolation or cold air advection in the context of frontal events. Warm spells fostered settling of the snow pack or melt events, enhancing the liquid water contents below the ground surface.

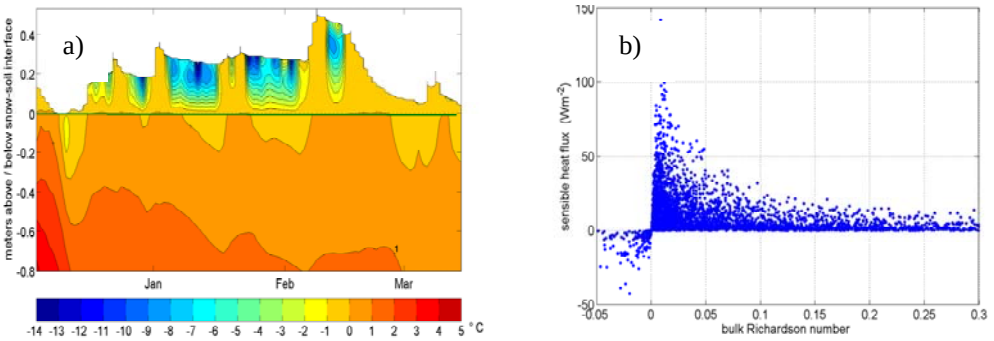

Fig. 7.11 a) Time-depth evolution of snow and ground temperature during the measurement period 05 Dec 2005 – 15 Mar 2006. b) Scatter plot demonstrating the effect of atmospheric stability on turbulent sensible heat fluxes calculated using data from the surface and 2 m AGL.

The energy balance during the accumulation (cold) period was characterized by net losses due to radiation and prevailing evaporation, which were offset by the positive contributions from turbulent sensible and conductive soil heat fluxes. During the ablation (melt) period, the snow pack experienced enhanced energy input, which was mainly due to the now positive radiation budget. This excess energy is used to bring the snow pack to the melting point and subsequent ablation generates liquid water infiltration into the soil and run off, respectively.

7.1.3.3 Temporal evolution of air pollution and meteorology

Time series of relevant parameters concerning air quality are shown in Fig. 7.12**.** Two exemplary periods with high air pollution burden are displayed, namely 18 Dec 2005 – 01 Jan 2006 and 05 – 19 Jan 2006. Note the correlation of stable layering (positive temperature gradient) and high air pollution burden combined with an accumulation effect over a couple of days in undisturbed periods, e.g. from 06 – 17 Jan 2006. An adiabatically stratified atmosphere in the lowest 180m AGL leads to a roughly uniform concentration profile between Schwaz and Arzberg. High wind speeds at the ground are usually connected with a change of the air mass and thus a cleaning effect. This is visible for example in the morning of 31 Dec 2005, before the New Year celebrations lead to a sharp increase in PM10. Generally outstanding high pollution episodes were found during 20 – 24 Dec 2005, 09 – 21 Jan and 25 Jan – 02 Feb 2006. The time-series of 19 – 26 Jan 2006 is shown in Fig. 7.39 in Section 7.1.5.2, giving a combined evaluation of noise and air pollution.

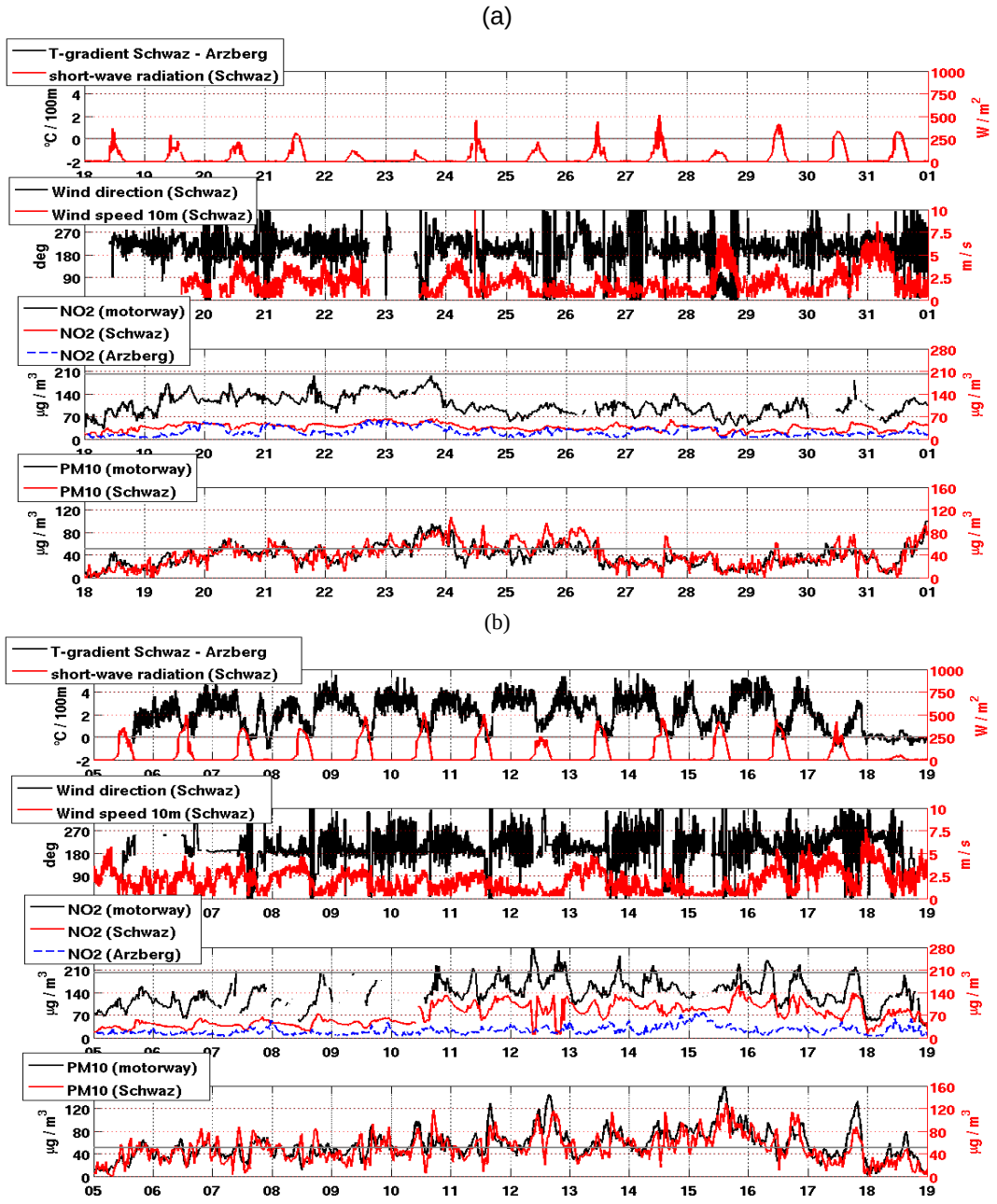

Fig. 7.12 Half-houly values of temperature gradient Schwaz – Arzberg (°C/100m) and short wave radiation (W/m^2) at Schwaz; wind direction (deg) and speed (m/s) at Schwaz; NO_2 across the motorway, at Schwaz and at Arzberg (all in $\mu g/m^3$) and PM10 at Vomp Raststätte and at Schwaz (all in $\mu g/m^3$) during (a) 18 Dec 2005 – 1 Jan 2006; (b) 5 – 19 Jan 2006. The zero temperature gradient line and the half-hourly NO_2-threshold as well as the daily PM10-threshold are marked by grey lines.

Tab. 7.3 The energy balance components during the whole measurement period (05 Dec 2005 – 15 Mar 2006). A positive sign denotes a gain of energy to the snow pack, units in W/m^2.

	whole period	accumulation period	ablation period
net radiation	-2.1	-6.9	11.0
sensible heat flux	5.3	3.8	9.4
latent heat flux	-4.5	-2.8	-9.4
soil heat flux	13.0	13.3	12.3
TOTAL	11.7	7.4	23.3

7.1.3.4 Spatial distribution of air pollution and meteorology – two case studies

During two selected days, the winter-time evolution of the atmospheric boundary layer (ABL) and its implications on air pollution in the presence of an area-wide snow-pack on synoptically undisturbed days is demonstrated. Both 13 Jan 2006 and 01 Feb 2006 are suited to study the typical wintertime valley dynamics.

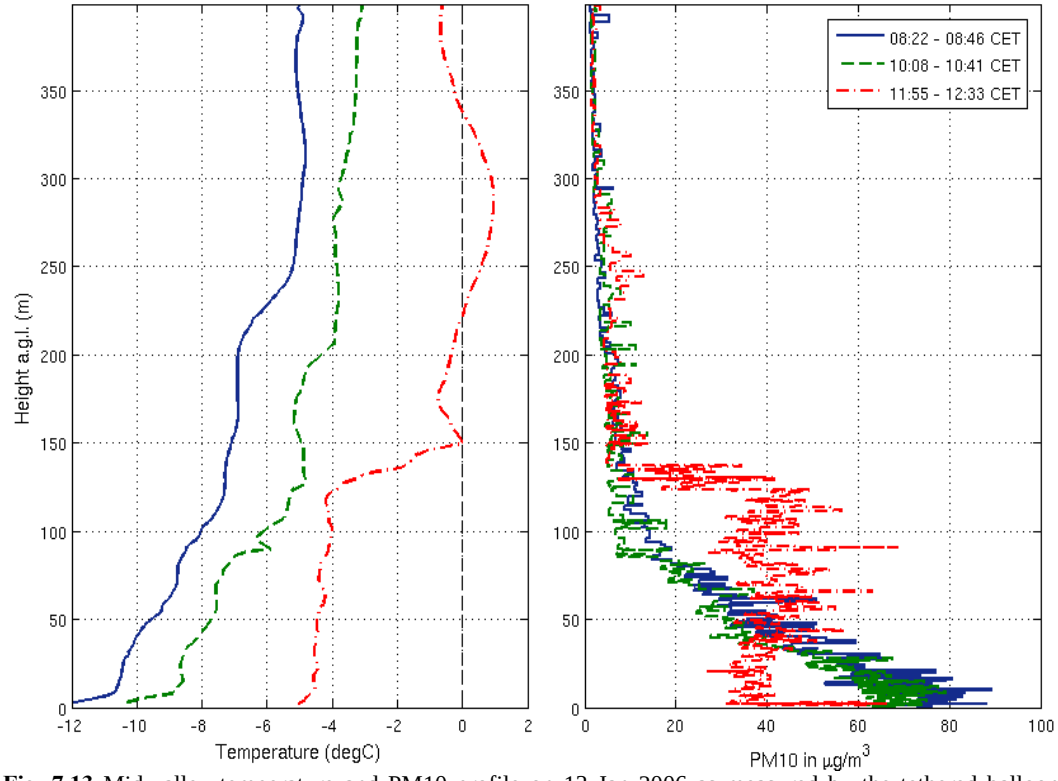

Fig. 7.13 Mid-valley temperature and PM10 profile on 13 Jan 2006 as measured by the tethered balloon system at 08:22 – 08:46 CET (solid blue line), 10:08 – 10:41 CET (dashed green line) and 11:55 – 12:33 CET (dash-dotted red line).

As shown in Fig. 7.13, 13 Jan 2006 starts with a stably stratified ABL (lowest 200 m) and valley outflow of the order 2 – 4 m/s. In the morning rush-hour, the valley ground concentration of NO_2 shows a relative peak as is usual. With increasing solar insolation the lowest layer becomes iso-

thermal, which is remarkable with respect to the presence of snow on the ground. The ground pollution decreases, which is mainly due to vertical redistribution. A short upvalley phase in the afternoon is not connected with a significant concentration transport in this case. Soon after sunset the lowest layer returns to a highly stable status leading to a pronounced increase in evening concentration and exceedance of the threshold close to the motorway.

The corresponding vertical profiles of temperature and PM10 as measured by the tethered balloon system are shown in Fig. 7.13. The highly stable morning profiles lead to a fine-dust concentration of 60 – 80 µg/m3 at the ground and interestingly a continuous decrease up to about 90 m AGL. Towards mid-day the temperature profile is almost isothermal, this less stable state allows for a homogeneous redistribution of PM10 up to approx. 140 m AGL.

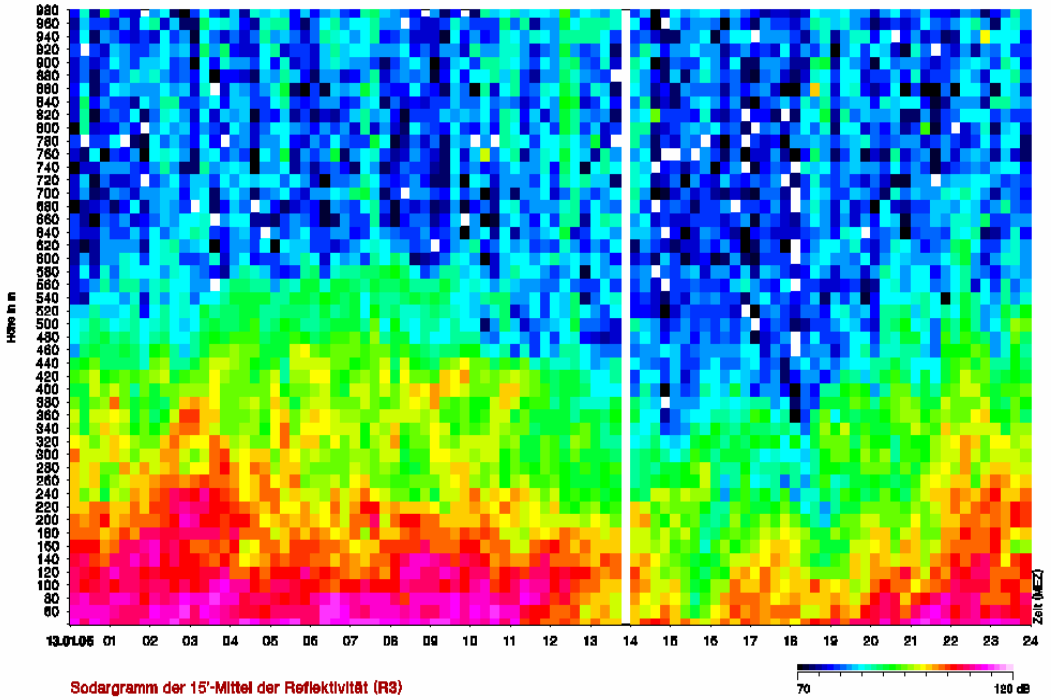

Fig. 7.14 Sodar reflectivity (dB) as a function of height on 13 Jan 2006. Times in CET.

The time height series of the Sodar reflectivity is given in Fig. 7.14. Reflectivity can be high due to either stable layering or high turbulence. For further discrimination, a combination with the standard deviation of the vertical wind velocity is useful (Emeis et al., 2007). Nevertheless the 100 to 200m thick stable layer up to midday is clearly visible. In the early afternoon a short “mixed” phase is demonstrated by the green mid-level reflectivities reaching the lowest detection level. Also a new build-up of the ground inversion from the surface at about 15 CET close to sun-set and the growing layer depth and strength in the course of the night is clearly visible.

The corresponding vertical profiles of temperature and PM10 as measured by the tethered balloon system are shown in Fig. 7.13. The highly stable morning profiles lead to a fine-dust concentration of 60 – 80 µg/m^3 at the ground and interestingly a continuous decrease up to about 90 m AGL.

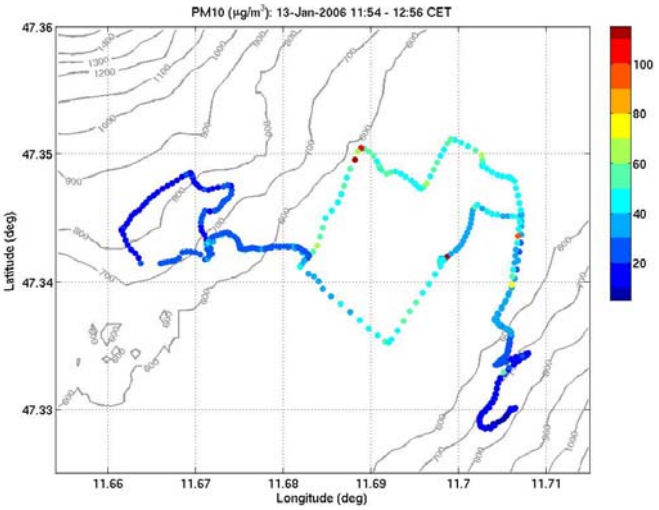

Fig. 7.15 PM10-distribution in µg/m^3 as measured by the mobil car platform in the area Schwaz-Vomp on 13 Jan 2006 between 11:54 and 12:56 CET with isolines of topography

Towards midday the temperature profile is almost isothermal, this less stable state allows for a homogeneous redistribution of PM10 up to about 140 m AGL.

Fig. 7.15 shows the fine-dust distribution between 11:54 and 12:56 CET as measured by the mobile car platform. At the valley ground the PM10 concentration is about 50 µg/m^3 interspersed with spikes from individual vehicles, e.g. at traffic lights in the city area of Schwaz. At the Vomperberg plateau on the NW side at about 300 m AGL the concentration is approx. 20 µg/m^3. On the opposite slope at 200 m AGL it only amounts to 10 µg/m^3. Note the dark blue colour at the south-eastern end points). This is a first hint for an asymmetric pollutant distribution with higher values on the sun-exposed slopes due to favoured up-slope flows.

This analysis is also confirmed by the slope temperature profile on the NW-facing slope at the southwestern edge of Schwaz. In Fig. 7.15 only 4 out of 8 sensors with a minor radiation error (see discussion above) were chosen for the background of the time-height plot of 13 Jan 2006. While losing vertical resolution the results are much more meaningful. The day starts with a stable profile up to 800 m AGL, the upper layer between 300 and 800 m AGL is nearly isothermal. A well-mixed layer – analysed as a slightly superadiabatic layer – develops between 11:00 and 16:30 CET and the layer is at least 112 m thick. After sun-set this lowest layer returns to an extremely stable state within a transition period of half an hour.

Additionally the mixing and boundary layer height from different data sources are depicted in Fig. 7.16. The results are comparable to those on other days in winter, the discrepancies and accordancies between the measurement systems are therefore typical of the methodologies and show, how difficult it is to uniquely define or measure the mixing layer height. The lowest layer without an inversion in the temperature profile is given by the thick black line. It represents the lower limit of the mixed layer and has been discussed above.

The MLH as analysed by the Sodar / ceilometer system is given in thick horizontal colored bars and is determined as the minimum of four different heights. For more information see Emeis et. al. (2007). The Sodar data are analysed for stable layers at the valley bottom (brown bar), lifted inver-

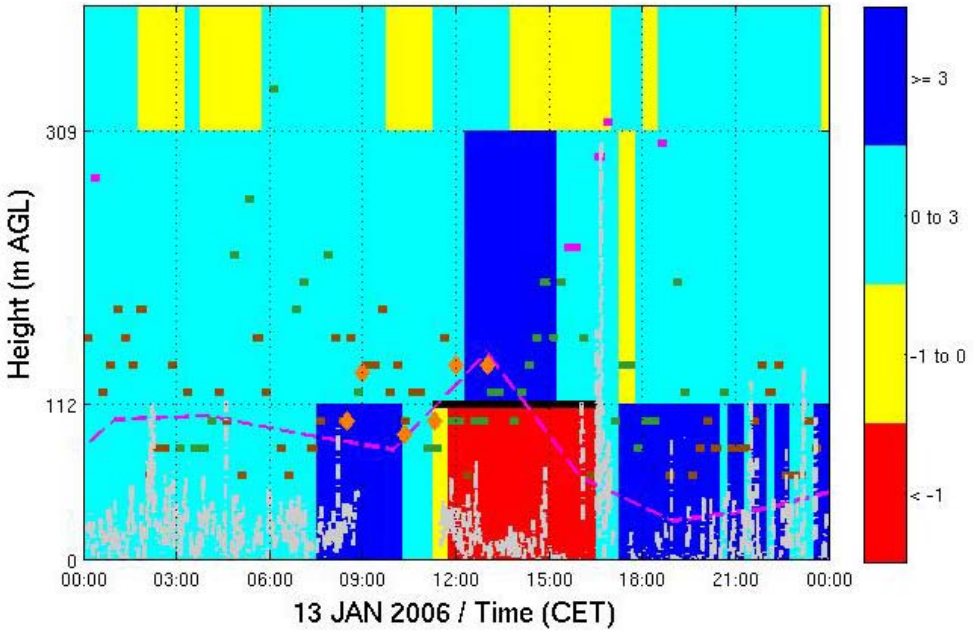

Fig. 7.16 Stability as analysed by selected sensors of the temperature profile. Colours denote stability range in °C / 100m as shown on the right, inversion layers in blue. Additionally mixing and boundary layer height as analysed from different data sources are printed. See text for a detailed description.

sions (green) and turbulent layers (orange). A magenta bar shows that the MLH was detected by the Ceilometer looking for the minimum of the vertical gradient of the optical backscatter intensity. In the night time the stable layers at the bottom of the valley are dominant with a height of 60 m (the lowest detection level) to 160 m AGL. In the early afternoon this layer has warmed sufficiently, so the mixing is then restricted by the lowest lifted inversion, which rises significantly after 1400 CET. After that the magenta bars indicate, that the top of the aerosol layer as seen by the ceilometer is slightly below the limiting inversion. The MLH reaches maximum values of about 300 m AGL at that time. After sunset a stable layer reforms starting at the bottom, which abruptly lowers the MLH.

The mixing layer height as analysed manually from the tethersonde data is shown in big orange diamonds (see Fig. 7.13 for a more detailed profile information). It represents the top layer of the pollutants emitted on that day just below the residual layer in a mid-valley position. The tethersonde analysis corresponds rather well with the Sodar / Ceilometer and temperature profile data.

Data from an ultra sonic anemometer (USA) at the mid-valley base station in Schwaz 5 m AGL was used to derive the stable boundary layer following Nieuwstadt (1981). The results are shown as a grey dashed line. During the night the lowest layer above the ground was extremely stable (see Fig. 7.13). Therefore mixing layer height calculations from the USA without any “knowledge” of the atmosphere aloft naturally tend to underestimate the MLH.

Finally the parameterized boundary layer height (BLH) from the ECMWF model with a three hourly resolution is plotted as a dashed magenta line. The temporal evolution is not quite correct,

namely the BLH at 16 CET is too low, when in reality the maximum heights are detected. Nevertheless, the overall magnitude is surprisingly accurate.

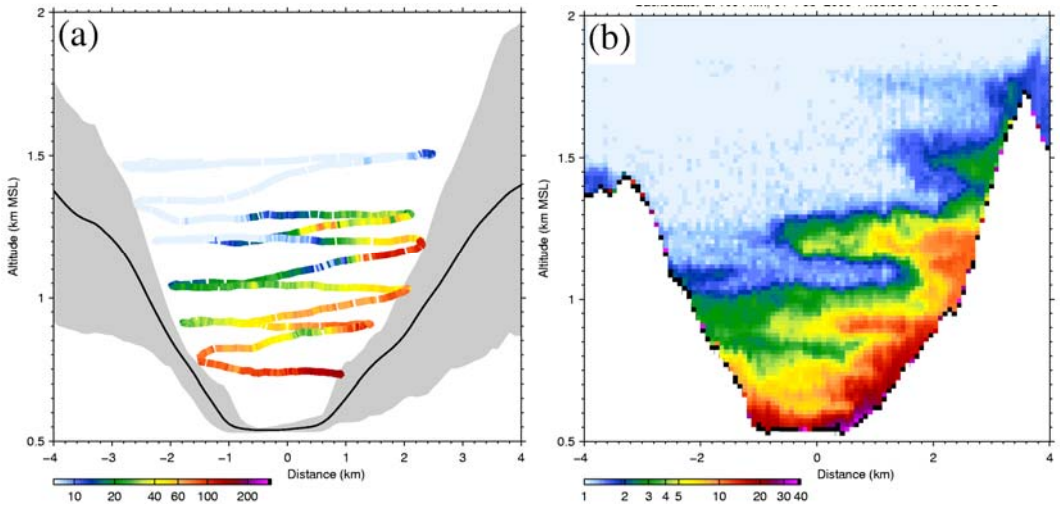

Fig. 7.17 Vertical transect across the Inn valley of (a) aerosol concentration for particles greater than 0.3 µm in particles per millilitre measured by the MetAir Dimona; (b) aerosol backscatter intensity at 1064 nm in logarithmic colour scale from the DLR TropOLEX lidar. The mean topography in (a) is shown as a solid line, and the limits of the topography in a 6 km corridor as gray shaded area. Topography in (b) is white. Figures are for the afternoon flights at 14 UTC (15 CET) on 01 Feb 2006. See text for further explanation.

The second case study presented here is 01 Feb 2006, again a day dominated by high pressure influence with some thin cirrus clouds. On that day and in the framework of the joint research projects INNAP[1] and INNOX[2] two research aircrafts were probing the atmosphere with an aerosol backscatter lidar and in-situ measurements, respectively. The collected data help to obtain a more detailed view of the aerosol distribution and specifically of the pollutant concentration asymmetry above the two valley slopes. While in the morning around 10 CET the highly polluted layer is still restricted to 100m AGL with a gradual decrease in the residual layer up to 500 m AGL (not shown), a strong asymmetry has formed in the afternoon at 15 CET (see Fig. 7.17). Both the absolute in-situ particle measurements by the MetAir Dimona motor glider and the backscatter from the DLR TropOLEX lidar in arbitrary units show the same picture: the aerosol layer has risen on the sun-exposed SE slope. When encountering elevated stable layers (in 900 m and 1250 m MSL, respectively), parts are also propagating towards the valley centre. On the other side the shaded NW slope apparently experiences slight upslope flow. This structure is also supported by other data. More detailed information on the results from these two projects is given in Harnisch et al. (2007) and Schnitzhofer et al. (2007).

This asymmetric feature is confirmed by the tethered balloon and car measurements at 10, 12 and 15 CET. As can be seen in Fig. 7.18, a general redistribution towards higher levels takes place throughout the course of the day leading to marked peaks at the top of the lowest stable layer(s)

[1] EUFAR project on the boundary layer structure in the Inn Valley during high air pollution
[2] EUFAR project on the NO_x-structure in the Inn Valley during high air pollution

and finally nearly homogeneous profiles in the afternoon. Nevertheless the higher concentration levels are clearly found on the sun-exposed SE facing slope, except for a still stable 30m deep layer at 12 CET on the NW-facing slope.

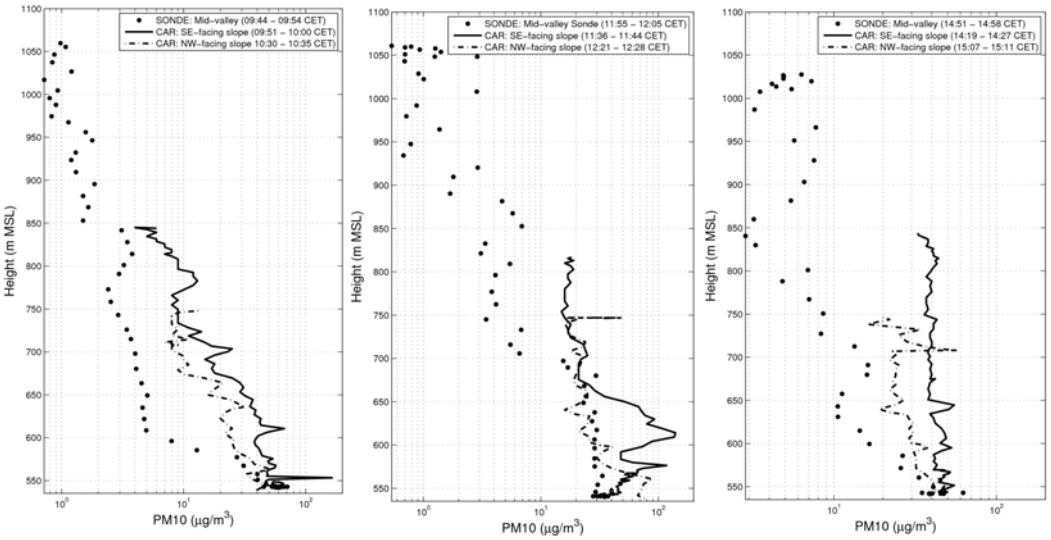

Fig. 7.18 Profiles from mid-valley sonde (black dot) and car-measurements along SE –facing slope (red solid line) and NW-facing slope (blue dashed line) on 01 Feb 2006 around (a) 10 CET, (b) 12 CET, (c) 15 CET. Note the redistribution of pollutants towards higher levels in the course of the day and the higher concentration on the sun exposed SE-facing slope as well as the formation of layers in the mid-valley profile.

7.1.3.5 Important factors for air pollution

In this chapter some preliminary results of the governing requisites for winter time air pollution in the lower Inn valley will be presented. Traffic is an important pollution source which is more relevant for nitrogen oxide than for fine dust. For this latter pollutant other sources like domestic heating have to be considered. Obviously the stability in the boundary layer and the horizontal wind speed as a measure of turbulence and dispersion conditions play an important role for the observed pollutant concentrations, but also the day to day accumulation under low inversions in the absence of synoptic disturbances is also addressed.

Traffic emissions have a quite well defined daily cycle also influenced by traffic regulations. Fig. 7.19 left, shows the number of vehicles of a four day period in Jan 2005. On weekdays a peak in the morning and late afternoon is connected to people driving to work. Note that the heavy duty vehicle traffic sets in before the light vehicle peak at 05 CET - directly after the end of the nighttime traffic ban. The weekend traffic is closely linked to weather and – in winter - snow conditions. Sunny weather can cause a lot of traffic to and from skiing areas peaking in the late morning. In general the weekends are characterised by almost no heavy duty vehicles, because they are banned, and thus an overall decrease in traffic.

There is some evidence that diesel engine emissions have shifted towards more NO_2 (Carslaw 2005). In other words, the overall NO_2/NO_x emission ratio has increased over the last few years. This tendency is also seen in the NO_2/NO_x concentration ratio at Vomp Raststätte between 1997 and 2006 (cf. Fig. 7.19 right) with an overall higher ratio since 2002.

The daily march for the period 01 Nov 2005 until 06 Feb 2006 is calculated for the hourly vehicle numbers, as well as for hourly concentrations of PM10 and NO_x (Fig. 7.20 left). In the morning hours (05 – 07 CET.) heavy traffic and NO_x concentration increase towards a first peak. The light vehicles have a first maximum at this time as well. The main peak of light vehicles is found in the late afternoon, where the second maximum of NO_x concentration occurs about 1 to 2 hours afterwards. A similar pattern is found in the diurnal variation of PM10.

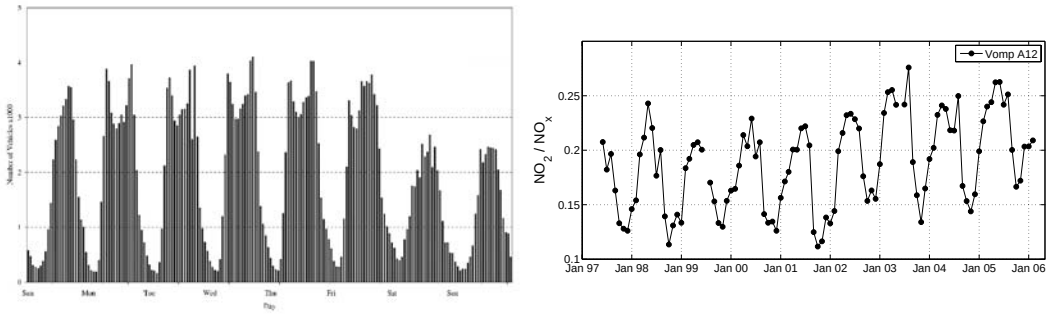

Fig. 7.19 Left: Total vehicles (blue) and total heavy vehicles counts (red) at Vomp Raststätte during the time period 11 until 14 Jan 2006 (Wednesday until Saturday). Right: Monthly mean of the NO_2/NO_x concentration ratio measured at Vomp Raststätte in 5 m distance to the highway A12 between Jun 1997 and Feb 2006.

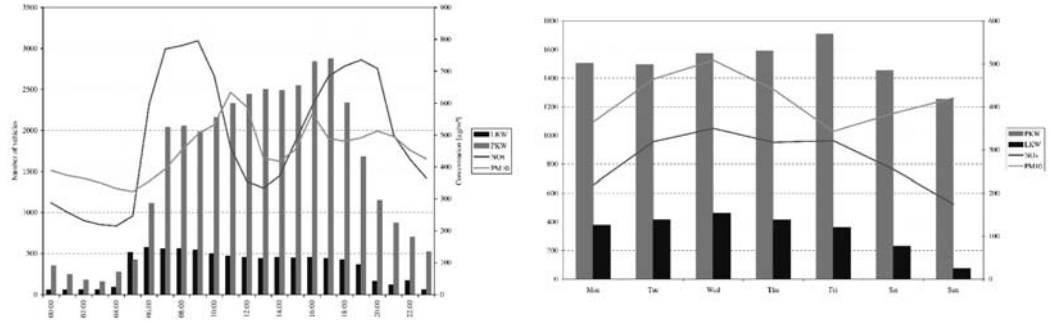

Fig. 7.20 Left: Mean diurnal variation of light vehicles (green bars), heavy vehicles (blue bars), NO_x concentration (red line) and PM10 concentration of LT station (orange line, diagrammed with factor 10) from 01 Nov 2005 until 6 Feb 2006. Right: Daily means for the different days of the week of light vehicles (green bars), heavy vehicles (blue bars), NO_x concentration (red line) and PM10 concentration of LT station (orange line, diagrammed with factor 10) from 01 Nov 2005 until 06 Feb 2006.

Daily averages for the different days of the week were also calculated (Fig. 7.20 right). Holidays were added to Sundays. Passenger traffic peaks on Friday and shows a slight decrease on weekends. Compared to the mean weekday a reduction of 8 % (20 %) was observed on Saturdays (Sunday and holidays). The peak maximum of heavy vehicles on the road is observed in the middle of the week. Towards the weekend, heavy traffic decreases. On Sunday the effect of a traffic ban on trucks is obvious. NO_x concentrations resemble the traffic emission march. They show a peak on Wednesday when heavy vehicles are most frequent. A secondary maximum can be found on Friday, when the volume of light vehicles is at its maximum. The weekly PM10 march is not clearly coupled to the traffic emission. This indicates the important role of other sources like domestic or industrial burning.

The distance from the source(s) is an important factor for the measured concentrations at a given location. Fig. 7.21 gives an example for 6 two-week periods during the ALPNAP field phase in winter 2005/ 2006. The NO_2 level measured by passive samplers is highest in the last two periods in January, reaching concentrations of 160 µg/m^3 in the vicinity of the motorway. In a horizontal distance of 200 m (500 m / 1000 m) this level is reduced by about 40 % (50 % / 60 %). At the northern and southern slopes the relative importance of the decrease due to horizontal and vertical distance is hard to distinguish. The higher NO_2 levels to the southeast of the motorway are probably due to the influence of the higher population density in the vicinity of Schwaz and do not give a clear indication of a general cross-valley asymmetry due to the different exposition angles of the slopes.

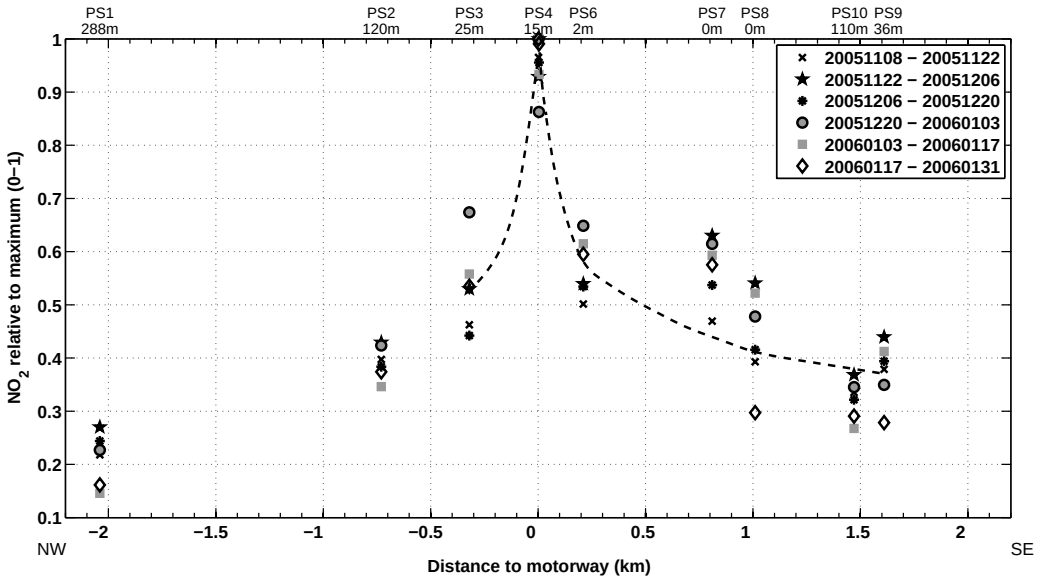

Fig. 7.21 Evaluation of the decrease of the NO_2 concentrations as measured by 10 passive samplers as a function of the horizontal distance from the motorway. The six two-week periods between 08 Nov 2005 and 301 Jan 2006 are outlined in the legend. Note that PS7 is influenced by the city of Schwaz. A rough mean winter estimate is given by the dashed line. The height above the valley floor of each passive sampler is given on top. The main northwest (NW) to southeast (SE) cross-section directions are indicated at the bottom.

Another important factor is the stability of the boundary layer. It is quite apparent, that stable conditions in the boundary layer foster an increase of air pollution close to the ground with new emissions being restricted to a shallow layer and low vertical dispersion. Fig. 7.22 (left) reveals the connection of the half-hour mean of the temperature gradient between the valley bottom and a slope station 180 m AGL to the measured mid-valley NO_2 concentrations. During the winter period NO_2 above 70 µg/m^3 occurs more often during inversion conditions than during mixed or neutral / slightly stable time periods and vice versa.

Wind acts on dispersion in two ways. First it is responsible for the horizontal or in case of topography also forced vertical advection of a potentially polluted air mass. But higher wind speeds are also connected to higher turbulence and hence mixing. During the measurement campaign in the Inn valley the mid-valley direction of the wind – mostly down valley in the night and short up-

valley periods in the early afternoon – showed almost no correlation with the concentration level. Nevertheless, higher wind speeds (turbulence) enhance dispersion, as expected, and are therefore linked with lower concentration levels in the valley concentrations for the four different wind classes up to 0.5, 0.5 – 1, 1 – 3 and 3 – 10 m/s. NO_2 concentrations higher than 70 µg/m^3 are clearly favoured by low wind speeds (see Fig. 7.22 right), nevertheless single events with moderate wind higher than 3 m/s and NO_2 exceeding 150 µg/m^3 could still be observed at the end of a long accumulation period in January.

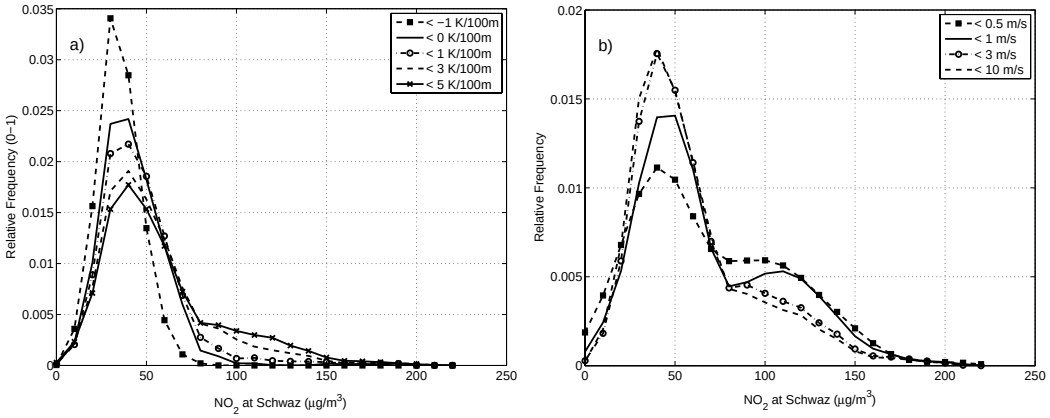

Fig. 7.22 a) Relative frequency of NO_2 at Schwaz for five different stability classes in the period 08 Nov 2005 to 04 Feb 2006. The mean stability from the valley bottom towards Arzberg (180 m AGL) as defined in the legend increases from blue to magenta. b) Relative frequency of NO_2 at Schwaz for four wind speed classes in the same period as in a. The wind speed is taken from mid-valley station Schwaz at 5 m AGL, the definition of the classes is given in the legend.

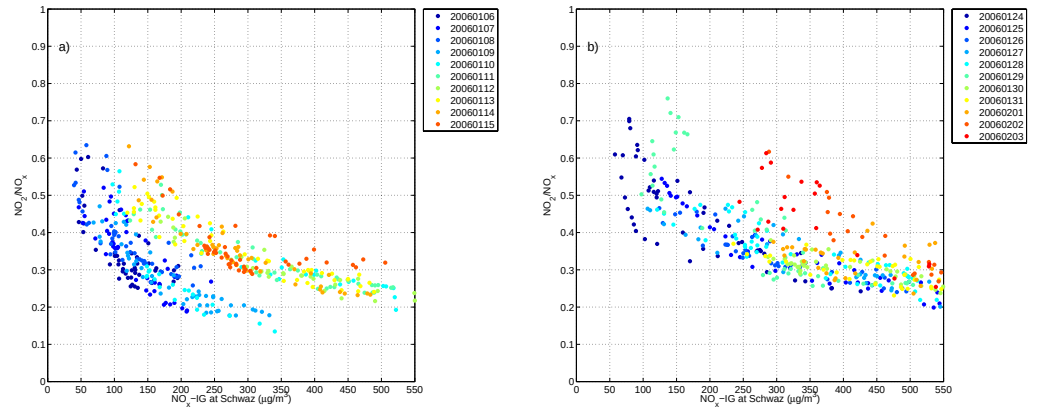

Fig. 7.23 NO_2 ratio to the total NO_x concentration at the station Schwaz from 06 until 15 January 2006 (left) and from 24 January until 03 February 2006 (right). The colours denote the date from 06 Jan (blue) to 15 Jan 2006 (red).

The role of air pollution accumulation is shown in Fig. 7.23. The figures demonstrate the influence of accumulating air pollution from day to day during stable meteorological conditions. During the first few days, which are the end of the holiday period, the maximum NO_x concentrations (left

part, blue points) reach values up to 350 µg/m^3 and the NO_2 ratio is about 0.40 for 100 µg/m^3 or 0.20 for 300 µg/m^3. From 09 Jan 2006 the traffic is growing and the values are at a new level (yellow, orange and red points in Fig. 7.23a). Due to the large amount of old air the amount of chemically formed NO_2 is high. The same effect of accumulation with higher chemical transformation rates is demonstrated during the second stable period from 24 Jan until 03 Feb 2006 (Fig. 7.23b).

The accumulation from day to day is connected to the regular valley wind system. In a high pressure period a cycle of nocturnal down-valley and daily upvalley flows establishes. Therefore polluted air is carried up and down the valley taking up new pollutants when sweeping over areas with relevant emission sources. This phenomenon is less pronounced in winter due to the only weakly developed upvalley flow but can still be of considerable importance; e.g. Griesser (2003) studied a high-pressure period in Nov / Dec 1999 with a conceptual model concentrating on accumulation processes along the Inn valley and found that the quasi-regular valley cycle is important for explaining the observed concentration patterns.

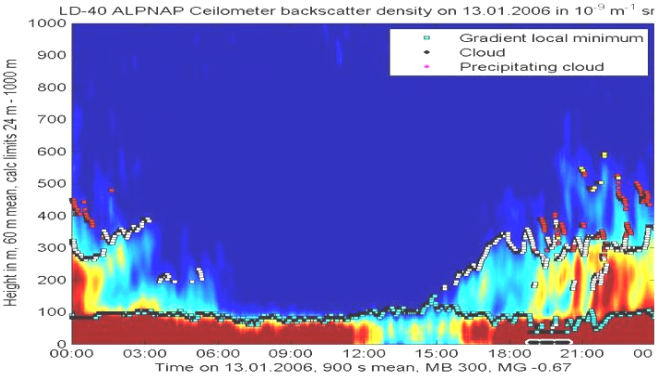

Fig. 7.24 Optical backscatter intensity (brown: high backscatter, dark blue: low backscatter) measured by the ceilometer on 13 Jan 2006 during 24 hours. Local minima of the vertical gradient of the ceilometer backscatter intensity are marked by dots with black shadow in the left-hand frame indicating a surface-based stable layer or lifted inversions.

The mixing-layer height (MLH) limits the vertical dilution of primary pollutants. MLH cannot be monitored from direct measurements but has to be inferred from ground-based remote sensing measurements (Emeis and Türk, 2004; Schäfer et al., 2004; Münkel et al., 2004). Fig. 7.24 shows an example from the Inn valley (more details in Emeis et al., 2007). Results from optical remote sensing with a ceilometer are displayed. Optical backscatter depends primarily on the aerosol concentration. MLH is at the top of the aerosol layer (light blue, yellow and red colours). The Sodar measurements on the same day have previously been presented in Fig. 7.14 in the section "Spatial distribution of air pollution and connected meteorology". Acoustic backscatter depends on temperature fluctuations (turbulence) and mean vertical temperature gradients (inversions). MLH is at the top of high near-surface backscatter (well-mixed surface layer) or at elevated secondary backscatter maxima (inversions).

Fig. 7.25 shows a special case with extremely pronounced vertical layering in the Inn valley. This happened on 29 Jan 2006. The acoustic backscatter intensity (left frame of Fig. 7.25) shows several secondary maxima below 700 m AGL during the first half of the day. This structure is interrupted around noon when the down-valley wind system is stopped and is replaced by up-valley winds in the lower layers (below about 200 m until 14:00 CET and then below 400 m above ground). The rather high backscatter intensities in the lower 200 m above ground between 15:00 and 18:30 CET also show that this flow is stably stratified. After 19:00 CET the down-valley wind starts again and the vertical structure from the morning hours is re-established. The right-hand frame of Fig. 7.25 demonstrates that this layering is also visible from the wind direction recordings made with the Sodar. We see that layers dominated by slope winds and layers dominated by down-

valley winds appear alternately one above the other. The main reason for the formation of a larger number of relatively thin stable layers one above the other in a larger valley is the interaction of nocturnal down-valley flow and nocturnal down-slope flows. Both flows are nearly laminar due to their small flow speed and high thermally stable stratification. Therefore the interaction between the different layers is very small and the layers can persist for hours without dissipating each other by friction.

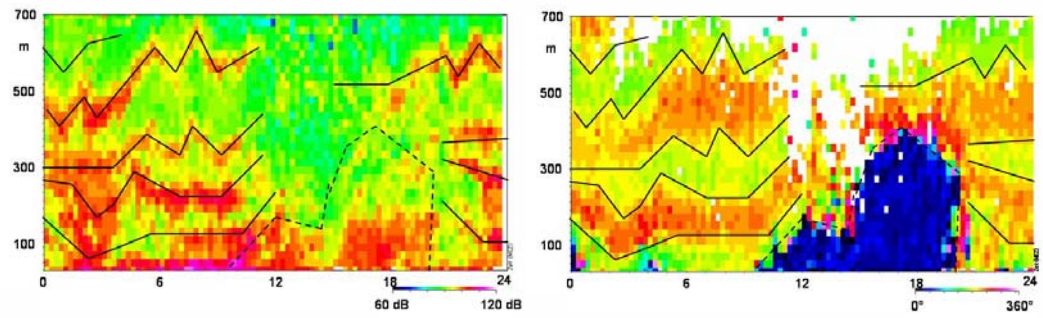

Fig. 7.25: Acoustic backscatter intensity (left; purple and red: high, green: low) and wind direction (right; green: down-slope winds, red: down-valley winds, and blue: up-valley winds) from the sodar measurements on 29 Jan 2006. The lines in the two graphs have been analysed from the wind direction changes in the right-hand frame.

Fig. 7.26 shows statistical evaluations of MLH using the combined results from both ceilometer and Sodar. The way this MLH is determined from the two instruments is explained in detail in Emeis et al. (2007). In winter, MLH only has a very small diurnal variation with slightly higher values in the second half of the day (left frame). The daily mean mixing layer height varies between 100 m and 325 m above ground with a peak frequency (right-hand frame) of about 29 % at 125 m above the valley floor.

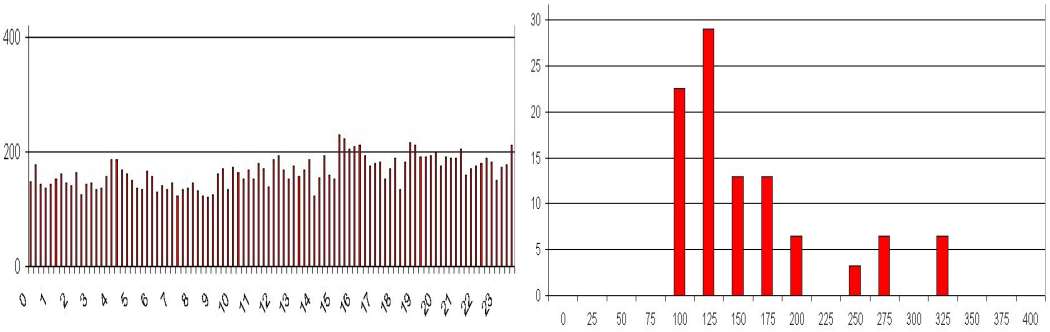

Fig. 7.26 Mean diurnal variation of mixing layer height in m plotted against the hours of the day (left) and frequency distribution of the mean daily-averaged mixing layer height in percent plotted against the height above ground in m (right) in the Inn valley for Jan 2006.

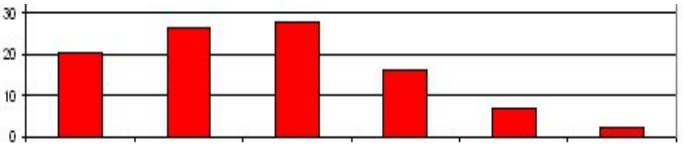

Fig. 7.27 Frequency of the occurrence of multiple lifted inversions in % from the Sodar data. "0" means that no lifted inversion was detected.

The occurrence of multiple lifted inversions is a special feature observed in Alpine valleys. Fig. 2.27 shows that in only 20 % of all 15 min time periods in this month no lifted

inversion could be detected. Most common (28 %) are two lifted inversions within the first about 600 m above ground. Four and five layers together still appear in about 10 % of the time.

7.1.4 Modelling results

7.1.4.1 Statistical forecasting of air quality in the Inn valley

As air quality threshold values are exceeded in wide regions of the transalpine transit corridors, a variety of strategies and measurement plans were set up. While some measures act towards a general reduction of emissions, others aim to reduce high pollution episodes. Giving support in steering this second kind of measurement was the major motivation in developing this forecast model for core pollutants as an online tool.

As a first step, the forecasting tool has been developed for five long-term air quality monitoring sites situated in the Inn valley and one in the exit region of the Wipp valley. For all sites, NO, NO_2, and PM10 forecasts up to 48 hours in advance are provided every morning.

Methodically, the forecasts are based on multiple linear regressions between the parameter to forecast – called predictant – and a set of possible influencing parameters. See section 4.4 for more information on the regression method.

To determine the relevant predictors and their regression coefficients, several years of measured air quality and potential predictors were analysed. The analysis was made for every forecasting time step (from +1 hour to +48 hours in half hourly resolution), leading to a set of 96 equations per station and forecasted parameter. Moreover, winter and summer half year were evaluated separately, to account for the fundamentally different dispersion conditions.

In forecasting mode, predicted or estimated values for the predictors are inserted.

The main groups of predictors and some detailed attributes are shown in Fig. 7.28. For all these parameters, accurate and long term data had to be collected or calculated retrospectively, in order to develop, analyse and test the model. Furthermore methods to predict their development in the near future had to be established to apply the forecast.

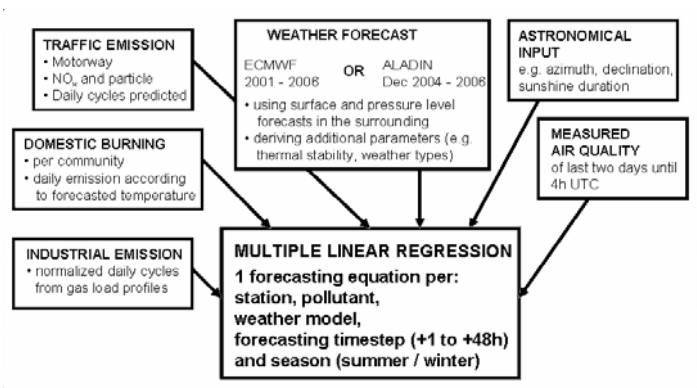

Fig. 7.28 Input scheme for the statistical model.

Emissions are included on an hourly basis as motorway emissions, emissions due to domestic burning and industrial emissions.

Motorway emissions were calculated on the basis of traffic counts between Apr 2004 and Dec 2006, differentiated in four relevant vehicle categories, by using standard emission factors. For temporal extrapolation (backwards until Jan 2001), typical daily traffic cycles were derived for all weekdays and months respectively. Administrative measures like a night time ban on heavy duty vehicles were accounted for. Additionally, changes in yearly total traffic amounts as well as

changes in the emission factors were applied. The prediction of motorway emissions in forecasting mode operates similarly, using estimations of daily traffic with respect to the accurate weekday, month or holiday to predict. An optional factor provides the capability of accounting for an increasing number of vehicles or a change in the vehicle fleet.

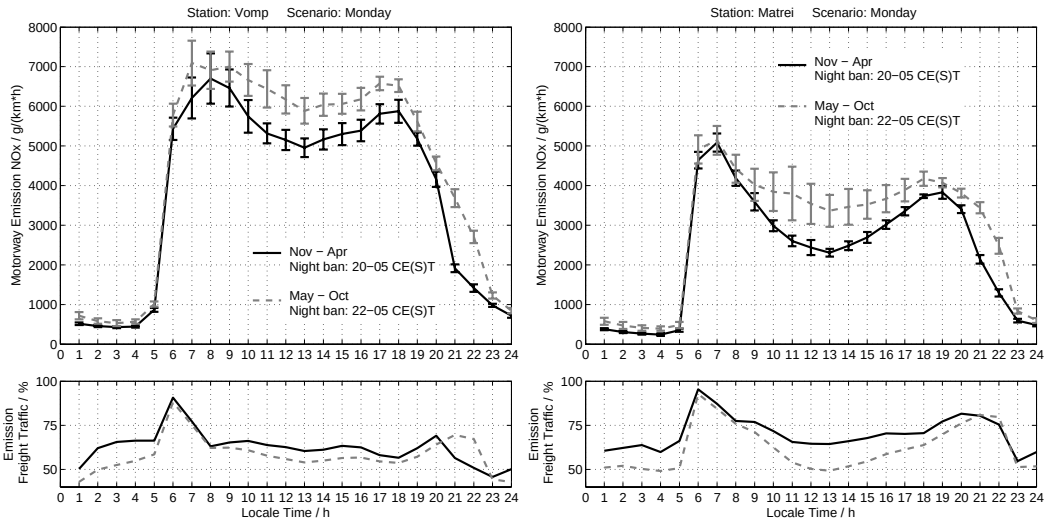

Fig. 7.29: Daily march of total NO_x emissions on the motorway. Left: Inn valley motorway A12 near Vomp; right: Brenner motorway A13 near Matrei. Total NO_x Emissions of summer months (May - October) in red and winter months (November to April) in black are shown in the upper part (mean values and standard deviations); the relative contributions from freight traffic are shown below.

Fig. 7.29 shows an example of daily motorway emissions on a typical Monday near Vomp in the Inn valley and near Matrei in the Wipp valley. Winter emissions are significantly lower during daytime, while the summer emissions, especially in the Wipp Valley, show much higher variabilities. On both sides, emissions from freight transport are dominant.

To estimate emissions from domestic burning, preliminary results from an emission inventory for North Tyrol were used, providing yearly sums of emission at a community level resolution. Combined with temperature measurements and a degree day approach, these emissions were calculated for each day and broken down to hourly resolution, according to heating energy consumption load profiles.

The same procedure is used to predict emissions from domestic burning in the near future, using temperature forecasts from the numerical weather models ECMWF or ALADIN.

Records on industrial emissions of North Tyrol are currently sparse, though an investigation in the frame of an emission inventory is in progress. Relative emission load curves were estimated from the consumption of process gas by industrial consumers.

As meteorological input, forecasts from one of the numerical weather forecast models ECMWF or ALADIN are used respectively. The spatial resolution of the global model ECMWF is rougher (50 to 25 km) compared to about 7.5 km of the mesoscale model ALADIN. Nevertheless, this is compensated by a more extensive parameter set and a longer data series of the ECMWF model. Additional air quality relevant parameters were derived for both models.

A smaller group of input data give astronomical information like the position of the sun by azimuth and declination or the maximum sunshine duration.

Finally, the initial pollutant level, in the form of measurements of the past two days, is included in the model.

The model was validated using an independent data set covering Dec 2005 and Jan 2006. Fig. 7.30 shows forecasted versus measured NO_2 for the station Vomp during the week 05 to 12 Jan 2006. This period is characterised by high pollution levels due to to ideal conditions for the generation of persistent inversions in the Inn valley and day by day accumulation of pollutants in the valley atmosphere. The reduced emissions on Sunday 08 Jan brought only a slight improvement of air quality.

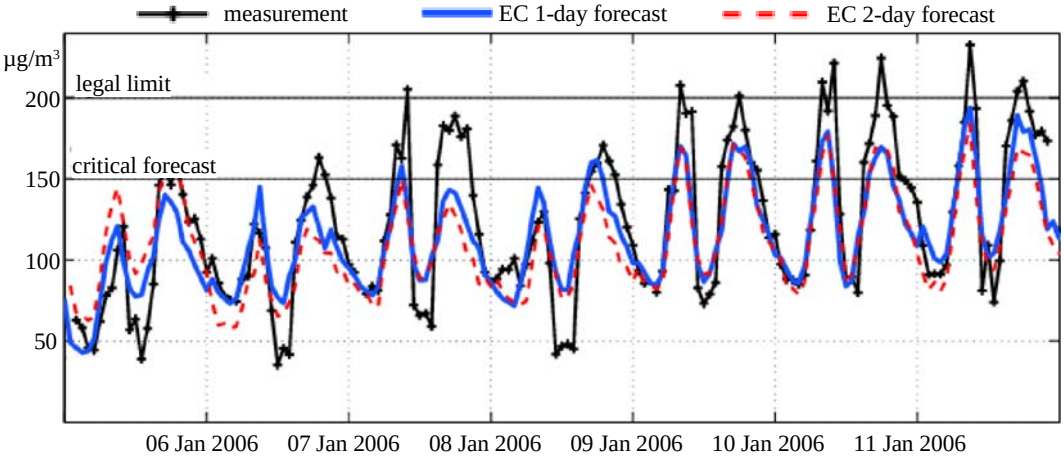

Fig. 7.30 Measurements and forecasts of NO_2 at the Vomp station during a highly polluted period from 05 to 11 Jan 2006.

The forecasts shown were calculated using meteorological forecasts from the ECMWF model. The daily marches of NO_2 concentrations are replicated quite well; extraordinarily high pollution peaks however are systematically underestimated. Also, remarkable reductions around noon on 06, 07, and 08 Jan are not covered. These events are highly governed by the evolution of the lowest boundary layer i.e. intensifying or breaking up of surface inversions, which is not resolved by the ECMWF model on the required scale.

In order to estimate the probability of exceedances of the legal half hourly mean threshold value of 200 µg/m³, the forecasts were statistically analysed and it was found, that – for this station – a forecast spike exceeding 150 µg/m³ fits best with a threshold exceedance, regarding false alarm and hit rates. Tab. 7.4 shows the score to predict threshold exceedances in the validation period.

Tab. 7.4 Statistical analysis of threshold exceedances predictability.

Legal threshold exceedances = measurement > 200 µg/m³	58	on 16 days out of 62
detected = forecasted peak > 150 µg/m³	55 (95%)	on all 16 days
not detected	3 (5%)	all on already "detected" days
false alarm	27 (55%)	on a total of 20 days; of which 13 days have exceedances at other times, and 7 days no exceedance

Due to the less complex emission situation for nitrogen oxides, their forecast is generally better than the one for PM10. The forecasts will be provided on an internet platform, allowing continuous observation and evaluation.

7.1.4.2 MM5 and CAMx modelling results

Here, simulation results are presented for a selected winter smog episode, obtained with the state-of-the-art model chain MM5-CAMx. More details can be found in Schicker and Seibert (2007). The simulation focussed on the lower Inn Valley. It illustrates capabilities as well as limitations of such models. In large Alpine valleys unfavourable dispersion conditions prevail in winter. Wind velocities are low and the atmosphere is very stable, especially in the presence of snow cover, so that pollutants emitted tend to accumulate near the valley floor. Realistic simulations of the meteorological conditions are difficult to achieve in these circumstances. The period 27 Jan 2004, 12 UTC, to 09 Feb 2004, 00 UTC, was selected for the simulation, as it represents such an anticyclonic weather phase with snow cover, weak winds and strong stability.

The latest version of the PSU/NCAR mesoscale model (MM5V3.7), described in detail in Dudhia (1993) and Grell et al. (1994) including modifications for Alpine topography by Zängl (2003a), was used to simulate the meteorological conditions. Simulations at first used four nested domains with a resolution of 2.4 km in the innermost nest (runs 1 and 2, with different boundary-layer schemes). Then a simulation with a fifth domain, having a resolution of 0.8 km in the innermost nest, was added (run 3). Topography of the two innermost nests is shown in Fig. 7.31. The MM5 model was initialised with the ECMWF analyses, and on the outer domain nudged towards the analysed fields to avoid forecast errors.

The observed temperatures in the Inn Valley (Fig. 7.32 left) during the high-pressure period are characterised by a large diurnal variation with minima below zero and maxima around 10 °C. The first runs with the coarser grid overestimate the temperature, and completely fail to reproduce the strong diurnal amplitude. Only the run 3 with 0.8 km highest resolution is able to simulate the observed temperatures well, though even then the minima are underestimated by several degrees. Domain 4 of run 3 is not much worse than domain 5, because of the two-way nesting employed. The different boundary-layer schemes have only little influence. At the mountain station Patscherkofel (approx. 2250 m ASL), close to Innsbruck (approx. 570 m ASL), the differences between the various simulations are much smaller, and they are also more accurate.

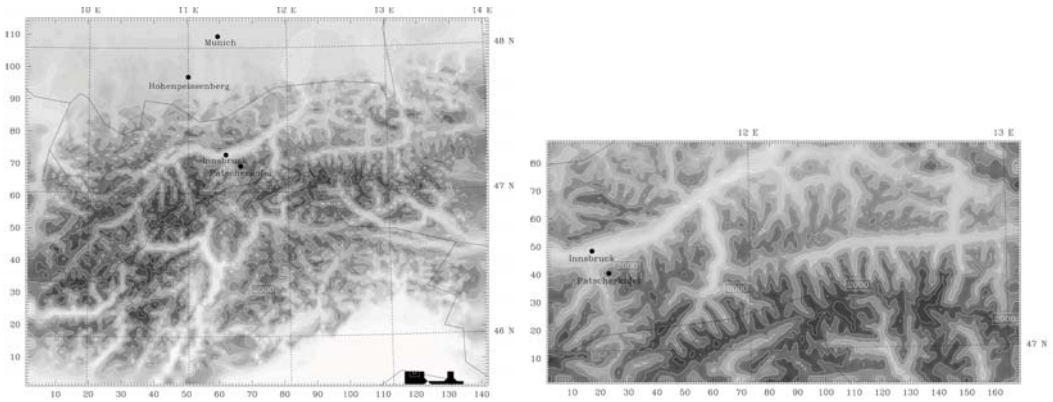

Fig. 7.31 Topography for MM5 model domain 4 (2.4 km horizontal resolution), with locations of Innsbruck Airport and Patscherkofel corresponding grid point in the left image and model domain 5 (0.8 km horizontal resolution) with locations of Innsbruck Airport, Innsbruck University (both ~570 m ASL) and Patscherkofel (~2250 m ASL) in the right image.

The stability of the atmosphere in the Inn Valley, expressed as the difference of potential temperatures (see Chapter 3) between mountain and valley station, was quite high during the whole period, especially during the nights (Fig. 7.32 right). The 2.4 km resolution run 2 completely failed to reproduce this high stability which is a major reason for the observed high concentrations of air pollutants in this episode, whereas the 0.8 km resolution run 3 is correct during daytime and moderately underestimates stability at night. In comparison, in the Alpine foreland the stability is much lower most of the time, and in general simulated well even with the coarse model resolution (Fig. 7.33).

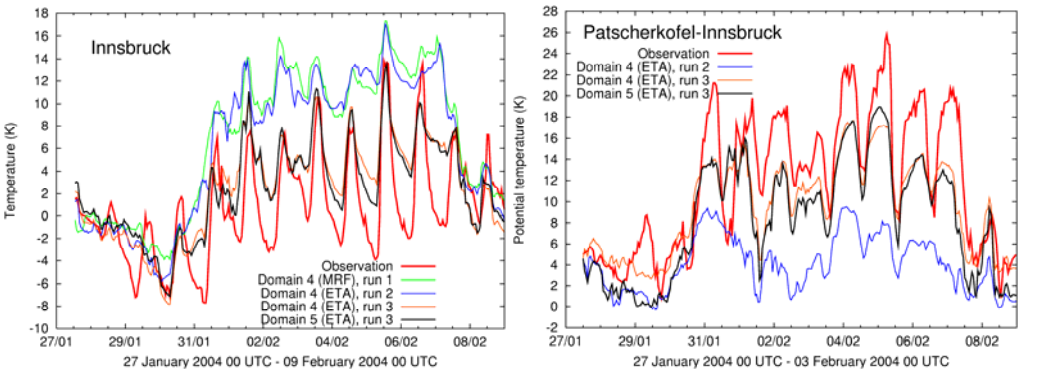

Fig. 7.32 Left: comparison of the modelled and observed temperature in Innsbruck (left). Right: comparison of the modelled and observed difference of the potential temperature between Patscherkofel (~2250 m ASL) and Innsbruck (~570 m ASL).

Winds (not shown) are not simulated well. There are probably two reasons for the deficiencies found even in run 3: In reality, the Inn Valley was snow-covered throughout this period, while in the model the snow was not intialised well and melted away quickly. Another problem is the fact that domain 5 was cutting through the Inn Valley too close to the region of interest.

This example shows that even the application of a sophisticated model does not guarantee success. A grid resolution of 2.4 km, which is considered high, may be good for flat terrain or lower moun-

tains, but is insufficient in high mountains. However, this step raises the computational costs of the simulation considerably (a simulation of domain 5 with 0.8 km costs the 27-fold computer time than a simulation of the same domain with 2.4 km). Also, the selection of the innermost domain is important. It needs to be sufficiently large. Finally, snow cover, a common situation in the Alps and important for pollution episodes, is not handled well enough by the MM5 model initialisation. Additional "Alpine improvements" are still necessary. These experiences also illustrate that meteorological competence is a prerequisite for successful application of this kind of models.

Modelling results of the Eulerian photochemical air quality model CAMx (ENVIRON, 2006) were performed with the same nested grid configuration as MM5. Fig. 7.33 displays the averaged hourly concentration of NO_2 in the innermost nest of 0.8 km resolution on 04 Feb 2004, at 17:00 CET. As expected the highest values concentrate within the valleys. The agreement of the model results with measured concentrations on NO_2 is only partly satisfying, however. One reason for the disagreement certainly is the coarse resolution of the used emission data. The NO_2 emission for the 2.4 km resolution grid is the sum of the hourly values for one day (Wednesday, 04 Feb 2004). These data are based on data from EMEP for 2003 with a resolution of 50 km (Vestreng et al., 2005). Within Austria the data were downscaled to 5 km resolution based on an emission inventory from 1995. However, this finer scale is not sufficient enough for modelling with higher resolution in complex topography. Another reason for the disagreement may be the limited agreement of the meteorological input data as has been described above.

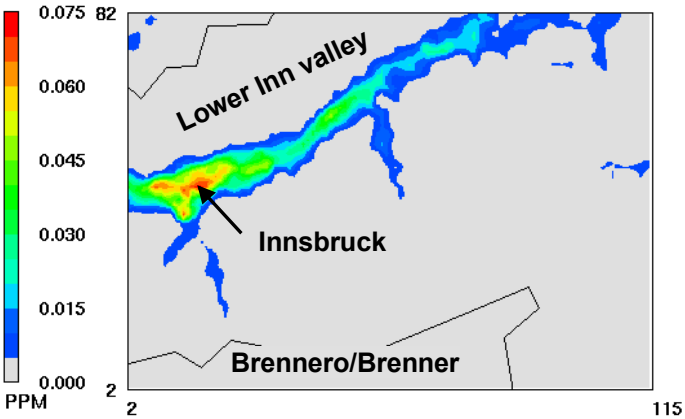

Fig. 7.33 Simulated NO_2 concentration (in ppm) in the nested model domain of Fig. 7.31 (right).

7.1.5 Noise

7.1.5.1 Noise measurements in the Unterinn valley

Relative measurements

The detailed traffic information needed for validating noise measurements and numerical calculations on a 1-minute timescale was not available. Therefore, the location closest to the road in each cross section was chosen as a reference measurement (Microphone positions MP2 in Cross Section 1 (Fig. 7.34), and MP6 or MP11 in Cross Section 2 (Fig. 7.35)). This relative approach will be used for validating the sound propagation model based on the parabolic equation (PE). The "Green's Function parabolic equation" method (see Section 5.4.1.4) was used, with a rotated reference frame to account for terrain undulations. The traffic intensity is assumed to be homogeneous over a sufficiently long stretch of the road near the receivers. A different traffic composition on the

road however influences the magnitude of the relative measurements: Each combination of vehicle type and vehicle speed results in a typical source spectrum. To account for this, the spread in sound pressure level caused by different vehicle types, driving at typical velocities, will be predicted.

As a result, there is an important spread in the measurements. First, traffic composition and vehicle speed may differ from minute to minute and is not known. Another reason is that atmospheric absorption changes over time. Since an average (clustered) air temperature profile is used, part of the variation could come from a different refractive state of the atmosphere within each cluster as well. The first two causes of variance are accounted for in the predictions, the last one is not for reasons of computational cost. To have statistically stable results, a criterion was set, demanding that at least 50 one-minute measurements are present in a cluster. Only results of such complete clusters are compared to calculations. This largely limited the number of possible comparisons between measurements and simulations, but was necessary to draw statistically sound conclusions.

Studying specific influences

Measurements are indicated by the boxplots in Figs. 7.36 and 7.37. Different sets of predicted relative noise levels are included as well in these Figures. The first set is the best available prediction, indicated by the blue symbols. An important advantage of performing simulations is the possibility of gaining understanding of the importance of the different factors involved. Additional calculations were performed to study the effect of terrain elevation and temperature profiles. Firstly, a homogeneous atmosphere was assumed in the presence of the actual relief. Secondly, a flat terrain is assumed in a homogeneous atmosphere. All other numerical and geometrical parameters remained unchanged.

A vertically isothermal atmosphere means that there are no vertical gradients in the temperature. As a result, temperature stays constant with height. The presence of gradients in temperature causes refraction of sound. Refraction can be directed upward or downward. For more details on this, the reader is referred to Section 5.2.2.

Results

The agreement between measurements and numerical predictions is adequate (see Figs. 7.36, 7.37 and 7.38). The average of the calculations lies close to the median of the measurements. Differences range up to 2 – 3 dB(A) in most situations.

To explain the measurements, some general aspects concerning sound propagation need to be considered, as discussed in Section 5.2.2.

Effects of snow cover

For receivers on the slopes, at sufficient height above the valley floor, direct sound is often the most important sound path. Interaction with ground reflected waves is often missing or less important than it is for flat ground propagation. For the receivers in the valley (the reference receivers used in our study), ground effect plays an important role.

The ground characteristcs are largely changed if the the ground is covered with snow. Snow has a typical value of 30 kPa s/m^2, while grassland has a value of 200 kPa s/m^2. The smaller the value, the better the sound waves can penetrate into the material. Air penetration in a material is essential for sound absorption.

Upslope receivers are hardly affected by ground. For the reference receivers, ground type is important, but propagation distances are too limited to see a significant effect. Since snow is a softer ground, the relative measurements above snow are much smaller than above grass. Long distance propagation over a very soft ground results in low levels at distant receivers. For the best available predictions, ground type is not important, and as a result, the difference between measurements (and simulations) with and without snow cover is limited.

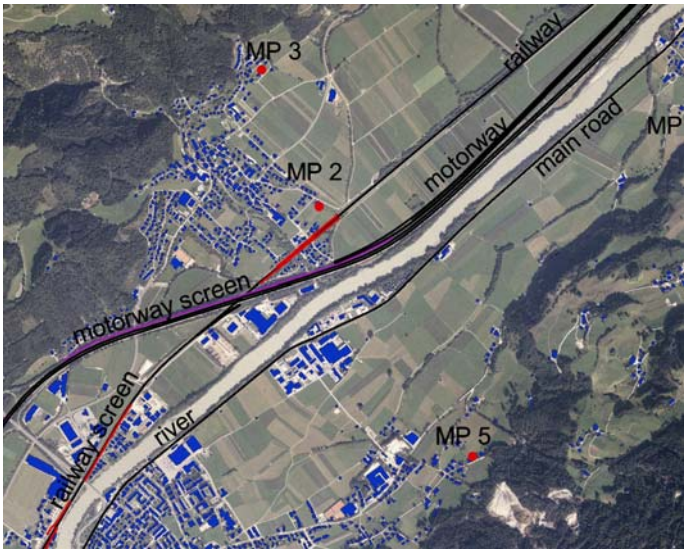

Fig. 7.34 Orthophoto of cross-section 1. Microphone position MP2 is taken as a reference. Photo credit: TIRIS

Inhomogeneous atmosphere

An inhomogeneous atmosphere results either in a decrease (see cross section 1, Fig. 7.34) or an increase (most cases in cross-section 2; Fig. 7.35) of the relative sound pressure level. Effects are in the range -3 dB(A) to 10 dB(A). For cross-section 2, a variety of temperature profiles occur, with upward and downward refracting parts. Nevertheless, these all tend to decrease the difference between reference and distant receivers. Qualitative analysis of what is happening is difficult because of the complex interaction of the mechanisms involved. Certainly, cross-section 2 is complicated. The terrain profile leading to microphone position MP24 is complex, and is characterized by a sudden increase in the elevation of the ground, close to the receiver. The ground profile also contains successions of pronounced concave and convex parts. The situation is further complicated because microphone MP 6 was placed on the roof of a building. This receiver was (slightly)

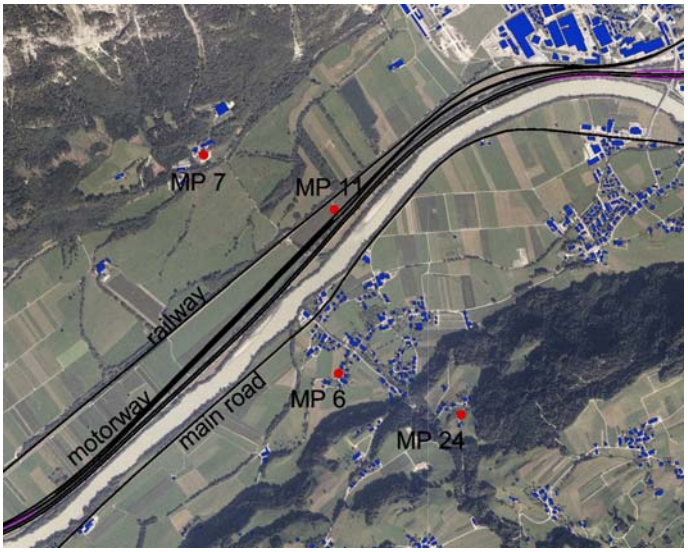

Fig. 7.35 Orthophoto of cross-section 2. During the summer measurements, microphone position MP7 is not used anymore and it is replaced by MP11. During winter, MP6 is taken as the reference. During summer, MP 11 is taken as the reference. Photo credit: TIRIS.

shielded by the edge of the roof, and this intensifies differences in sound pressure level by the different states of the atmosphere. In contrast to a situation with direct sound, the contribution caused by atmospheric refraction, although small, results in an important increase in the sound pressure level. The numerical model nevertheless manages to produce sufficiently accurate results.

MP11 is taken as a reference in the cross-section 2. As a result, the effect of the upward refracting atmosphere becomes very limited. This can be explained by the fact that this receiver is very close to the road, so refraction does not play a role. The (elevated) receivers far away are mainly determined by direct sound (see previous paragraphs). It is known that is such cases, refraction is not important either.

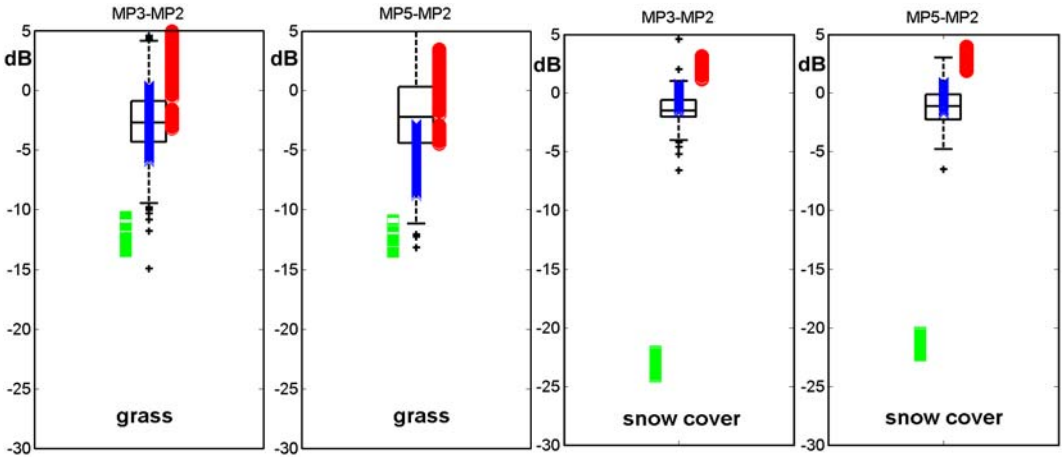

Fig 7.36 Measurements (indicated by black boxplots) and numerical predictions for the cross-section 1 (blue crosses: actual terrain and inhomogeneous atmosphere; red circles: actual terrain and homogeneous atmosphere; green squares: flat terrain and homogeneous atmosphere) for grass and snow covered ground.

7.1.5.2 Combined evaluation of air pollution and noise

Synchronous measurements of the pollution and noise in the Inn valley cross section near Schwaz were carried out during the 7-day period from Thursday 19 Jan 2006 (16 CET) to Thursday 26 Jan 2006 (13 CET). This enables a combined evaluation of both environmental nuisances together with the meteorological situation and the emission condition.

Meteorology, air pollution and noise were measured on the valley bottom (meteorology and air pollution at Schwaz, noise at Vomperbach) and on the south-eastern slope of the Inn valley at Arzberg. The station Schwaz is situated near the southwestern outskirts of Schwaz about 750 m south-east of the A12 motorway. The position of the noise measurement station Vomperbach is about 1500 m southwest of the station Schwaz and about 400 m away from the A12 motorway. The slope station Arzberg is located at 720 m ASL (180 m above the valley bottom) on the southern slope. The closest horizontal distance between the station Arzberg and the A12 motorway amounts to 1690 m. More information about the stations is given in Section 7.1.1. Although the motorway A12 is the most important emitter in the area, all stations were also exposed to extraneous emissions from some local traffic and nearby operating machinery. The measurements at Vomperbach were additionally affected by the noise of trains passing by at a distance of about 150 m away.

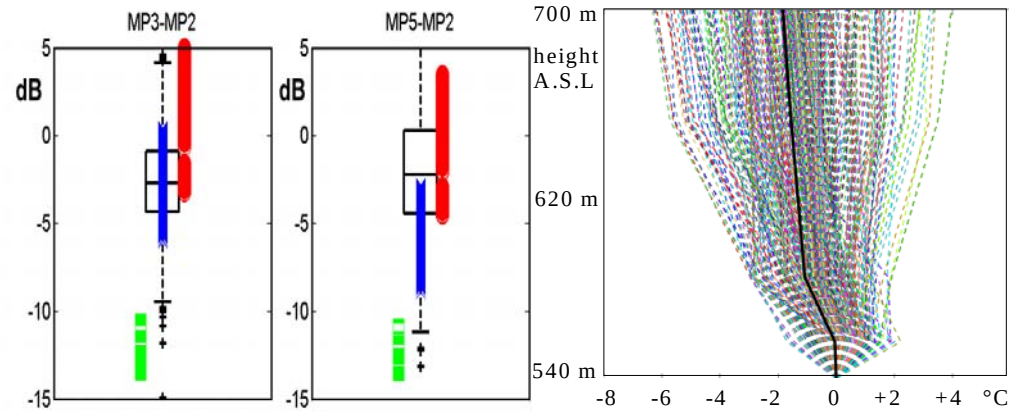

Fig 7.37 Measurements (indicated by black boxplots) and numerical predictions for the cross-section 1(blue crosses: actual terrain and inhomogeneous atmosphere; red circles: actual terrain + homogeneous atmosphere; green squares: flat terrain and homogeneous atmosphere). On the right, the corresponding temperature profile cluster is shown, relative to the temperature at the lowest sensor, with the average profile in the full black lines. Shown are the cases without snow cover.

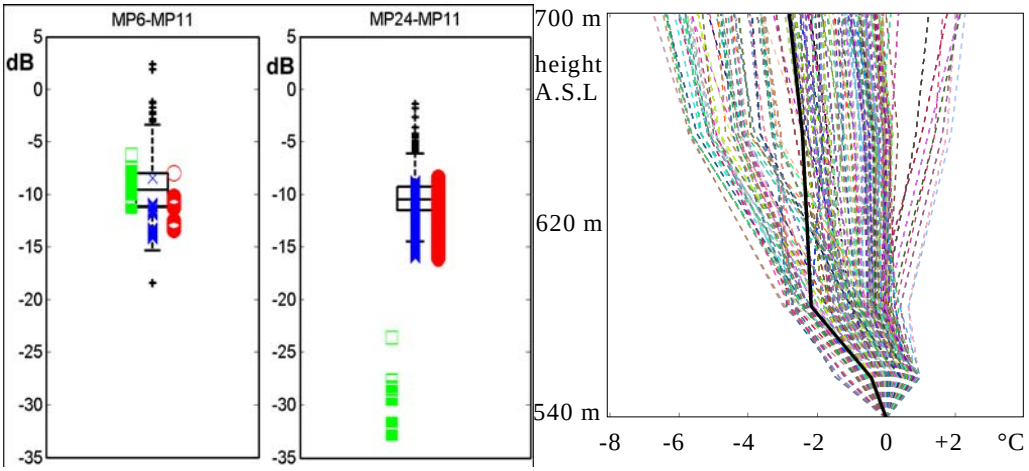

Fig. 7.38 Measurements (indicated by black boxplots) and numerical predictions for cross-section 2 (blue crosses: actual terrain and inhomogeneous atmosphere; red circles: actual terrain + homogeneous atmosphere; green squares: flat terrain + homogeneous atmosphere). On the right, the corresponding temperature profile cluster is shown, relative to the temperature at the lowest sensor, with the average profile in the full black lines. Shown are cases without snow cover.

The weather of the first part of the period considered was influenced by a weak low-pressure activity with a northerly to westerly large-scale flow while from 24 Jan 2006 on a high-pressure ridge was dominating the weather in the area. The development of autochthonous wind systems was largely suppressed during most of the time under consideration. Indications for such circulations are only found on 25 Jan 2006.

Air pollution and noise exposure depend on the respective emissions and transmission conditions. The latter are largely determined by meteorological parameters (wind speed and direction, vertical temperature profile, etc.) and the ground properties (e.g. vegetation, porosity). If the traffic flow

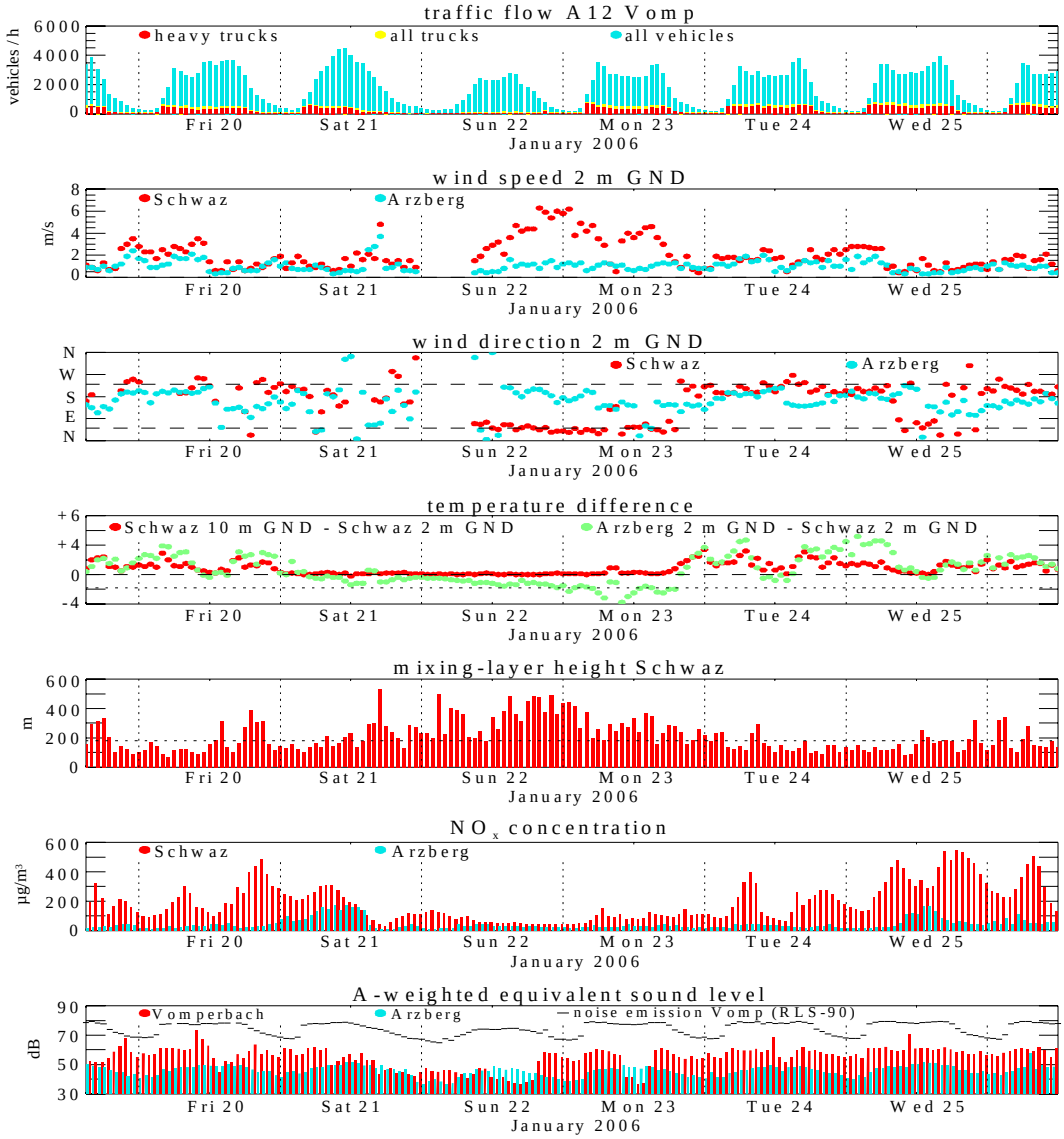

Fig. 7.39 Time series of (from top to bottom) traffic flow on the A12 motorway near Vomp, wind speed at 2 m GND at Schwaz and Arzberg, wind direction at 2 m GND at Schwaz and Arzberg (the broken lines indicate the direction of the Inn valley), temperature difference between Arzberg and Schwaz (the dotted line corresponds to a lapse rate of 1 °C per 100 m), mixing-layer height above Schwaz (the dotted line indicates the altitude of Arzberg), NOx concentration at Schwaz and Arzberg, A-weighted energy-equivalent sound levels at Vomperbach and Arzberg (the black curve shows the emission noise level 25 m away from the A12 motorway as calculated according to the German RLS-90 standard for road noise). All parameters are 1-hour average values.

doubles under the same transmission conditions the concentration of air pollutants doubles and the noise level increases by 3 dB (= doubling of the sound intensity). The transmission conditions that are favourable for high levels of air pollution are normally also favourable to noise levels and vice versa. A major difference between air pollution and noise consists is the fact that the transmission speed of air pollutants is in the order of the mean wind velocity (1 – 10 m/s), while the transmission speed of noise is determined by the much higher speed of sound in air (310 – 340 m/s). Therefore, air pollutants can accumulate while noise energy cannot. Hence, the local pollutant concentration is often the consequence of a long (up to severaly days) history of emission and transmission conditions, above all in weak wind situations. On the contrary, the actual noise exposure is exclusively determined by the emission and transmission during the last few seconds.

The temporal evolution of a greater selection of relevant parameters is shown in Fig. 7.39. The top panel of the figures shows the traffic flow on the A12 motorway (ASFINAG traffic counting station Vomp). The usual weekday peak of commuter traffic in the morning and evening hours are evident. On Saturday and Sunday the traffic flow is rather different from the weekdays. On Sunday the traffic is significantly reduced and trucks are almost completely banned from the motorway. A night-time ban on trucks of more than 7.5 t is effective between 20 CET and 05 CET on all days.

In the following panels of Fig. 7.39 the time series of some meteorological parameters which control the transport of air pollutants and the propagation of noise through the atmosphere are shown. The wind speed and direction at Schwaz is rather variable. High wind speeds (up to 6 m/s at 2 m AGL, up to 8 m/s at 10 m AGL) were observed on 22 and 23 Jan 2006 with the advection of cold air into the Inn valley. During this episode the wind at Schwaz blows parallel to the valley axis from the northeast. Weak winds occurred from 20 Jan at noon to 22 Jan 2006 in the morning and after the morning hours of 25 Jan 2006. At Arzberg the wind speed is generally low (< 3 m/s at 2 m AGL) and blows from the south-east, i.e. in a downslope direction, or south-west, i.e. in a down valley direction. Only on 25 Jan 2006, the behaviour of the wind at Schwaz shows the typical pattern of a thermally induced mountain-valley circulation with southwesterly down-valley flow during the night and the morning hours and northeasterly up-valley flow during the afternoon and evening. The slope wind circulation at Arzberg is not well developed.

The mean temperature stratification of the lowest 180 m thick layer of the valley, indicated by the temperature difference between Arzberg and Schwaz (positive values: inversion, i. e. elevated slope position warmer than valley bottom), does not show a diurnal variation from 21 until 22 Jan 2006. During the strong wind episode on 22 and 23 Jan the air layer between Schwaz and Arzberg is well-mixed and the temperature difference between both stations sporadically exceeds 1.8 °C, which corresponds to the dry adiabatic lapse rate. The mixing-layer depth (derived from Sodar measurements at Schwaz; see Sections 3.2.2.3 and 7.1.3.5) is consequently high (> 300 m). In the remaining of the 7-day period, the air at the elevated slope station Arzberg is warmer than air down in the valley bottom at Schwaz, i.e. a temperature inversion exists. Only around noon on 20, 24, and 25 Jan the air at Arzberg is slightly colder than at Schwaz (also during the whole of 22 – 23 Jan 2006).

However, the temperature difference is smaller than for a well-mixed layer between the levels of both stations (-1.8 °C). This is corroborated by the mixing-layer height which hardly extends up to the altitude of the “Arzberg” station (180 m) at these times.

The two lowest panels of Fig. 7.39 show the temporal behaviour of the concentration of NO_x and the A-weighted sound level. Both parameters are used here as representative indicators of the air quality and the noise burden.

The NO_x concentrations show low values throughout the period of strong winds and enhanced mixing (deep mixing layer and negative temperature difference between Arzberg and Schwaz). At Arzberg considerable NO_x concentrations were observed during only two episodes on 21 and 25 Jan 2006. In both cases the wind speed is rather low while the vertical mixing only became efficient at noon. Both episodes follow an accumulation phase in the valley bottom during the morning hours. On 25 Jan the upward mixing led to a corresponding decrease of the concentration in the valley due to the enhanced mixing volume, which cannot be explained by the slight reduction of traffic during midday.

The time series of the noise levels shows a few short periods for which the level at the elevated slope station Arzberg (1690 m away from the A12) is higher than the level at the station Vomperbach at the valley bottom (400 m away from the A12). These periods coincide with a temperature decrease with height and correspondingly adverse propagation conditions (upward refraction). This has an attenuation effect for nearly horizontal propagation from the motorway along the valley bottom towards Vomperbach, while the slantwise propagation up to the slope station Arzberg is much less affected. Therefore the noise level at Arzberg more or less follows the variations of the emission noise level.

The NO_x concentration and the sound level at Schwaz/Vomperbach and Arzberg are shown as scatter plots in Fig. 7.40. In this figures, the mixing-layer height and temperature difference between Arzberg and Schwaz are colour-coded. The figures suggest a certain relationship between air pollution and noise. All events with low noise levels (< 50 dB at Vomperbach, < 45 dB in Arzberg) are associated with low NO_x concentrations at Schwaz and Arzberg, respectively. Vice versa, all high NO_x pollution events (> 200 µg/m^3 at Schwaz and > 100 µg/m^3 at Arzberg) occur in combination with high noise levels at Vomperbach and Arzberg. This behaviour is caused by meteorological effects to some extend which are either favourable or adverse for both air pollution transport and noise propagation. A strong influence is exerted by the temperature stratification. If the temperature decreases with height (negative difference between the temperatures at Arzberg and Schwaz), the probability for low concentra-

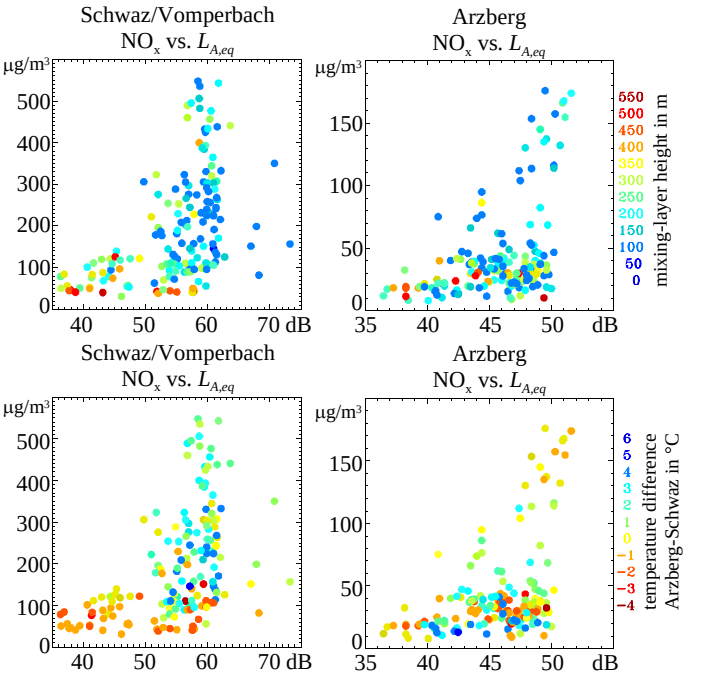

Fig. 7.40 Scatter plots of the NOx concentration (in µg/m^3) vs. the A-weighted energy-equivalent noise level ($L_{A,eq}$ in dB) at Schwaz/Vomperbach (left panels) and Arzberg (right panels). The mixing-layer height (in m) above Schwaz (upper panels) and the temperature difference (in °C) between Arzberg and Schwaz (lower panels) are colour-coded. All parameters are 1-hour average values.

tions and low noise levels at the valley bottom is high. Low concentrations at Schwaz are also associated with a deep mixing layer. However, the mixing-layer depth has no influence on the noise level. At the slope location of Arzberg (180 m above the valley bottom) the relationship between concentration and noise level is still present, but the relationship with the selected meteorological parameters is weak.

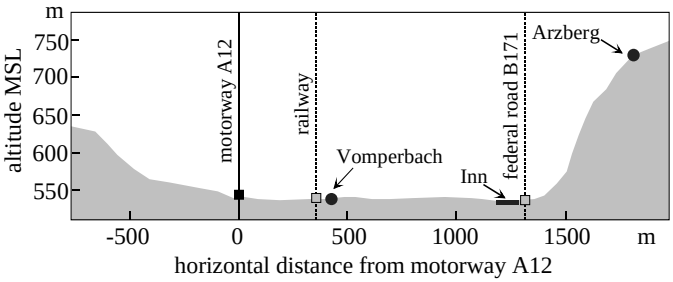

Fig. 7.41 Cross-section through the Inn valley near Schwaz with the positions of the noise measurement points Vomperbach and Arzberg and the major noise sources, i.e. the motorway A12, the ÖBB railway line and the federal highway (B171).

7.1.5.3 Noise propagation in the valley cross-section south of Schwaz

The noise level measured at a given measurement point, at a given time is determined by (1) the actual noise emission and (2) the actual propagation condition. The latter depends on the meteorological and ground conditions (see Section 5.2.2). Noise emissions of the contributing sources are not exactly known. Therefore, it is principally not possible to isolate the propagation effect.

In the following, the evaluation is focused on overlapping noise measurements at the temporary noise monitoring stations Vomperbach (valley bottom, 540 m ASL) and Arzberg (slope, 740 m ASL) from 19 Jan 2006 (16 CET) to 26 Jan 2006 (14 CET) and the wind and temperature measurements of the automatic weather stations of the University of Innsbruck at Schwaz (10 m mast) and Arzberg (2 m mast). The meteorological station Schwaz was located on the bottom of the valley at an altitude of 540 m ASL. It is equipped with a 10 m high mast with sensors mounted at 2, 5, and 10 m above ground. The meteorological station Arzberg was situated close to the noise station Arzberg on the slope at an altitude of 720 m ASL, this is 180 m above the valley-bottom. The terrain profile and the location of the major sources of noise and the noise measurement points are provided in Fig. 7.41.

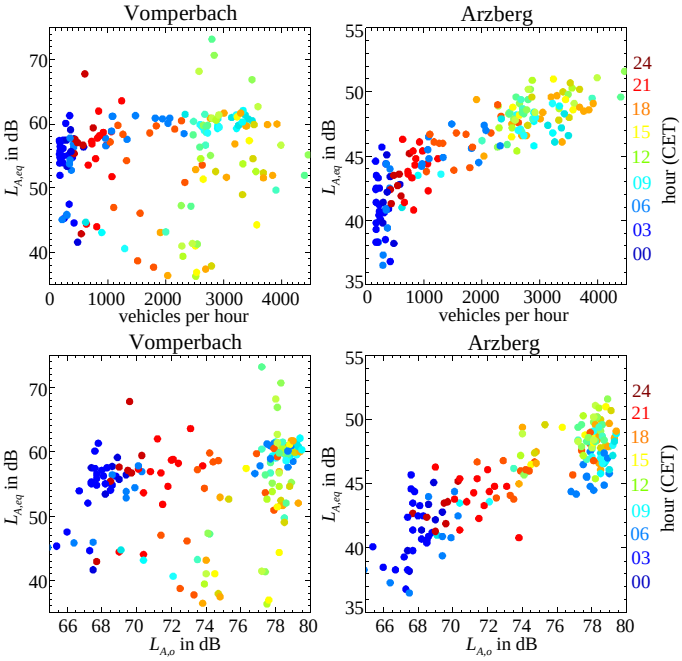

Fig. 7.42 Hourly 1-hour A-weighted average energy-equivalent noise levels $L_{A,eq}$ at Vomperbach and Arzberg versus the A12 traffic flow at Vomp (top) and the noise emission level $L_{A,o}$ according to RLS-90 based on the traffic flow at Vomp. The hour (CET) is colour-coded.

Fig. 7.42 shows the measured noise levels at Vomperbach and Arzberg (hourly A-weighted 1-hour average levels $L_{A,eq}$) as functions of the traffic flow at the motorway A12 counting station Vomp and the noise emission level (A-weighted noise level at a standard distance of 25 from the motorway). The latter was derived from the traffic counts and the fleet composition (passenger cars, trucks) according to the German standard procedure for road traffic noise RLS-90. The figure shows that the measured sound level at Vomperbach is rather independent of the traffic flow on the 400 m distant motorway, while at Arzberg (1680 m distance from the A12 motorway) a rather clear correlation is indicated. The reason for this behavior is twofold: Firstly, propagation from the motorway to Vomperbach (valley bottom) follows the ground and is therefore greatly influenced by the ground (reflection) and meteorological effects (refraction) while the propagation from the motorway to the elevated slope station Arzberg crosses a rather deep atmospheric layer and is no longer quasi-parallel to the ground surface such that propagation effects do not vary much with time. Secondly, both stations are exposed to extraneous noise from unknown noise sources (railway noise, local traffic, machinery, animals, etc.). However, in the following is it assumed that the motorway is the dominant source of noise at both stations.

Fig. 7.43 shows that the noise level at Vomperbach quite clearly depends on the mean vertical gradient of the effective sound speed between 2 and 10 m AGL. The mean vertical gradient of the effective sound speed is the decisive meteorological parameter which controls the refraction of sound in the atmosphere due to the vertical gradient of the sound speed relative to the air and the horizontal wind component in the direction of sound propagation (see Section 5.2.2). The gradient of the effective sound speed was derived for each hour from the temperature and wind measurements at the meteo station Schwaz between 2 and 10 m AGL. The direction of sound propagation was assumed to be from 293° (WNW) to 113° (ESE) which is about the direction of the closest connection between the motorway and the station Vomperbach.

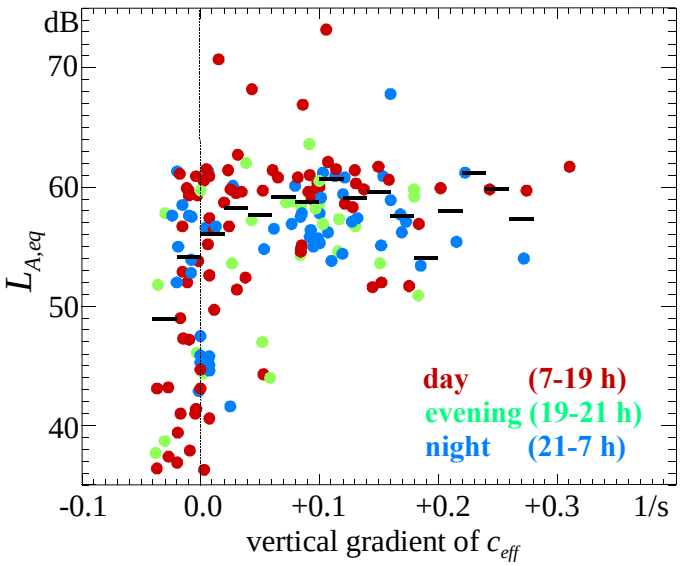

Fig. 7.43 Measured A-weighted 1-hour L_{eq} values at Vomperbach as a function of the mean vertical gradient of the effective sound speed c_{eff} between 2 and 10 m above ground. The colours refer to the day time as indicated. The black bars are average levels for 0.2 1/s wide intervals of the vertical gradient of the effective sound speed.

The sound level at Vomperbach is significantly reduced in cases with a negative gradient of the effective speed of sound. In these situations the station Vomperbach lays in the acoustical shadow zone which is caused by the upward refraction of sound waves. This is due to the vertical temperature lapse (negative gradient) and/or propagation against the wind. Under these circumstances sound energy can only arrive by diffraction or scattering at turbulent eddies in the atmosphere (for details of the sound propagation we refer to Section 5.2.2). Since most cases with low levels are

observed during the day and although the traffic flow is rather strong at this time of the day, the temperature effect seems to be dominant.

Two-dimensional simulations with the Lagrange-type sound particle model (Heimann and Groß, 1999; see Section 5.4.1.5) were performed to investigate the situation in the cross-section south of Schwaz. The terrain elevation along a cross-section perpendicular to the motorway was derived from digital elevation model data and interpolated to intervals of 5 m.

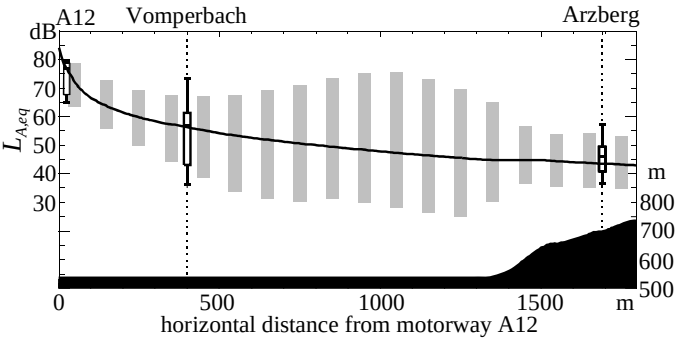

Fig. 7.44 Variability (grey bars) of the simulated A-weighted sound levels at a receiver height of 2.5 m above ground according to the variations of the traffic emission, the mean vertical temperature gradient (-1 to +2 °C per 100 m), and the ground property (grass, snow). The black curve is the result of the ISO 9613-2 standard noise prediction. The box and whisker plots indicate the variability of the noise emission level at 25 m distance from the A12 motorway and the noise measurements at Vomperbach and Arzberg.

A set of simulations was performed for three different vertical temperature gradients: 0 °C/m (isothermal atmosphere – no refraction), +0.02 °C/m (temperature inversion – downward refraction), -0.01 °C/m (temperature lapse – upward refraction). Wind was not considered in this set of simulations. In addition, two types of ground were considered: grass-covered ground (flow resistivity = 300 kPa s m^{-3}) and snow-covered ground (flow resistivity = 30 kPa s m^{-3}).

The line source (motorway) was set to a height of 4.5 m above the valley-bottom in order to account for the embankment. In each simulation 12,000 sound particles were released at the source point with elevation angles from -20° to +20°. The source is assumed to emit a spectrum typical of road traffic. All 1/3 octave band centre frequencies from 10 Hz to 20 kHz were considered. Since the noise emission level does not affect the transmission an arbitrary sound power was assumed. The simulation results were calibrated with the noise emission levels at a distance of 25 m from the motorway as it was calculated from the traffic flow data with the help of the RLS-90 standard procedure. Other sources of noise were disregarded.

The results of all simulations are presented in Fig. 7.44 as functions of the distance from the motorway source (averaged in 100 m intervals). Variability of the simulated noise levels results from the variability in the noise emission data (because of the time-dependent traffic flow), the assumed temperature gradients which cause different refraction, and the two ground types considered which control the ground effect. For comparison, the variability of the noise emission level and measured noise levels at Vomperbach and Arzberg are also indicated. In addition, the result of a standard noise prediction (ISO 9613-2, see Section 5.1.3.4) is plotted in the figure. The latter was calibrated to meet the median of the noise emission levels near the motorway.

The simulated variability of the sound level increases with growing distance from the source (motorway). This is caused by the meteorologically induced refraction effects on the near-ground sound propagation. Of course, the three considered meteorological conditions and the two ground types do not reflect the full variability of possible meteorological and ground effects. Highest noise levels are simulated at a distance of approx. 1000 m from the motorway. This is a consequence of multiple reflections on the ground under the condition of downward refraction in the case of a

temperature inversion. Above the slope the variability is significantly reduced. Here the sound does not propagate along the ground anymore but crosses the valley atmosphere so that ground and refraction effects become less important. The remaining variability is mainly caused by variability of the noise emission. Simulated behaviour of the variability and the values of the levels match observations at Vomperbach and Arzberg quite well. The (black) curve of the ISO 9613-2 standard noise prediction result matches the median of noise levels at Vomperbach quite well. At Arzberg however, the median is underestimated by about 3 dB.

7.1.6 Effects on health and well-being from traffic exposure combinations

In most real-world situations traffic exposure involves more than one source and a variety of specific exposures (air pollution, noise, vibrations, visual intrusions) are occurring at the same time. Tab. 7.5 shows some of the potential combinations of critical importance.

Tab. 7.5 Basic traffic exposure combinations in transportation.

noise / sound	vibration	air pollution	context
road	+	+ +	+
rail	+ +	+	+
aircraft	+	+	+
special *	+ +	+	+

* low frequency noise and impulse noise
\+ possible modifier of effect
\+ + important modifier of effect

Typically, this complexity is not sufficiently investigated nor reflected in environmental health assessments. In EHIA, the cumulative assessment has largely been neglected and interactions are mainly dealt with in a qualitative manner (Burris and Canter, 1997, Cooper and Sheate, 2002), although the combined or cumulative assessment is required in EIA (CEC 1985, 1997, Cooper and Sheate, 2002).

The standard practice to assess the community response to traffic separate by source and type of exposure runs the risk of getting an incomplete picture of the overall burden of the concerned communities. Incompleteness of the exposure inventory is usually exacerbated by the omission of subjective information about the perceived effects of exposure at the population level. The side effects of incomplete assessments are often population mistrust or even charges of misfeasance due to the incompetence of the responsible authorities. This can further lead to additional costly investigations or even litigations (Staples 1997). In the following paragraphs some demonstrations of combined assessments within the health study are outlined.

7.1.6.1 The effect of exposure to combined noise sources on annoyance

Although increasing consideration has been given to the effects of noise from combined traffic sources at conferences during the last decade the scientific community still lacks a full understanding of this issue. Therefore, it is not surprising that in current practice the community response to noise is assessed source by source, although proposals to handle mixed source assessment are available (Vos, 1992; Botteldooren and Verkeyn, 2003; Miedema, 2004; Schomer, 2005). It is tacitly assumed that the single standard exposure-response curves are also appropriate for mixed exposures. Theoretically, one would expect deviations in reactions in both directions, depending

on the nature of the source. A continuous source (like a motorway) could mask other sources if some of the frequency ranges overlap. On the other hand, there are good reasons to assume that an intermittent source (such as rail or aircraft) which has a different frequency spectrum, additional tonal components, vibrations or non-acoustical features (e.g. air pollution) may increase the reactions of the concerned population due to additional interfering sensory information input.

Railway noise exposure-annoyance by motorway sound exposure

Exposure-annoyance curves for railway are shown by three levels of motorway exposure (Fig. 7.45, left) or by four difference levels between rail and motorway (Fig. 7.45, right). Around 60 dB(A), L_{den} rail noise exposure annoyance lines cross: higher rail exposure is more annoying when road exposure is low. The lowest exposure-annoyance curves result when the difference between rail and motorway noise exposure is between 0 and 6 dB(A). When motorway noise is larger, i.e. difference ≤ 0 dB(A), a parallel shift to overall greater annoyance is observed. When rail dominates by more than 6 dB(A) the curve starts with lower annoyance but exceeds the motorway annoyance curve at higher rail sound levels.

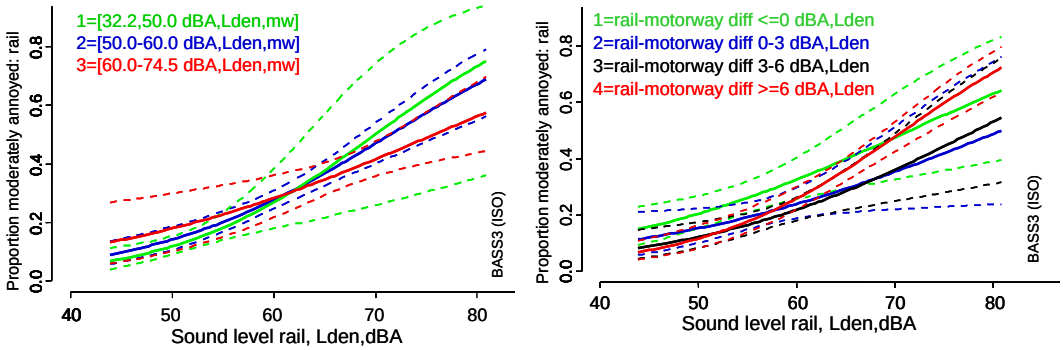

Fig. 7.45 Exposure-annoyance curves for railway noise by 3 levels of motorway (mw) exposure (left) or by 4 levels of difference between rail and motorway (right).

Railway noise exposure-annoyance by distance: overall combined assessment

Since we have shown earlier that exposure response curves in alpine areas deviate from the END-curves (Lercher, 1998) we also tested the exposure-annoyance relationships by distance and adjusted for the presence of the other sources (motorway or main road exposure). Whereas no difference in annoyance can be observed within 300 m of the rail track when an additional road source is present, there is a significant upward trend in annoyance when another noise source is present beyond 300 m (Fig. 7.46).

Railway noise exposure-annoyance by distance: combined assessment by type of source

Following up on the results reported in Fig. 7.47 we specifically tested for the situation of the combined road noise exposure beyond 300 m from the rail. In both cases (Fig. 7.47) you can observe a higher exposure-annoyance curve when road sources show lower exposure levels and less annoyance when road sources are louder.

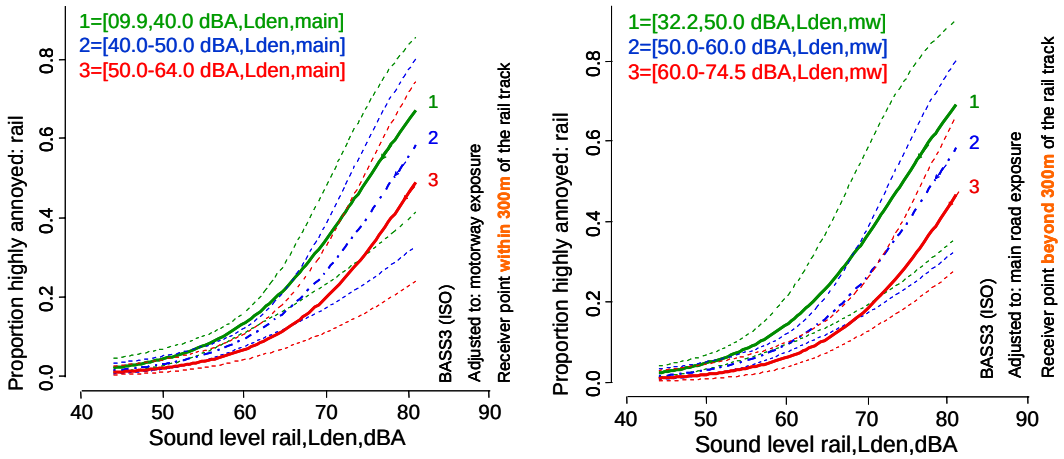

Fig. 7.46 Exposure-annoyance curves for railway noise in the presence of other sources of road noise near (within 300 m, left) and far (beyond 300 m, right) from the rail track.

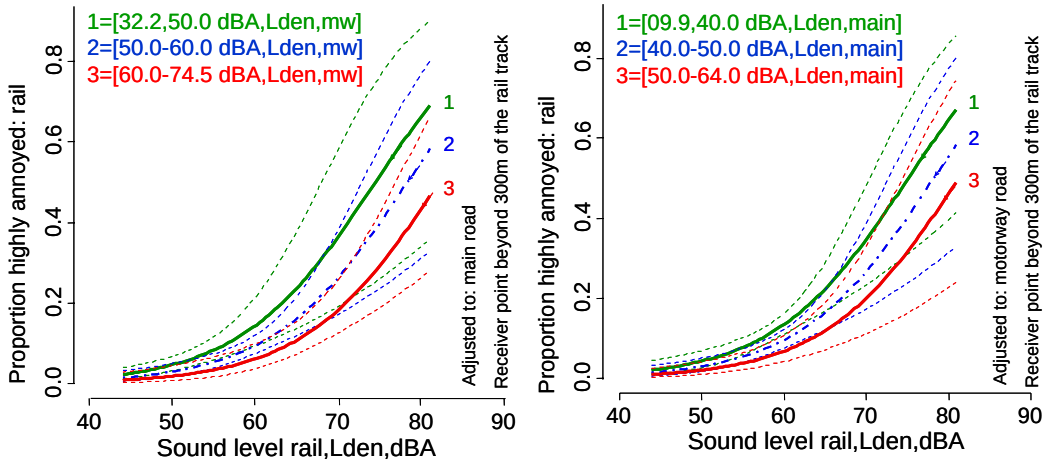

Fig. 7.47 Exposure-annoyance curves for railway noise by 3 levels of additional road noise exposure (main road, left and motorway, right): receiver point beyond 300 m of the rail track

7.1.6.2 The effect of combined exposure to noise and traffic pollution on annoyance

It is well recognized in the scientific community that the (psycho-social and physiological) reaction toward noise is modified by features of the noise itself, but also by other accompanying factors of the traffic exposure pattern. Wanner et al. (1977) and Hangartner (1987) were among the first to report correlations between noise and air pollution related annoyance frequency (0.78 and 0.81). Haider et al. (1990), quoting a study from Wien from 1984, showed even higher correlations (noise and exhaust gases: 0.90, noise and dust/particles: 0.97). The correlations can substantially differ, however. Due to regional and yearly differences in climate or wind direction background air pollution or noise levels may vary between towns and years. This means that correlations beetween noise and air pollution indicators become smaller in multi-site or multi-year studies than in single site – one-shot studies. For instance, in the Oslo multi-site and multi-year studies a correla-

tion of 0.50 was reported between yearly average indicators of NO_2, PM10, PM2,5 and L_{den} (Klæboe, 2000). Correlations are highest for yearly average air pollution indicators, and substantially lower for indicators of air pollution episodes where variability may be high and reliability of calculations or representativity of measurements may be low.

Thus, effects may simply surface due to the high intercorrelation between these factors, but may also being triggered by true interaction (one factor sensitizes individuals towards the other factor). However, the biological basis of these interactions is often poorly understood.

It has been shown in some studies, however, that accompanying factors of vehicular or rail traffic such as air pollution and vibrations may substantially modify the noise annoyance ratings (Sato 1988, 1994; Howarth and Griffin, 1991; Zeichart et al., 1994; Öhrström et al., 1996, 1997; Klæboe, 1998; Passchier-Vermeer, 1998; Passchier-Vermeer and Zeichart, 1998; Zeichart, 1998; Lercher et al., 1999; Klæboe et al., 2000; Klæboe et al., 2003; Yano et al., 2005; Yokoshima and Tamura, 2005; Yokoshima and Tamura, 2006; Lercher, 2007b; Öhrström et al., 2007). It is currently hypothesised that combined exposures tax or may exceed common human coping resources and that additional stressors lead more rapidly to the depletion of these resources (Lepore and Evans, 1996).

The effect of combined exposure to noise and vibration on annoyance

Some studies have dealt with the effect on annoyance by a combination of noise and vibrations in a laboratory context (e.g. Meloni and Krüger, 1990; Howarth and Griffin, 1991; Paulsen and Kastka, 1995). Larger field studies have been carried out in Austria, Germany, Japan, Sweden, and Norway (Sato, 1988, 1994; Öhrström et al., 1996, 1997, 2007; Knall, 1996; Zeichart, 1998; Passchier-Vermeer and Zeichart, 1998; Lercher et al., 1999; Yano et al., 2005; Yokoshima and Tamura, 2005; Yano et al., 2006; Ota et al, 2006).

Similar to the analyses carried out nearly 10 years ago (Lercher et al., 1999) the MUI health study found strong moderation between the annoyance response to railway noise and accompanying annoyance due to railway vibrations. However, it is not possible to fully separate the modifying impact of vibrations from individual sensitivity to noise and vibrations in these relationships. Since sensitive persons will typically be overrepresented in the vibration annoyance category.

We also saw a modfiying effect of perceived vibrations from road traffic on motorway and main road annoyance. A stronger effect is observed with main road annoyance – this is consistent with the fact that vibrations are often stronger due to the smaller distance of houses to the main road. The modifying effect starts at lower levels than for motorway noise

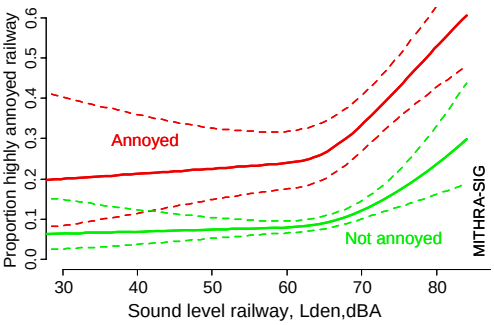

Fig. 7.48 Exposure-annoyance curves for railway noise by degree of annoyance from perceived vibration exposure.

The effect of combined exposure to noise and air pollution on annoyance

There are only three groups that have addressed this combination in major field studies (TOI, 1991; Clench-Aas et al., 1991; Lercher, 1992; Lercher et al., 1993; Lercher and Kofler, 1995; Lercher et al., 1999; Klæboe et al., 2000; Job and Hatfield, 2004).

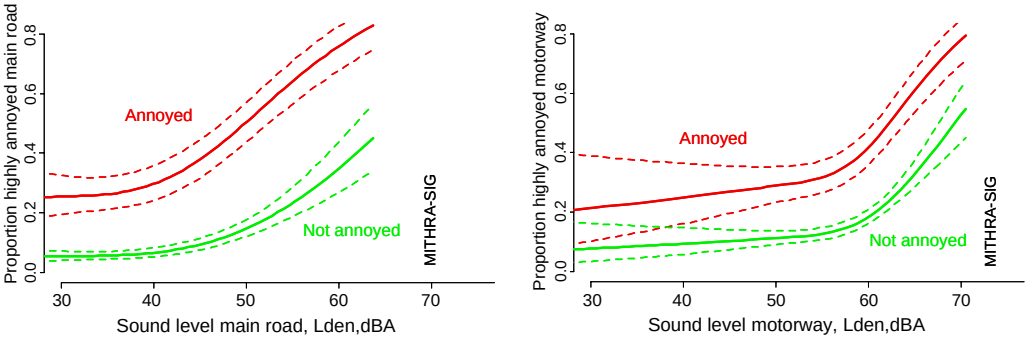

Fig. 7.49 Exposure-annoyance curves for main road (left) and motorway (right) noise by degree of annoyance from perceived vibration exposure.

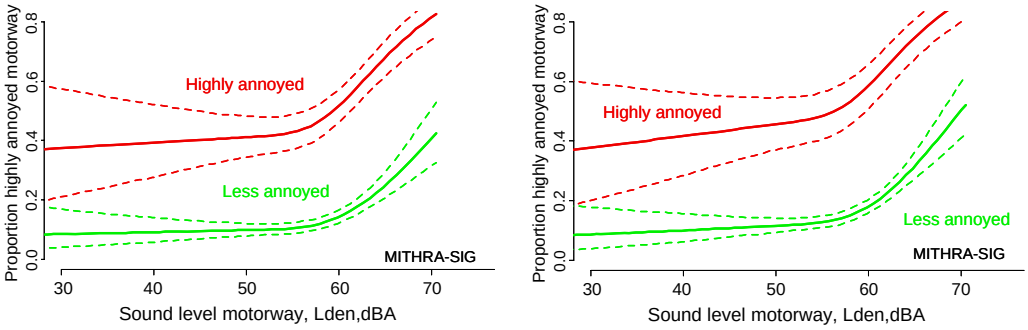

Fig. 7.50 Noise exposure-annoyance curves for motorway noise by degree of annoyance from perceived particles/soot exposure (left) and perceived traffic exhaust (right).

Similar to the analyses carried out nearly 10 years ago (Lercher et al., 1999) the Medical University of Innsbruck health study found strong moderation between the annoyance response to noise and air pollution with motorway and main road noise exposure (Figs. 7.50 and 7.51) in the target area. The modifying effect of perceived particle/exhaust exposure is larger at lower levels with motorway exposure than with main road exposure. However, overall, the modifying effect is larger at main road sites by contributing more to the explained variance (26 % vs. 13 %). Furthermore, the moderation through perceived air pollution is also stronger than the modifying effect of vibration (see Figs. 7.49 and 7.50).

There is also a modifying effect of perceived air pollution exposure on railway noise annoyance visible – although this effect is smaller than the perceived vibration effect (Fig. 7.52).

When the analysis combines perceived additional vibration and particle exposure the explained variance still increases somewhat (see Tab. 7.6). Residents living within a main road environment show a larger increase in explained variance than those living near railways and motorways.

From a health impact point of view it is of significance to note that people who are sensitive to one exposure are also often impacted by other exposures. From a methodological point of this view it means that it is necessary to deepen these analyses. However, such additional analyses carried out by Klæboe et al. (2000) indicate that the heightened response is indeed caused by an interaction effect.

Tab. 7.6 Cumulative increase in variance explanation with the combination of air and vibration exposure.

Source	Vibration	Particles	Exhaust gas	Vibration and Particles
Railway	12.02 %	11.29 %	9.27 %	14.98 %
Motorway	13.46 %	23.16 %	17.92 %	25.06 %
Main road	25.70 %	27.14 %	26.70 %	33.44%

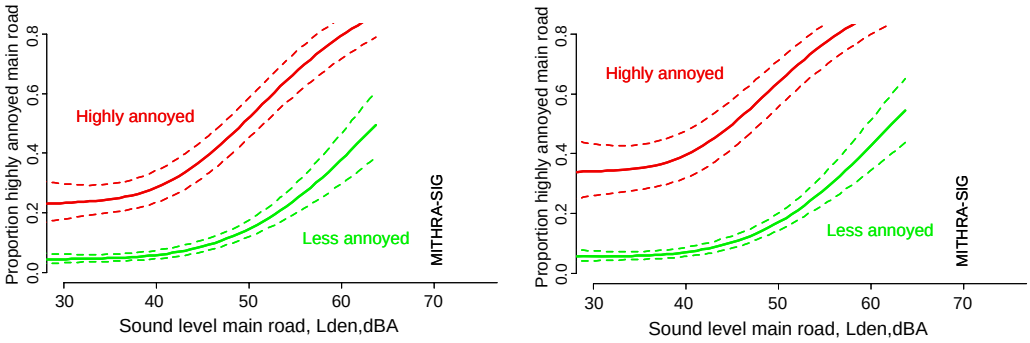

Fig. 7.51 Noise exposure-annoyance curves for main road noise by degree of annoyance from particles/soot exposure (left) and traffic exhaust (right).

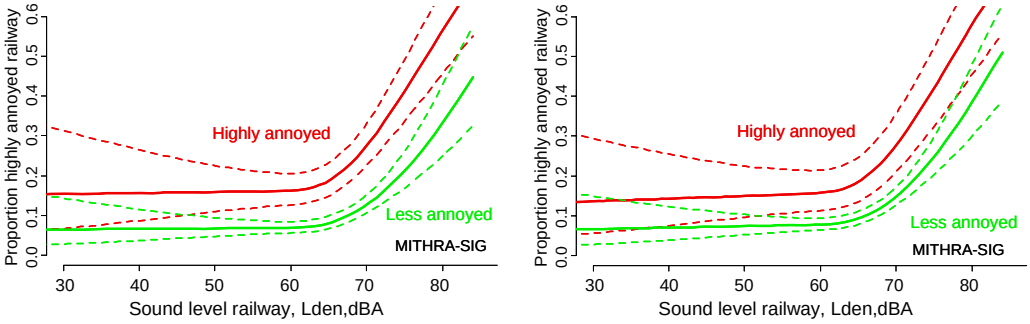

Fig. 7.52 Noise exposure-annoyance curves for railway noise by degree of annoyance from particles/soot exposure (left) and traffic exhaust (right).

7.2 Brenner Corridor: Adige/Etsch valley

A major part of the Brenner corridor crosses the Provinces of Trentino and Alto Adige/South Tyrol running along the Adige/Etsch valley, which connects the Po plain (with an inlet close to the city of Verona) to the basin of the city of Bolzano/Bozen and the Isarco/Eisack Valley towards the Brennero/Brenner Pass. Since the upper part of this route has already been the subject of many studies concerning the Brenner Basis Tunnel, the interest has been devoted to the lower part which crosses three different Provinces.

An intensive observing period (IOP) was designed for the beginning of 2006 and in the following the area and the experimental setup will be briefly described, along with the meteorological conditions, the results of the measurement campaigns and of the whole modelling chain.

7.2.1 General information

7.2.1.1 The Brenner-South transit route

Mountains are a major component of the regional landscape, with peaks reaching 3905 m ASL with an approximate average height around 1500 m ASL. Indeed, rather high mountain chains (around 1500 m with respect to the valley bottom) flank the Adige/Etsch Valley all along its course, characterizing a typical U-shaped valley. The characteristics displayed by the orography, the location of the main infrastructures and populated areas, motivated the rationale and planning of the measurement campaigns which are described below (see Section 7.2.1.2).

The Autobrennero-A22 motorway runs for more than 220 km, out of a total of 313 km, in the Italian Alpine region (source Autobrennero S.p.A.[3]). An important aspect of this route is that although travelling towards an alpine pass at an altitude of 1375 m ASL, the motorway maintains minimum slopes: only on the last stretch Vipiteno/Sterzing-Brennero/Brenner the slope reaches 3.8 %, but the average from Brennero/Brenner to Bolzano/Bozen is 1.4 % and even less in the lowest part of the route which appears almost horizontal. All these aspects have to be carefully taken into account when evaluating the emission factors of the different vehicle categories (see Section 2.2.1.1 and 2.5.2 for more details).

The motivations of the present project and the implemented investigations are supported by the fact that throughout the

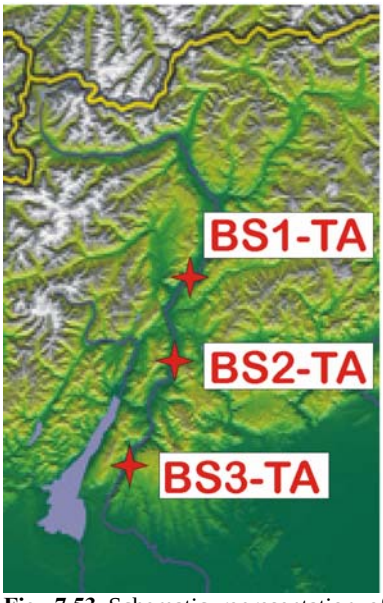

Fig. 7.53 Schematic representation of the three Target Areas (BS1-TA Salorno/Salurn; BS2-TA Aldeno; BS3-TA Rivalta) along the "Autobrennero-A22" motorway south of the Brennero/Brenner Pass.

[3] www.autobrennero.it

last few years, the Autobrennero-A22 motorway had to deal with a continuous increase in traffic, the heavy flow during the various seasons and traffic jams along the motorway. This trend follows the national average and highlights a problem which touches all of the cities in the Alpine arc.

7.2.1.2 Climatic situation of the Brenner-South target area during the IOP

As described in Section 3.2.3.2, the temporal representativeness of a short-period measurement campaign is of great relevance. Since the intensive observing period (IOP) covered the period 9 Jan – 13 Mar 2006 and was designed to sequentially investigate three different Target Areas (hereafter TAs) along the Brenner-South (BS) transit route for approximately 20 days (Fig. 7.53), it is important to briefly describe the overall meteorological conditions of this period.

January 2006 has been characterized by relatively stable weather with air temperatures below the mean values of the period 1978 – 2005, and precipitation values registered below the seasonal average for both periods 1961 – 1990 and 1978 – 2005: only the southernmost part of the region was affected by large amounts of precipitations due to its exposition to southerly flows. Events were particularly concentrated on the 27 – 28 Jan 2006 with intense snowfall also in the Adige valley.

February 2006 displayed two different regimes: relatively stable and fair weather in the first half and more variable in the second half. Temperatures have generally been lower than the average, but mountain stations registered higher values. With respect to the period 1978 – 2005 precipitations was greater during Feb 2006, even if the comparison with the period 1961 – 1990 displays a decrease of the total monthly amount.

March 2006 displayed substantially changing weather conditions, which typically sets the transition from winter to spring: temperatures were lower than the seasonal average again and especially during the first two decades of the month, and precipitations were mainly concentrated in few events even though their spatial distribution was highly inhomogeneous depending on the specific perturbation which crossed the region.

From the above description it may be stated that the IOP has been completed during a period of time which represents typical winter conditions well for the area under investigation and therefore is suitable for the scope of the project.From the above description it may be stated that the IOP has been completed during a period of time which represents typical winter conditions well for the area under investigation and therefore is suitable for the scope of the project.

Moreover, it is worth briefly addressing the rationale behind the IOP design, which was discussed in detail with local authorities and observers and can be summarized in the following:

1) Choice of one TA for each province and observer involved in the monitoring phase to explore the spatial variability of the various phenomena under investigation along a relevant part of the whole route.

2) The measurement period had to cover for each TA for at least more than one week (in order to observe different traffic flows) and a sufficient number of representative weather conditions, especially those which are most critical for pollution episodes during winter.

3) Each TA had to be far enough from the main urban areas to minimize their direct influence on pollutants concentration.

4) Small towns had to be included in those areas in order to apply the health impact assessment (see Chapter 6) within a realistic context.

5) The air quality measurements had to be located perpendicular to the valley axis in order to measure concentration gradients in the direction normal to the road axis. In particular:

    a. one site had to be close to the motorway in order to measure concentrations representative of traffic emissions/immissions (Fig. 7.55);

    b. a second site located in rural areas between the motorway and the towns;

    c. a third one inside the towns where other major sources of pollutant can be expected (namely local traffic and domestic heating);

    d. the last site at a location higher on the slopes of the valley in order to capture the background concentrations and/or vertical gradients.

6) The turbulence measurements, the energy-balance instrumentation and the wind profiler (see below for more details on the specific setup and Section 3.2.2 for general instrument description) were located in the middle of the valley section in order to provide information nearly representative of the whole TA.

7) On one slope at each TA 5 temperature sensors were located to collect useful information about the vertical thermal structure of the atmosphere within the valley (see Section 3.2.2.3).

Fig. 7.54 The complete energy-balance measurement system during the BS2-TA field phase.

Fig. 7.55 The air-quality mobile station of the Environmental Protection Agency of the Autonomous Province of Bolzano during the BS2-TA field phase.

7.2.1.3 Instrumental setup

One of the goals of the IOP field measurements has been that of displaying the added value of a detailed investigation of the complex meteorological fields expected to realize within a mountainous area such as that crossed by the Brenner transit route.

Following the rationale of the campaigns described above, besides conventional state-of-the-art air-quality mobile stations made available by the local environmental agencies (to which the reader is referred for further information), advanced sensors and measurement systems have been deployed in each TA for investigating specific atmospheric processes. The latter are summarized in the following:

- An ultrasonic anemometer (Gill Mod. HS-Research – hereafter sonic) for determination of the three wind components at a high frequency acquisition rate, coupled with an infrared gas analyzer (LiCor Mod. LI-7500 – hereafter IRGA) for the measurement of H_2O and CO_2 concentrations, and an independent resistance temperature device (PT100 DIN B) for the measurement of air temperature (Fig. 7.54). The system was designed and set up to acquire all the physical quantities at 20 Hz by means of the sonic analog inputs: this solution allowed perfect synchronization of all the signals, although a major drawback was the huge amount of data to be stored in raw format for accurate post-processing. The measurement height of the sonic and IRGA was 6.4 m AGL for all three TAs, and has been chosen in order to allow the instruments to measure flows influenced by uniform up-wind fetches (see Lee et al., 2004 for recent developments in this field).
- A Sodar (Scintec Mod. MFAS-64) for the retrieval of the vertical wind speed and direction profile. The system was set up to acquire data with a spatial resolution of 10 m up to 600 m AGL, depending on the meteorological factors affecting the sound propagation and on the background noise which is nearly impossible to exclude. Data were averaged over 30 min periods and archived every 10 min, thus giving the same temporal resolution as the other advanced instruments deployed in each TA.
- A 4 channel net radiometer (Kipp & Zonen Mod. CNR-1) to measure the incoming and outgoing short- and long-wave radiation components separately. Measurement height varied for the 3 TAs between 1.5 m AGL and 1.7 m AGL due to the need of looking at a representative surface, i.e. minimizing the influence of obstacles or even of the supporting masts and the datalogger enclosures on the radiative footprint. The instrument was pointed toward South in order to correctly measure the complete diurnal radiation cycle; special care was put in the perfect horizontality of the instrument as requested for reliable and comparable energy flux measurements.
- A ground heat-flux plate (Lastem Mod. DPE-260) to quantify the heat exchange across the soil-atmosphere interface. The sensor was put 1 cm below the surface and special attention was paid to avoid undesired modification of the state of the surrounding ground which needed to be representative of a larger area.
- An infra-red surface temperature sensor (Apogee Mod. IRTS-P) was also installed at a height of 45 cm AGL looking downward at a terrain plot which included the ground heat-flux plate and may be considered representative for the investigated area.

– A set of 8 fine-wire thermocouples (of type T, Copper-Constantan) at different heights from the ground (0.1 – 0.3 – 0.6 – 1.0 – 2.0 – 3.0 – 4.0 – 5.0 m) to investigate the surface layer air temperatures and how they are affected by the energy balance at the surface in detail. Due to the very small dimensions of the sensors (less than 1 mm in diameter) no radiation shield was provided, also in order to allow for faster response of the thermocouples to air temperature changes.

– Five temperature and humidity sensors (Onset Mod. HoBo H8 Pro) equipped with solar radiation shields have been located along suitable slopes at each TA. Data acquisition rate was set up to 5 min which is an optimal compromise between the temporal resolution needed for this study, the time response of the sensors and the available storage capacity. Since the sensors were deployed to get a pseudo-vertical air temperature profile representative of the thermal structure within the valley, the best location would have been that of slopes which remain in the shadow all day long in order to avoid/minimize the influence of local surface-layer processes on the measurements. Unfortunately this has not always been possible (especially for the second measurement campaign) and therefore the data analysis requires great attention for correct interpretation of the measurements.

The design and implementation of a measurement campaign always requires a well balanced compromise between theoretical and practical needs (e.g. representativeness of the site, measuring heights and sensors positioning with respect to obstacles, etc.) and possible limitations and constraints. For what concerns the aforementioned measurement systems, following considerations need to be stressed:

– Air-quality mobile stations are "power-hungry", thus not all interesting sites will be suitable for locating the vans and in many cases the simple use of power-line extensions may not guarantee adequate stability of the power supply.

– The "sonic + IRGA" measurement systems provides a detailed investigation of the surface-layer turbulent exchanges, but besides the specific requirements in terms of sensor position and height (due to theoretical assumptions implied by the investigation method itself: see Kaimal and Finnigan, 1994; Lee et al., 2004) the system produces a very

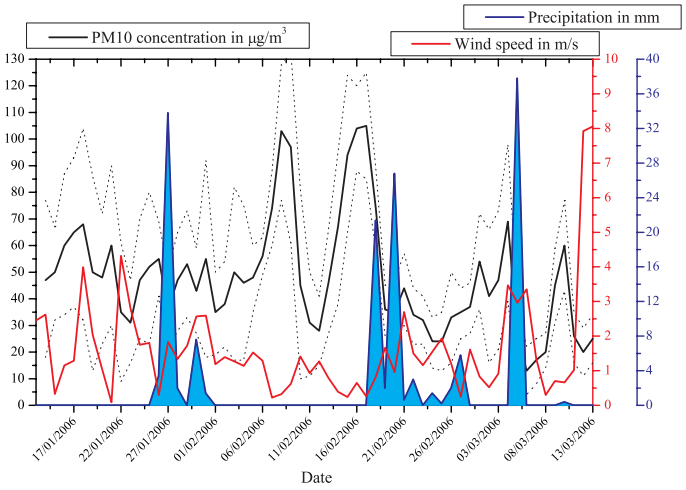

Fig. 7.56 Overview of the main meteorological quantities along with daily PM10 concentrations along the Adige Valley (black solid line: data averaged over all available stations between Bolzano and Verona. Black dotted lines: ±1 standard deviation interval). The atmospheric pressure is the average along the whole TA, as well as the PM10 concentrations. The wind speed and directions are referred to the 3 BS-TAs, while the reference daily total precipitation refers to Trento.

large amount of data which may not be easy to manage. For these reasons frequent surveys by trained personnel are necessary to guarantee the quality of the data.

– Radiation and energy balances need to be performed over rather uniform areas, i.e. the presence of small-scale inhomogeneities or very site-specific conditions must be avoided as much as possible; otherwise a detailed mapping of the situation up to distances of 1 km from the measuring site may be needed for reliable analysis of the collected data.

7.2.1.4 Data analysis

Besides the temporal/meteorological representativeness discussed in the previous Section 7.2.1.3, whether the pollution episodes measured during the investigations at one TA were due to the specific site or were common to the whole valley it was also checked. Fig. 7.56 shows, among others, all available PM10 daily averages between Bolzano/Bozen and Verona: apart from slight site-to-site variability (in connection with both local-scale meteorological phenomena and local emissions), the pollution episodes were almost the same at the different sites. This result clearly suggests the spatial representativeness of the IOP design, and also strongly supports the need to adopt common measures to ameliorate air-quality inside a valley due to the specific nature of the environment in which the processes occur (or in other terms that "local-scale" minimization strategies may bring very little benefits).

Moreover, since the daily and weekly cycles of traffic along the motorway are very similar during the whole measurement period (Fig. 7.57 for an overview of the total daily transit close to the three BS-TAs), air-quality data confirm the relevance of meteorological factors in determining the concentration levels (the schematic comparison of PM10 concentrations and meteorological quantities is reported in Fig. 7.56), as expected from considerations based on physical processes and previous experiences in this field.

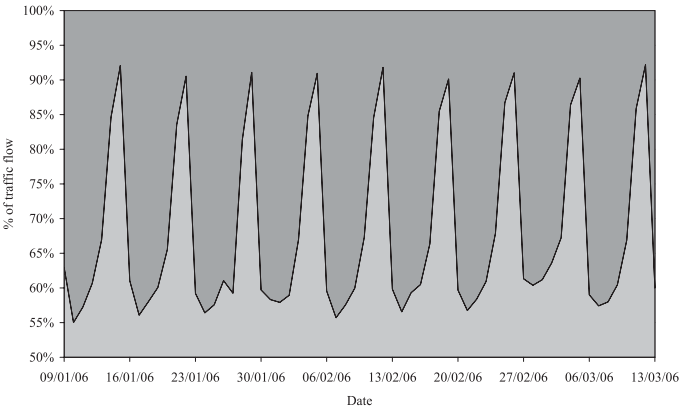

Fig. 7.57 Percentage of total daily transits along the Brenner-South motorway route during the whole IOP for both light duty vehicles (light grey: LDV – including passenger cars) and heavy duty vehicles (dark grey: HDV). Dates reported on the x-axis are Mondays.

The field measurements performed in the BS-TAs also highlighted, among others, the relevance of proper investigation of the vertical structure of the air temperature and wind speed and direction, as well as the surface energy budget which triggers most of the atmospheric processes at a local scale. Conventional observation networks only rely on ground measurements of the various meteorological variables, where many of the pollution sources are indeed located, but commonly miss the upper air features which are relevant for a more reliable understanding and prediction of the pollutant transport and dispersion processes. As a matter of fact, one of the key issues in mountainous environments is the complexity of the vertical structure of the atmosphere within a valley (see Section 3.1) and its effects on pollutant concentrations. Fig. 7.58 displays such complexity by means of one day of wind speed and direction measured by means of the Sodar during the meas-

urements in the BS2-TA. These and similar data will be discussed in more details in Section 7.2.2.2 along with concurrent measurements to provide useful description of typical interaction between emissions and meteorology which lead to the first of two episodes of high concentration levels.

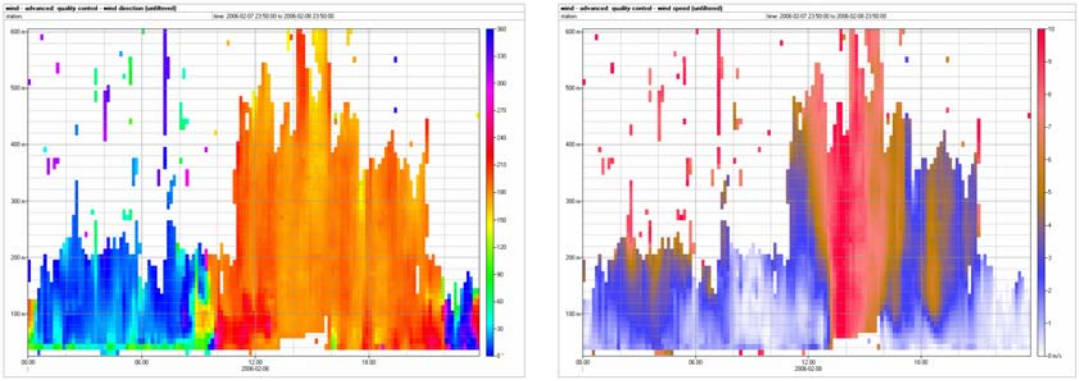

Fig. 7.58 Wind direction (left panel; warm colours indicate south) and speed (right panel; colour scale ranges from 0 to 10 m/s) measured by the Sodar on the 07 Feb 2006 during the first high-pollution episode registered during the BS2-TA measurement campaign. Height is above ground level.

7.2.1.5 Correlation between traffic and pollution

A direct correlation between NO concentration and traffic has only been considered for the air-quality stations close to the motorway where the effects of daily traffic cycles (Fig. 7.60) are easily recognizable. This also holds true for NO_2, although a weaker variation is observed, due to inertial effects. The rather low NO concentrations measured far away from the linear source are mainly determined by chemical transformation from NO to NO_2. On the contrary, less difference in NO_2 concentration may be observed among different stations, probably due to higher background values, typical of winter situations, displaying strong atmospheric stability and therefore allowing persistent stagnation of pollutants. Moving away from the motorway, this source becomes no longer dominant, so that the daily traffic cycle effect is no longer evident from the pollutant concentration values, since other sources are present (mainly domestic heating and national roads).

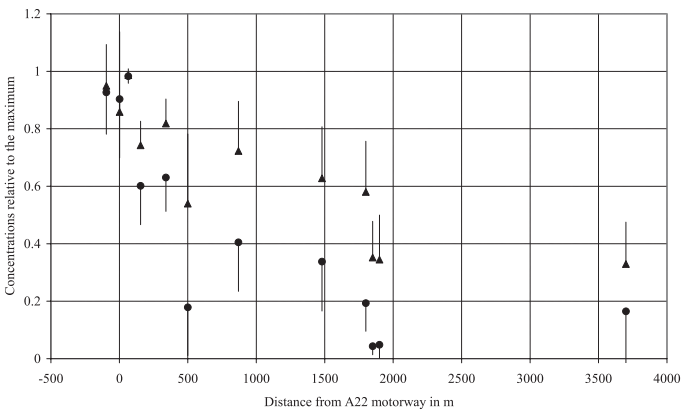

Fig. 7.59 Normalized NO (squares) and NO_2 (triangles) concentrations for the Brenner-South target areas. Vertical bars denote one standard deviation

Further interesting considerations may be drawn from Fig. 7.59 which displays the concentration gradients for both NO and NO_2: NO concentrations show a quite rapid decrease with increasing distances from the motorway, while the NO_2 concentrations tend to remain higher for longer

distances, mainly due to the chemical transformations which take place in the near- and medium-range. The investigation of distances up to 4 km from the motorway has been made possible by using all available data from all TAs in one single graph. For each hour of the IOP the concentrations at each station have been scaled with the maximum value (measured by the air-quality station closest to the motorway), then the average daily normalized concentration has been calculated and finally mean values along with standard deviations have been evaluated over the whole measurement period at each TA. The vertical bar on the graphs represents the standard deviation around the average at each measurement point and is mainly due to the meteorological variability which induced day to day variations in the pollution loads.

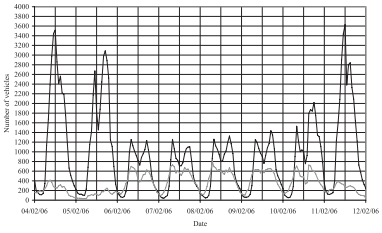

Fig. 7.60 Hourly transits of Light Duty Vehicles and passenger cars (black line) and Heavy Duty Vehicles (grey line) at the motorway measuring section closest to the BS2-TA. See Section 2.2.1.1.

It is worth of noting that Fig. 7.59 is comparable to that obtained in the Lower Inn valley (see Fig. 7.21 in Section 7.1.3.5) in a different manner, thus underlining the general validity of the considerations drawn here with respect to the horizontal attenuation of the NO and NO_2 concentrations at increasing distances from the source.

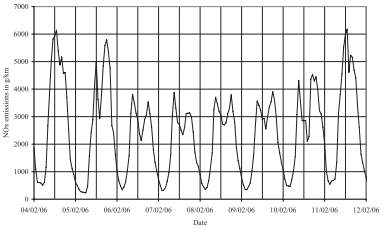

Fig. 7.61 Hourly NO_X emissions in g/km at the BS2-TA evaluated by means of the COPERT III methodology (see Section 2.5.2.2).

7.2.2 Demonstrations

In the following a specific episode of the BS2-TA measurement campaign will be briefly be presented as an example of the interactions of emissions/meteorology/immissions. Afterwards, details about the whole modelling chain (along with other considerations on measured data) will be given following the same logical sequence as before, with the addition of the health impact evaluation.

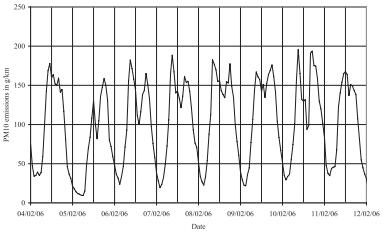

Fig. 7.62 Hourly PM10 emissions in g/km at the BS2-TA evaluated by means of the COPERT III methodology (see Section 2.5.2.2).

7.2.2.1 Traffic and emissions

The first step when approaching the problem of traffic pollution is straightforward analysis of traffic flows also because this is usually considered the quickest indicator for the influence of traffic on the overall pollution in a certain area. In the present case the weekly and daily patterns are clearly recognizable (see Fig. 7.60) and the predominance of light duty vehicles and passenger cars is also evident. Heavy duty vehicles are mainly crossing the Alps during the week, while buses travel during the weekend. It is also worth mentioning the relevance of tourists-related traffic typical of the winter in the Alps and especially in the area under investigation: an almost doubled amount of cars during the weekend (also with a different diurnal cycle) may already suggest a strong increase of emissions during these days.

In order to quantify the effect of traffic on air pollution a further step is required, such as the evaluation of emission factors for the different types of pollutants in terms of g/km for each hour

of the day. For NO_X and PM10 the results of the COPERT III methodology as described in Section 2.5.2.2 are reported.

Directly comparing traffic emissions (Figs. 7.61 and 7.62) with pollutant concentrations (Fig. 7.68 and 7.69 in Section 7.3.2.3), clearly shows that the traffic flow alone is not sufficient to explain the pollutant loads within the valley for many reasons: on one hand the different vehicle categories, types and especially Euro-classes are responsible for very different emission factors (in terms of g/km), not to mention the behaviour of the average driver; on the other hand the weather factor plays a very important role on pollutant transport and dispersion (see Chapter 4 and following Section 7.2.2.2). Nevertheless, with the methodology adopted here one may easily notice that there is a substantial increase of NO_x during the weekend, while this is not the case for PM10.

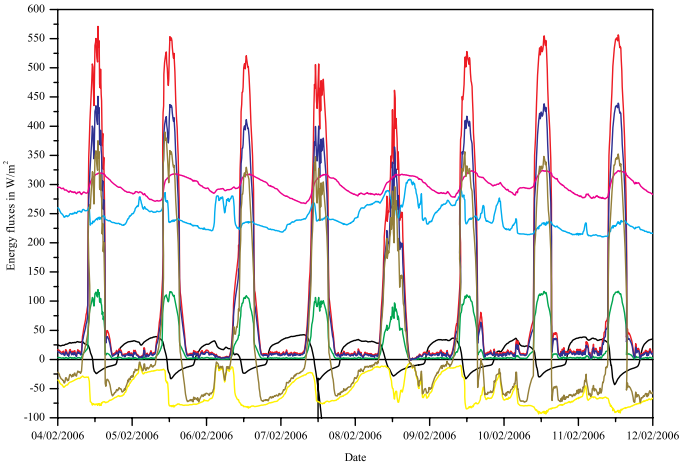

Fig. 7.63 Diurnal cycles of different components composing the surface energy balance during the BS2-TA measuring campaign. Black: ground heat flux; red: incoming short-wave; light-green: outgoing short-wave; blue: short-wave net radiation; cyan: incoming long-wave; purple: outgoing long-wave; yellow: long-wave net radiation; olive: total net radiation. Data are 10 min averages

7.2.2.2 Meteorology

All meteorological processes are forced by the energy budget which is realised at the Earth surface. In the present case, the diurnal cycles of different components are displayed in Fig. 7.63**,** which helps in understanding the amount of energy made available at the surface (i.e. the total net radiation) for heating/cooling the atmosphere close to the surface itself. One of the consequences of these ground-based processes is the thermal stratification of the atmosphere within the valley (for which we consider as representative measurements the pseudo-vertical temperature data ob-

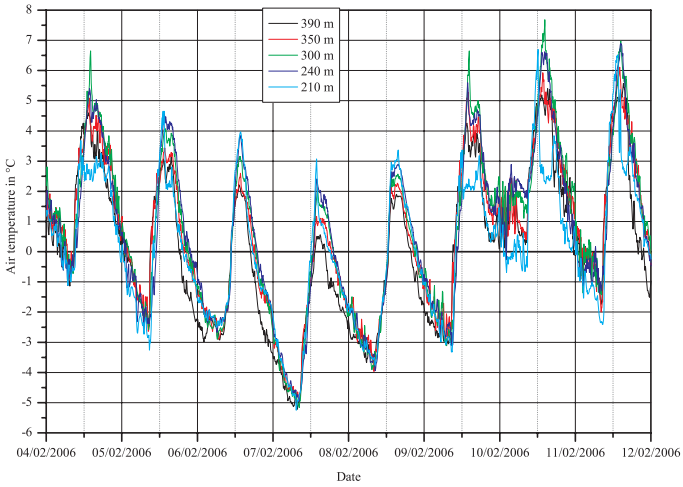

Fig. 7.64 Air temperature measured by the sensors placed along the eastern slopes of the valley during the BS2-TA measuring campaign. Legend indicates the height above mean sea level of the different sensors.

tained along the slopes and reported in Fig. 7.64), as well as the development of local wind circulations.

The latter are highlighted by wind speed and direction measurements (Fig. 7.65) taken in the middle of the valley sections: winds blow in the up-valley direction (i.e. from south) for many days during the afternoon and in the opposite direction during the remaining of the day. This pattern is also very well represented by the Sodar measurements especially when only the along-valley components are plotted (see Fig. 7.67, bottom) where positive values indicate southerly winds). It is interesting to notice that these winds may reach heights of more than 400 m AGL during the day, while in most of the cases nocturnal circulations are confined to shallower layers approximately 200 m AGL thick. The thickness of such circulations is an important factor for both highlighting the diurnal variation of the dilution volume inside the valley and supporting the evidence that the whole valley is affected“at the same time” by pollution episodes which are not confined to single locations, i.e. single towns or valley sections.

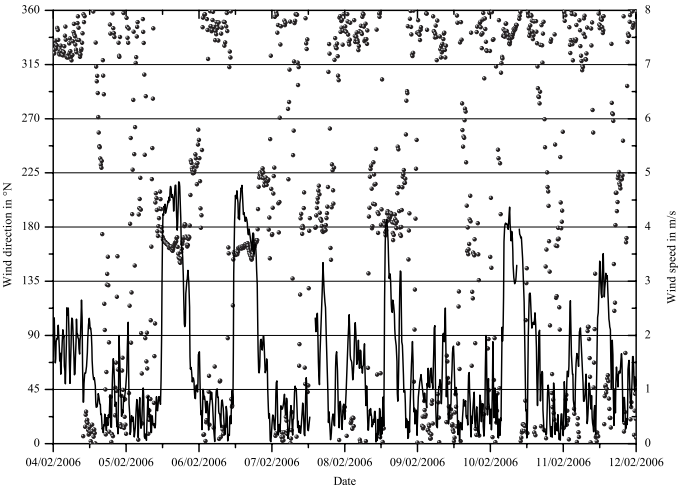

Fig. 7.65 Wind speed and direction measured by the ultrasonic anemometer in the middle of the valley section at the BS2-TA. Data cover the period 04 – 12 Feb 2006 and are half-hourly averaged with 10 min final temporal resolution.

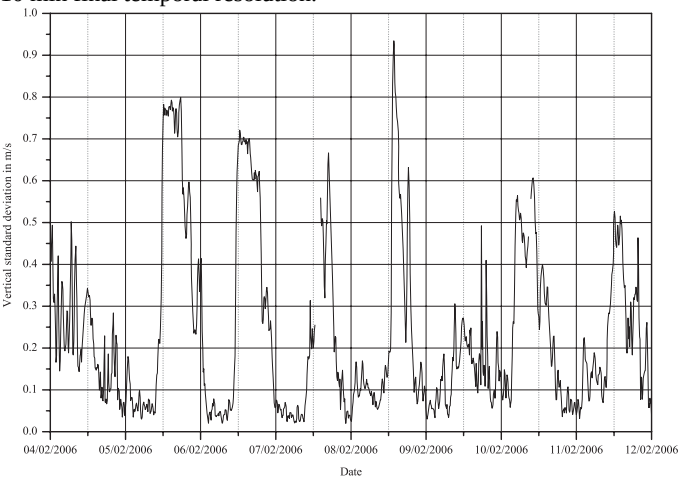

Fig. 7.66 Same as **Fig. 7.65** but for the standard deviation of the vertical wind speed component. Higher values denote higher turbulent mixing in the vertical direction.

Whilst the transport of pollutants may be easily related to the wind intensity, the dispersion has to be related to turbulence parameters, among which the standard deviation of the vertical wind speed components is a key factor. Measurements taken close to the ground (Fig. 7.66 obtained from ultrasonic anemometer measurements) and up to approximately 200 m AGL (Fig. 7.66 obtained from Sodar measurements) provide explanations of the strong drop in NO_X and PM10 concentrations in the early afternoon of 05 – 07 Feb 2007 (Fig. 7.68 and 7.69 in Section 7.3.2.3) with the rapid increase of both the wind speed (Fig. 7.65) and vertical standard deviation (Fig. 7.66) measured at 6.4 m AGL.

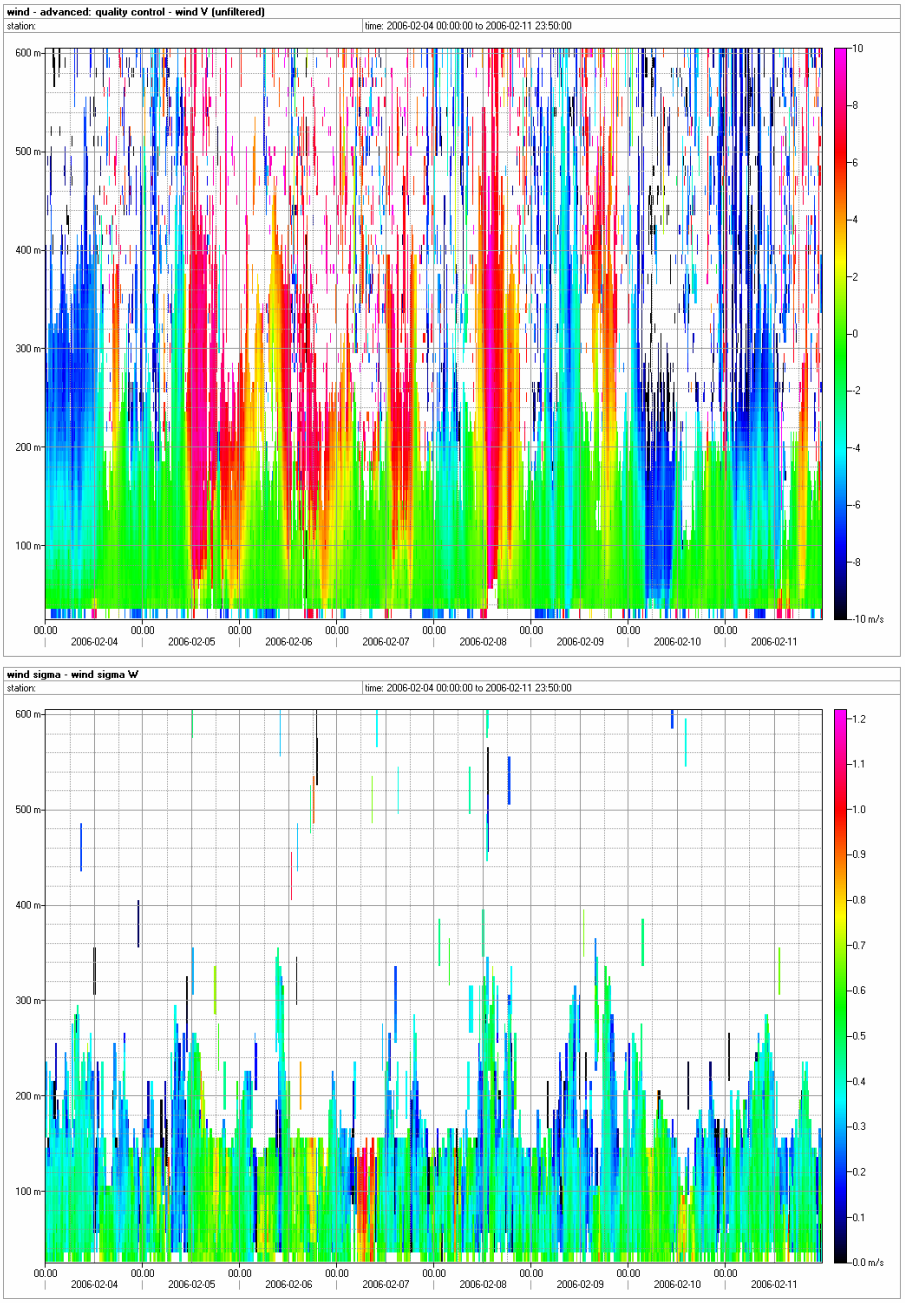

Fig. 7.67 Top: along-valley wind components measured by the Sodar at the same site and during the same period as for Fig. 7.65. Positive values indicate southerly winds. Bottom: same as top panel, but for the standard deviation of the vertical wind component. Higher values (redish colours) denote higher turbulent mixing in the vertical direction.

7.2.2.3 Pollutant concentrations

The result of the interaction between emissions and meteorology is the development of pollutant concentrations. The analysis of a high-pollution episode during the BS2-TA (Figs. 7.68 and 7.69 for NO_X and PM10 respectively) shows the superimposition of at least two modulation patterns. The first one may be viewed as a long-term accumulation of pollutants amenable to the rather continuous emission from the various sources within a substantially well confined environment. The second one usually displays a diurnal variation which is related to both the emission characteristics (however, it must be kept in mind that major sources other than the motorway are present along the valley) and the meteorological processes, as previously discussed.

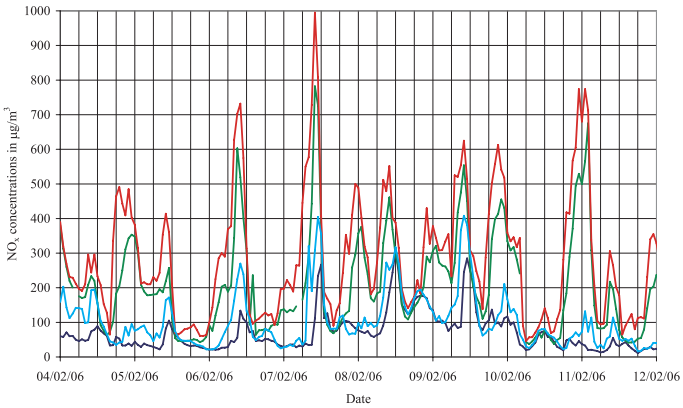

Fig. 7.68 Hourly NO_X concentrations in µg/m^3 at the BS2-TA. Different colours identify the position at increasing distance from the motorway: red, green, light blue, blue.

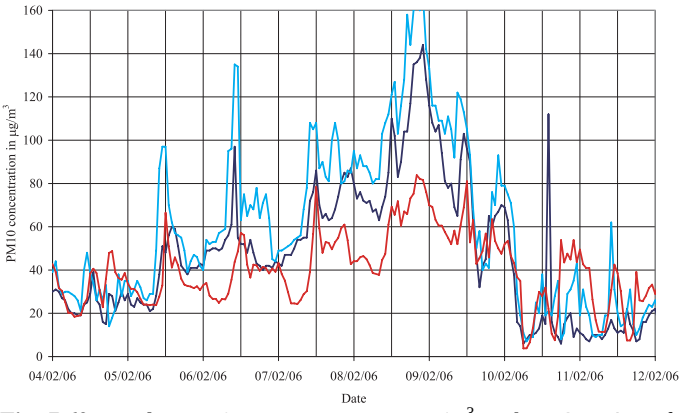

Fig. 7.69 Hourly PM10 concentrations in µg/m^3 at the BS2-TA. Different colours identify the position at increasing distance from the motorway: red, light blue, blue.

7.2.2.4 The air quality modelling chain

The basic concept of the dispersion models adopted here is to calculate air pollutant levels in the vicinity of the motorway by considering it as line sources. The models take source characteristics into account such as traffic volume, vehicle speed and type, and fleet emission; in addition, roadway geometry, surrounding terrain and local meteorology are addressed. Model validation has also been performed with field data: this step is not usually warranted, because the best models have been extensively validated over a wide spectrum of input data variables.

The product of the calculations is usually a set of isopleths (air pollution contour maps) in plan view. Cross sectional view has been added to evaluate the difference with respect to measured data. Calculations have been performed for carbon monoxide, total hydrocarbons, nitrogen oxides and particulate matter, but only the latter two have been reported here.

Prior to the description of the modelling chain, it is important to recall that for correct and reliable application of such a system, proper calibration of the models is needed. Under the word “calibration” careful application of a model developed for more general conditions to a specific case by well trained and skilled personnel is intended.

In the present case this phase can be sketched as follows:

1. calculation of emissions through COPERT III emission model (see Section 2.5.2.2);
2. application of the CALINE Gaussian model;
3. comparison with observed air quality data near the traffic source (where it is supposed to be dominant);
4. estimate of initial turbulent diffusion parameters (near-field diffusion);
5. final CALPUFF and CALGRID dispersion model calculation using the previously calibrated parameters;

Details are given in the following paragraphs.

Traffic

The analysis and evaluation of emission factors was performed using the registered transits and speeds on the A22 motorway. The transit data near the motorway toll-points were made available for the years 2003 and 2004. The daily data are divided into heavy and light vehicle. As far as the monthly data is concerned, only transit for the five motorway toll classes is available (see also Section 2.2.1.1).

Traffic flow analysis

The daily mean transits from Brennero/Brenner to Verona reported in Fig. 7.70 shows a mean increase of about 3 % between 2003 and 2004, which is mainly due to the increase of heavy vehicle traffic (about 8 %). The highest transit is in San Michele – Mezzocorona, especially for the light vehicle class, which is probably due to the commuter traffic from and to Trento. Interestingly, a greater amount of transit occurs on the weekend: on Saturday in the northerly direction, and Sunday in the southerly direction. Since trucks cannot circulate on the A22 motorway during the weekend, the reported heavy vehicles are probably buses, cars with caravans and motor caravans. The traffic is generally higher in the summer months, especially in July and August, but in December some events of high traffic have also been recorded, corresponding to Christmas holidays.

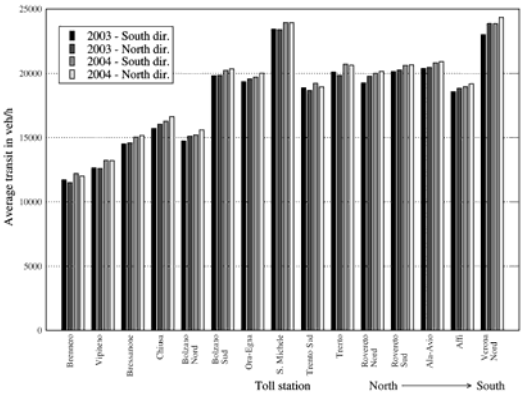

Fig. 7.70 Mean daily traffic transit at the motorway toll stations from Brennero/Brenner (on the left) to Verona (on the right).

A deeper analysis has been performed on the total number of vehicles for one sections at each target area, namely near Salorno/Salurn (km 102.0 south from Brenner) near Aldeno (km 138.1 south from Brenner) and finally near Rivalta (km 205.5 south from Brenner).

Fig. 7.71 shows the total number of vehicles registered during Jan 2006, in the three sections, going from north (Salorno/Salurn) to south (Rivalta) where the traffic intensity increases more or less by 40 %. The hourly transit data also highlight more characteristics of the traffic in the area: the days with the highest number of transit are 02 Jan 2006 and the first weekend of January, because of the traffic due to Christmas holidays. During these days the high number of vehicles causes stop-and-go traffic and traffic jams.

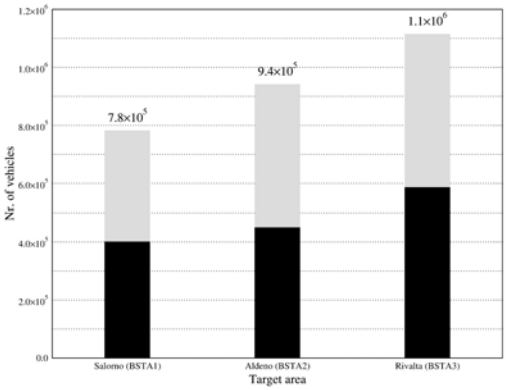

Fig. 7.71 Total traffic transits in the month of January 2006 at measurement-points near Salorno, Aldeno and Rivalta.

During weekdays there is generally a regular repetition of the traffic flows with two peaks: one in the morning, at about 09 CET, and the other in the afternoon at about 18 CET. During the weekend traffic appears greater, especially on Saturday. The cycles are less regular, probably because of influences of tourist flows and therefore traffic is also related to the weather. Looking at the traffic direction, it is interesting to observe that the flows in the northerly direction are generally higher on Friday and on Saturday, maybe because of tourist arrivals in ski resorts, while the return is concentrated in a few hours with the peak on Sunday afternoon.

Further considerations involve the vehicle density (expressed in veh/km), which is the ratio between the traffic count (in veh/h) and the vehicle speed (in km/h). This parameter is very effective in identifying traffic obstructions or jams, since under normal traffic conditions the density does not exceed the value of 20 – 25 veh/km, while in traffic jams the density may reach values of 120 veh/km and the speed is not determined by the typical velocity of the vehicle but by the presence of the queue. Fig. 7.72, 7.73 and 7.74 show an example of this analysis, referring to 17 Jan 2004. The typical bimodal daily distribution may be observed with one peak at 07 CET and another one in the late afternoon. During the day the traffic remains quite high, while during the night a consistent reduction is observed. Mean vehicle speed has some variation depending on the fraction of heavy duty vehicle over the total and the density of the traffic.

Particular attention was put on identifying daily traffic cycles, in order to explain features in emission and air quality patterns. In Fig. 7.75, for example, week-end days are depicted in grey and they show a quite a different traffic pattern with respect to the remaining 5 days of the week.

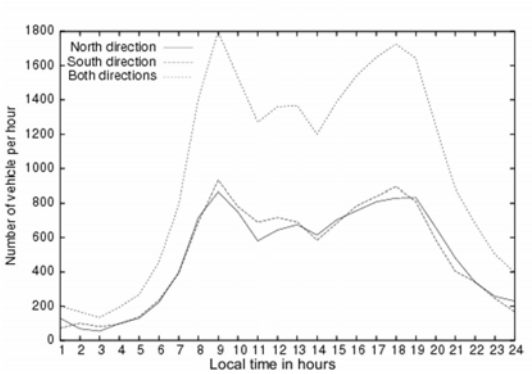

Fig. 7.72 Daily traffic distribution in the section of Salorno (km. 102.0), on 17 Jan 2006

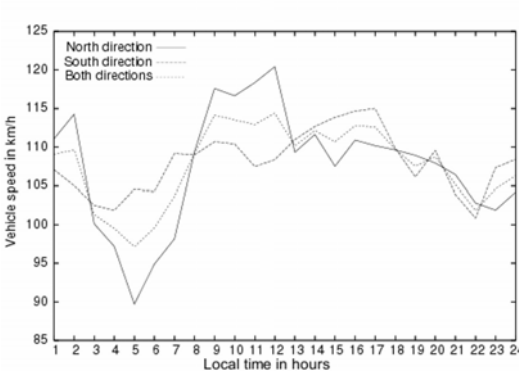

Fig. 7.73 Hourly mean speed in the section of Salorn (km. 102.0), on 17 Jan 2006

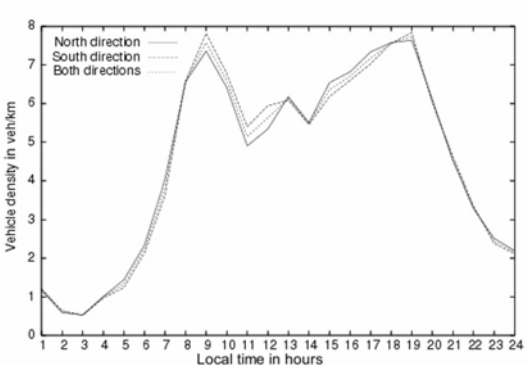

Fig. 7.74 Hourly vehicle density in the section of Salorno (km. 102.0), on 17 Jan 2006

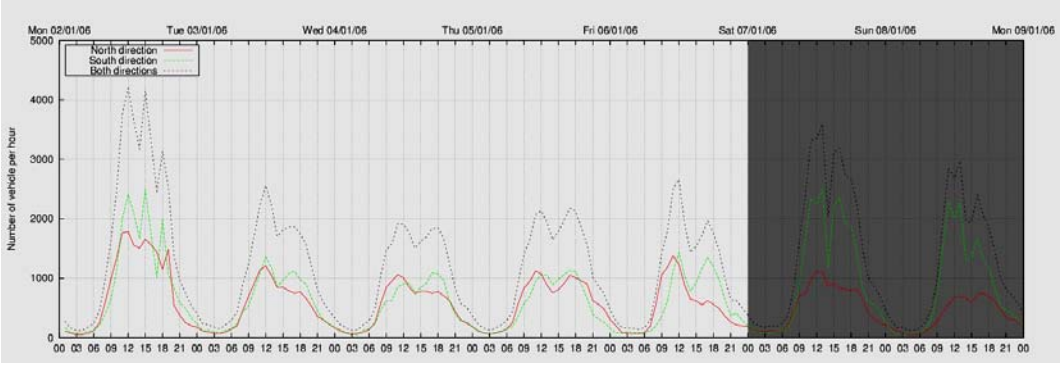

Fig. 7.75 Example of traffic counts during the IOP in the BS1-TA (km 102.0); weekend days are highlighted in grey.

Traffic classification

Following the description reported in Section 2.5.2.2, emission factors have been computed through COPERT III methodology and using the Automobile Club Italia (ACI) national vehicle fleet (integrated with other databases to make it more representative of the A22 traffic). Since no further information is available, A22 motorway transit classes have to be mapped into COPERT emission classes. Initial information is the traffic transit made available for several sections between Brennero/Brenner and Verona for the IOPs (Jan to Mar 2006):

Tab. 7.7 Length classification.

COPERT sector	Motorway count category
Sector 1 (cars)	Short vehicles
Sector 2 (light duty vehicles < 3.5t)	Short vehicles
Sector 3 (heavy duty vehicles + busses)	Long vehicles
Sector 4 (mopeds)	[does not apply]
Sector 5 (motorcycles)	Short vehicles

- Number of vehicles per hour
- Mean hourly speed
- Length class (short/long)

The latter was setup to distinguish between vehicles shorter or longer than 5.25 m and the scheme used for mapping between A22 motorway transit categories and COPERT technology sectors is reported in Tab. 7.7.

Selected traffic counts corresponding to the target areas have been used and compared to tollbooth data (see Chapter 2) in order to check for continuity. It is important to notice that in case of traffic jams, when cars and trucks are very close to each other, the reliability of the measurement tends to decrease significantly.

The continuity check shows some discrepancies between tollbooth and automatic traffic count, which can be explained by the occurrence of traffic jams, by occasional malfunction of the measuring system, or, since the logger measures separate lanes transit, by a non–perfectly aligned position of vehicles (only partially within the lane).

Emission factors

For the emission factors estimate the COPERT III methodology (see Section 2.5.2.2) has been applied using automatic traffic counters which provide hourly data along with the length classification which is more useful to be linked to COPERT categories. The present Italian vehicle fleet and annual average mileage per vehicle class have been used as additional information.

This is the outcome of the deficiency in reflecting the year of vehicle production and, subsequently, the engine and after-treatment technology which is implemented for achieving the emission standards. Thus, for the purpose of COPERT, a more detailed vehicle category split is used: 105 categories are used, grouped in five main classes (passenger cars, light duty vehicles, heavy duty vehicles, urban buses and coaches, two wheelers) and classified on the basis of the emissions and not the size as done for the toll classes.

For the present case (motorway) cold emissions may be safely neglected and total emissions can be calculated as:

$$E_{TOTAL} = E_{HOT} + E_{COLD} + E_{EVAP}$$

where:

- E_{TOTAL}: total emissions (in g) of any pollutant for the spatial and temporal resolution of the application
- E_{HOT}: emissions (in g) during stabilised (hot) engine operation
- E_{COLD}: emissions (in g) during transient thermal engine operation (cold start)
- E_{EVAP}: emissions (in g) from fuel evaporation. Emissions from evaporation are only relevant for non-methane OC species from gasoline powered vehicles.

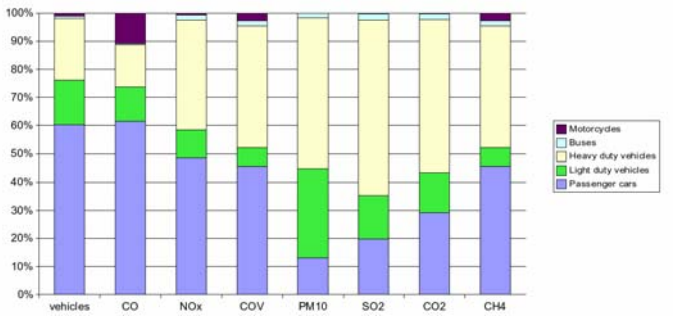

Fig. 7.76 Estimate of relative contributions of the different motorway vehicle categories to each pollutant considered for the base year 2004.

Vehicle fleet

Statistical data released by ACI refering to the year 2005 were made available and adopted as a reference for the ALPNAP project (Tab. 7.8). A correction was introduced in the COPERT classification to account for annual average mileage per each vehicle class: heavy duty vehicles, diesel passenger cars and newer vehicles are indeed characterized by a greater average annual mileage. Therefore, empirical functions of vehicle parameters derived through statistical analysis have been adopted, consisting of linear regression functions in the form:

Tab. 7.8 Vehicle fleet in year 2005

Type	**Number**
Motorcycles	4938359
Light duty vehicles	344827
Passenger cars	34667485
Buses	94437
Heavy duty vehicles	4179659
Trucks	148173
Other	812161
Total	**45185101**

$$AAM = m \cdot A + q$$

where AAM is the annual average mileage (in km), A represents the age of the vehicles (in years), q is the intercept of the regression line and m its slope.

For all the classes where similar data were not available, i.e. motorcycles, buses, duty vehicles, the ACI data updated to 1996 has been used and extrapolated to 2005. For motorcycles only 1/3 of the fleet has been considered as > 125 cm^3 or, in any case, using the motorway.

As a conclusion, the percentage of transit assigned to each COPERT class has been computed on the basis of all the previous considerations.

The same has been made for heavy vehicles, considering that buses and gasoline duty vehicles have average annual mileage approximately 50% lower with respect to heavy duty vehicles.

Further working hypotheses have been made in the estimate of emission factors. In particular:

1. All emissions are considered to be “hot” ones. Cold start emissions are obviously not present for motorway traffic and evaporative could be only suitable for petrol stations (this possibility is already foreseen in air quality modelling).
2. Heavy duty vehicles have been considered as travelling with full load and a corrective coefficient for fuel consumption and emission factors has been used.
3. In the computation measured vehicle speed has been used. Nevertheless, for speed greater than the legal limit (and outside of COPERT range), the COPERT upper limit has been adopted.

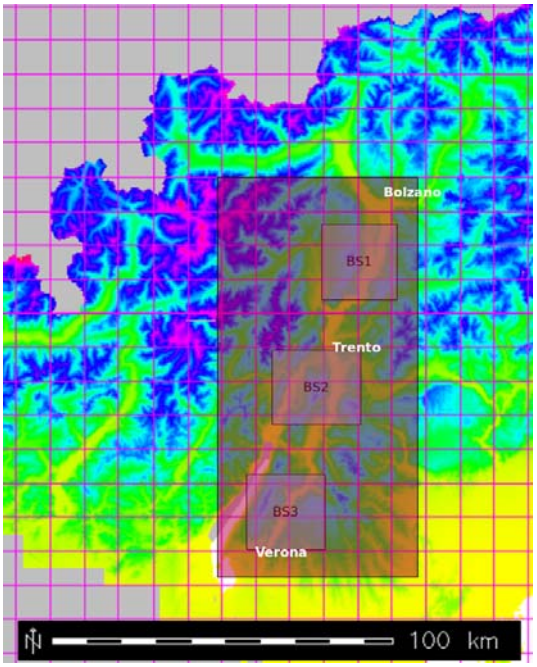

Fig. 7.77 Modelling domains covering the whole Brenner-South Target Areas.

A synthetic result is shown in Fig. 7.76 where the contributions of each vehicle category to the pollutant emissions from the motorway in the year 2004 are reported: duty vehicles, even if in lower number with respect to private cars show a significant contribution to both primary PM10 emissions and to NO_X (thus to secondary particulate matter); on the contrary passenger cars, both Diesel and unleaded gasoline fed vehicles, are principly responsible for VOC and CH_4 emissions.

7.2.2.5 Meteorological simulations

The CALMET model was used for the diagnostic simulations over a domain of 45 km (East) × 115 km (North) wide, and a horizontal resolution of 250 m in both the *x* and *y* directions has been adopted (see Fig. 7.77). In the vertical direction the levels are not equally spaced: an unequally spaced distribution has been used in order to achieve a higher resolution near ground level: 10, 20, 50, 100, 200, 300, 500, 800, 1200, 1600, 2000, 2500 and 3200 m AGL. Horizontal layers are expressed in terrain-following coordinates, and the absolute values are actually referred to the lower cell in the whole domain. Thus, a total number of 460 × 180 × 12 cells are used for calculation. Simulations were performed both for the reference year 2004 and for the IOP campaigns.

Meteorological data from the automatic weather stations located within the Adige/Etsch valley and in the surroundings have been used for simulations (Fig. 7.78).

Meteorological simulations for several reference days have been performed, choosing them among the most significant IOP in order to check simulated and measured values. After that the base year simulation was performed. The computed parameters are the 3D field of the wind compontents *u*, *v*, *w* and the temperature *T*; moreover 2D stability parameters have been computed, i.e. Monin-Obukhov length, friction velocity, vertical convective velocity scale, sensible heat flux. An example of wind field at ground level is shown in Fig. 7.79.

The CALMET simulation was run from 01 Jan 2006 to 31 Mar 2006, covering the intensive observation periods in the three target areas. To get sufficient information on the synoptic conditions

while still resolving locally driven dynamics, the station of Monte Tomba was used as a fictitious upper air station. The CALMET model was also utilized in a trial run, wherein sodar data was used as upper air sounding inside the domain to get an initial guess wind field, also applying the normal diagnostic adjustments for terrain and employing the objective analysis procedure with all available observations.

Nevertheless, some suitable extrapolation is needed in this case, as the Sodar profile does not reach the upper range of the model domain. As wind direction at lower levels is significantly influenced by the valley directions, results are not realistic and the CALMET simulations in this mode fail to reproduce the above vertical structure. Therefore only the fictitious upper air station in Monte Tomba has been left which is located within the domain but quite far away from the sub-target areas. CALMET simulations with this hypothesis are probably less accurate but successfully simulate the lower levels.

As far as temperature is concerned, the lowest level estimate is quite accurate if the altitude correction foreseen in CALMET is adopted; otherwise, only horizontal interpolation between two stations at the same altitude but divided by an orographic obstacle, can in some case produce non-realistic spatial variation in the temperature field.

The computational costs involved in running a coarse prognostic meteorological model and introducing its output to a fine resolution diagnostic model are significantly lower than running a fully nested prognostic meteorological model with horizontal resolutions comparable to those of the diagnostic model. The CALMET model incorporates an advanced version of the diagnostic wind model and produces mixing height fields and other meteorological parameters that are then utilized by the Lagrangian puff dispersion model CALPUFF, and also by the Euler photochemical transport model CALGRID.

Difficulties are still present, mainly in comparing wind directions at lower levels, as the module of CALMET computing terrain driven winds uses a local approach and sometimes tends to overestimate terrain effects. In any case, while the relative errors for the horizontal component of velocity decrease when CALMET is operated without terrain adjust-

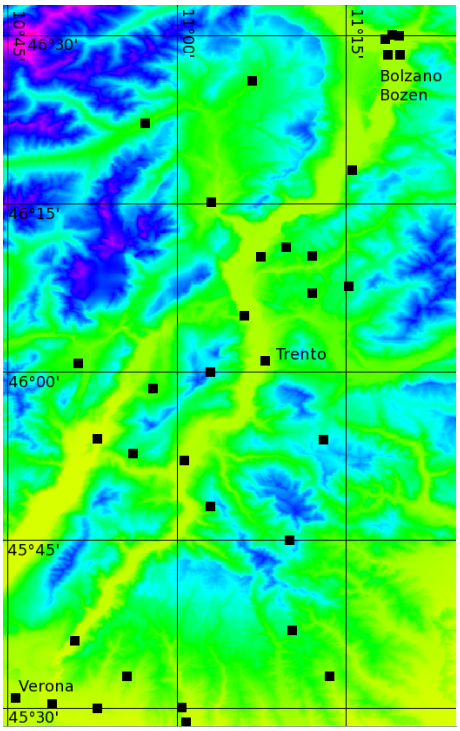

Fig. 7.78 Location of the automatic weather stations used for CALMET simulations over the base year.

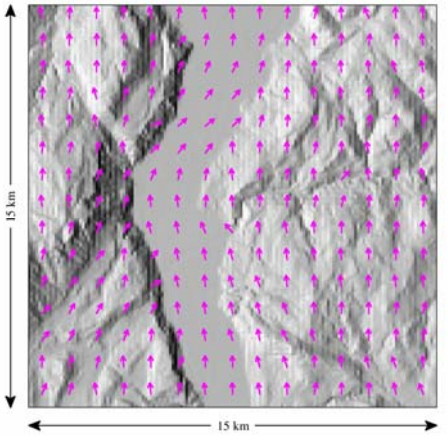

Fig. 7.79 Lowest level wind field simulated by CALMET (BS2-TA, 08 Feb 2006).

ment, wind direction results would be completely wrong. On the contrary there is no significant increase corresponding to the relative errors of the local velocity module in the first mode.

7.2.2.6 Model calibration

The calibration procedure of the air quality models can be sketched as follows:

- calculation of emissions through COPERT emission model
- application of the CALINE Gaussian model
- comparison with observed air quality data near the source traffic data (where it is supposed to be dominant)
- estimate of initial turbulent parameters (sigmas in the near field diffusion)
- final CALPUFF and CALGRID dispersion model calculation using the previously initial diffusion parameters

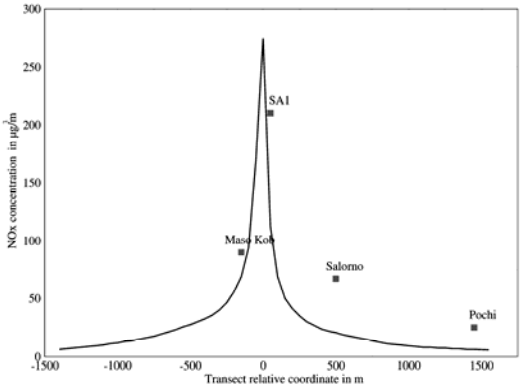

Fig. 7.80 Simulated and measured NO_x concentration along the section shown in **Fig. 7.81**.

Calibration at small spatial scale has been performed using a modified version of CALINE with 20 m grid spacing. Traffic data, meteorological input and air quality surveys during the IOP have been used. The first aim was to calibrate turbulent diffusion parameters in the near range, which is important if we want to estimate the impact contribution of the motorway along the cross section of the valley. Moreover emission factors can be double-checked, as the vehicle fleet is not given in detail and therefore, adopted emission factors are in some way approximated. An example of the results is shown in Fig. 7.80. Influence of the source turns out to be significant in the first 500 m from the centreline.

In this example the simulation shows good agreement near the linear source, but underestimations in Salorno/Salurn and Pochi/Bucholz. As a generally valid consideration it should be pointed out that in Salorno/Salurn also other sources are present (domestic heating, local traffic) which explains the underestimation of the model. On the other hand, Pochi/Bucholz is located on the valley side, i.e. it is representative of the background concentration.

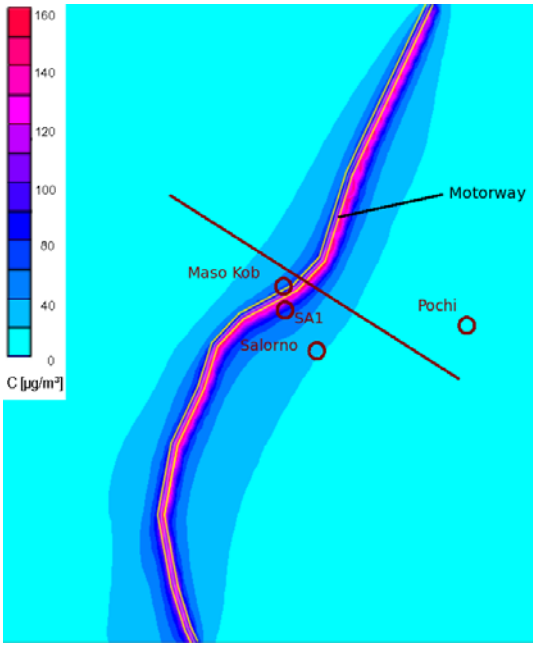

Fig. 7.81 CALINE model output NO_x concentration.

7.2.2.7 Air quality simulations

Two different approaches are being adopted for dispersion modelling. A small scale approach, using the CALINE model, has been used to calibrate the initial mechanical diffusion induced from high traffic and speed: this factor is in fact not negligible for motorway emissions. Only in the vicinity of the source the Gaussian CALINE model is applicable; on the other hand, most of the impact is effectively estimated to be within 0.5 km from the source for the target area in Salorno/Salurn, Aldeno and Rivalta (see example in Fig. 7.81).

The second approach has been carried out by using the Lagrangian puff model CALPUFF and the Euler model CALGRID. Both can use the meteorological parameters estimated by CALMET, also including a complete complex-terrain module.

The CALPUFF model has been applied in order to characterise the main feature of the pollutant dispersion phenomena. The horizontal extension is the same used for the meteorological simulations. Mainly particulate matter and nitrogen oxides have been considered both in data analysis and in the simulations, as they are the most critical pollutants. Airborne particulate matter represents a complex mixture of organic and inorganic substances. The same computational domain as CALPUFF was also used for the CALGRID simulation.

A particular focus has been held on the three sub-areas using the CALINE model. In these areas intensive observations are being used for model calibration especially for temperature vertical profiles on valley sides and turbulence parameters. In any case the adoption of a small scale dispersion model was useful to estimate dispersion length scale and consequently adjust the CALPUFF setup.

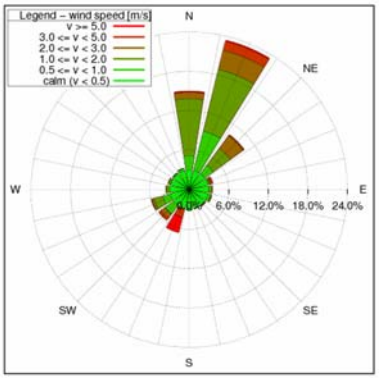

Fig. 7.82 Simulated wind rose for BS2-TA, near Aldeno.

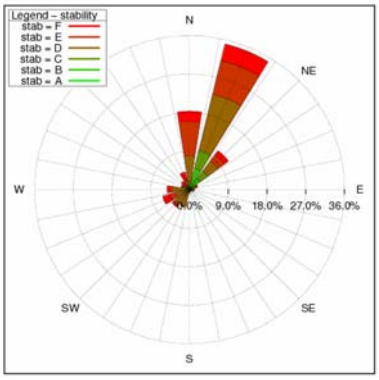

Fig.7.83 Simulated stability rose for BS2-TA, near Aldeno.

For the air quality simulations meteorological fields obtained by CALMET were used. They were checked for consistency with respect to the nearest measured data. Figs. 7.82 and 7.83 show the wind-rose and stability-rose for the BS2-TA respectively. Pasquill-Gifford stability class is derived by CALMET along with analytical parameters such as mixing height, friction velocity, etc.

Every simulation has been performed by using hourly variable emission factors, in accordance with traffic flows, for all days of the intensive observation period (IOP). Note that the sources are differently treated in our air quality models. While CALINE directly support linear sources for road modelling and considers traffic-induced turbulence CALPUFF does not. For the latter mod-

els, the volume source approach for line sources has been used. Initial vertical dimension for adjacent volume sources was fixed at 3 m.

In Fig. 7.84 the comparison of the output produced by CALGRID and CALINE is reported. This rather raw example aims at showing how the grid resolution can affect the results in terms of concentration maps thus changing the degree of detail, also when the same input is used. In brief, the following spatial resolutions have been adopted for simulations:

CALINE: 20 m

CALPUFF: 100 m (and 250 m on the largest domain for the base year simulation)

CALGRID: 500 m

As may be expected, the spatial resolution strongly influences the interpretation of data. For the BS1-TA (Salorno/Salurn) the simple cross-correlation of observed and measured values of NO_2 at the nearest point to the source is reported in Fig. 7.85 and it is quite clear that at this scale the better performance can be obtained by using the model CALPUFF. Another comparison for the BS2-TA (Aldeno) is sketched looking at the cross-section with respect to NO_2 and PM10 (Fig. 7.86 and 7.87, respectively). It is clear that the greater the model grid size, the larger the area over which the results are averaged and thus the greater the differences with single-point measurements.

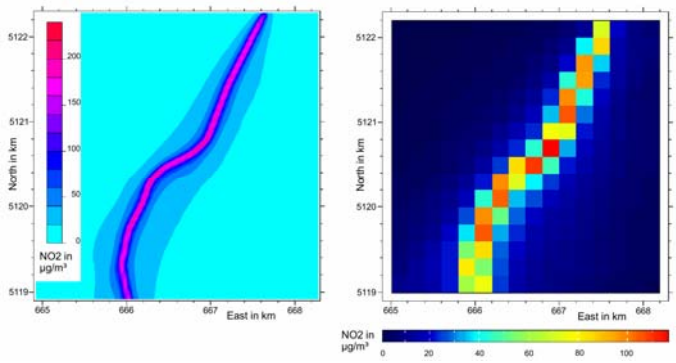

Fig. 7.84 Comparison between small and large scale results: CALINE – CALGRID (24-h average on 18 Jan 2006 – BS1-TA)

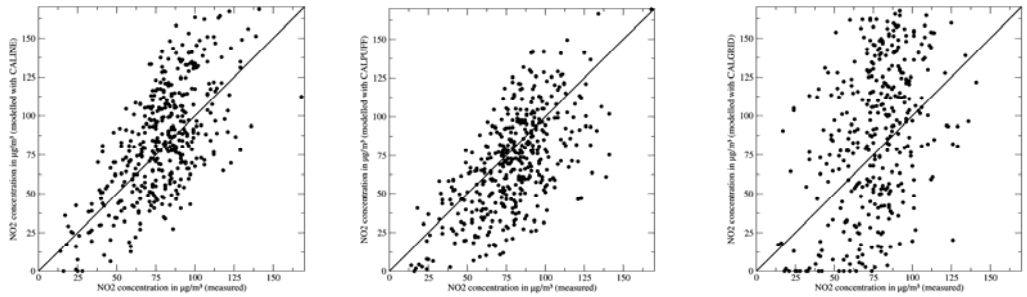

Fig. 7.85 BS1-TA NO_2 correlation (measured vs. observed) over the IOP for the CALINE model (left), the CALPUFF model (centre) and the CALGRID model (right).

From the above considerations, the CALINE model works well in the near range, but, due to the Gaussian approach, it does not accounts for "memory effects", i.e. in periods when wind direction changes from downwind to upwind with respect to the source axis, the concentration suddenly changes from a higher value to near zero or vice versa. This effect may give a poor overall performance.

On the other hand, the results of the Euler model CALGRID model are remarkably smoothed, because this model is not able to work with grid cells smaller than 0.5 km for numerical reasons. Therefore, the model tends to underestimate the concentration near the source, because the Euler scheme immediately spreads the emission over the whole volume of the grid cells which contain the motorway.

These drawbacks are clearly related to the specific kind of application for which the models are adopted, i.e. the spatial and temporal scales requested for the evaluation of air-pollution loads.

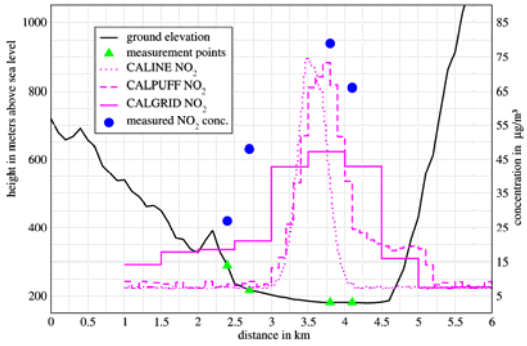

Fig. 7.86 BS2-TA cross section: NO_2 average values obtained by means of the different models and compared with measured values. Data are referred to the IOP.

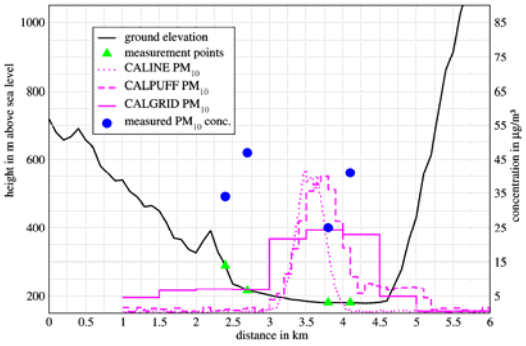

Fig. 7.87 BS2-TA cross section: PM10 average values obtained by means of the different models and compared with measured values. Data are referred to the IOP.

7.2.2.8 Conclusions

Some indications can be given on the basis of the shown results with respect to the three tested simulation models:

CALGRID is not suitable for local scale analysis of the motorway impact, as it is quite impossible to catch the near field dispersion in the simulation; on the other hand it seems to perform better on the long range transport.

CALINE performs well only in the near range near the source if well calibrated (it is the case of the IOPs) and where the main source is dominant. It should not be used for distances beyond some hundreds of metres from the source or where orographic influence is present in any case.

For the scope of the project CALPUFF comes out to be the most suitable and performs better than the other two models in the middle range simulations

As a conclusion, the CALPUFF results for the yearly average (referred to the 2004 base year) of both NO_2 and PM10 concentrations due to the A22 motorway between Bolzano/Bozen and Verona along the Adige/Etsch Valley are reported in Fig. 7.88**.**

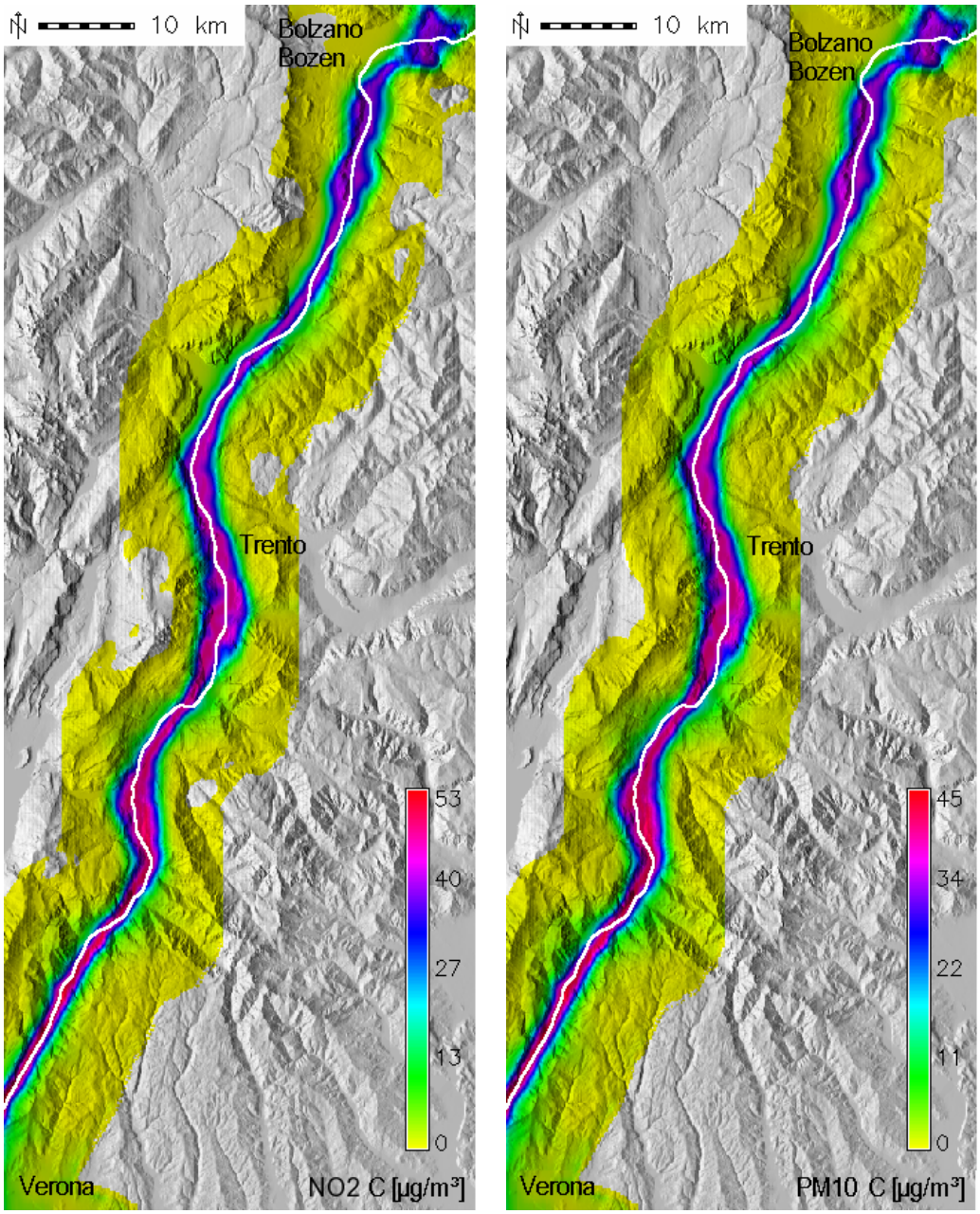

Fig. 7.88 NO_2 and PM10 yearly average concentration determined by the motorway as the result of the modelling chain described in **Section 7.2.2.7**.

7.2.3 Health impact

7.2.3.1 Exposure assessment

The first step for assessing health risk of transport-related air pollution is the evaluation of the population exposure to air pollutant concentrations. Beginning from the emission scenario (traffic flow, traffic composition, emission factors) and meteorological data, the air pollutant concentrations can be modelled using air quality dispersion model such as CALPUFF. Using a GIS support (GRASS in the present case) the population living near the motorway can be combined with the air pollution concentrations. Combining data of population with the same spatial resolution of the air dispersion model one can obtain maps of the distribution of exposed population. The use of exposure-response functions subsequently allows to quantifing the health effects and their distribution on the examined territory.

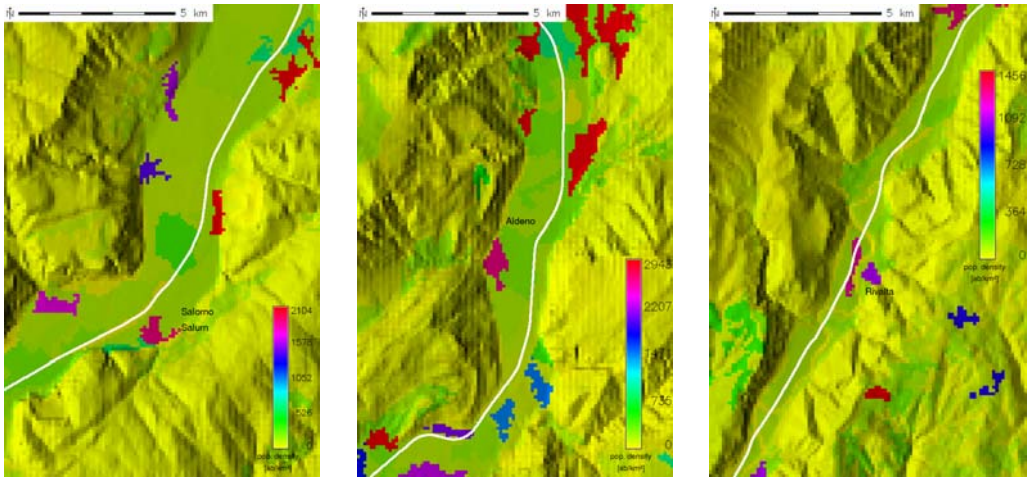

Fig. 7.89 Details of the distribution of the population living in the three target areas. From left to right: BS1-TA Salorno; BS2-TA Aldeno; BS3-TA Rivalta.

This kind of exposure assessment can be applied to evaluate the effects of the macro-pollutants emitted by road transport, such as PM and NO_2. In fact people are exposed to these pollutants exclusively by inhalation route. For assessing exposure to toxic and persistent atmospheric pollutants multiple pathways impacts must be considered. All possible routes by which contaminants enter the body of an exposed person must be taken into account – inhalation, ingestion of food or drink, ingestion of soil and adsorption through skin – because such patterns directly affect the magnitude of exposure to substances present in different indoor and outdoor environments. The assessment of exposure combine information regarding soil pollutants deposition, use of the soil, and modality of permanence of the subjects in different exposure places.

7.2.3.2 Health risk assessment

In order to have less uncertainty related to the proposed health impact assessment methodology some additional information about the population living in the impact area is necessary. Besides, more information on population lifestyle may improve the results.

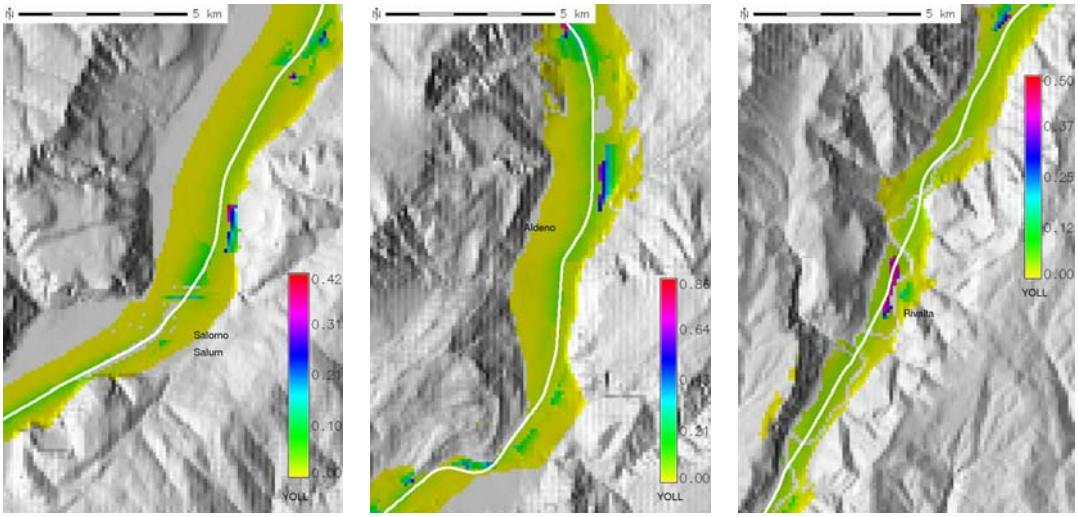

Fig. 7.90 GIS impact representation in the three target areas: coloured scales represent the exposure impact in terms of years of life lost (increasing from yellow to red). From left to right: BS1-TA Salorno; BS2-TA Aldeno; BS3-TA Rivalta.

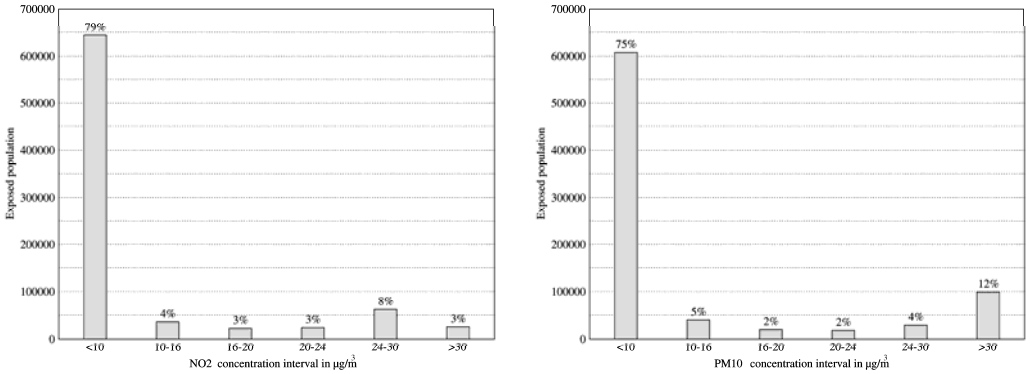

Fig. 7.91 NO_2 and PM10 exposure indicators representing the population amount living under specific pollution concentration levels.

The procedure described in Section 6.3 has been applied, taking into consideration all the available information, namely the pollutants concentration, the population living in the area and the exposure-response functions. In the present case the methodology implicitly considers the specific meteorological conditions of the alpine territory too.

The three target areas are characterized by different living conditions (Fig. 7.89): the most populated one is the BS2-TA (Aldeno), southern of the city of Trento, with about 30,000 residents. In the BS1-TA (Salorno/Salurn) live about 12,000 people whereas in the BS3-TA (Rivalta) the population consists of about 6,500 people. The adopted "exposure indicator" (see Section 6.3.3.3) represents the portion of the population living under specific pollution concentration levels. The levels have been determined as a function of the legislative air quality standard.

The exposure of the population and the consequently impact depend on pollutants concentration and population density within the area. The population exposure can be therefore displayed as a map in which each grid cell value is given by the product of population by concentration, as shown in Fig. 7.90 for each single target area during the IOP. It can be observed that in BS3-TA the population appears to be relatively more exposed.

The analysis carried out on the three target areas has been used for the model setup and validation; nevertheless, in order to assess the economic impact a more extended spatial domain and a reference period at least one year long should be taken into consideration. Therefore, the same assessment methodology has been applied to the whole area for the base year 2004.

The distribution of the population living in the area is reported in Fig. 7.92. The area is characterized by the presence of two relatively populated towns (Trento and Bolzano) and some smaller ones; the city of Verona is located just at the south-west border of the computational domain. Most of the population is situated along the valley bottom, quite close to the motorway route.

The indicators representing the population amount living under specific pollution concentration levels are reported in for NO_2 and PM10 in Fig. 7.91.

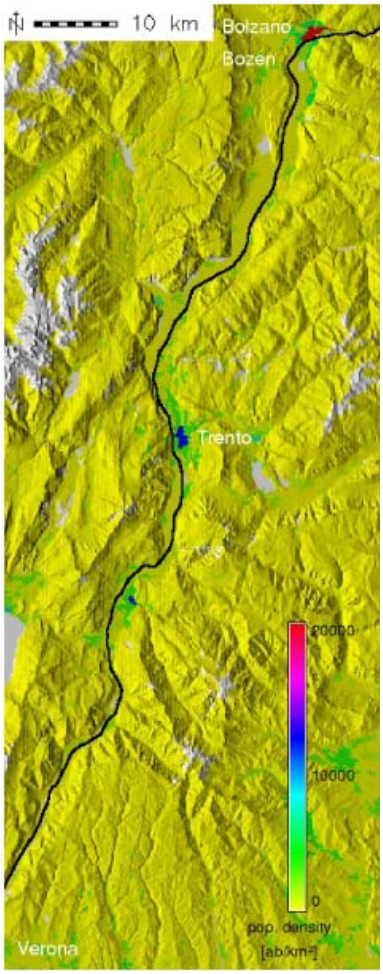

Fig. 7.92 Distribution of the population living in the whole Brenner-South Target Area.

It clearly appears that, especially for PM10, a still considerable fraction of citizens are living under the highest concentration class condition; this could be typical in the alpine valleys where the residents are frequently living along the valley floor, close to the major transit routes. This observation is also supported by the map of the population exposure, representing the product of population by concentration, as reported in Fig. 7.93.

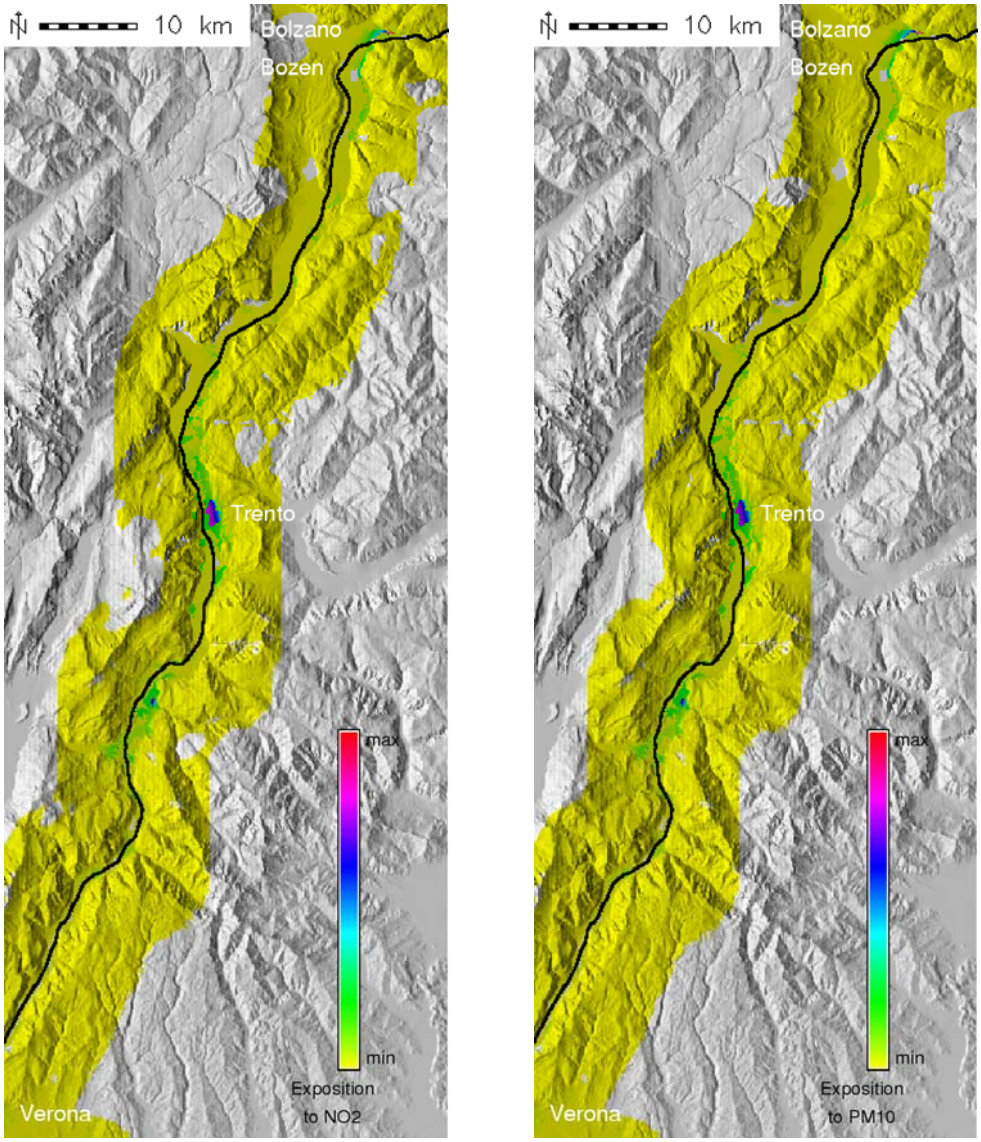

Fig. 7.93 GIS impact of NO_2 (left) and PM10 (right) representation in the whole Brenner-South Target Area.

In order to quantify the health impact, two parameters have been adopted: the "hospital admissions" (number of additional cases of hospitalization) and the YOLL (Years Of Life Lost) referred to the motorway traffic pollution. The parameters refer to one year (namely the 2004 base year taken as a reference) and to the total population living in the whole area.

The results of applying the functions defined in Tab. 6.19 of Section 6.3.4.2 are summarised in Tab. 7.9.

Subsequently to the impact calculation, also the economic assessment has been carried out, considering a unitary cost of 4,320 € for the hospital admissions and 50,000 € for the YOLL index. These unitary costs refers to those applied in the EcoSense software (IER, 2004) adopting the ExternE methodology. The results of the costs evaluation are reported in terms of EUR per capita in **Tab. 7.10.**

Tab. 7.9 Externalities of damages

	NO_2	PM10
Hospital Admissions [number of cases / year]	7	13
YOLL [number of Years Of Life Lost / year]	1.320	2.449

The obtained results show as the relative costs due to the emissions of PM10 mainly contribute to the total costs (65 %) while the NO_2 contribute for 35 %. It is to be marked also that the costs are due almost exclusively to mortality.

Tab. 7.10 Economic assessment of the hospital admissions and YOLL (€ per capita)

	NO_2	PM10
Hospital Admissions	0.04	0.07
YOLL	81.05	150.38
TOTAL	81.09	150.45

It should be remarked that these results are peculiar of this target area and can not be transferred to different condition. However, the obtained costs are comparable with the results of analogous studies. In the WHO study of evaluation of externalities due to traffic in Austria, Switzerland and France (Sommer et al., 1999) they have been calculates costs, regarding only the PM10 pollutant, between 158 and 588 € pro capita with the lower value related to the alpine regions. In his study the weight of the morbidity costs result greater because of the consideration, besides the hospital admissions, of some others morbidity costs like chronic bronchitis, bronchitis, restricted activity day and asthma attacks. Furthermore it has to be considered that that analysis refers to the total impact of the traffic in the whole national territory.

7.3 Fréjus Corridor

7.3.1 General information

7.3.1.1 Road traffic data

One difficulty when handling traffic data, is to deal with heterogeneous information. This is due to the fact that different management authorities (motorway, main roads), from different countries (France-Italy) are involved. An important part of the work was dedicated to the construction of a consistent traffic database, introducing assumptions to complete possible lacks of information. Year 2004 was chosen as the base year for the studies made on the Fréjus corridor, with focuses on February and July months.

Base-data needed for air pollution simulations (the most constraining) are hourly distributed traffic flows, and ratios between different categories of vehicles. However, hourly distributions of traffic were not available for all homogeneous sections of motorways and main roads. These data have been reworked separately for the all the roads depending on the level of accuracy provided by counting stations.

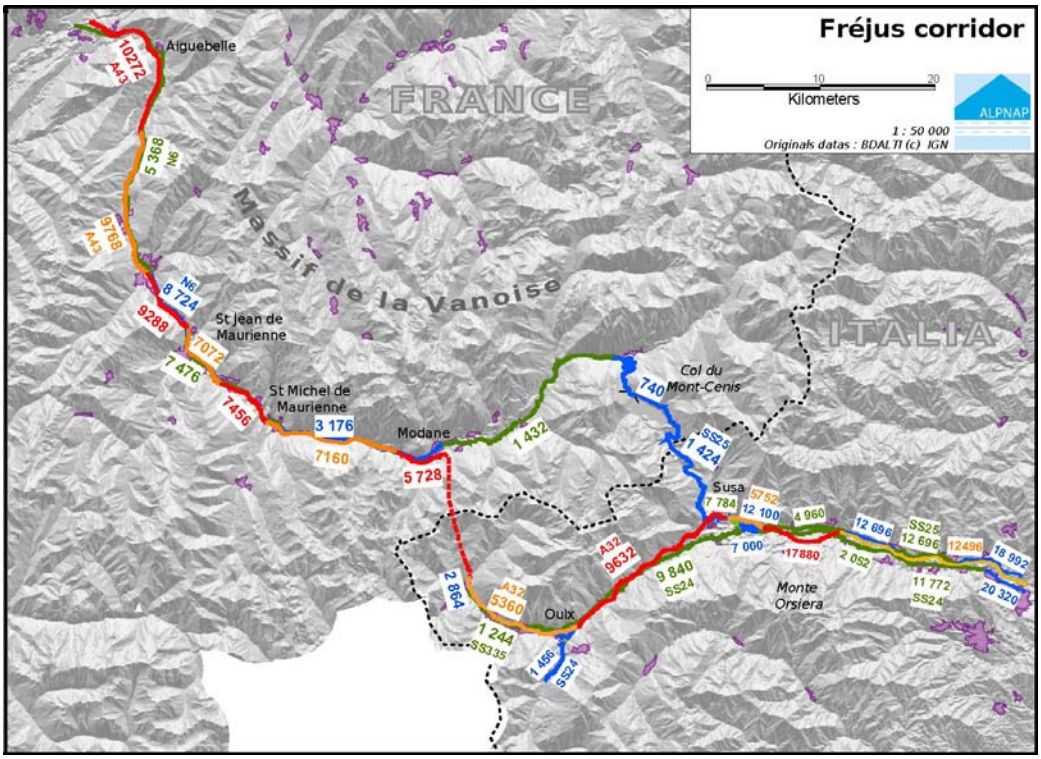

Fig 7.94 Roads traffics (annual average daily traffic (AADT) in the base year 2004) on the Fréjus target area.

French A43 motorway is divided into seven homogeneous parts, for which annual average daily traffics were available from SFTRF (Société Francaise du Tunnel Routier du Fréjus).

The counting station situated at the toll station of Modane, records hourly and daily data. The assumption was made that these distribution should be approximately the same on the six others sections where detailed temporal information is missing. The error made is probably small for heavy vehicles since their number is almost constant all over A43 sections (between 3100 and 3400 veh/h).

On the national French road network, the data base given by the local road administration (DDE de la Savoie) are detailed, by vehicles categories (heavy and light), day by day, all over 2004 from six permanent traffic counting stations: 5 along the RN6, from downhill to uphill, Argentine, Pontamafrey, Saint-Michel de Maurienne, Orelle et Mont-Cenis and one along the RD902 in Bessans. From the hourly data, given separately for light and heavy vehicles in front of three permanent traffic counting stations in Argentine, Pontamafrey and Orelle, during two weeks on 2003, it has been possible to rebuild spreadsheets of hourly data, by category (LV and HV), and according to the typology of day (workday, Saturday, Sunday and holiday). The very good coherency between these three distributions allowed to generalize them with average distribution histograms for the whole national network, and to distinguish workday, Saturday, Sunday and holiday traffic volumes (see Fig. 7.95).

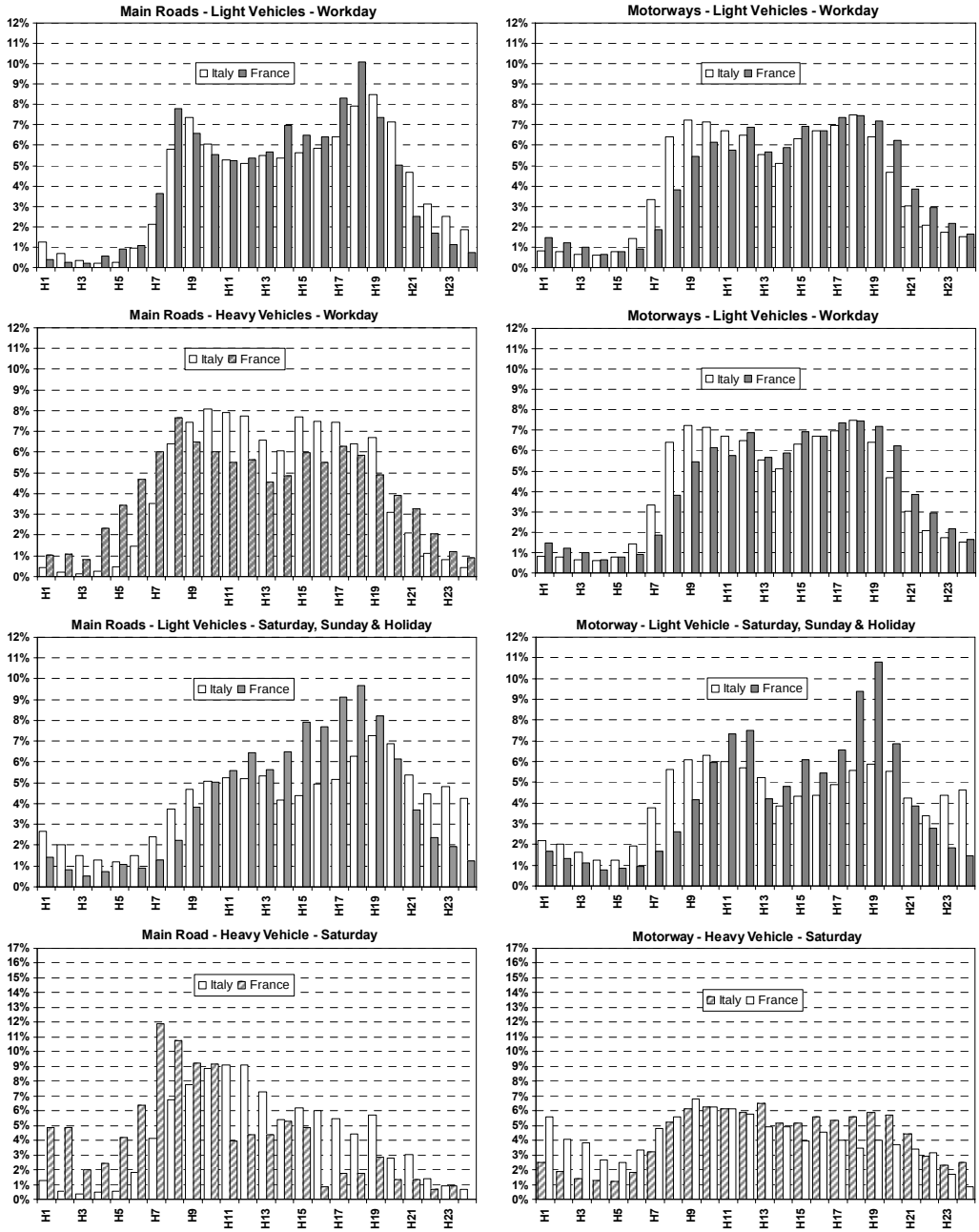

Fig. 7.95 Traffic modulations on main roads and highways of the Fréjus corridor for both light and heavy vehicles.

On the Italian side of the Fréjus corridor, traffic related data comes from traffic modelling completed with punctual counting records. This modelling is based on a simplified geometry of the major roads network. It gives, among others results, the traffic during the ninth hour of an average weekday for each way. The hourly distribution is rebuilt from given hourly distributions based on the ninth hour of a reference day. The same process is used to obtain daily and monthly data. Distribution histograms are available for both motorways and secondary roads.

Considering the value given by the modelling as an average month, it was possible to reconstruct hour by hour, and day by day, the whole traffic data el (light plus heavy vehicles) on each section of the model in the year 2004.

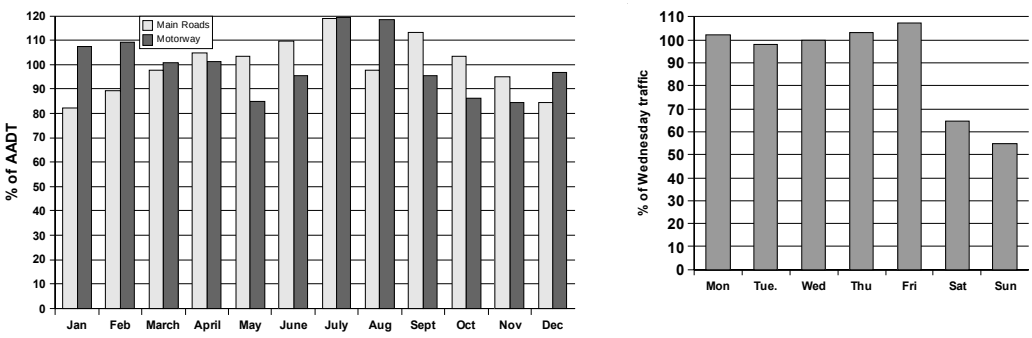

Fig 7.96 Example of monthly distributed traffics (in % of the AADT) on the Italian networks.

Concerning the traffic data across the highway A32, significant traffic discrepancies between the Italian modelling data and the French counting data have been noticed. Its origin has not been determined. After consulting of the « Società Italiana Traforo Autostradale del Fréjus » SITAF[4], we observed this time a good coherency with the data collected on the French side. The average daily traffic data of the A32 motorway at Italian entrance of the Frejus tunnel, the Salbertrand's pay toll (between Oulx and Suza), and the Avigliana's pay toll (downhill from Bussoleno) were utilised.

The Italian main roads network is composed of 3 itineraries, SS335 between Bardonecchia and Oulx, SS24 relating Sestrières – Oulx – Susa – Bussoleno (the south of the valley) and SS25 linking Montcenisio – Susa – Bussoleno (north of the valley).

The traffic data that vary from section to section on each itinerary have been simplified. Homogeneous sections have been merged on the basis of average traffic values. In-situ observations helped to perform this simplifying process. The number of heavy vehicles was determined from a few punctual counting stations, placed on the downhill side of the Susa valley (district of Susa along SS24 and SS25). It has to be underlined that the portion of heavy trucks is extremely low (between 1 and 2 %). Finally the upper bound estimating was kept, excepted for the Mont-Cenis pass access where the data collected by French counters have been propagated on the Italian side. Finally the national road network has been split into fifteen homogeneous sections, along the three itineraries. Comparison of average hourly distributions estimated on Italian and French sides shows a good correlation between data. Some discrepancies can be noticed for heavy trucks revealing contrasted

[4] http://www.sitaf.it

driving habits in both countries. Some adjustments were finally made to insure the coherency between Italian and French data at the border, inside the Frejus tunnel and at the Montcenisio pass.

7.3.1.2 Railway traffic data

The choice and accuracy of railway traffic data was driven by noise indicators. Then, the traffic distributions over each regulation period [6-18h], [18-22h] and [22-6h], and according to three great classes of trains (freight, regional train, international train) have been collected from Italian and French sources. Data, provided by the French railway infrastructure manager "Réseau Ferré de France" (RFF), are traffic distributions for an average week of October 2004, on a model cross section of the Maurienne valley, near Saint-Avre-La-Chambre. Daily average traffic data on the French acoustic regulation period [6-22h] and [22-6h] were also available on the different sections of the Maurienne valley.

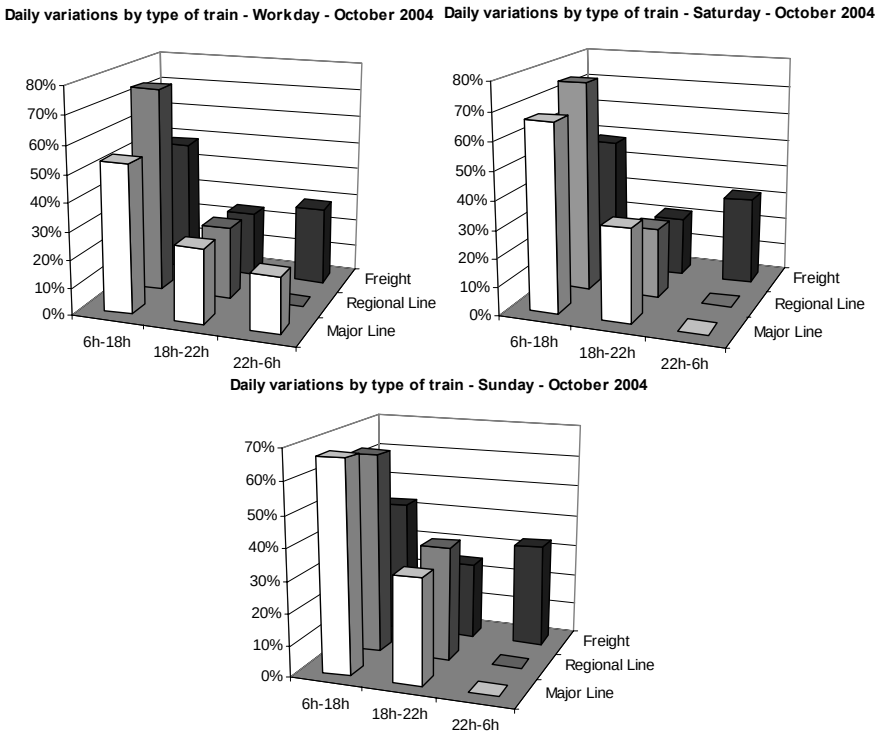

Fig. 7.97 Distributions of trains for a average workday, an average Saturday and an average Sunday.

Traffics are given according to six types of trains (freight, goods, regional train, major line train, TGV high speed train, isolated locomotive). A top and a commercial speed are associated to each type of train, and each section. The minimum of these two speeds was retained for the acoustic simulations.

The French railway network in the Maurienne valley has been split into 7 homogeneous sections with regard to traffic volumes and speed (Tab. 7.11).

Tab. 7.11 Train traffic. The seven homogeneous sections in the Maurienne valley

Sections	Daily Average Trains Traffic (trains/day)	Top speed (km/h)
Saint-Pierre d'Albigny – Aiguebelle	386	150
Aiguebelle – Saint-Jean de Maurienne	386	130
Saint-Jean de Maurienne station	386	110
Saint-Jean de Maurienne – Saint-Michel de Maurienne	210	110
Saint-Michel de Maurienne – Modane	210	95
Modane station	440	30
Modane – tunnel	440	75

From all these data, traffics corresponding to an average week for the year 2004 have been derived, for finally three categories of trains, as mentioned in Section 2.2.1.2. These traffic data are annual averages since the information about annual fluctuations was not available.

Traffic data on the Italian side were far less detailed as only passenger trains traffics (with hourly and daily distributions) were accessible, on the five following sections: Modane - Bardonecchia, Bardonecchia – Salbertrand, Salbertrand – Bussoleno, Susa – Bussoleno et Bussoleno – Borgone Susa.

For freight trains we assumed that all trains passing the Modane station on the French side run as far as Bussoleno on the Italian side. The same hourly distribution was implemented, but shifted to account for the travel time. Finally, traffic has been averaged for each period of an average workday, Saturday and Sunday, as illustrated in Tab. 7.12.

Tab. 7.12 Example of railway traffic data in the Susa valley. Number of trains for an average workday.

Sections	Type of trains	Day	Evening	Night	Speed (km/h)
Borgone Susa – Bussoleno	Regional	35	14	3	120
	International	3	3	0	130
	Freight	21	11	13	85
	Foods	49	23	29	95
Bussoleno – Susa	Regional	18	7	3	120
	International	0	0	0	130
	Freight	0	0	0	85
	Foods	0	0	0	95
Bussoleno – Salbertrand	Regional	9	4	0	110
	International	2	2	0	110
	Freight	11	5	6	75
	Foods	24	12	14	85
Salbertrand – Bardonecchia	Regional	17	7	0	110
	International	3	3	0	110
	Freight	21	11	13	75
	Foods	49	23	29	85
Bardonecchia – Modane	Regional	1	0	0	75
	International	3	2	0	75
	Freight	21	11	13	70
	Foods	49	23	29	70

7.3.2 Emissions

7.3.2.1 Air pollutant emissions

During Alpnap project, the choice was made to estimate emissions of nitrogen oxide and particulate matter with an aerodynamic diameter less or equal to 10 µm (PM10). Both pollutants are not concerned with fuel evaporation. At last, as the road network under consideration is only composed of main roads and motorways, the warming-up phase was neglected. Indeed, most of vehicles moving on main roads have already done some kilometres on secondary road network. The warming up phase is specially an important factor in case of urban networks. During Alpnap pro-

ject, methodology COPERT III (see Section 2.5.2.2) is used to determinate exhaust emissions from the thermal stabilised engine operation, also called “hot emissions”.

The rate load of heavy duty vehicle, which influences hot emissions, is fixed to 74 % as observed by the French National Institute of Transports and Safety (INRETS).

As COPERT III methodology is not able to take non exhaust emissions into account. The potential contribution of non-exhaust emissions can not be neglected, and emissions such as tyre wear, brake wear, clutch wear or road wear particles must be accounted for.

Tab. 7.13 PM10 non exhaust emissions (mg/km.vehicle)

Vehicle type	tyre	brake	clutch	road	Total
Passenger cars	7.7	3.2	2.5	7.5	20.9
Light Duty Vehicle	12	4.5	2.5	7.5	26.5
Heavy Duty Vehicle	83.3	12.4	2.5	38	136.2

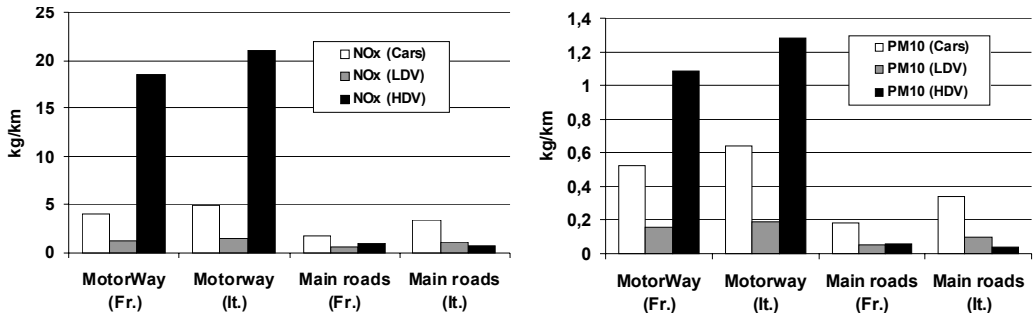

Fig. 7.98 Average daily NOx (left) and PM10 (right) pollutants emissions from motorways d main road on the French and Italy parts of the Frejus corridor. Base year 2004.

These non exhaust emissions have been computed using emissions factors suggested by a French interministerial workgroup[5].

The following values are used to estimate the non exhaust emissions of PM10. These emissions are directly added to hot emissions coming from COPERT III to obtain total emissions.

The study domain being localised at the border area, vehicles classification (according to the fuel used), the cylinder capacity of vehicles, and the legislative or technology steps as regards pollutants emissions, were considered as the same for Italy and France.

The graphs in Fig. 7.98 show the contribution of road infrastructures on both sides of the Frejus corridor for base year 2004. Data represent the daily average emission per kilometre computed from average annual traffic flows, and the contribution of each type of vehicle. Three categories of vehicles have been distinguished: cars, Light Duty Vehicles (LDV), Heavy Duty Vehicles (HDV). Ratio of LDVis not directly available from counting stations but was set to 23 % of cars according to national French figures.

Unsurprisingly motorways reveal to be the predominant source and emissions are quiet homogeneous between countries, slightly larger on the Italian side. This reflects the transit nature of the axis. More significant relative discrepancies are observed between main roads, indicating heavier local traffic in Italy. Overall, heavy vehicles are the main contributors to NO_x and PM10 emissions

[5] http://www.sante.gouv.fr/htm/dossiers/etud_impact/axgt_ei52.pdf

per km on motorways with a ratio between 4.2 and 4.5 compared to cars for NO_x and about 2 for PM10. The high proportion of HDV, lying between 25 and 60 % depending on the section, is responsible for this result. Conversely, cars emissions are predominant on main roads but remaining far below motorways total emissions on average.

The comparison of base year and modal shift scenarios leads logically to a dramatic decrease of the quantities of emitted NO_x and PM10: -53 % in the Maurienne valley, and -43 % in the Susa valley on average.

7.3.2.2 Acoustic properties of road pavements

The CPX measuring method, described in Section 2.6.2, has been used to characterize the acoustical properties of road pavements of main roads and motorways in both Maurienne and Susa valley. A two-day measuring campaign was performed during spring 2006, under good weather conditions (no rain).

For safety and practical reasons, the measurements were made on the slow lanes, and in only one direction. The assumption that both sides of the infrastructures have the same properties was judged acceptable for the roads under test. Hence, on A43 and A32 properties of pavements were determined in the France to Italy direction, and reversed for the main roads network. The large amount of data (10 m resolution) obtained during the experimental campaign have been stored in a database and analysed in a GIS tool (Fig. 7.99).

Using a thematic analysis, the road pavement characteristics have been estimated for each section, and the deviations to the reference pavement (see Section 2.6.2) ere applied to the noise power levels of roads simulated in MITHRA-SIG (Section 7.3.4.1). With this aim, the resolution was lowered to 100 m for easier handling of data. The results illustrated by Fig. 7.100 obtained on the Italian side, show the importance of characterizing road pavements accurately: about 10 dB (corresponding to a factor 10 on acoustic energy!) separates the best and worse pavements from the acoustical point of view. It can also be noticed that pavements on the motorway are on average, about 2 dB more silent than on main roads, in the Susa valley. Pavements in the Italian valley are also globally better than on the French part, with a difference of one to two 3-dB categories on average. These discrepancies can be due to different technical choices, and also to different years of achievement.

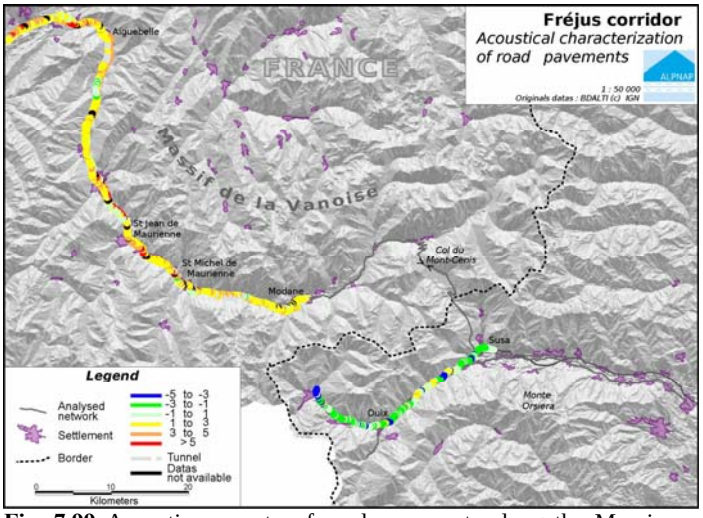

Fig. 7.99 Acoustic property of road pavements along the Maurienne and part of the Susa valleys.

7.3.3 The numerical simulations of high-pollution episodes

The study of the atmospheric pollution due to the traffic in a mountain valley involves a lot of physical processes and possible problems, related to the peculiarity of both meteorological and dispersive characteristics in such complex topography. The mean flow, having as a forcing the large scale motion, is heavily modified by the complex orography, and secondary circulations, like mount-valley breeze, superpose on it generating daily cycles of complex wind regimes. Also the turbulence due to the interaction of the flow with the topographical features, and thermodynamically by solar radiation, plays a fundamental role, especially in the dispersion of pollutant emissions. These particular conditions are clearly of great importance in determining the effectiveness of the dispersion of road traffic pollutant emissions, and cannot be treated with simplified models or parameterisations. Thus it is necessary to apply or develop properly sophisticated models that are able to reproduce this level of complexity.

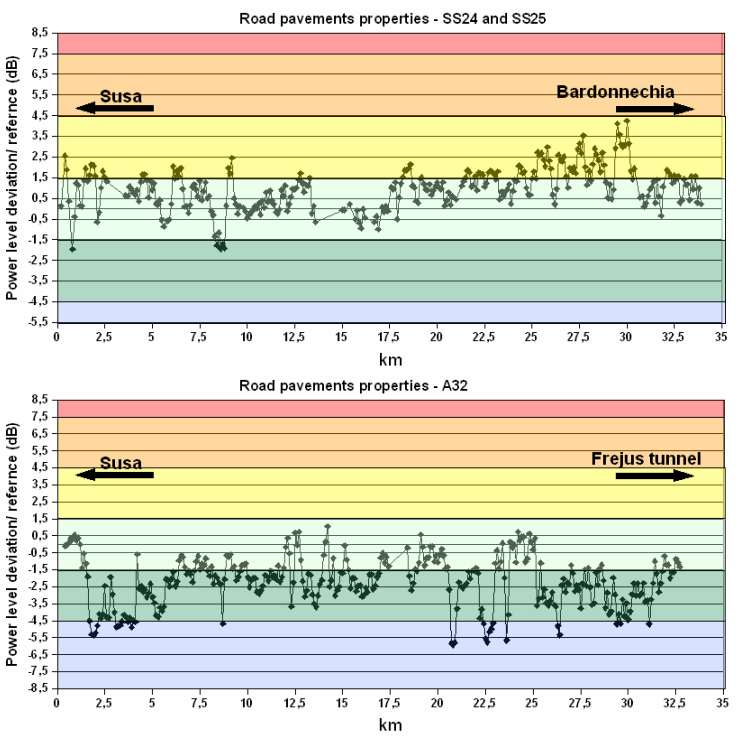

Fig. 7.100 Acoustical characteristics of roads pavements in the Susa valley, determined using the CPX method.

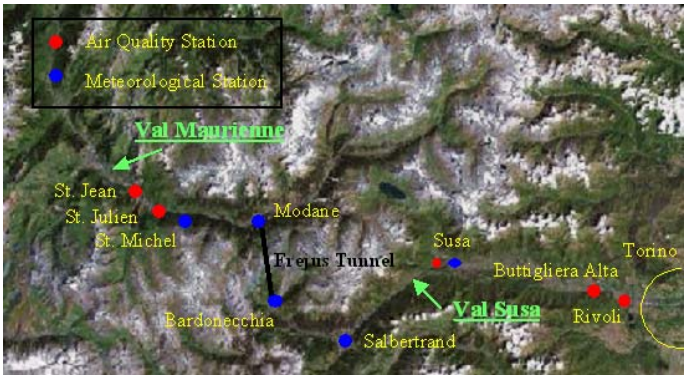

Fig. 7.101 The two valleys (Maurienne on the left and Susa on the right) with the air quality stations (St Jean and St Julien for the French side, Susa, Buttigliera Alta and Rivoli for the Italian side).

For a detailed reproduction of the atmospheric circulation in

Frejus transect area, a methodology to downscale from the regional to the local scale was applied. The pollutant dispersion, related to the emissions from the major traffic routes in Susa (Italy) and Maurienne (France) valleys, was then simulated in subdomains where the highest grid resolution of the meteorological fields is applied, namely 1 km and 100 m. Three periods, characterized by critical conditions of the dispersion scenarios, were chosen in the reference year 2004. The prognostic modelling system RMS (RAMS-MIRS-SPRAY) was used for the simulation of atmospheric circulation and pollutant dispersion down to 1 km resolution. To obtain the meteo fields at 100 m resolution, a mass-consistent diagnostic model, MINERVE was used in cascade after RAMS and in input to SPRAY. Here, a discussion of the methodology and some illustrative examples of the main results are presented.

7.3.3.1 Selection of the simulation periods and domains

One of the final goals of the ALPNAP Project was to present and make available advanced methodologies to estimate the traffic-induced air pollution and noise along the major Alpine routes and to evaluate their impact. In this frame, the approach adopted for the Frejus transect was to interface the different skills and tools of the participating partners and to establish a common procedure and methodology that can be adopted for further applications.

On this basis, we firstly proceeded in identifying some episodes, in the base year 2004, typical of both winter and summer seasons, in order to characterise the most critical meteo-diffusive situations at the local and regional scale. For this reason, we considered the observed concentrations of the main pollutants in 2004, that is the annual trends of hourly averaged NO_2 and daily averaged PM10, in all the available measuring stations in Susa valley (Susa, Rivoli and Buttigliera Alta) and Maurienne valley (St. Jean and St. Julien), also referring to the European law limits. Anomalous values of concentration records in particular conditions were highlighted, like peaks in the traffic correspondent to week-ends or summer/winter holiday periods.

It was thus possible to single out some critical episodes, characterized by high pollutant concentrations during a well marked period. Since the high pollution episodes of course do not generally occur simultaneously in the Italian and French sides, we took care of including the most interesting periods identified for the two across-Alps domains.

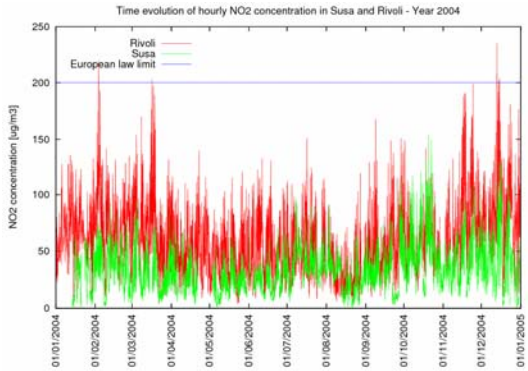

Fig. 7.102 Annual trend of hourly NO_2 observed concentration in Susa valley for base-year 2004.

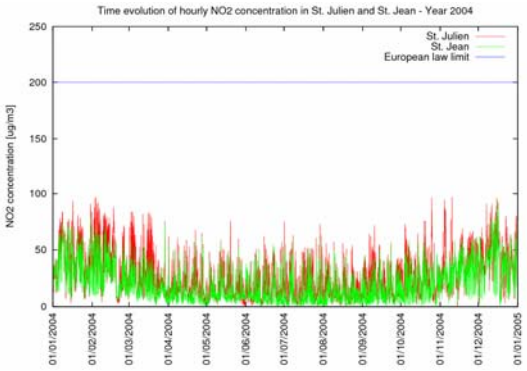

Fig. 7.103 Annual trend of hourly NO_2 observed concentration in Maurienne valley for base-year 2004.

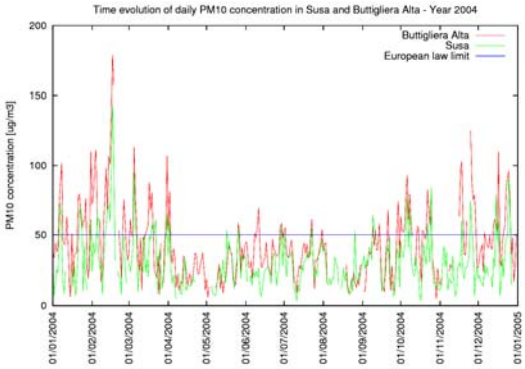

Fig. 7.104 Annual trend of daily PM10 observed concentration in Susa valley for base-year 2004.

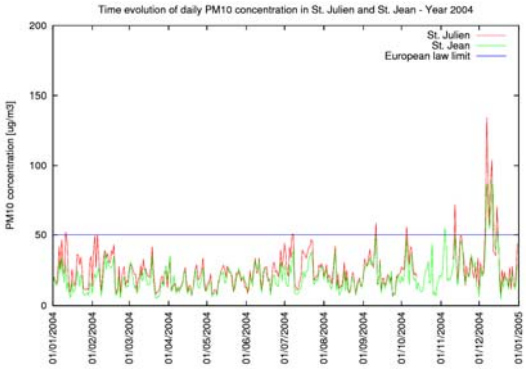

Fig.7.105 Annual trend of daily PM10 observed concentration in Maurienne valley for base-year 2004.

Figs. 7.102 to 7.105 depict the diagrams of the annual observed concentration trends, hourly for the NO_2 and daily for the PM10, in three towns of the Susa valley, Susa, Rivoli and Buttigliera Alta, and in two urban centres of the Maurienne valley, St Julien and St Jean, for the year 2004.

The diagrams show that there are several periods of the year during which the peaks of concentration exceed the European law limits. We selected the three episodes looking at periods where in both Italian and French sides or the limits were exceeded (this in particular for PM10) or, if not, there was anyway a contemporary concentration peak.

We identified three periods, as follows:

– one Summer episode: 03 – 13 Jul 2004

– two Winter episodes: 10 – 20 Dec 2004 and 08 – 18 Feb 2004

To confirm the suitability of the choice of these episodes, we also examined the related meteorological conditions.

The selected periods were generally characterized by atmospheric high pressure, no perturbation and consequent absence of precipitation. To detail the atmospheric conditions during the highest concentration days, we analysed the wind speed and temperature time evolution at the surface and, to gather information on the atmospheric stability of the boundary layer, the temperature vertical profiles in Cuneo Levaldigi and Milano Linate radiosounding stations. For each episode, a full week was simulated with our modelling system, so to analyse the typical cycles, daily and weekly, of interest. From the simulation results, the ground level concentration distribution and its hourly and daily maximum values were extracted for the different pollutants.

The results of the simulations, both of meteorology and dispersion, can be then compared with the observed meteo fields and air quality data, available from Italian (ARPA Piemonte) and French Agencies (Meteo France, CETE and CSTB).

A second important aspect for a reliable and efficient numerical description of the atmospheric circulation and dispersion is the proper definition of the simulation domains. The area of interest includes the Susa valley, extending along the East - West axis from the town of Torino to the village of Bardonecchia, at the Italian Frejus entrance, and the Maurienne valley, extending mainly along the South - North axis, from Modane village to Aguibelle, towards Chambery. The full domain of interest is then about 150 km E–W and 100 km S–N. To identify sub-regions of interest

for critical conditions of noise and air pollution impact on 07 and 08 Nov 2005 a survey in the Susa and Maurienne Valleys was organized. The location of urban centres, the positioning of the highways and national roads inside the valleys, the characteristics of the air and noise pollution sources, the typology of the traffic and the road infrastructures (tunnels, viaducts) were assessed.

In complex terrain the mesoscale and local scale circulations, related to the presence of main and lateral valleys, ridges and landuse heterogeneity (resulting in features such as air stagnation regions in the lee of obstacles, separation of the flow and differentially heated valley walls) superimpose over the large scale circulation. Thus, to correctly reproduce the meteorology of the region, we have to take into account also the forcing of the synoptic circulation, possibly describing the interaction between the large scale processes and the local and small scale ones.

In RAMS metorological model (see Sections 3.3.3.2 and 7.3.3.3) a two-way nesting procedure allows to optimise the interaction between the different scales. We configured the simulation using four nested grids: the main outer one covers a domain of 1000 × 1000 km^2, where the main large-scale topographical features of Northern Italy and Southern France, till the Pyrenees and the Northern Mediterranean Sea to the West, and the total Alpine arc from West to East, are included (Fig. 106). The next two intermediate grids zoom over the area of interest and they are chosen to be compatible with the main local topographic features. The last domain, having the highest resolution, is focused over the selected Frejus area previously introduced. In the vertical, a stretched grid is used, with the highest resolution of about 25 m at the surface.

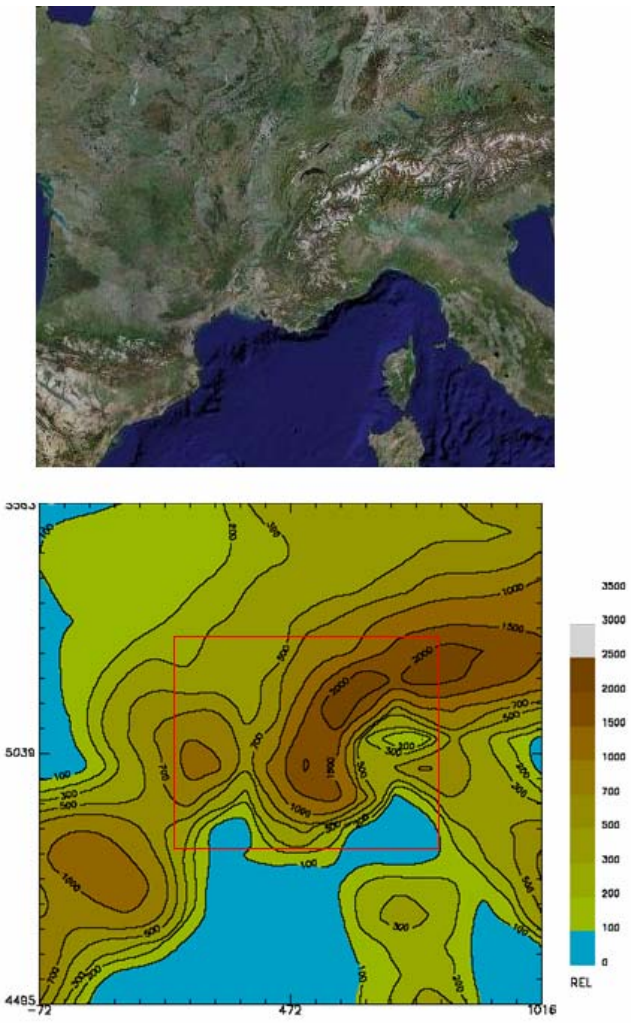

Fig. 7.106 Outer grid domains for the simulations 1 and 2.

The 3D configuration of the grids 1 and 2 is respectively 1088 × 1088 × 17 km^3 with a horizontal grid mesh of 64 × 64 km^2, and 592 × 464 × 17 km^3 with a grid mesh of 16 × 16 km^2.

For the study of the regional scale, in cascade to the circulation model RAMS and after MIRS boundary layer processing, the simulation of the dispersion with SPRAY model was thus performed in the smallest

and most refined domain, 1 km resolution.

For the study of the more local characteristics of the flow and dispersion, after RAMS the MINERVE mass-consistent model was applied to downscale to 100 m in horizontal and using a finer streched grid in the vertical, over the same smallest RAMS domain. Afterwards, some sub-domains in this area were chosen to run SPRAY dispersion model, using the meteorological fields obtained on the grid with the finest resolution of 100 m.

In modelling the atmospheric circulation with RMS, we performed two kinds of simulations that we define as *preliminary* and *definitive*. In the first case, the fourth smallest inner RAMS domain includes a large part of the two valleys, the city of Torino and part of its surrounding plain. The aim of these simulations is to provide an estimation of the possible differences in the performance of the modelling system when applied in flat or complex topography. Moreover, the presence of an important urban centre like Torino, where many good quality and accurate observation datasets are available, represents a valid benchmark for testing the reliability of the models in such heterogeneous conditions.

The definitive simulations consider instead a reduced domain for the smallest inner grid, including the most part of the two valleys converging into the Frejus transect, with their main roads and railways but excluding the big urban centre of Torino.

We stress that all these choices are also conditioned by a reasonable compromise between the degree of details of the output information and the affordable computational effort, both in time - duration of the simulation - and in space - collection and storage of all output files and data.

7.3.3.2 Brief description of the modelling system used in ALPNAP Project

The RMS modelling system is built as the off-line interface between the meteorological model RAMS (Regional Atmospheric Modeling System, Pielke et al., 1992; Cotton et al., 2003) and the Lagrangian stochastic particle model SPRAY (Tinarelli et al., 1994a and 1994b; Tinarelli et al., 2000), through the boundary-layer parameterisation code MIRS (Method for Interfacing RAMS and SPRAY, Trini Castelli and Anfossi, 1997; Trini Castelli, 2000). The advantage of an off-line approach is the independence of the two models and the consequent flexibility, so that different configurations for the dispersion description can be set and tested once that the meteorological fields are given.

RAMS is a prognostic non-hydrostatic model, world-wide adopted in the atmospheric numerical modelling community, and it is briefly described in Section 3.3.3.2**.** The RAMS versions 4.4 and 6.01 (an ISAC-CNR modified version of RAMS 6.0) are used by ISAC-CNR. In the ALPNAP Project we took advantage of the two-way grid interactive procedure and of the non-hydrostatic option, to downscale from a large-scale area to smaller scale domains characterised by higher resolutions, in this way accounting for most spatial scales that are relevant for the Alpine meteorology.

In the RMS system, two RAMS components are used, the data analysis package and atmospheric-core, while the post-processing phase is handled by the interface code MIRS.

MIRS is a boundary-layer module, which ingests the meteorological fields produced by RAMS or, alternatively, other kind of data fields, deriving by observations or diagnostic models. Topography, wind speed, potential temperature is the minimum information requested, then turbulent kinetic energy, diffusion coefficients and surface fluxes are treated when available. MIRS calculates the surface layer and boundary layer parameters, the friction velocity, the temperature scale and Monin-Obukhov length, the PBL height, the convective velocity, the variances of the velocity

fluctuation, the local velocity decorrelation time scale and the third and fourth moments of the vertical velocity fluctuations. Several alternative options are available for the parameterisations of the atmospheric boundary layer and turbulence processes. The fields of data are then processed to prepare a meteorological file in the appropriate format and with the temporal sequence of interest to be used by SPRAY as input information. The version 3.0 of MIRS is used as interface between RAMS 4.4 and SPRAY 3.0, while a new version MIRS 4.0 is linking the most updated models RAMS 6.01 and SPRAY 4.0.

SPRAY is a Lagrangian particle model simulating the 3D dispersion of chemically neutral airborne species in complex real conditions, and it is briefly described in Section 4.4.2.2. The version adopted for this work uses the most recent developments, optimizing the performances in complex simulations.

7.3.3.3 Numerical simulations for the meteorology: RAMS and MIRS

To present the results of the simulations of the atmospheric processes and meteorology, in the following we focus our discussion on the comparison between the model predictions and observations at the surface. As discussed in Section 3.4.1, from a direct comparison between observations and predictions we cannot expect a point-to-point agreement. We may consider results as satisfactory when the typical atmospheric observed daily cycle is reproduced, when the range of values of the mean variables (ex. wind speed and direction, temperature and humidity) is well caught and representative of the seasonal characteristics, that is when simulated variables correctly reproduce the mean trend of measurements.

In general, to produce the simulated fields at a specific surface station, it is possible to interpolate on its location the values simulated at the grid points surrounding it, considering also a vertical interpolation from the closest model levels to the height of the site.

Since we are dealing with highly complex topography and landuse heterogeneity, in particular when considering a 1 km grid resolution, we decided to plot the predicted data of the first model level (about 24 m high) at the four grid points around the station, in order to highlight the possible differences due to the different altitudes of the points (as noted in the figure's legend, the altitudes of two next grid points can be even 300 m different). We recall that, in general, the surface station wind velocity is measured at 10 m above the ground and the temperature at 2 m or, when the mast is located over a roof, generally in urban sites, at higher heights (for instance, in Torino three meteorological stations – Torino-Consolata, Alenia and CSELT – are located on a building roof at a height of 30 m above the ground level).

For every considered period, we compared the time evolution of the simulated wind speed and direction and air temperature against the measured data. The comparisons have been carried out at several stations in urban centres and villages in the two valleys, Torino, Susa, Salbertrand, Bardonecchia for the Susa valley and Mont Cenis, Modane, St. Michel de Maurienne and St. Marie de Cuines for the Maurienne valley. In the following, we present a few results that are representative of the most important outcomes and findings.

Preliminary simulations and results

For the group of preliminary simulations, inside the smallest domain we have included the town of Torino and part of its surrounding plain. The 3D configuration of the grids 3 and 4 of RAMS-MIRS models is respectively $196 \times 132 \times 17$ km^3 with an horizontal grid mesh of 4×4 km^2, and $133 \times 61 \times 17$ km^3 with a grid mesh of 1×1 km^2.

As it can be seen comparing Fig. 7.106 with Fig. 7.110, with a resolution of 4 km and 1 km the details of the topography definition improve with respect to the larger domains (grid mesh widths of 64 and 16 km respectively). In particular, thanks to the finer resolution, it is possible to better characterize the main Alpine range in the territory.

In Fig. 7.107 we compare the simulation against observations at Torino-Consolata station, located in the centre of Torino. We consider this station as a reference since it provides measured data of high quality and it is fully representative of the urban characteristics. It represents a severe test for the reliability of the model simulations, since the city is identified in the regional scale mainly through its landuse and roughness, while of course the urban scale is not resolved. When the model is able to capture, on average, the mean variables at such kind of stations, then we can be confident in its good performances in less critical part of the domain. For instance, the relatively good agreement of the measured wind speed with predicted values at the four grid points around the station justifies the application of the modelling system at this resolution.

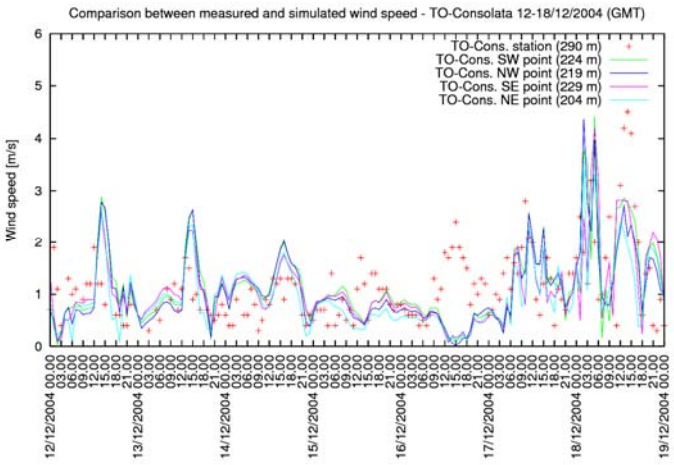

Fig. 7.107 Comparison between wind speed measured and simulated in Torino-Consolata station, December episode.

Analogous results are found also at high-mountain stations, like Bardonecchia and Modane, as in Fig. 7.108, which are the two villages hosting the entrances of the Frejus tunnel, both in the summer (July) and in the winter (December) episodes.

These preliminary runs were useful also to highlight a well known problem related to the modelling of the surface temperature in highly complex terrain, which occurs especially when simulating the meteorology in winter time. In fact, generally the mesoscale models, and in our case RAMS,

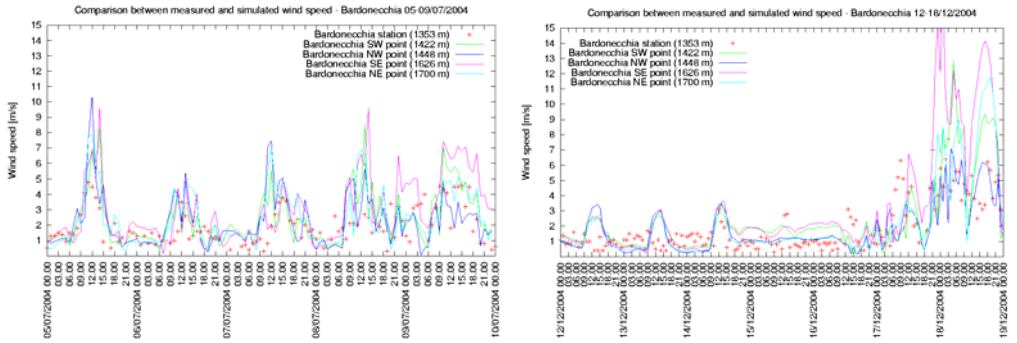

Fig. 7.108 Preliminary simulations. Comparison between wind speed measured and simulated in Bardonecchia for July (left) and December (right) episodes.

need an initial profile of temperature and humidity in the soil. These profiles represent the triggering-start of the soil model, which is part of the "engine" of the surface layer and boundary layer physical processes.

The international community of modellers and meteorologists recognised that the lack of observed data and information about the soil thermodynamic variables is one of the limits which can affect the performances of the numerical models. This problem becomes even more 'dramatic' for simulations of winter periods, since also the quality of information about the snow coverage is not yet optimal.

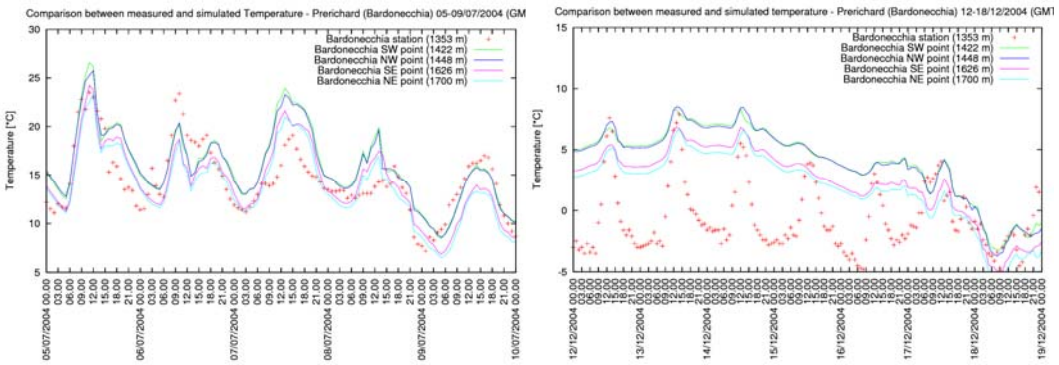

Fig. 7.109 Preliminary simulations. Comparison between temperature measured and simulated in Bardonecchia for July (left) and December (right) episodes.

In our preliminary simulations, we adopted as initial soil profiles of temperature and humidity the values extracted by the ECMWF analyses, which are provided with a resolution of 0.5 degree (that is, at our latitudes, about 50 km). In Figs. 7.108 and 7.109 wind speed and temperature trends at Bardonecchia in the episodes of July and December are plotted. In both episodes the wind speed is well reproduced, while for the temperature in July the agreement is satisfactory, but in December a very large difference between predictions and observations is registered. This was the worst case, but it is representative of the problem. We notice that in December episode the model is hardly able to become independent from the initial conditions, and only after 1 day of run startup and 5 days of simulation the predicted temperature start to match the measured value. In the first days, the daily cycle is not correctly reproduced and, in particular, the minimum values are not captured at all. This deficiency does not occur in the July episode, where the same 1 day run startup time was used.

To overcome this inaccuracy, we varied the initial profiles of soil temperature and humidity on the basis of our previous experiences and of discussion within the community of RAMS modellers.

We found out that using a constant profile of humidity with lower values than the ECMWF ones improves the performances of the model, due to a better budget of the soil-air fluxes in the soil model. An example of the results is given when presenting the results of the "definitive" set of simulations.

Another approach could be to produce mesoscale simulations on a single coarse grid for a long period, at least a few months, and then use its final output values of the soil thermo-fields as input to the simulation of episodes. This approach would help overcome the problem of the initial-condition dependency in time, but of course is computationally expensive and needs further tests.

Definitive simulations and results

In the "definitive" set of simulations, we reduced the domain to focus on the area of interest, the centre part of Susa valley from Bussoleno to Bardonecchia, and the most of Maurienne valley, from Modane to Aguibelle. In Fig. 7.110 the areas covered by nested grids 3 and 4 in the final configuration and the 3D-orography of the smallest inner domain are illustrated. The 3D configuration of grids 3 and 4 of RAMS-MIRS models is respectively 196 × 132 × 17 km^3 with a horizontal grid mesh of 4 × 4 km^2, and 101 × 81 × 17 km^3 with a grid mesh of 1 × 1 km^2.

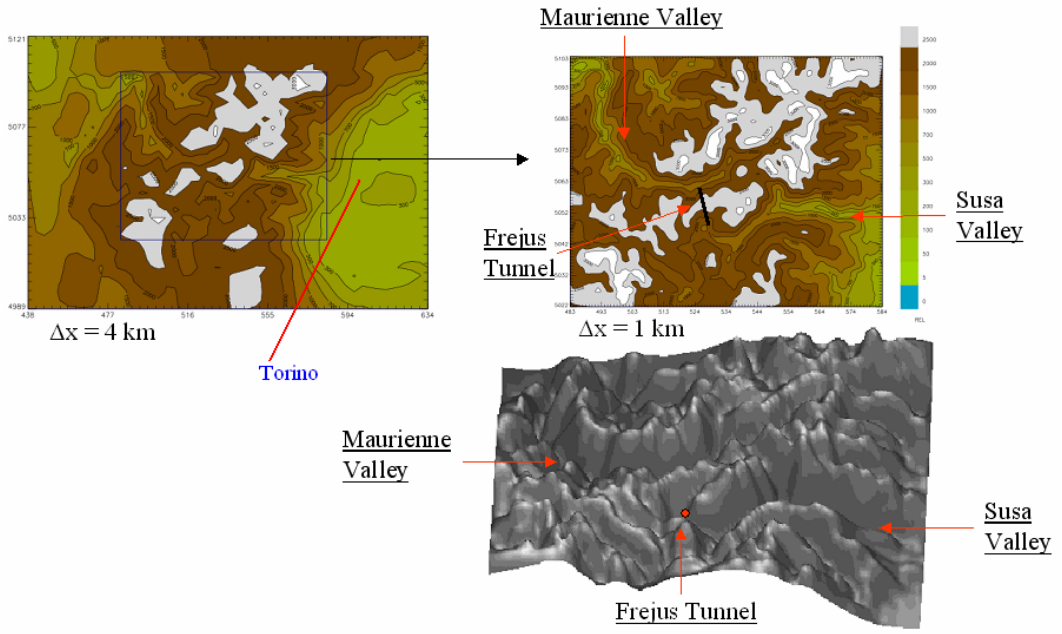

Fig. 7.110 Grids 3 and 4 for the definitive simulations (top) and image of 3D orography contained in the smallest domain (bottom).

In Fig. 7.111 we show the temperature trends at Susa when varying the initial soil moisture profile, passing from the preliminary to the definitive set of simulations in the critical episode of December. Improvements in the daily cycle and in the temperature range are obtained, even if the deficiency is not completely overcome. In some of the other stations, like Mont Cenis, the improvement in the December episode simulation was larger. On the other hand, simulating in the same configuration the other winter episode of February always gave satisfactory results, as seen in Fig. 7.112.

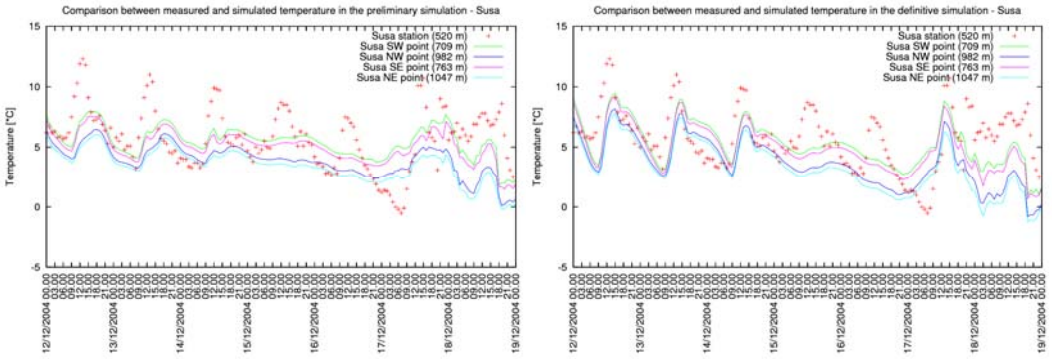

Fig. 7.111 Comparison between temperature measured and simulated in the preliminary (lef) and in the definitive (right) simulations in Susa.

The quality of the reproduction of the wind velocity field was anyway unaffected by the changes in the initial soil profiles. In Figs. 7.113, 7.114, and 7.115 examples of the wind speed recorded and simulated in Susa and St. Michel stations are depicted for the three episodes. We notice that the observed data at French stations, provided as standard datasets by Meteo France, have the limitation of giving only integer values of the wind speed, hiding the real ranging of the values and, as a consequence, heavily affecting the comparison with predictions, particularly considering that the wind is, in many cases, moderate or low.

We also reviewed the 3D structure and time development of all the meteorological fields, to evaluate their consistency and check possible misbehaviours. The results appear to be reliable both for the dynamical and thermal variables. As an example of the wind field produced by RMS simulation, in Fig. 7.116 we report the wind field vectors predicted at 18 m height, correspondent to two foehn episodes, also registered in the wind speed time development, on 09 Feb 2004 (maximum wind speed value at 18 m was 22 m/s) and 17 Dec 2004 (maximum wind speed value at 18 m was 23 m/s).

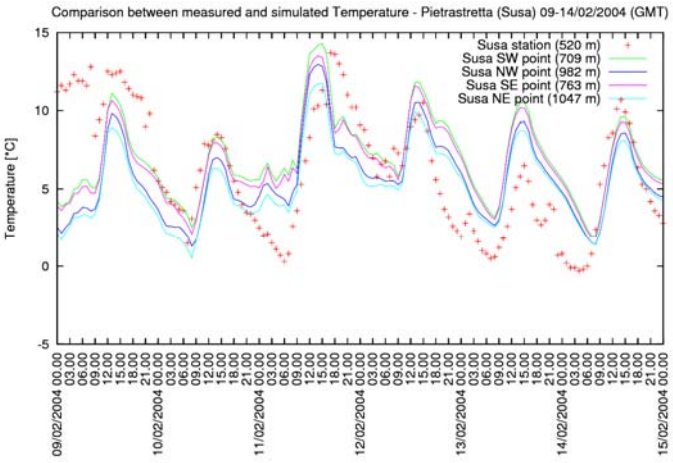

Fig. 7.112 Comparison between temperature measured and simulated in Susa in February episode, definitive simulations.

The meteorological fields provided by RAMS-MIRS interfaced modelling system were then used as input to drive the dispersion model SPRAY on the entire 1 km resolution domain.

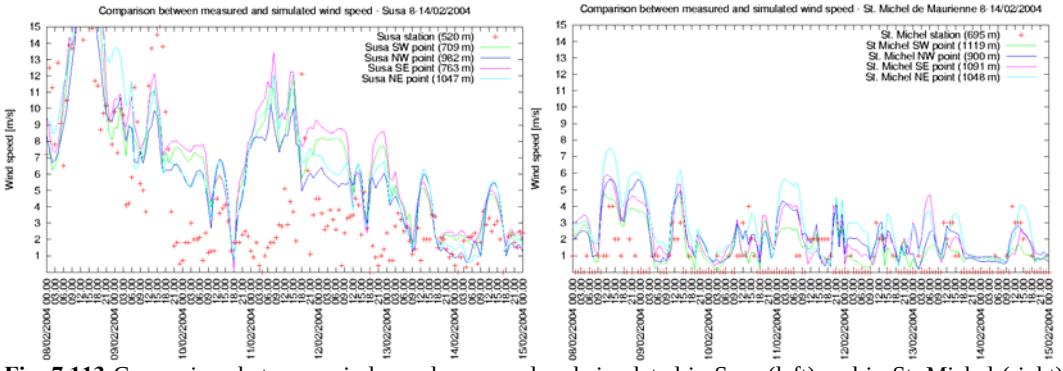

Fig. 7.113 Comparison between wind speed measured and simulated in Susa (left) and in St. Michel (right) for the February episode

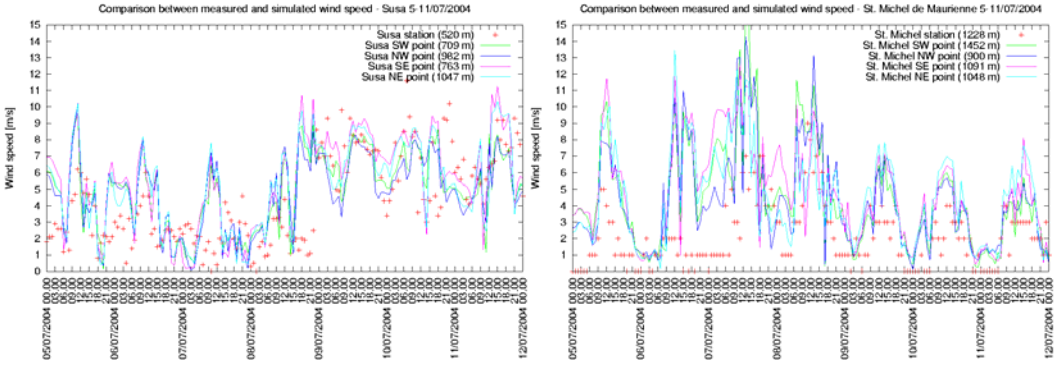

Fig. 7.114 Comparison between wind speed measured and simulated in Susa (left) and in St. Michel (right) for the July episode.

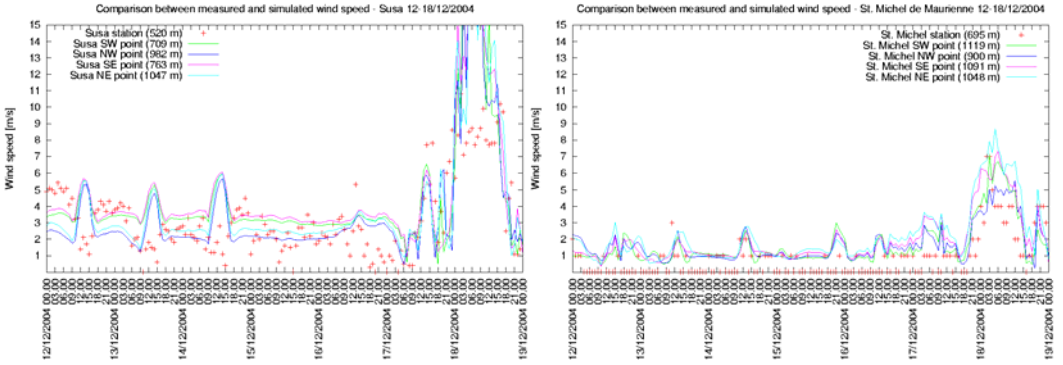

Fig. 7.115 Comparison between wind speed measured and simulated in Susa (left) and St. Michel (right) for the December episode.

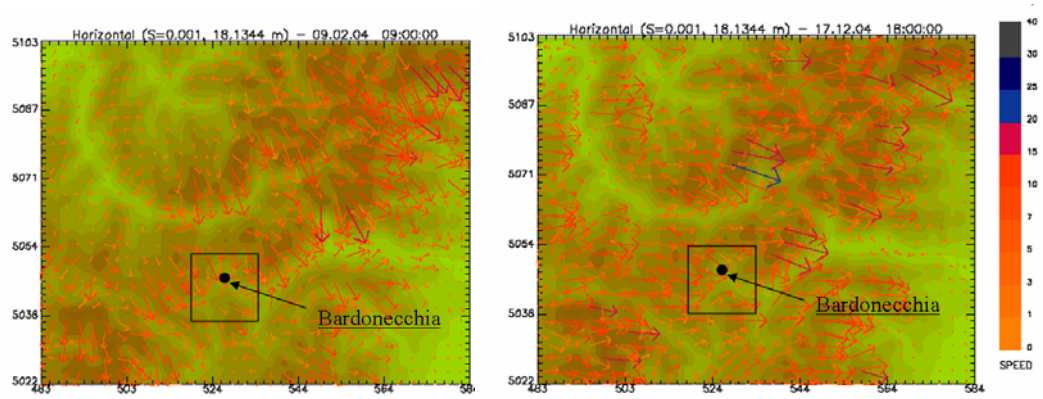

Fig. 7.116 RMS wind field at 18 m, foehn episodes 09 Feb 2004, 09 UTC (left) and 17 Dec 2004, 18 UTC (right).

7.3.3.4 Numerical simulations for the meteorology: downscaling with MINERVE

In order to improve the description of the meteorological fields in the target areas, we operated a further downscaling from RAMS-MIRS outputs on the 1 km grid mesh to a grid resolution of 100 × 100 m^2 using the mass consistent model MINERVE.

MINERVE is a diagnostic 3D model which interpolates the input 3D wind field on the new domain through an objective analysis based on the mass conservation equation (see Section 3.3.3.1). In this way, it is possible to better account for the effect of the local scale forcing over the synoptic and mesoscale fields.

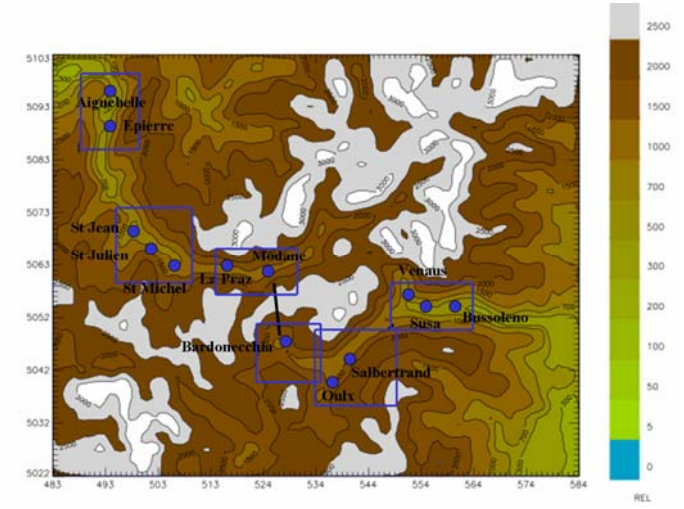

Fig. 7.117 Examples of subdomains (blue) for the local simulations at 100 m resolution

Increasing the resolution implies a much larger number of grid points and a heavier computational cost. For this reason, we decided to select, inside the 1-km-mesh RAMS domain, several subdomains of interest, with a horizontal extension between 10 × 10 km^2 and 15 × 15 km^2, a vertical extension up to 8 km, zoomed on different zones of the Maurienne and Susa valleys, as for instance depicted in Figs. 7.117. To finalize this part of the work with MINERVE, we identified six sub-areas of interest where the highest resolution fields are requested. These subdomains include the main urban centres and villages in the two valleys. The final output of the simulations provided meteorological data fields on the selected subdomains with 100 m resolution.

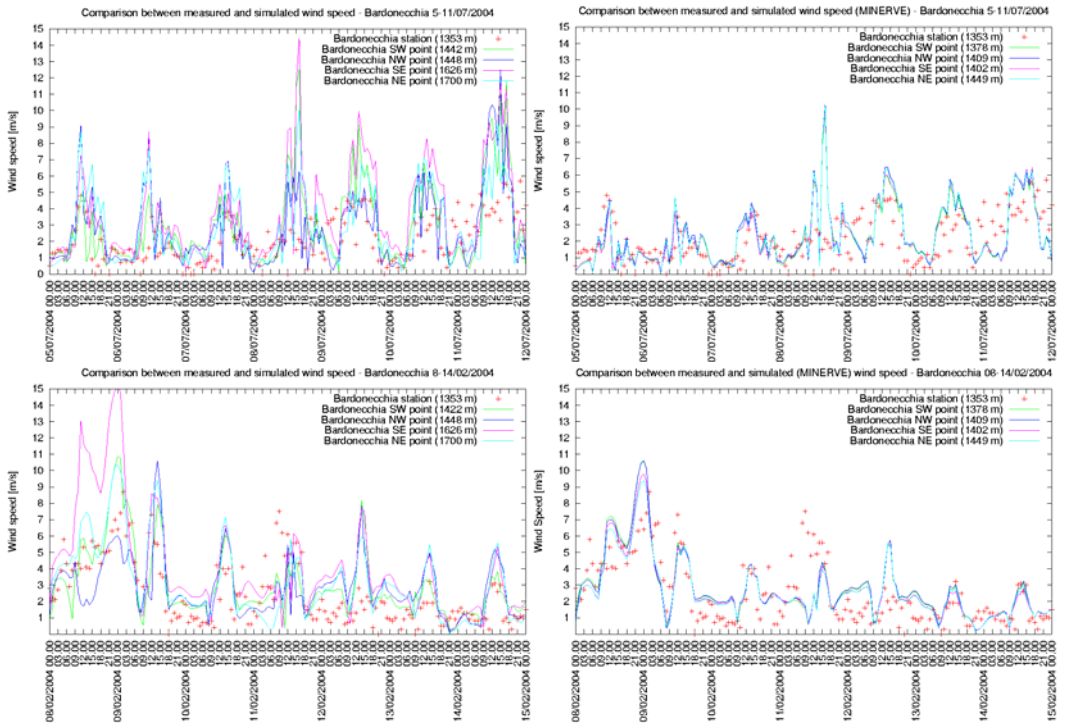

Fig. 7.118 Comparison between wind speed measured and simulated with RAMS (left) and MINERVE (right) models in Bardonecchia station, July (top) and February (bottom) episodes.

To estimate the improvement obtained through the MINERVE application, we made a comparison between the values obtained with RAMS at 1 km resolution and the results obtained with MINERVE at 100 m resolution on the four grid points around the same stations.

We performed simulations on all 6 different subdomains, including 13 of the main urban centres and villages, in summer and winter episodes. As an example, here we present results from the domain including the village of Bardonecchia in the Italian side.

Fig. 7.118 shows the wind speed time evolution simulated in Bardonecchia. The comparison

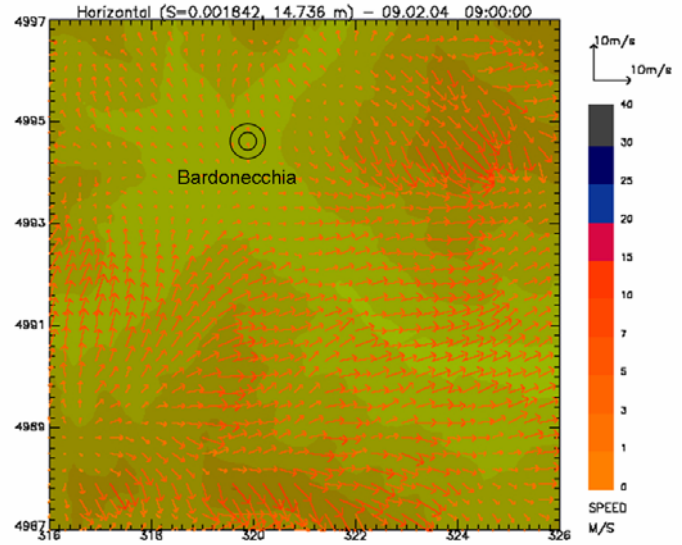

Fig. 7.119 MINERVE wind field at 15 m height in Bardonecchia subdomain, foehn episode 09 Feb 2004, 09 UTC.

between the left graphs, referring to the RAMS output on the 1 km resolution grid, and the right graphs, referring to the correspondent MINERVE output, well illustrates the improvement of definition that was obtained in the near ground wind velocity simulation by using the grid. Having a resolution of 100 × 100 m^2, the reduction of the scatter among the lines corresponding to the four grid-points closest to the station is evident and the agreement with observed data improves. The possibility of downscaling to higher resolution is important to provide more refined information not only for air pollution study, but in particular for the noise propagation studies, where the typical scales can be of the order of a few metres. As analogously done for RAMS simulation, in Fig. 7.119 we present as example the wind field vectors correspondent to the foehn episode on 09 Feb 2004 in the subdomain containing Bardonecchia village (maximum wind speed value at 15 m was 15 m/s). It is evident that the downscaling provides a better detail of the local circulation.

7.3.3.5 Numerical simulations of the pollutant dispersion: SPRAY runs

The highest pollutant impact in the valleys, both for air and noise, is clearly given by the major routes, which will also be mostly affected by possible variations of the traffic scenarios in the future. For this reason we established to consider the contribution of the main roads in the two valleys that are the two Italian National roads SS 24 (that becomes SS 335 between Oulx and Bardonecchia) and SS 25, the Italian highway A32, the French National road RN6 and the French highway A43.

To proceed with the dispersion simulations, Version 3.0 of SPRAY model was installed, the road emission data were processed and the various SPRAY input and configuration files were prepared.

The collection and merging of the NO_2 and PM10 emission data related to these routes was possible thanks to the collaboration between the partners and the support of external institutions, like the French National Geographical Institute (NGI) and the Italian Society of the Frejus Tunnel Highway (SITAF).

To perform reliable simulation of the dispersion, a further processing of the provided emission data was performed so to include the presence of both viaducts and tunnels and treat their emissions properly. When not accounting for viaducts and tunnels, the road emission segments are just lying on the topography. This means, for instance, that the segments of the tunnels possibly lay on the top of the correspondent mountain, while the segments for viaducts are set on the orography floor and not at their heights. Clearly, this introduces errors in the dispersion simulation, in the estimation of concentrations and in the evaluation of the environmental and health impact. To avoid these inaccuracies, we adopted a simple approach. As viaducts need specific segments to identify their different slopes, the subdivision of the original emission arcs was modified by ARPA so that viaducts were divided into subsequent sub-arcs and characterized by their specific height over the terrain. In this way, 2D (x, y) emission segments corresponding to viaducts were rearranged as 3D $(x, y, \Delta z)$ segments ascribing them a height Δz over the topography. An example of the procedure and resulting segments is depicted in Fig. 7.120**.**

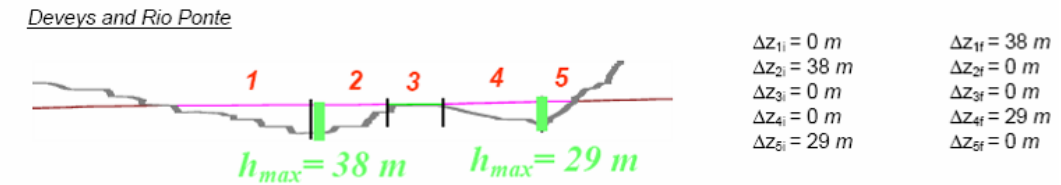

Fig. 7.120 Example of the modification of emission segments to account for viaducts (courtesy of ARPA).

To account for the presence of tunnels, the tunnel emitted mass was split in two contributions and attributed to emission-segments adjacent to the tunnel entrances (Fig. 7.121). After some preliminary tests to identify a criterion to define the emission boxes at the tunnels entrances, the segment length was set 50, 100 or 200 m when the tunnel length was respectively less that 1 km, between 1 and 5 km and longer than 5 km. In this way it was possible to modulate the emission boxes depending on the mass of pollutant emitted in the tunnel.

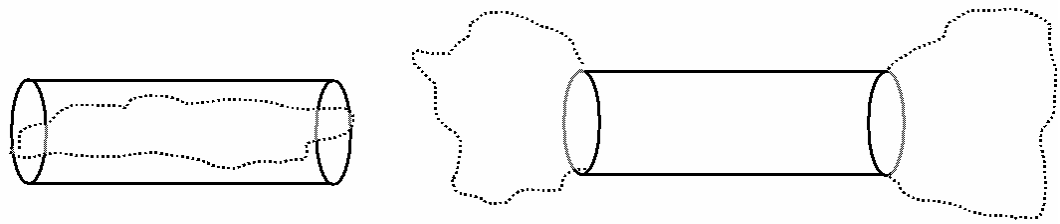

Fig. 7.121 Example of the modification of emission segments to account for tunnels.

An example of the differences when accounting for (or not) the presence of tunnels is shown in Fig. 7.122, or the preliminary testing phase with RMS at the two villages closest to the Frejus tunnel. When not treating tunnels, the concentrations are much lower than when accounting for tunnels. When working with MINERVE the sensitivity to the segment length was higher and lead us to the final choice of modulating the segment-lengths as function of the tunnel length.

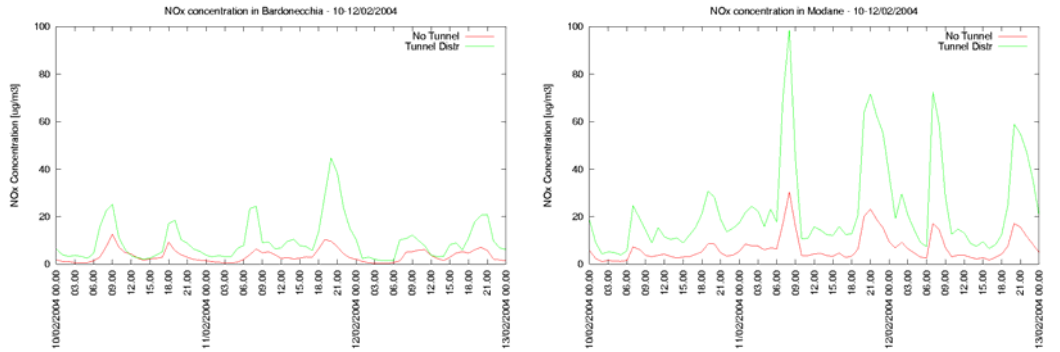

Fig. 7.122 Example of the difference in concentration values when accounting (green line) or not (red line) for the presence of tunnels. Bardonecchia centre (left) and Modane centre (right).

SPRAY model was run both on the 1 km-mesh domain covering all the Frejus transect, using RAMS-MIRS meteo and turbulence files, and on several subdomains, from 10 × 10 km^2 to 15 × 15 km^2 with 100 m resolution, using MINERVE wind fields. These were interfaced with an associate module, called SurfPRO, used to produce the relative turbulence on its grid.

In Figs. 7.123 and 7.124 we report some examples of the final results for the mean and maximum concentration of NO_x calculated over the period in February and July episodes. This kind of analysis allows identifying the most critical zones for the air pollution impact. As expected, ground level concentrations exhibit larger values in the winter period due to the more stable atmospheric conditions (lasting several hours). During summer more convective, thus more dispersive, conditions are generally present, the pollutant is spread over larger areas and secondary maxima occur in the domain. In Fig. 7.124 for NO_x maximum, the subdomains relative to the downscaling with

MINERVE are marked and the concentration contours at 100 m are reported in blue palette. Analogous analyses were performed also to simulations with PM10, but to discuss a homogeneous comparison to the illustrative figures for NO_x.

To highlight the improvement in detailing the concentration fields thanks to the downscaling, in Fig. 7.125 the concentration contours obtained by MINERVE + SPRAY, inside the red square, are superposed over the contours of RAMS + SPRAY simulation.

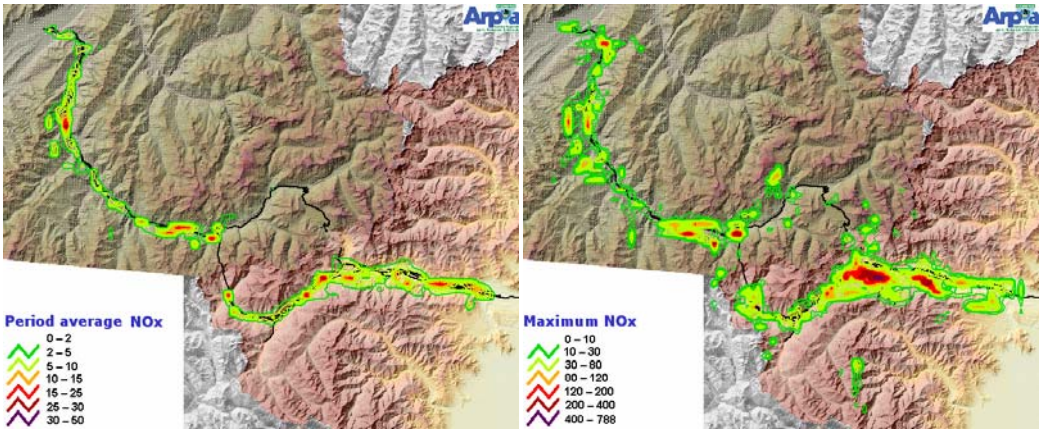

Fig. 7.123 Example of mean (left) and maximum (right) NO_x concentration from RMS simulations of the February 2004 episode.

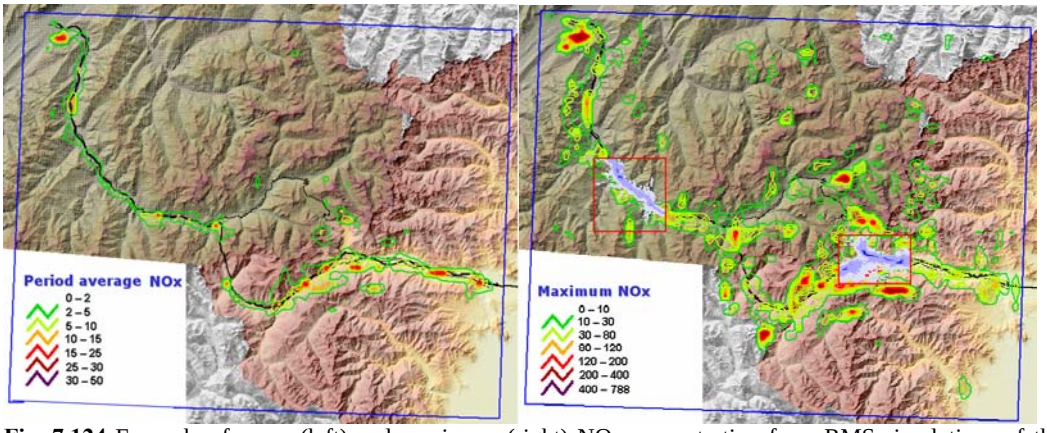

Fig. 7.124 Example of mean (left) and maximum (right) NO_x concentration from RMS simulations of the February 2004 episode.

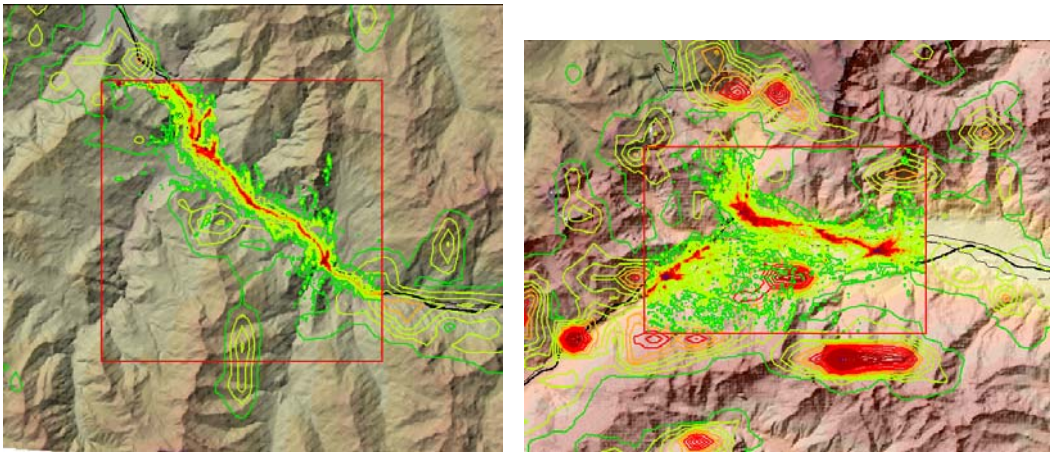

Fig. 7.125 Comparison of maximum NO_x concentration contours from RMS and MINERVE+SPRAY simulations in the two subdomains of the February 2004 episode.

In all graphs it is possible to appreciate the effect of including the presence of tunnels and viaducts. The absence of concentration in correspondence of the tunnel is correctly described and maxima occur at the tunnel entrances. The pollutant emitted by a viaduct is dispersed at levels much higher than the ground, thus reaching the ground highly diluted and possibly displaced with respect to the position of the viaduct itself.

7.3.4 Noise mapping

7.3.4.1 MITHRA-SIG software

MITHRA is a powerful code developed about fifteen years ago by CSTB and dedicated to outdoor noise level predictions in complex environments (Gabillet and Van Maerck 1995). It is based on a fast ray-tracing algorithm. The standard methods used are either the ISO 9613-2 or the NMPB (The French method which is the proposed interim computation methods for road traffic noise in the European Noise Directive 2002/49/EC).

For large scale noise mapping, a version of MITHRA coupled with the Geographical Information System "SIS" (Spatial Information System) is used. This complete software is named MITHRA-SIG and is developed, for the acoustical part, by CSTB and for other elements by GEOMOD. MITHRA-SIG gives the opportunity of investigating traffic noise propagation on a whole Alpine valley. For ALPNAP purposes, only the NMPB will be used with application of specific local long term meteorological occurrences of conditions favourable to noise propagation.

7.3.4.2 Input data

The data processing is an important part of computing large scale noise maps. Input data can be divided in three categories: geographical data, traffic data and meteorological data.

Geographical data

A first step concerns the preparation of geographical data. Input data are 3D databases from IGN (national geographical institute in France) giving relief, buildings, roads, railways. This data has to be cleaned in order to delete inconsistencies. Then, roads and railways have to be separated in sections according to traffic data. Tunnels and bridges are kept with different properties since there specificities play a role in the acoustic processing. Noise barriers are also considered when the data is provided.

Traffic data

The traffic data is needed to have accurate acoustical simulations. For the French side of the Fréjus corridor permanent traffic counting stations or toll systems, either managed by "Société Française du Tunnel Routier du Fréjus" SFTRF (the French highway A43 manager) or the "Direction Départementale de l'Equipement de la Savoie" DDE73 (the French national roads RN6 and RD902 manager) have been used to acquire the required information. On the Italian side of the Fréjus corridor data have been obtained from traffic modelling based on punctual traffic counters. Those traffic data represent the Year 2004.

For roads, the traffic data is the number of light vehicles, the number of heavy vehicles and their speeds. For railways, it is the number of trains, their description and their speeds. Motorways, main roads and main railways are divided in several sections where the traffic data is specified for the three periods: day / evening / night. In order to make simulations as accurate as possible, some measurements of road pavements properties have been carried out and taken into account for the achievement of noise maps.

Meteorological data

The meteorological conditions have a significant influence on noise propagation, especially in mountainous areas. For the software MITHRA-SIG, the input data required is the percentage of favourable conditions depending on the direction of propagation and the period (day / evening / night). Those percentages are calculated from measurements and/or simulations of wind speed, wind direction and temperature.

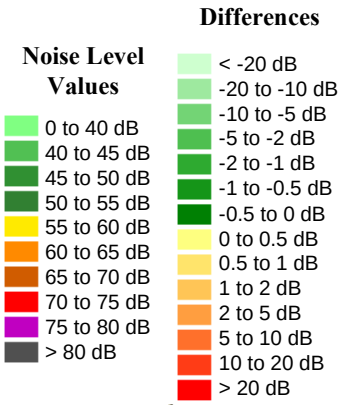

Fig. 7.126 Colour scale for noise level values on the left and for differences on the right

7.3.4.3 Results

There are two main kinds of results: horizontal maps and 3D façades results:

- Horizontal maps: calculations at a specified height of a chosen acoustical indicator (L_{den}, L_{eq}, L_{day}, etc.) and representation with a scale of colours. As an example, Fig (horizmap maurienne) and (horizmap suza) give horizontal noise maps of Lden levels at a height of 4 m for the traffic data of Feb 2004 in the Maurienne valley (Fig. 7.127) and for the traffic data of Jul 2004 in the Susa valley (Fig. 128) respectively.
- Receivers in facades: calculations for receivers located 2 m away from each facades (the number of receivers for each facades depends on some parameters specified). Several acousti-

cal indicators can be calculated. This kind of results, when related to population data, allows to evaluate the exposed population (according to the European Noise Directive). For receivers in façades, the last façade reflection can be deleted for calculations as recommended for strategic noise maps asked by the European Directive. An example of 3D facades representation of noise level is given in Fig. 7.130.

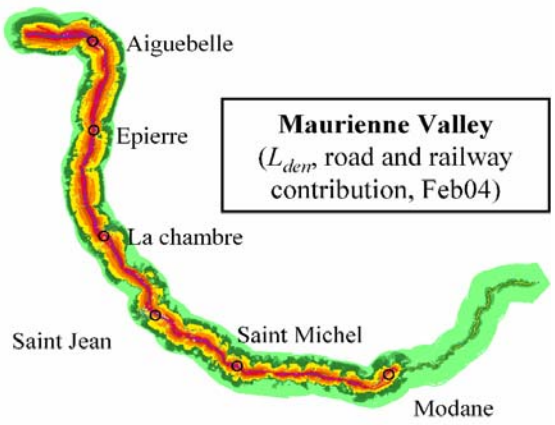

Fig. 7.127. Noise maps representing L_{den} indicator in the Maurienne valley for contribution of both roads and railways and for the period of February 2004. For the colour code see Fig. 7.126.

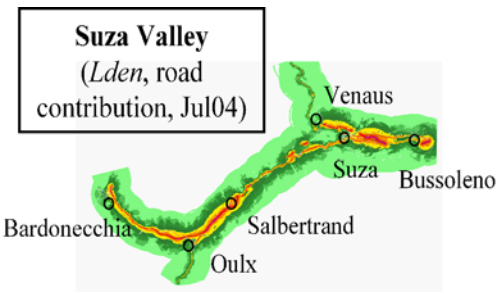

Fig. 7.128 Noise maps representing L_{den} indicator in the Suza valley for contribution of roads only and for the period of July 2004. For the colour code see Fig. 7.126.

The colour scale is given in Fig 7.126. On the left it is the scale for maps representing noise levels for a given indicator and on the right it is the scale for maps of differences between two situations.

It has been chosen to compare the scenario of measured traffic in 2004 with another scenario considering modal shift. This new scenario (Scenario 1) considers no changes on national roads. For motorways, there are no changes for light vehicles whereas the number of heavy vehicles is reduced and the number of trains, especially freight trains is strongly increased. As it is shown on the Fig 7.129, this new scenario has a strong impact on noise levels; the increase is between 2 and 5 dB in a large area.

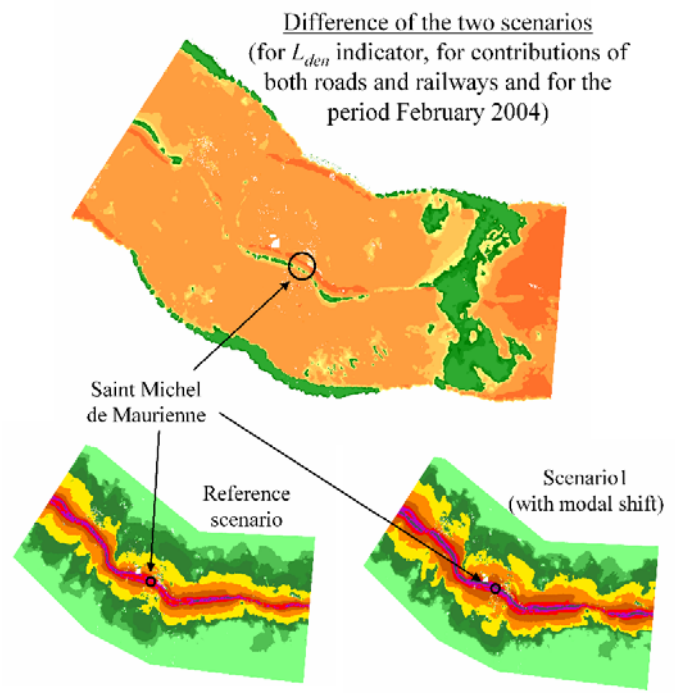

Fig.. 7.129 The map on the top gives the difference between the one for Scenario 1 on the bottom right and the one for reference scenario on the bottom left. For the colour code see Fig. 7.126.

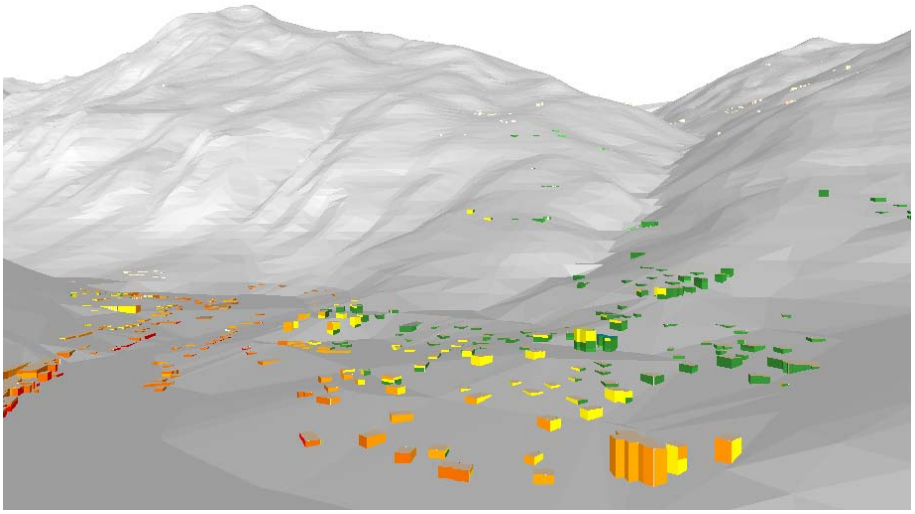

Fig. 7.130 3D facades representation of noise levels (L_{den} indicator) in the area of Saint Michel in the Maurienne valley. For the colour code see Fig. 7.127.

7.4 Scenario assessments

7.4.1 Scenarios for the Brenner corridor: Lower Inn valley

7.4.1.1 Emission modelling results for the Lower Inn valley scenarios

The project MONITRAF provided a detailed traffic development model comprising four traffic scenarios on the A12 from 2005 – 2010. The scenarios are based on traffic count data at the station Vomp and a survey of the HDV fleet composition of HDV near Vomp in 2005, and a prognosis of the emission standard fleet composition by Hausberger (2006). Here, the different scenarios are only described briefly, details are given in Allinger-Csollich (2006):

1. The scenario "Business As Usual" scenario (BAU) assumes a HDV traffic increase of 2.5 % and an increase of 1 % for coaches and passenger cars. Currently, there is a nocturnal driving ban for tractor-trailer combinations and trucks without trailer with the exception of Euro 4 and Euro 5 heavy goods vehicles. This exceptional rule will be abandoned for tractor trailers in 2008 and for trucks without trailers in 2010.
2. The first future scenario (V1000) is mainly based on:
   - Driving ban for Euro 0 and Euro 1 tractor-trailer combinations > 7.5 t modelled from 2007 onwards
   - Driving ban for Euro 2 tractor-trailer combinations > 7.5 t modelled from 2009 onwards
   - Driving ban for Euro 0 and Euro 1 heavy goods vehicles without trailers modelled from 2009 onwards
3. The second future scenario (V0100) is mainly based on:
   - A sector driving ban for heavy goods vehicles (shift to rail) which leads to a reduction of -7.3 % modelled from 2008 onwards.
   - Except for 2007/2008 (-7.3 %) there is an increase in heavy goods vehicles of 2.5 % per year
4. The third future scenario (V1100) is a combination of V1000 and V0100

The output of these scenario computations for 4 × 6 years was calculated and stored as annual means for 5 different vehicle classes (VC): passenger cars, LDV, coaches, trucks without trailers, tractor-trailer combinations and trucks without trailer and 5 pollutants (NO_x, PM10-exhaust, PM10-non-exhaust, HC and CO). In addition, the results were calculated for the road gradients of 0 %, 0.5 %, 1 %, 2 %, 5 % and -0.5 %, -1 %, -2 %, -5 %. Finally, the emissions given in kg/(km·h) can be calculated for each "average" hour of the year by the simple formula given in the previous sub section.

The results of these emission computations were used for two air quality simulation scenarios for the Lower Inn valley and for the entire Brennero/Brenner corridor (see Section 7.4.2). The results of the base case for 2005, the BAU scenario for 2010 and a combination of the driving ban for older Euro classes and the sector driving ban (SCEN-2010) is shown in Figs. 7.131 and 7.132 for NO_x, PM10, HC and CO. For all four pollutants a significant decrease from the base case to the BAU scenario 2010 (BAU-2010) is calculated. This decrease is attributable to higher emission standards and the fleet renewal of cars, LDV and HDV.

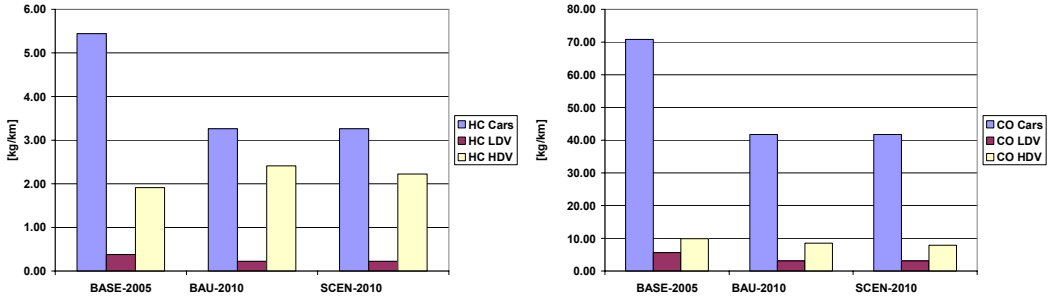

Fig. 7.131 HC emissions (left) and CO emissions (right) calculated for MONITRAF scenarios.

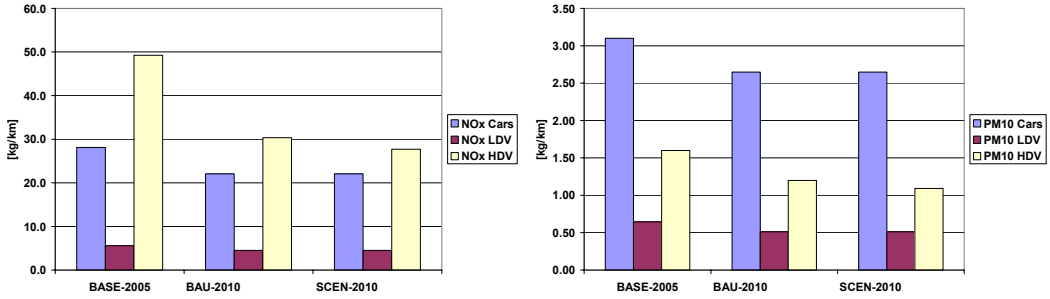

Fig. 7.132 NO_x and PM10 emissions (exhaust and non-exhaust) calculated for MONITRAF scenarios.

The difference between BAU-2010 and the combination of measures is small. For passenger cars and LDV the there are no differences because these vehicle classes are not affected by measures. For HDV there is for SCEN-2010 a decrease of some percent related to BAU-2010 for all four pollutants. The small changes between BAU-2010 and SCEN-2010 and the significant changes between the base case 2005 and BAU-2010 have both the same reasoning, namely the expected fleet renewal, i.e. the replacement of old cars, light and heavy duty vehicles vehicles with low emission standards by new ones with higher emission standards. Already now, due to the nocturnal driving ban, with the exception rule for Euro 4 and 5 heavy goods vehicles, the HDV fleet on the A12 is modern. Therefore, the ban of Euro 0 and 1 (in 2007) and Euro 2 (in 2009) may have some impact in 2007 and 2009, respectively, but it will not be until 2010 for most of these HDV to be abandoned. The sectoral ban assumed from 2008 onwards leads to a sudden reduction in HDV by about 7.3 %. However, three years later the 7.3 % are outnumbered by the assumed increase in HDV traffic of 2.5 %.

More effective measures from the viewpoint of emission modelling would be a general speed limit of 80 km/h or even 70 km/h for all vehicle classes, so that in practice the real average speed is close to the emission optimum of around 80 km/h. If HDV, LDV and passenger cars have to go at the same speed, this might take the advantage of a quite steady driving behaviour on both lanes on the motorway, leading to less acceleration cycles of cars and HDV and therefore less emissions. However, due to meteorological reasons acting upon dispersion conditions such drastic measures should be only considered to be applied during severe air pollution episodes or in combination with measurements like temperature profiles or forecasts indicating severe unfavourable dispersion conditions or air pollution forecasts.

However, there might be a conflict of interest in many places with noise generated by HDV. Noise levels are increased with increasing HDV speed. For instance in Austria there is a nocturnal speed limit for HDV on motorways and express-ways of 60 km/h between 22:00 – 05:00 CET.

In summary, within the next years higher emission standards are expected to have major impact on NO_x and PM10 emissions, although a significant increase in HDV on A12 motorway traffic is also expected. Additionally, due to the already existing quite effective measure of the nocturnal driving ban on HDV (below Euro-IV), future measures like modal shift (reduction of HDV traffic by 7.3 %) will affect only a modern fleet and hence result only in minor emission reductions in NO_x and PM10.

7.4.1.2 Lower Inn valley air quality modelling study base case

Annual means for NO_x, NO_2 and PM10 were calculated for 2004 and compared with air quality stations maintained by the state of Tyrol and BEG (Brenner Eisenbahn Gesellschaft). The BEG stations are used to monitor the effects of the construction work within the lower Inn Valley, i.e. the expansion from 2 to 4 rail way tracks. The predicted annual mean values for NO_2 and PM10 were used for the health assessment study by MUI (see Chapter 6). For these air quality computations the model system GRAL (for details see Section 4.4.2.2) together with the street network emission model NEMO was used. Both models were developed at TU Graz.

The size of the chosen model domain is 27 km (W-E) × 23 km (N-S). Around 300 flow fields were calculated with GRAMM (for details see chapter 3) on a horizontal resolution of 250 m × 250m representing about 95% of all classified situations. The smallest vertical resolution was chosen to 10 m on the lowest grid cells. For each flow field a dispersion calculation with GRAL was carried out on a very fine horizontal resolution of 10 × 10 m^2. In this study, the lowest counting grid cell was chosen to 2 m. The fine horizontal resolution enables to resolve the dispersion close to strong sources such as motorways. Hence, the model results can be compared with measurements from air quality monitoring stations located very close to busy roads. Thereafter, each run is weighted due to its meteorological classification and frequency. Annual, summer and winter means were calculated by post processing and weighting the numerous dispersion calculations. The NO_x to NO_2 conversion is calculated according to the scheme of Romberg et al. (1996) using the following formula:

$$NO_2 = \left(\frac{103}{NO_x + 130} + 0.005 \right) \cdot NO_x$$

The Romberg scheme is a simple regression model, based on current results of field measurements, describing the conversion rate as a function of NO_x concentrations only. The scheme works for annual means and 98-percentiles but not for single hours. Due to the shift of NO_x emissions to larger a and larger NO_2 primary emissions with increasing Euro standards for diesel passenger cars the application of the Romberg scheme may result in an underestimation of NO_2 when calculating future scenarios.

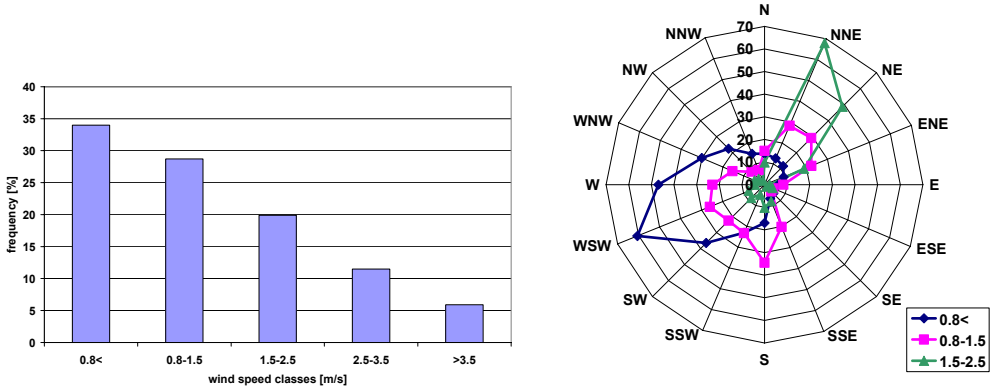

Fig. 7.133 Analysed wind frequency distribution and wind rose for three wind speed classes at the air quality station Vomp.

7.4.1.3 Flow fields

For the flow field simulations, one year of meteorological measurements for 2004 have been used. Fig. 7.133 provides information about the analysed wind frequency distribution and main wind directions measured at Vomp. Fig. 7.134 provides information about the classification into stability classes based on 15,420 half hour intervals for 2004. The derivation of stability classes was a crucial part in this work, because the method applied here is based on wind speed and cloud cover using a matrix which relates these parameters to the respective stability class (ÖNORM M9440). Usually for computations (with the GRAL model system) radiation balance measurement are used to derive near surface stability classes because it has been proven as the most suitable parameter to be used for air quality modelling studies. Unfortunately, routine radiation balance measurements are not carried out in Tyrol. Because the cloud cover method produced too many instable and neutral conditions during the winter month, the classification for December, January, and February has been corrected. A large share of stable classes (42 %) followed by neutral near surface conditions resulted. Radio sonde measurements can not be used, because the classification used for the GRAL system is based on an hourly basis.

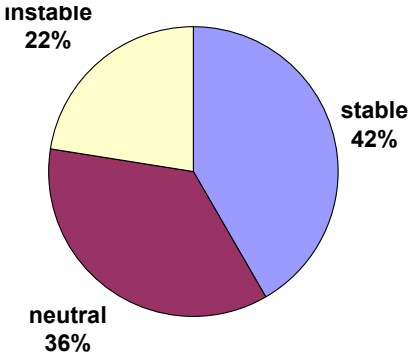

Fig. 7.134 Analysed stability classes based on meteorological data from Innsbruck airport

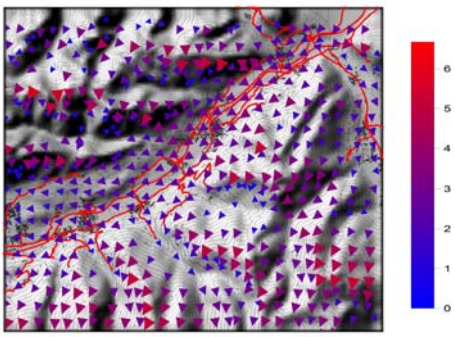

Fig. 7.135 Exemplary flow field for neutral conditions computed with GRAMM.

Fig. 7.135 shows the simulated wind field initialized with a mean flow of 2.5 m/s from NE and neutral stratification. Highest wind speeds are simulated near the mountain tops, and the lowest wind speeds in the valleys, where channelling effects in the side valleys (like the Ziller valley) are

represented. In Fig. 7.136 simulated annual mean distrubution of wind directions (wind roses) are compared against observed ones. The overall agreement is good, however there seems to be a model bias of one wind sector between NNE to SSE sector. This might point towards a too strong channelling, i.e. slope winds might be not represented well enough. However, even on the fine resolution of 250 × 250 m^2 differences between the real and model topography may be attributable for this differences

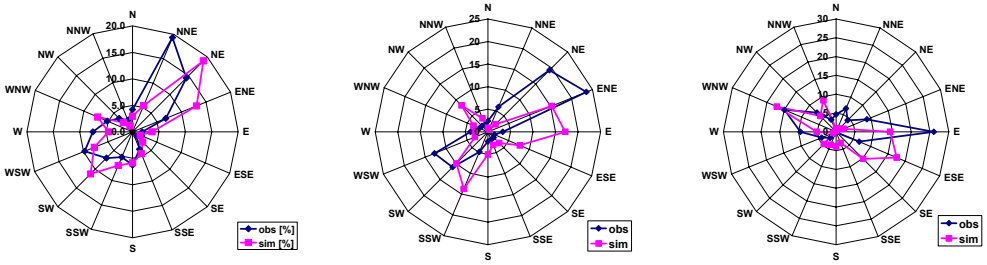

Fig 7.136 Comparison of simulated wind roses against observed ones for Vomp (left), Terfens (middle) and Fritzens (right).

7.4.1.4 Evaluation of the air quality modelling results and determination of the background (reference case)

Model results for NO_x, NO_2 and PM10 were compared with the results of seven air quality monitoring stations located within the model domain (see Fig. 7.1 in Section 7.1.1). The model results were evaluated by scatter plots. The respective background values were determined by regression analysis (see Fig. 7.137 and 7.138). The background value should set the intercept to zero. The derived background values for the Annual Mean Values (AMV), and for the winter and summer season and are shown in Tab. 7.14.

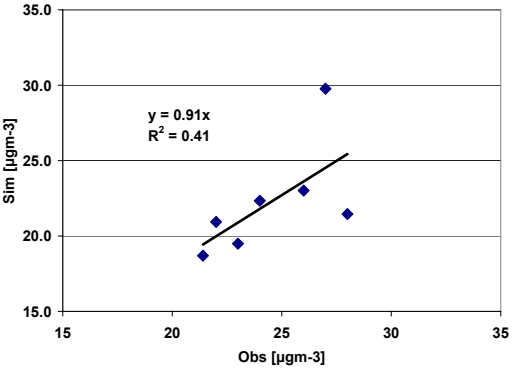

Fig. 7.137 Comparison simulated results versus observation and derivation of the background value. Scatter plot for the annual mean PM10.

The chosen background values accommodate for the following shortcomings of this model approach:

- Non consideration of emission sources (e.g. construction industry)
- Non consideration of secondary particle formation and growth
- Under/over estimation of emission sources (e.g. cold start traffic emissions)
- The effect of strong sources outside the model boundaries and inflow through the system boundaries. In example, westward advection (from the Innsbruck area) and eastward advection (from the Wörgl–Kufstein area)

The background values within this study were height corrected according to Seinfeld and Pandis, 1997. Another localized problem when comparing the model results with the air quality simula-

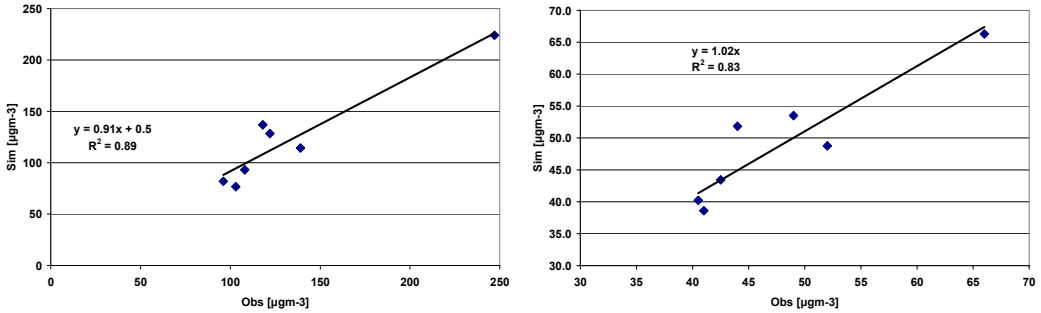

Fig. 7.138 omparison simulated results versus observation and derivation of the background value. Scatter plots for the AMV NO_x (left) and the AMV NO_2 (right).

Tab. 7.14 Derived background values for NO_x and PM10

	AMV (in µg m^{-3})	DJF (in µg m^{-3})	JJA (in µg m^{-3})
NO_x	25	40	11
PM10	14	21	10

tions is the very intense construction activity of the Brenner Rail Company (BEG) in 2004 between Baumkirchen and Fritzens.

In Figs. 7.139, 7.141, and 7.142 the modelled NO_2 concentrations are shown. The highest concentrations are close to the motorway A12 and near the larger towns of Wattens, Schwaz/Vomp and Jenbach (see Fig. 7.1 in Section 7.1.1). In Jenbach there is also heavy industry located. The concentration pattern is confined by the topography especially during the winter time. Another important feature in the AMV and winter (Dec, Jan, Feb) concentration pattern is that larger concentrations are eastward of major sources. These features are visible eastward of the three major settlements in Figs. 7.139, 7.140 and 7.142.

The reason for this behaviour is that during stable conditions catabatic down valley flows prevail and dispersion conditions are less favourable at these conditions. During instable conditions prevailing rather during the summer months air pollutants are better mixed within the Inn valley due to larger mixing layer heights and upslope winds. In addition up-valley flows have a larger frequency. Therefore, the simulated NO_2 concentration pattern is significantly changed compared to winter months. The AMV NO_2 level at the valley floor is large; the current Austrian NO_2 air quality standard of 40 µg m^{-3} is exceeded in large areas along the motorway A12. During the winter month the NO_2 concentration level close to the A12 and near the largest settlements is even increased. In contrast, during the summer month the NO_2 concentration level close to the A12 is much lower.Given the uncertainty in meteorological input data for the derivation of stability classes and industrial NO_x emissions, the model results for AMV of NO_x and NO_2 are in good accordance with measurements. A good agreement between simulated results and observations was obtained for the summer months (Jun, Jul, Aug). In winter due to the large background the overall agreement between simulations and measurements is fair. The large uncertainty concerning PM10 emissions is evident when the modelling results are compared against the observations (see Fig. 7.138).

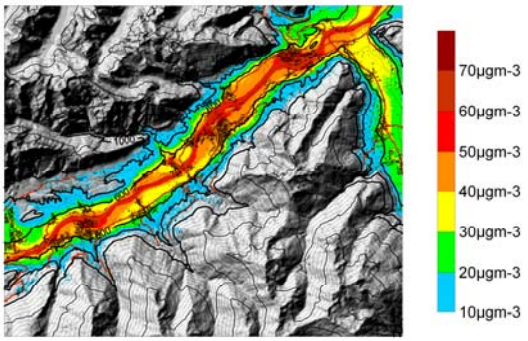

Fig 7.139 Modelled annual mean value for NO_2 within the Lower Inn valley.

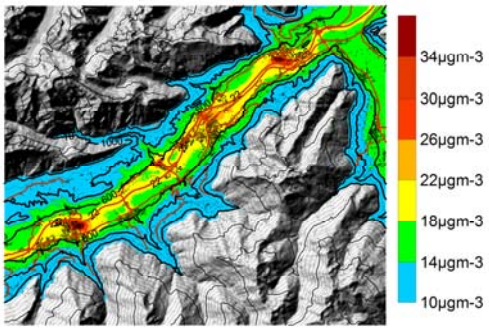

Fig 7.140 Modelled annual mean value for PM10 within Lower Inn valley.

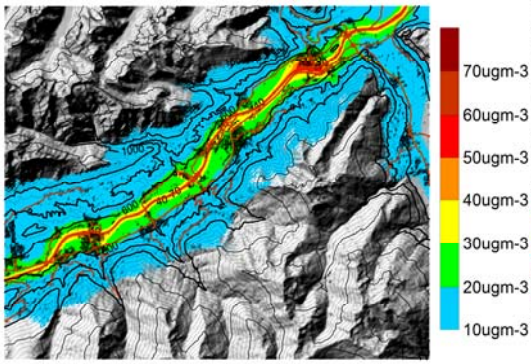

Fig. 7.141 Modelled JJA mean value for NO_2 within Lower Inn valley.

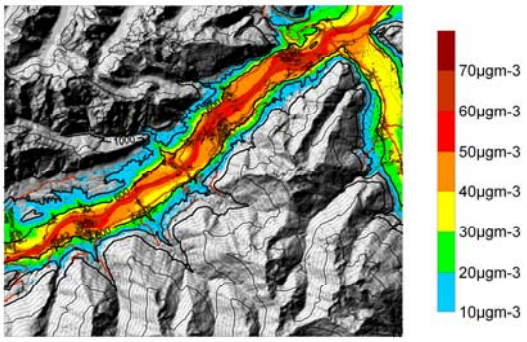

Fig 7.142 Modelled DJF mean value for NO_2 within Lower Inn valley.

The scatter plot derived PM10 background is very large related to the simulated values, especially during the winter season. During the winter season a significant fraction of PM10 may consist of secondary aerosol which was not accounted. The correlation coefficients based on only seven air quality monitoring stations for NO_x and PM10 give some indication about the poor PM10 emission data. Within the EU-Life Project KAPA-GS significantly better results for PM10 were obtained with the same model system (Sturm et al., 2007). In the KAPA-GS air pollution modelling work variance is about 0.88 for the AMV PM10 and about 0.79 for the winter PM10 based on 10 stations. The increased background values for NO_x and PM10 (during the cold season) and lower ones during June – August compared to the annual means points to a deficiency/drawback in the general model approach. Due to CPU limits (4 GByte RAM) the urban area of Innsbruck could not be represented in the air pollution modelling work. During winter time there are prevailing catabatic down valley flows acting together with flow channelling, both from south westerly to north easterly directions. Hence, due to the location of Innsbruck close to the westerly-border of the model domain a strong inflow of air pollutants in a shallow layer near the ground is attributable for enhanced winter background values of NO_x, NO_2 and PM10. In addition, using only one stable stability class may not account for severe winter inversion situations with low wind speeds and highly stable near surface conditions. The simulations results may be improved by using 2 – 3 stable stability classes.

7.4.1.5 Scenarios

Based on the traffic count data and fleet composition at the station Vomp A12 (in 2005) and the base case presented before, the increase in traffic volume was extrapolated to all motorway sections of the A12 within the Lower Inn valley domain. The HDV fleet composition (tractor-trailer combinations, trucks without trailer and coaches) was taken constant. Fig. 7.143 shows the simulated NO_2 concentration for the BAU scenario 2010. Compared with Fig 7.139 there is already some clear alleviation in the NO_2 concentration pattern visible due to higher emission standards. However, the Austrian air quality standard for the AMV of NO_2 of 35 µg m^{-3} for 2010 (from 2012 it will be 30 µg m^{-3}) is exceeded in large areas along the motorway A12.

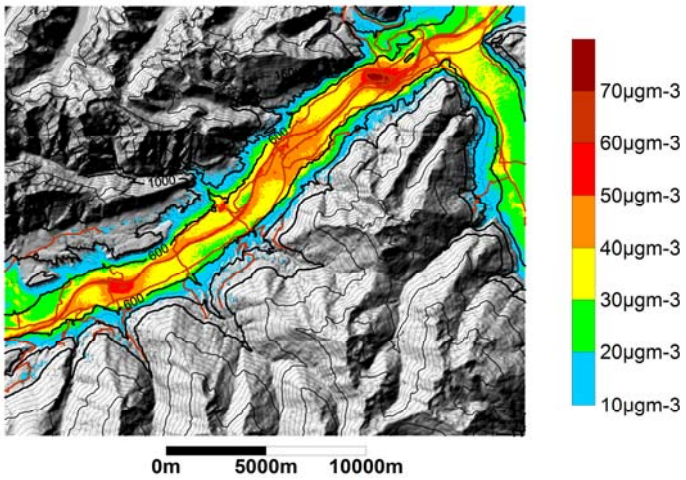

Fig 7.143 Modelled annual mean value for NO_2 within the Lower Inn valley.

The measures (modal shift and ban of older HDV EURO classes) until 2010 as proposed by MONITRAF show only a very small impact close to the motorway A12. Fig. 7.144 shows the difference in NO_x between the scenario BAU-2010 and the scenario with measures SCEN-2010; the differences in NO_2 are even smaller (not shown).

7.4.1.6 Annual diurnal impact of atmospheric conditions/processes on dispersion

Based on the modelling work presented for the base case, the interplay of two single emission sources and the meteorological processes was examined by the following approach. The NO_x concentration fields owing to HDV and Car traffic were calculated for annual mean 3-hour intervals as shown in Fig. 7.145. The diurnal NO_x emission cycle was accounted for each 3-hour interval in the reference run (for Vomp A12 data see

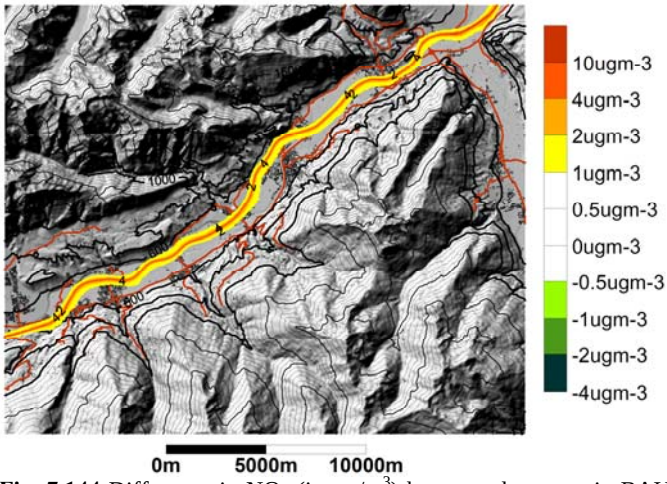

Fig. 7.144 Difference in NO_x (in µg/m^3) between the scenario BAU-2010 and the scenario with measures SCEN-2010.

Fig. 7.6 in Section 7.1.2.1). In the experimental model set-up the traffic emissions were distributed evenly for each hour, i.e. the non-dimensional factors f_{diurn} were set to one. Averaging over all 3-hour intervals at the chosen receptor points yields higher concentrations (due to HDV and car motorway traffic) for the scenario than for the reference run. Importantly, during the night time the values for different receptor points are significantly increased because the same emission can lead to higher concentrations e.g. due to more stable conditions prevailing at night. However, stratification is one important meteorological process which may impact on the annual mean diurnal cycle. Also the location to the motorway and prevailing or altering wind systems are of importance. The low impact at the receptor point Baumkirchen can be explained by the more "sheltered location", i.e. larger distance from the motorway and catabatic flows. At the other receptor points the largest and smallest concentrations vary up to a factor of 2.5. In principle this analysis can be carried out for each hour in order to evaluate e.g. the impact of temporal driving bans.

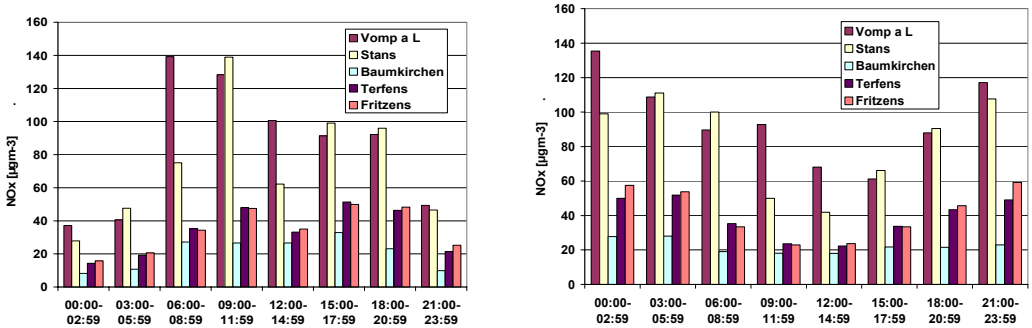

Fig 7.145 Concentrations for 3-hour intervals owing only from motorway emissions (HDV + Cars) for control run (left) and omitted diurnal cycle (right).

7.4.2 Scenario assessment for Brenner transit route

7.4.2.1 Regional air quality simulations with MCCM

Regional air quality modelling is an essential tool for the estimation of the effect of emissions and meteorological conditions on the regional distribution of pollutants. It is a requisite for the assess-

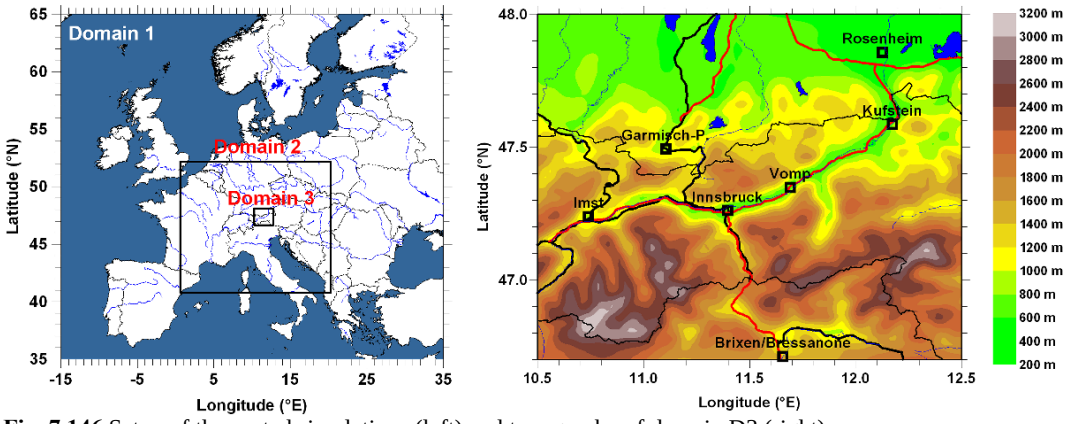

Fig. 7.146 Setup of the nested simulations (left) and topography of domain D3 (right).

ment of the spatial and temporal distribution of pollutants (e.g. background conditions on PM10 or ozone), for the introduction of emission and abatement strategies, as well as for health impact assessment studies. For the present example, simulations with the model MCCM (Grell et al, 2000, see also Section 4.4.2.2) were performed for the region of Tyrol for the year 2004.

MCCM is an online coupled meteorology-chemistry model, i.e. meteorology and atmospheric chemistry are computed by one single model. Its meteorological part is based on the nonhydrostatic NCAR/Penn State University model MM5. As MM5 is a widely used community model, the meteorological part has been extensively evaluated for numerous different regions of the earth, and MCCM was validated for different meteorological and chemical conditions and regions (e.g. Forkel and Knoche, 2006; Haas et al., 2007; Grell et al., 2000; Jazcilevich et al., 2003; Suppan and Schädler, 2004). Nevertheless simulations for the Alpine region are a challenging effort for any modelling study.

7.4.2.2 General setup

The simulations with MCCM were made for three nested model domains. Fig. 7.146 displays the model domains together with representation of the topography for the region of Tyrol in the model. Domain D1 (horizontal resolution 60 km) covers whole Europe, domain D2 (horizontal resolution 12 km) the Alpine region, and domain D3 (horizontal resolution 2.4 km) the region of Tyrol.

Simulations were carried out for the entire year 2004 and for two emission scenarios: a baseline case with 2004 emission data and a traffic emission scenario for 2010 ("Business as usual" + some additional measures). Meteorological conditions refer to the year 2004 and were identical for both simulations. The meteorological boundary values for the largest domain, which determine the large scale meteorological conditions in the modelling area, were derived from

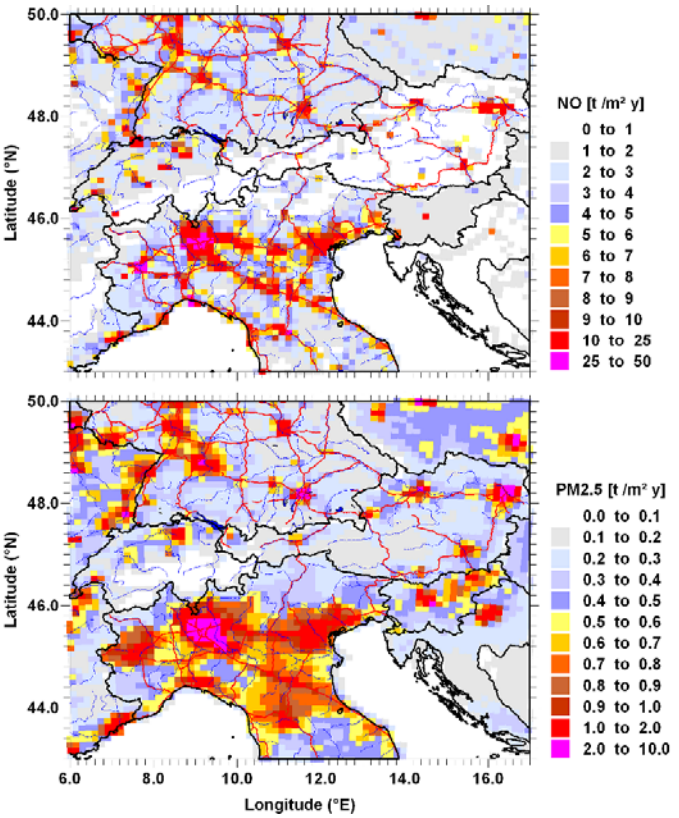

Fig, 7.147 Yearly NO (top) and PM2.5 (bottom) emissions for D2 for all sectors.

global reanalyses from the Global Forecast System (GFS)[6]. Typical values were used as chemical boundary conditions for the largest domain while the nested domains D2 and D3 receive their boundary values from the results of the larger domain.

7.4.2.3 Emissions

One of the most crucial points of regional air quality modelling is the provision of anthropogenic emissions for all emission sectors and all emitted species in an appropriate spatial and temporal resolution. The emissions must be made available for the whole modelling domain and for all emission sources. Gridded emissions for Europe, for example, are made available with a horizontal resolution of 50 km by EMEP (Co-operative programme for monitoring and evaluation of the long-range transmission of air pollutants in Europe, www.emep.int).

For the present study, an emission data set (except for PM) for Europe with 10 km horizontal resolution, provided by the LFU (Bayerisches Landesamt für Umwelt), was used for domains D1 and D2. Emissions of particulate matter (PM) were derived from a data base with 0.25° × 0.125° resolution supplied by TNO (Visschedijk and Denier van der Gon, 2005). As an example, Fig. 7.147 shows the spatial patterns of area emissions of NO and PM10 for domain D2. Fig. 7.147 demonstrates that the anthropogenic emissions for Tyrol/Austria are lower than the emissions in southern Germany or Northern Italy. In particular there seems to be some evidence that industrial emissions for Tyrol may be underestimated.

For the simulations for domain D3 with 2.4 km horizontal resolution the local traffic emission inventory from the Tiroler Landesregierung was incorporated into the coarser emission inventory of domain 1 and 2. For Tyrol, detailed data on yearly traffic emissions were supplied for the main motorways, roads, and urban traffic. These data were distributed to the grid of D3 using a geographical infor-

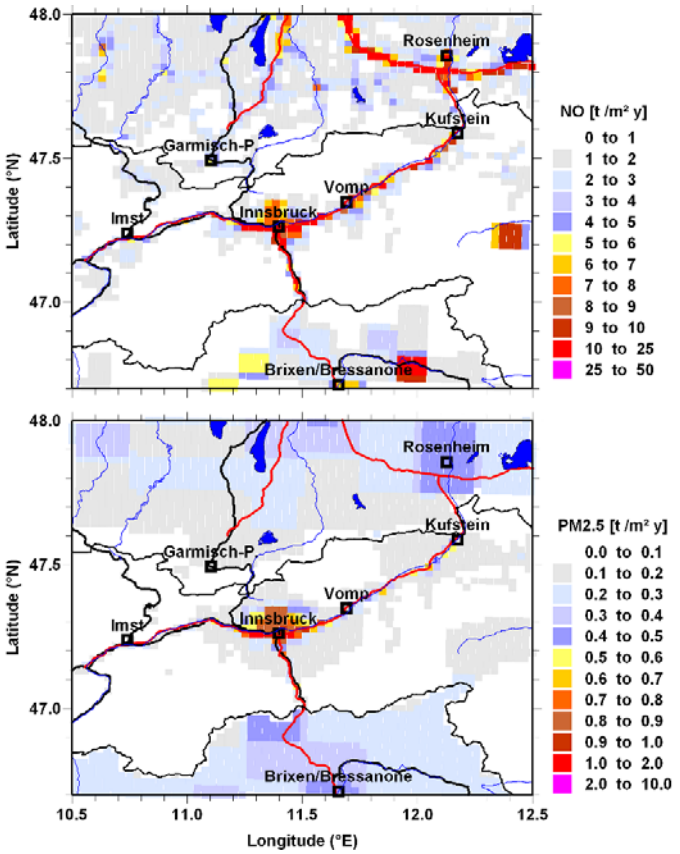

Fig. 7.148 Yearly NO (top) and PM2.5 (bottom) emissions for D3 for all sectors.

[6] www.emc.ncep.noaa.gov/gmb

mation system (GIS). The emissions of total volatile carbons included in this data set were split into compound groups (Friedrich et al., 2002). A ratio of 0.1/0.9 was assumed for the partition of NO_2 and NO emissions. Hourly emissions were derived from the yearly traffic emissions on the basis of seasonal, weekly, and daily cycles as described in Section 7.1.2.1. Data on emissions from domestic heating in Tyrol were also supplied by the Amt der Tiroler Landesregierung. For all the other emission sectors, i.e. industrial combustion, emissions from production processes, fuel refinement and distribution, solvent use, mobile sources besides road traffic, waste treatment, and agriculture, the data with 10 km resolution from LFU had also to be used for Tyrol. Whenever appropriate these data were aggregated to the areas of communities in Tyrol. For the part of D3 belonging to Germany emission data of gas phase compounds with a horizontal resolution of 2 km were available. Emissions of particulate matter were included in the traffic and domestic heating emissions for Tyrol. For all other emission sectors and all regions outside of Tyrol the particulate matter emissions were taken from the TNO data base with 0.25° × 0.125° resolution. The resulting NO and PM2.5 emissions are shown in Fig. 7.148. Similar to the emissions in Fig. 7.147 the emissions for D3 display a noticable and certainly unrealistic drop at the Austrian border.

For the scenario simulations a traffic emission scenario for 2010 from TU Graz was used which relies on a detailed traffic development model by MONITRAF. Details on the computation of the scenario emissions can be found in Section 7.4.1.1. The traffic development scenario is composed of a "Business As Usual"-scenario (BAU) in combination with additional measures for heavy duty vehicles, i.e. driving ban for Euro 0, Euro 1, and Euro 2 classes and sector driving ban for heavy goods vehicles. As shown by Figs. 7.131 and 7.132 in Section 7.4.1.1 most emissions are considerably lower for the scenario than for the year 2005 due to the expected fleet renewal, i.e. the increase of the number of vehicles with higher emission standards For the year 2004 considered here, emissions are 4 – 7 % higher than the "BASE-2005" emissions from Figs. 7.131 and 7.132 in Section 7.4.1.1. Hydrocarbon emissions of heavy duty vehicles, however, these are expected to increase slightly until 2010.

7.4.2.4 Simulations of the baseline case

The air quality situation of the year 2004 was characterized by several violations of threshold values, although no extreme situations were observed (Amt der Tiroler Landesregierung, Abt. Waldschutz/Luftgüte). Violations of the 200 $\mu g/m^3$ threshold for NO_2 were found at 4 of 13 measurement stations of the Tyrolean air quality measurement network (Bericht über die Luftgüte in Tirol 2004, Amt der Landesregierung). These events occurred during inversion situations in February 2004 and December 2004. Exceedances of the target value of 80 $\mu g/m^3$ for the daily mean were found at the majority of the stations during the winter time. However, between April and October the target value was only exceeded on two days at a station near the motorway A12. For particulate matter (PM10) the threshold of 50 $\mu g/m^3$ for the daily mean was found do be exceeded on up to 84 days of the year, depending on the location. Observed ozone never exceeded the threshold of 180 $\mu g/m^3$ for the hourly mean at any station. However, the target value of 120 $\mu g/m^3$ for the 8-hour mean was exceeded in 2004 at approx. 10 to 20 days at the stations in the Inn valley and around 60 days at the stations located at higher altitudes.

Fig. 7.149 shows the regional distribution of the annual mean of simulated NO_2 and PM2.5 for domain D3. In accordance with the patterns of the NO emissions the highest NO_2 concentrations in Tyrol are found along the Inn valley and for the area of Innsbruck. Simulated PM2.5, which is about 70 to 90 % of PM10, matches the order of magnitude that can be expected according to the observed PM10 concentrations. Simulated PM2.5 is strongly dominated by secondary aerosol material (in particular HNO_3 formed out of anthropogenic NO). On single days with stable conditions primarily emitted particulate matter can contribute about 25 % to the total PM2.5 concentration in Innsbruck. However, the annual mean of the PM2.5 concentration does hardly reflects the patterns of the comparatively weak primary emissions which contribute by approx. 10 % to the total mass of PM2.5.

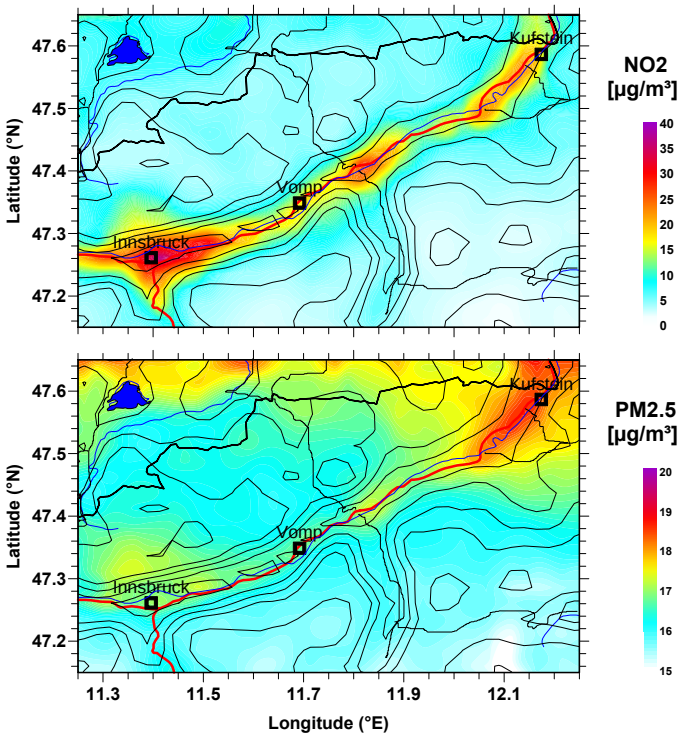

Fig. 7.149 Simulated annual mean of near surface NO_2 (top) and PM2.5 (bottom).

The temporal course of pollutant concentrations depends strongly on the meteorological conditions, which is generally well reproduced by the model. For example, the duration of inversion situations and frontal passages are simulated in good agreement with the observations. This holds also for the reproduction of the main valley wind systems. Although the simulations reflect the general observed features of the regional distribution, it is also obvious that a resolution of 2.4 km is not sufficient to resolve small-scale details. In particular, the simulated nocturnal cooling in the Inn valley (during inversion situations in the winter) was found to be too small at this resolution which resulted in an underestimation of the inversion strengths.

The scatter plot (Fig. 7.150) shows that the NO_2 concentrations are generally underpredicted as compared with the observations. This can be partly attributed to the underestimation of the inversion strengths by the model. However, a major part of the discrepancy is due to the fact that most of

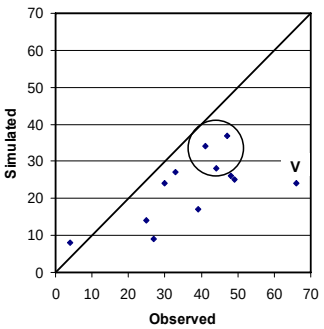

Fig. 7.150 Scatter plot of annual mean NO_2. The value of "Vomp Raststätte" station is indicated by "V".

the measurement stations are located near motorways and roads and are not representative for a larger area. The model results on the other hand represent an area of 2.4 × 2.4 km^2. This can be illustrated for the measurement site "Vomp Raststätte", which is directly located at the motorway with no other sources nearby. As in the model the traffic emissions are instantaneously spread over the full grid cell, the concentration near the motorway is much lower than observed. As the city of Innsbruck represents a more extended source region, the observations are more representative for a larger area and consequently the model results are closer to the observations (marked by the circle in Fig. 7.150**)**. Finally, the probable underestimation of the NO and PM emissions for Tyrol in the available emission inventory contributes further to the underprediction of pollutants.

7.4.2.5 Effect of changed traffic emissions

In order to estimate the effect of changed traffic emissions on the regional distributions of pollutants in Tyrol the simulations were repeated using the 2010 traffic emission scenario from TU Graz. The differences in the simulated fields of NO_2 and PM2.5 are shown in Fig. 7.151**.** The NO_2 concentrations are significantly lower for the city of Innsbruck and along the main motorways. Here, a decrease of up to 25 % was found and the effect declines rapidly with increasing distance from the NO sources. For PM2.5 the pattern is less pronounced due to the comparatively high background of secondary aerosol material.

Air quality simulations including chemical transformations also permit the investigation of the impact of emission reductions on secondary pollutants. For example, more than 50 % of the decrease in PM2.5 for the scenario can be attributed to the decrease of secondary HNO_3 formed by oxidation of emitted NO_x. Summertime ozone is a further compound that can be investigated this way. Near surface ozone is to a large extent a product of NO and volatile organic carbon compounds from traffic emissions. Therefore, changes in the amount and composition of traffic emissions can have an effect on ozone concentrations as well as on the days where threshold values are exceeded. As already mentioned, violations of the threshold of 120 µg/m^3 for the 8-hour mean for ozone are frequently observed at mountain sites as near surface ozone is not titrated by local NO emissions at these sites. Generally, the spatial patterns of the simulated mean ozone and the number of days with threshold exceedances

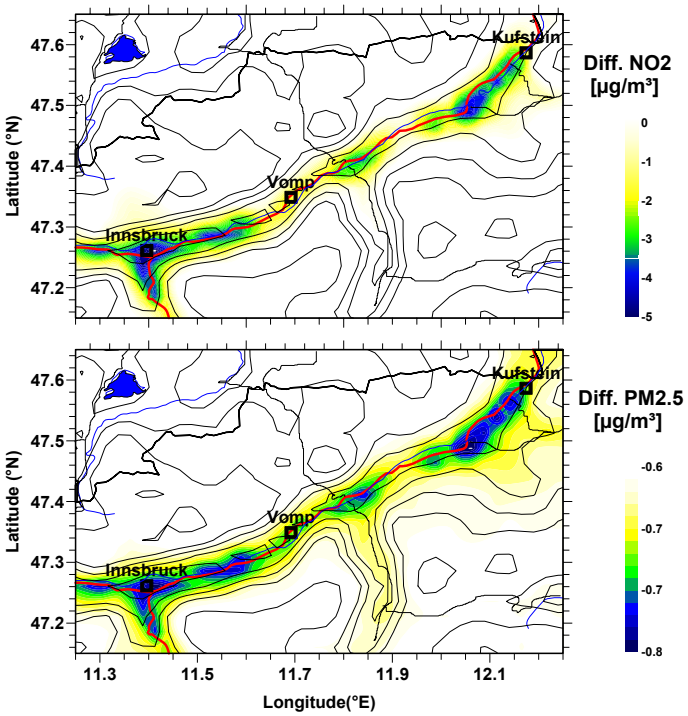

Fig. 7.151 Difference between base case and scenario for annual mean of NO_2 (top) and PM2.5 (bottom).

(Fig. 7.152) reflect rather well the observations with the exception that simulated local mean ozone concentrations are not that low as observed near stations at motorways with very high measured NO_x concentrations. The reduced NO_x concentration of the 2010 traffic scenario causes a reduced titration of ozone, in particular during the night-time, and consequently in a slight increase of the number of days with exceedance of the threshold of 120 µg/m^3 for the 8-hour mean. Since the effect is mostly restricted to the vicinity of roads and highways and does not reach into the more susceptible mountain regions this is not an issue so far. However, it must be taken into account that the shift towards larger NO_2 primary emissions with increasing Euro standards for Diesel passenger cars in the future (see also Section 7.4.2.3) will change the NO_2/NO ratio. This might result in an additional slight increase of ozone concentrations. Nevertheless, it can be expected that, besides high PM exposures, high NO_2 concentrations in the Inn valley will remain a major issue in Tyrol as compared to the possible increase in near surface ozone.

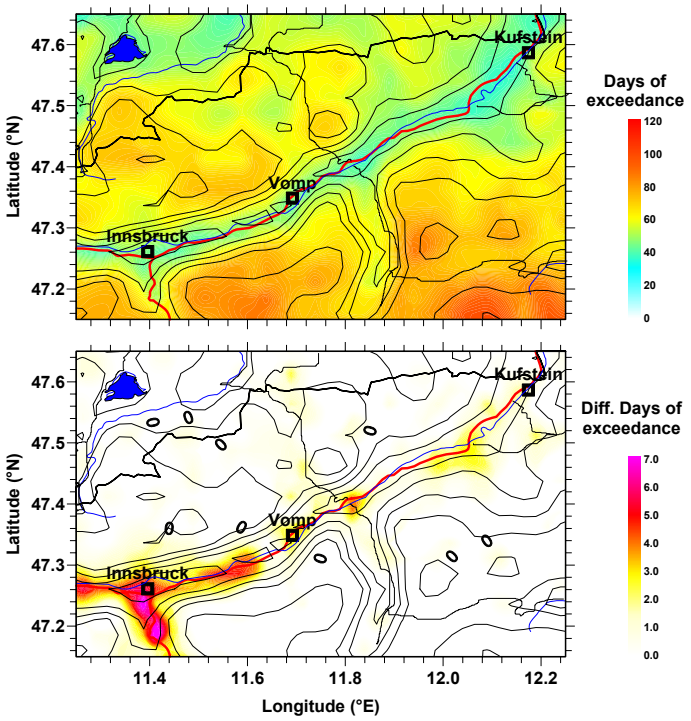

Fig. 7.152 Simulated number of days with exceedances of the threshold of 120 µg/m³ for the 8-hourly mean ozone for the base case (top) and difference between scenario and base case (bottom).

Regional air quality modelling is a tool for the estimation of the effect of emission reduction measures on the background fields of primary and secondary pollutants. For the investigation of the effect of strong local sources regional air quality modelling should be combined with microscale modelling. The combination of regional and microscale models is still an ongoing task.

In order to obtain more realistic patterns for simulated particulate matter concentrations more effort must be put into the development of a complete inventory of PM emissions.

7.4.3 Scenarios for the Fréjus corridor

7.4.3.1 Assessment of a future air pollution scenario

The dispersion simulations in Section 7.3.3.5 were repeated considering a possible "future" emission scenario suggested by CETE. It was considered that an amount of goods equivalent to about 1700 heavy lorries per day are moved from the highway to the rail transport system, taking into account the railway capacity. New calculations of the emissions on the highway, with 1700 heavy lorries less with respect to the original year 2004 emission dataset, were produced for both French and Italian sides (taking into account no changes on the national roads). The mean and maximum concentration of NO_x for the future scenario is plotted in Fig. 7.153 for July episode.

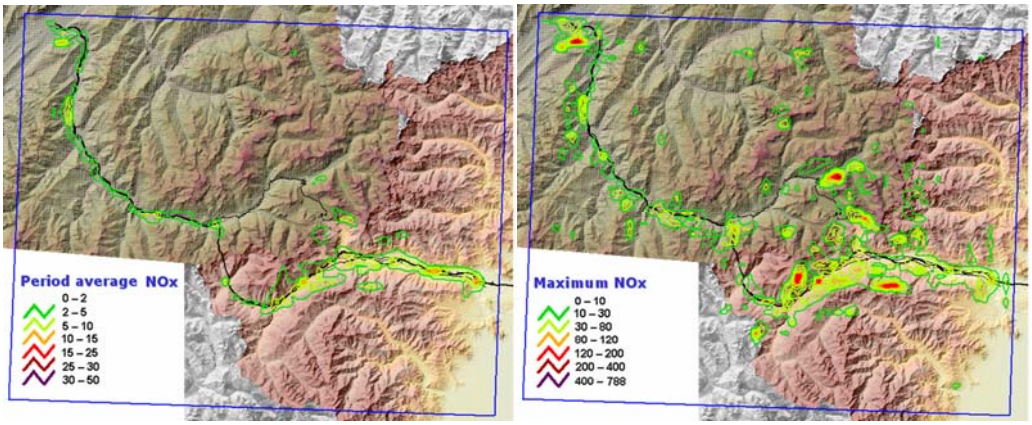

Fig. 7.153 Example of mean (left) and maximum (right) NO_x concentration from RMS simulations, future scenario, July episode.

To quantify the reduction in concentration related to the future scenario with respect the 2004 base year emissions, we calculated a normalized concentration reduction, expressed as percentage, with the formula:

$$\%R = \frac{\overline{C}_{2004} - \overline{C}_{\text{future}}}{\overline{C}_{2004}} 100$$

where $\overline{C}_{2004}$ and $\overline{C}_{\text{future}}$ are averaged ground-level concentrations for the base year 2004 and the future scenario, respectively. To have an overall estimation of the reduction, we calculated the *%R* for the concentrations averaged on all period of time for the different episodes in the full simulated domain. In Fig. 7.154 the distribution of relative frequency occurrences for the NOx normalized reduction values is plotted as a histogram for the July episode. We can infer that in 30 % cases the future emission scenario leads to a reduction in concentration, with respect to the 2004 year, ranging between the 25 % and the 30 %. Another 20 % cases fall in both 20–25 % and 30–35 % classes of reduction, thus giving a total of 70% cases between 20 % and 35 % reduction. Also the normalized reductions of the ground-level concentration for the 12-hour mean at single stations were computed. An example is presented in Fig. 7.155 for Susa and St. Julien stations. In most cases the improvements occurring in St. Julien are larger than those in Susa. In fact, in Susa two National roads contribute to the emissions while in St. Julien only one National road is present,

implying that the relative weight of the highway traffic reduction over the total of the emissions is different in the two cases. Therefore, comparing the future scenarios to year 2004 scenarios, an improvement, corresponding to lower concentrations, is registered both in the area distributed concentrations and at the single station. To finalise this analysis, in Fig. 7.155 a map of the differences between 2004 and future scenarios for mean and maximum concentrations in the July period are plotted. They quantify the improvement in air pollution in all domains which are achieved by the assumed transfer of heavy lorries to the rail transport.

Concentration maps were produced also for the subdomains where 100 m resolution simulations were performed: in Fig. 7.156 an example of the results for maximum NOx, for year 2004 and future scenario is given in Susa subdomain. In Fig. 7.157 the difference between the two scenarios is shown for both subdomains, centered on St. Julien and Susa.

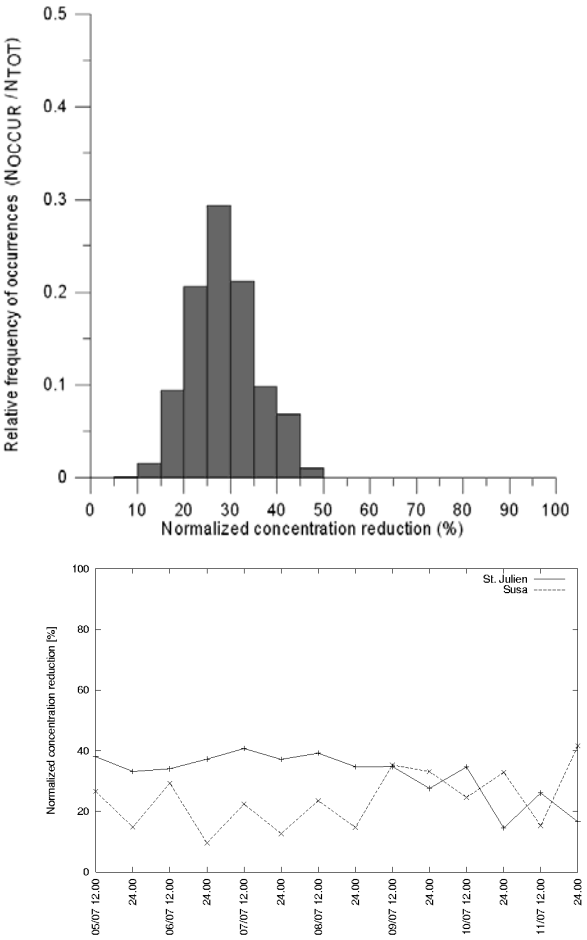

Fig. 7.154 Normalised NO_x concentration reduction. Histogram of future to 2004 reduction distribution for the mean of all July period in the full Frejus domain (top). Percentage reduction for 12-hours averaged concentration at Susa and St. Julien stations in July episode (bottom).

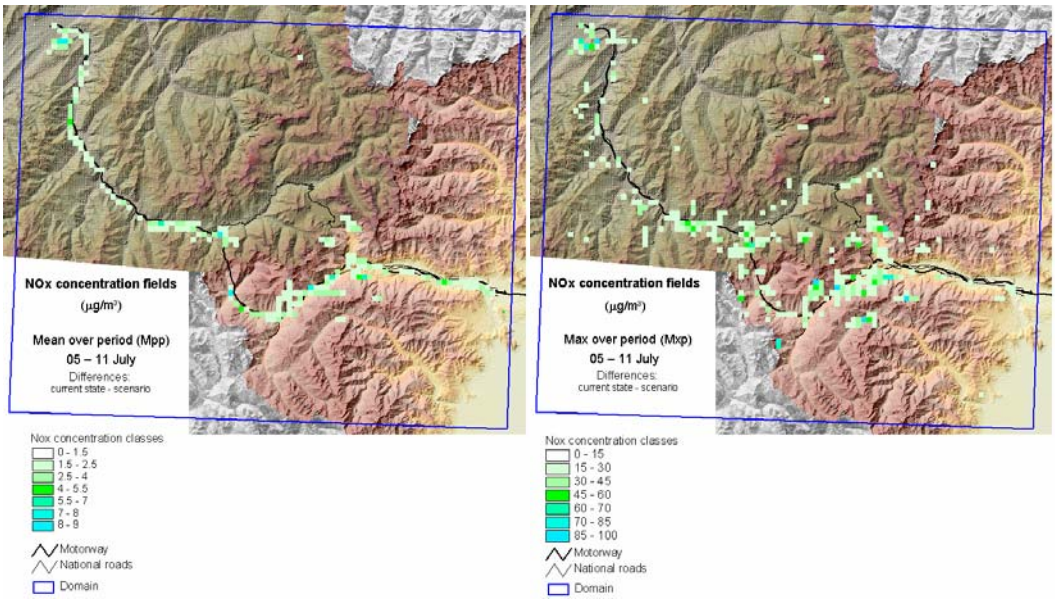

Fig. 7.155 Example of mean (left) and maximum (right) NO_x concentration difference between year 2004 and future scenarios, RMS simulations, July episode.

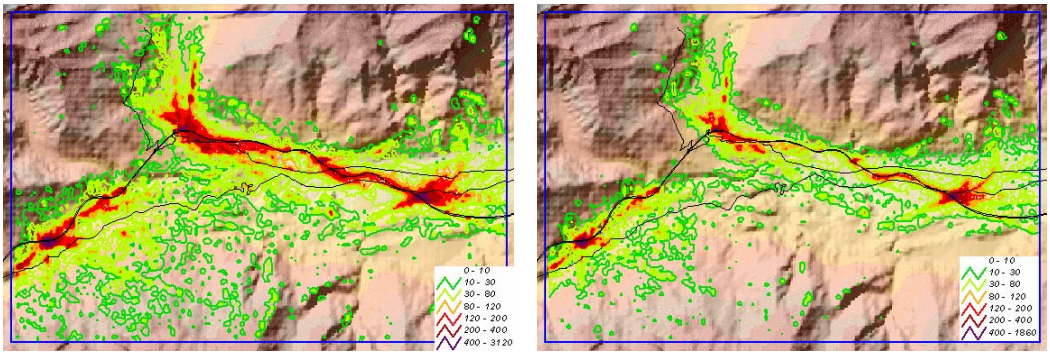

Fig. 7.156 Comparison of maximum NO_x concentration contours from MINERVE+SPRAY simulations, year 2004 (left) and future scenario (right), July episode, Susa subdomain.

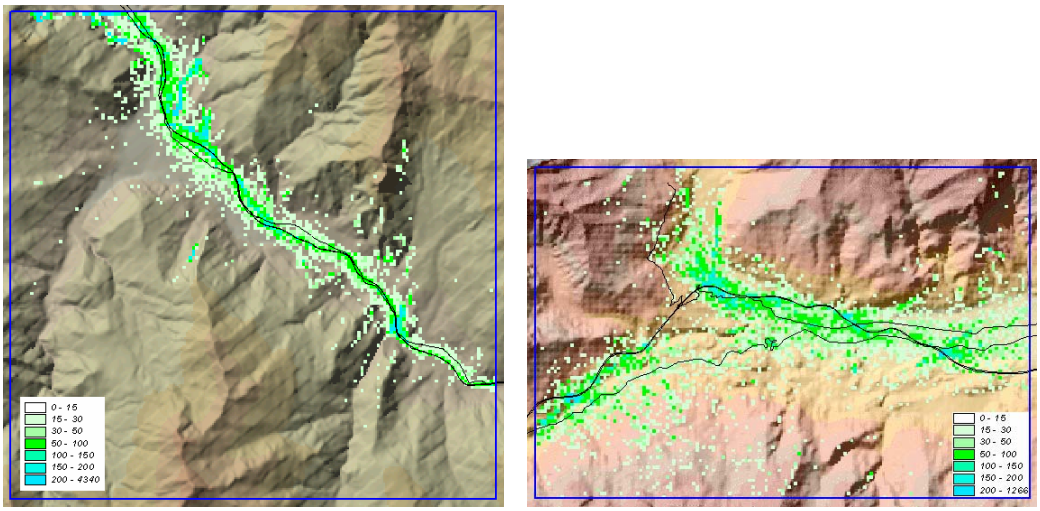

Fig. 7.157 Example of maximum NO_x concentration difference between year 2004 and future scenarios, MINERVE+SPRAY simulations, July episode, St. Julien (left) and Susa (right) subdomains

7.4.3.2 Modal shift scenario

Modal shift is one of the most promising measures to improve transalpine transports in a sustainable way. In 2003, the experiment of the railway motorway, also known as "rolling-road" between Aiton-Bourgneuf, in the Maurienne valley, and Orbassano, close to Torino, marked a watershed in freight transport practices in this area. Until the end of 2008, four shuttle trains, each one composed of eleven "Autostrada Ferroviaria Modalohr" (AFM) wagons, are operated daily, using the historical line and the Mont-Cenis tunnel. Despite the innovative nature of this experiment, the results of the first three years of operating reveal some room for improvement (IGC-CGPC, 2006). For instance the filling ratio (65 % at the moment) must be improved and should reach 80 % for increasing cost-effectiveness. The extension to 15 wagons per trains is also suggested. Another problem is the limited capacity of the actual line on which passengers (transnational, and regional), freight (classic and AFM) coexist and compete. In the name of sustainable development, aiming at conciliation between social, environmental, and economical interests, the Lyon-Turin railway project has been identified as a priority by the EC as early as 1994. It is considered as the missing link to connect thousands kilometres of railway lines of the European network, and it should greatly contribute to the development of modal shift.

The complete and complex chain of models (i.e. advanced meteorological, air pollutant dispersion, and sound propagation models as presented in the previous chapters), was tested on one scenario based on fictitious modal shift hypothesises inspired by the context. They are in no way officially supported, but should only be considered as input for testing the sensitivity of the methodology. A recent report addressing the potentials of freight transport through the Alps (COWI, 2006; ordered by EC) helped us to define a traffic scenario in a more consistent way.

This theoretical scenario suggests the effects of shifting as much freight as possible from motorway to railway. All technical, commercial, or political constraints are supposed to be removed. In this view, the volume of the shifting is limited by the capacity of the actual railway, considering that no new line is built. Traffic of long-distance passenger (9 trains) and regional trains (6 trains)

is kept constant and the motorway railway traffic is increased to its maximum to fill the capacity of the line. Therefore, 40 AFM trains (20 in each direction), would be added to "classic" freight trains representing a total of 188 freight trains. The 40 AFM could transport a maximum of $18 \cdot 40 = 720$ heavy vehicles. Assuming that service would operate 300 days a year and that the average capacity of each HV is about 16.4 tons, 3.55 Mt (millions of tons) of goods could be transported by the AFM. In the COWI report, the annual maximum capacity of the line is estimated at between 16.5 and 18.2 Mt of freight. On the basis of 188 freight trains per day (94 in each direction with 545 t of freight from France to Italy and 320 t in the opposite direction) operting on 260 days per year, the annual average tonnage of freight transported amounts to 21.1 Mt. This theoretical valuation exceeds the values given in the COWI report, however it was decided to keep this maximal value, counting on the fact that unused passenger train slots could be could be used by freight trains. Subtracting the tons of freight transported by AFM and those already transported by regular trains (8.4 Mt), the shifting of freight from road to rail would finally correspond to 9.15 Mt which is an equivalent of approx. 558,000 heavy vehicles per year or 1690 heavy vehicles (HV) per day. 35 % and 65 % of these HV would be "gained" or catched on the Mont Blanc and Fréjus corridors, respectively. The later would be relieved of:

$$\Delta HV = (720+1690) \cdot 0.65 = 1566\ HV/\text{day}$$

On the one side, this scenario leads to a dramatic decrease (-45 %) of heavy vehicles driving through the Fréjus tunnel that would positively affect air pollutants emissions. On the other side, the increase of freight trains traffic will have negative consequences on the acoustic situation, if no abatement measures are planned. We must keep in mind that this scenario relies on very fictitious assumptions.

Two situations are finally compared: the reference scenario based on year 2004 data, and the modal shift scenario, applied to base year 2004. This analysis is of course unrealistic, but the interest is to limit the number of variables, and to analyse the intrinsic effect of modal shift.

7.4.3.3 Air Pollution Index

On the basis of air pollutants concentrations simulations performed by ISAC-CNR and ARPA, the Air Pollution Index (*API*), presented in Section 6.3.3.2 and derived from the Swiss index, was computed over the Fréjus target area. This index, based on NO_2 and PM10 concentrations, has been spatialized on a 1 km² resolution square-grid, and the results are given in Figs. 7.158 and 7.159 for both scenarios. The maximum concentration of NO_x and PM10 over the two episodes was used to compute the indices. Doing so, the exposure is probably overestimated regarding impact on populations. However, it helps to point out most critical areas. Moreover, the tests performed on average values of concentrations showed a very limited sensitivity of the method that does not allow comparing seasons or transporting scenarios between each others.

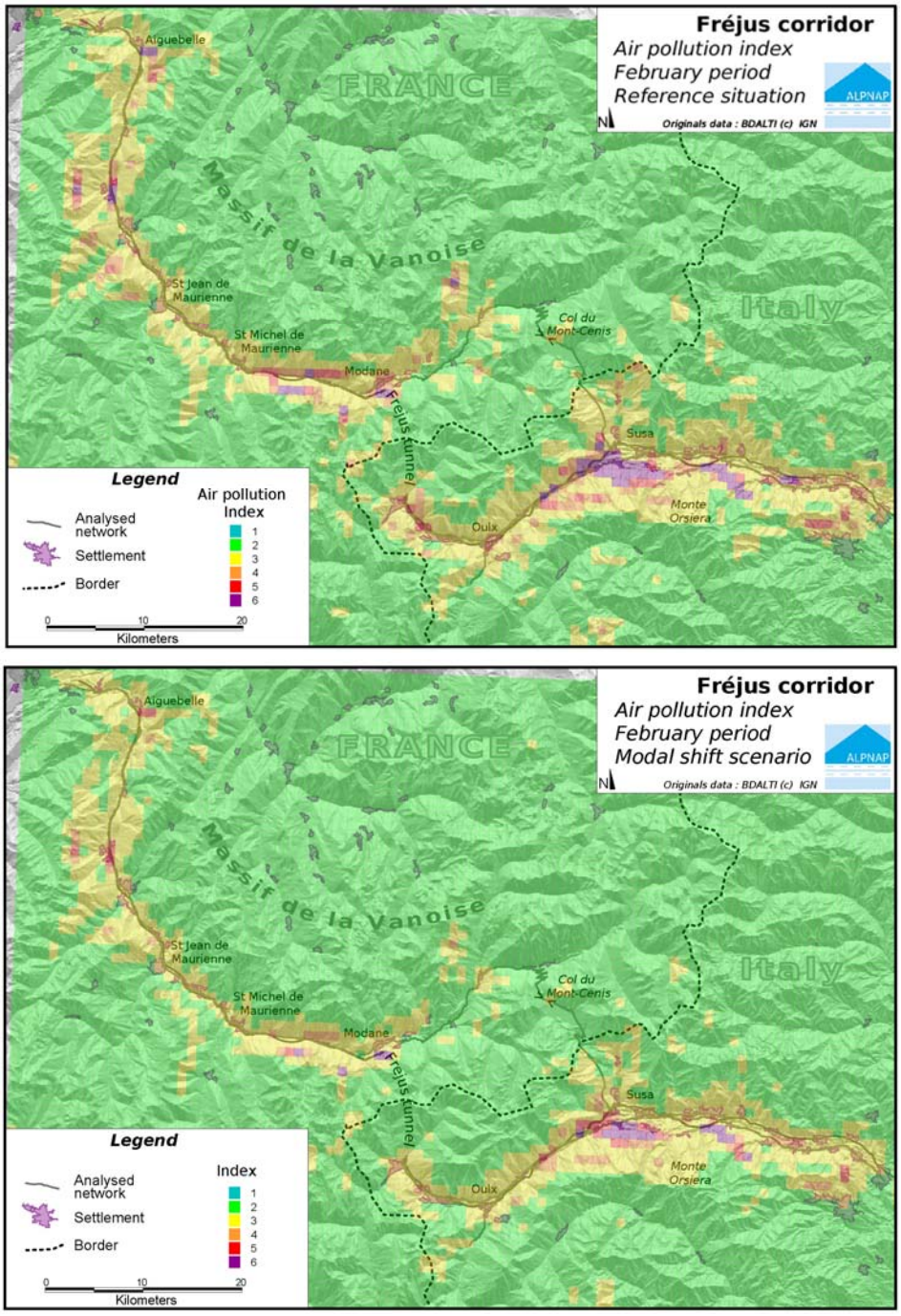

Fig. 7.158 Comparison between Air Pollution Index (*API*) computed over the Fréjus target area for the two scenarios: February episode.

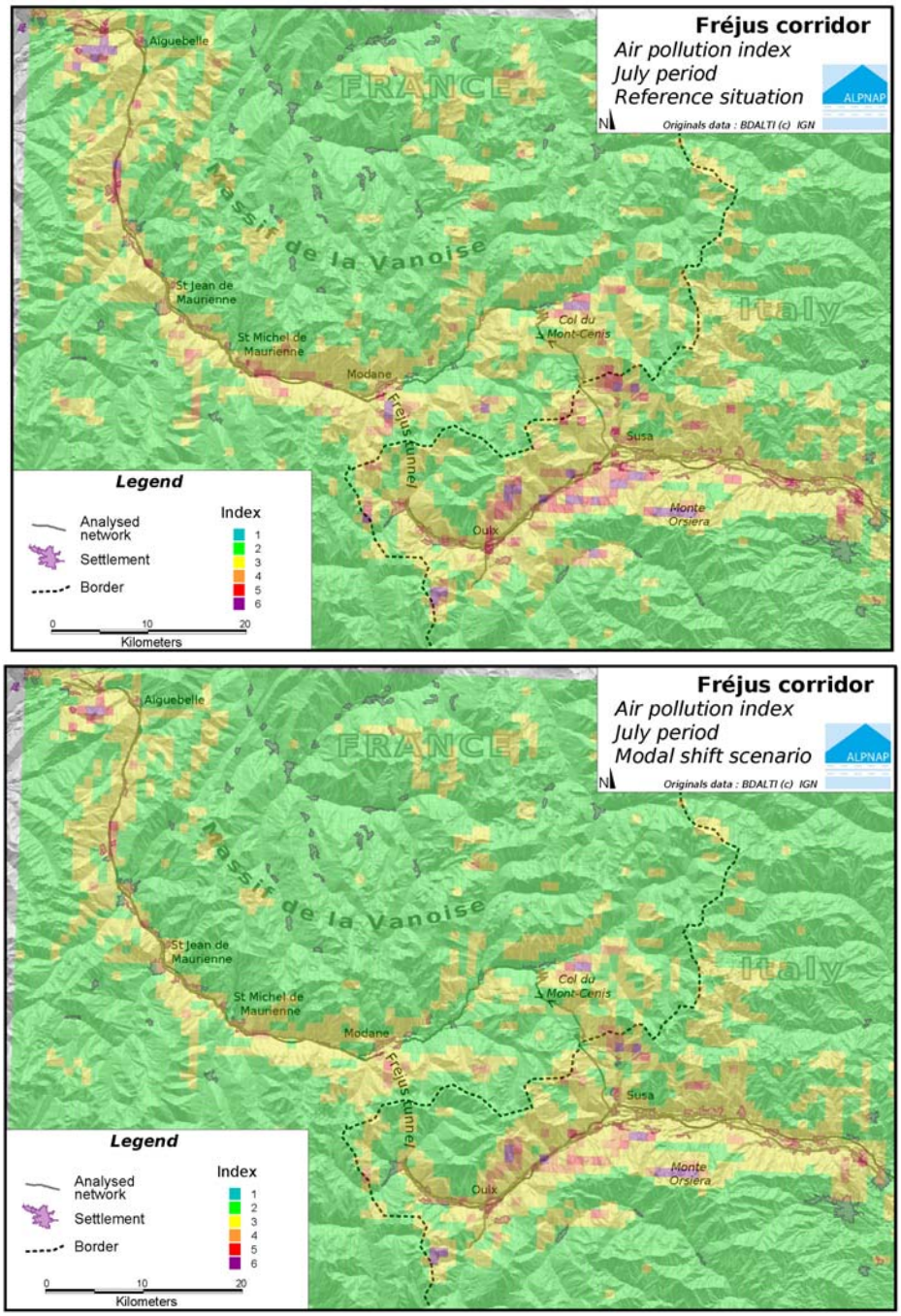

Fig. 7.159 Comparison between Air Pollution Index (*API*) computed over the Fréjus target area for the two scenarios: July episode.

Since it has not been possible to estimate the correct NO_2/NO_x ratio, a maximalist value of 1 was finally kept. The computation of the index reveals that its value is governed by NO_2 which is not surprising since only road emissions have been simulated.

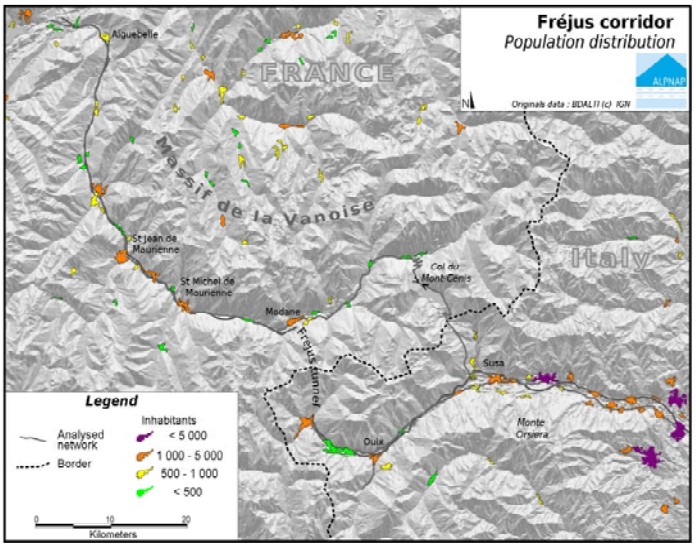

Fig. 7.160 Population distribution over the Fréjus target area.

Based on the population distribution (Fig. 7.160) the corresponding number of inhabitants exposed to each index category is calculated. It reveals that more than 87 % of the total population (approx. 146,000 in the domain of study) are exposed to moderate pollution levels, i.e. an API less or equal to 3, for both winter and summer episodes (see Tab. 7.15). The effect of contrasted meteorological conditions between the two episodes can be seen on higher API values. During the winter period pollutants are more confined to the deep valleys near the sources, whereas summer conditions promote dispersion. The result is a significant change in indices distributions. Even if traffic volume is generally lower during February compared to July, the number of people exposed to *API* is larger or equal to 4. This exposure is 1.5 times larger during the winter episode, and the number of inhabitants affected by *API* of Category 6 is radically increased. This is explained by the proximity between sources and high density of population areas for instance near Susa combined with bad dispersion conditions in February.

Tab. 7.15 Air Pollution index and corresponding number of exposed people for February and July periods– Reference scenario

API	February	July
1	0	0
2	65735	66481
3	62042	68022
4	14517	6992
5	839	4846
6	3198	0

The consequences of the massive modal shift scenario on the exposure to air pollution are noticeable in the *API* maps for both episodes (Figs. 7.158 and 7.159). Higher indices areas are significantly decreased, the spatial footprint of pollution is reduced, and indexes distributions are shifted correspondligly.

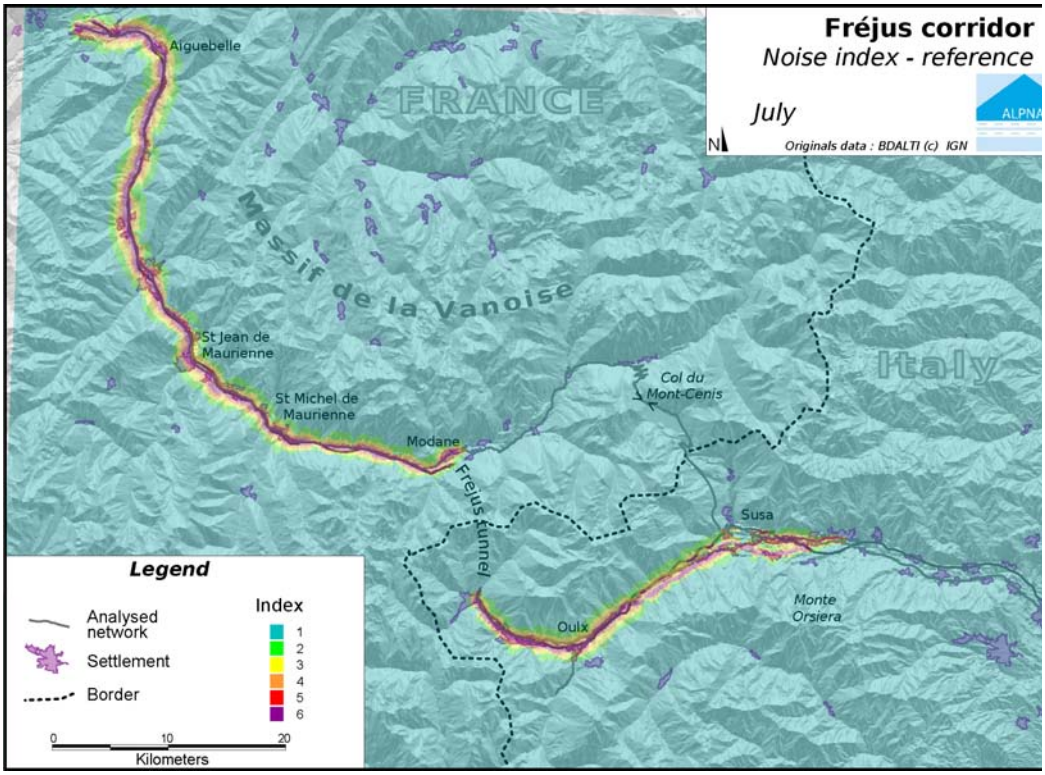

Fig. 7.161 Noise Pollution Index map. Reference year 2004, July episode.

7.4.3.4 Noise Pollution Index

Noise levels maps computed separately for roads and railways (provided by CSTB) were used to estimate the multi-exposure noise index (*NPI*) as defined in Section 6.3.3.3. The resolution of the results was decreased in order to adapt the data to the scale of the domain. However the difficulty is that noise levels vary quickly on small distances (about few meters) close to the source, and any aggregation at upper scale is synonymous of information loss. A 100 m² squared meter grid was finally used to represent the index (Fig. 7.161). The value in each mesh being the maximum of the index computed on a 10 m² squared. Of course, the process tends to inevitably overestimate the index. It must be kept in mind that this kind of map is not intended for performing accurate noise impact study, but should help identifying areas specially subjected to noise pollution. A local study, at building scale, is necessary to complete the analysis.

Tab. 7.16 Noise Pollution index and corresponding number of exposed people for both scenarios

NPI	Reference	Modal shift
1	79.8 %	78.3 %
2	5.3 %	4.1 %
3	4.0 %	3.9 %
4	3.1 %	3.2 %
5	2.3 %	2.9 %
6	5.3 %	7.3 %

Following the same procedure as for air pollution index, the noise pollution index map has been crossed with the population layer of the GIS tool. This allow us to evaluate the number or percentage of people of the domain exposed to each *NPI* category (Tab. 7.16).

The results worked out for both scenarios are depicted on Fig. 7.162. More than 80 % of the population living in the valley are outside the zone affected by transportation noise (NP = 1). The contribution of road and railways sources to noise pollution is located in the vicinity of the infrastructures. In these areas, the number of people concerned with NPI higher than 1 is more or less equally distributed. The consequence of the transfer of heavy vehicles from motorway to railway is an increase of inhabitants exposed to indices 5 and 6. The reason is that built-up areas are already protected from motorway noise contribution and the diminution of HV do not lead to significant noise reduction. On the other hand, the modal shift scenario was built without considering any new additional noise abatement system or strategy for railways, leading to more nuisances from these sources.

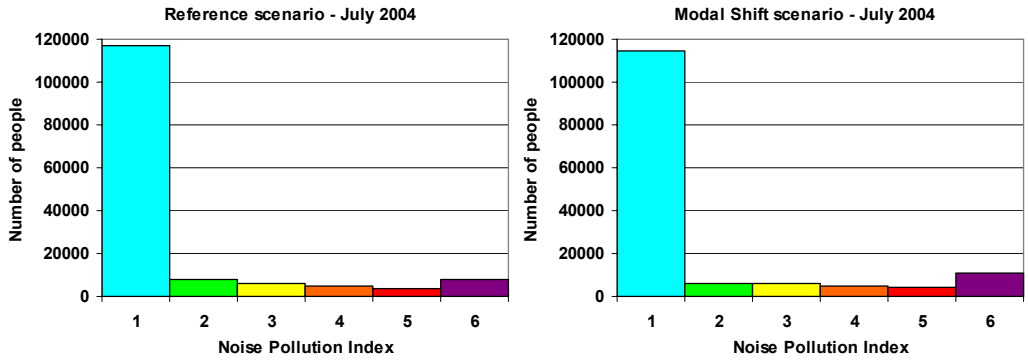

Fig. 7.162 Noise Pollution Index/Population distributions over the Fréjus target area. Comparison between the reference situation and the modal-shift scenarios for the July episode.

From a methodological point of view the index based method turns out to be sensitive and efficient to compare transports scenarios. However it must be underlined that moving tons of freight from road to railway, without suggesting compensatory measures, is somewhat unrealistic.

Hence, on 19 March 2007 an intention protocol was sign between French ministry and political authorities, and the French railway management authority (RFF), reaffirming that the priority character of the Lyon-Turin project (www.transalpine.com). The protocol clarifies the content of the programme of the first phase, with the goal to propose a capacity of 20 Mt of freight per year, after the opening of the base tunnel. This tunnel will help to reduce the freight traffic and the acoustic emissions on the historical line. Moreover, a complementary program of noise abatement measures is planned along the historical line where the railway is not underground. Therefore, the comparison of exposure values between reference and modal shift scenario must be considered as indicative all things being equal.

7.4.3.5 Global Air and Noise Exposure Index

As explained in Section 6.3.4, several aggregation functions could be considered, with the difficulty to justify the mixing between pollution effects of different kind. This is something actually already done with air pollution indices when aggregating sub-indices based on pollutants having different health impacts. Two methods of aggregation are proposed in chapter 6. The first one is based on the use of a maximum function applied to *API* and *NPI*. According to the second one, the Exposure Index is computed using weighted values of each sub-index. Results given by the first procedure are now discussed, and are compared below to the weight-method.

Computation of the Air and Noise Exposure Index based on the maximum function

The exposure index (*EI*) is defined as the maximum of both air and noise sub-indices computed in each grid mesh. While a 100 m² square-grid was used for the acoustic data, air pollution is resolved in 1 × 1 km² grid cells. The projection of the air pollution index to the finer noise grid does not add further information.

Fig. 7.163 presents the results for the EI distribution as an example.

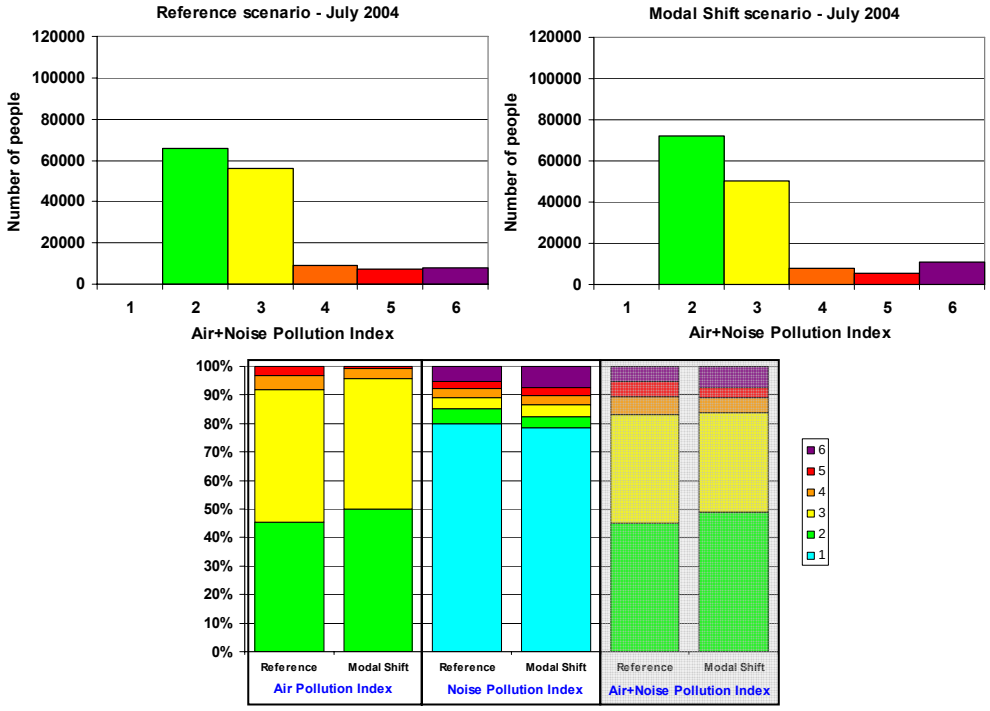

Fig. 7.163 Distribution of Air and Noise Exposure Indices (*EI*) computed over the Fréjus target area: July episode.

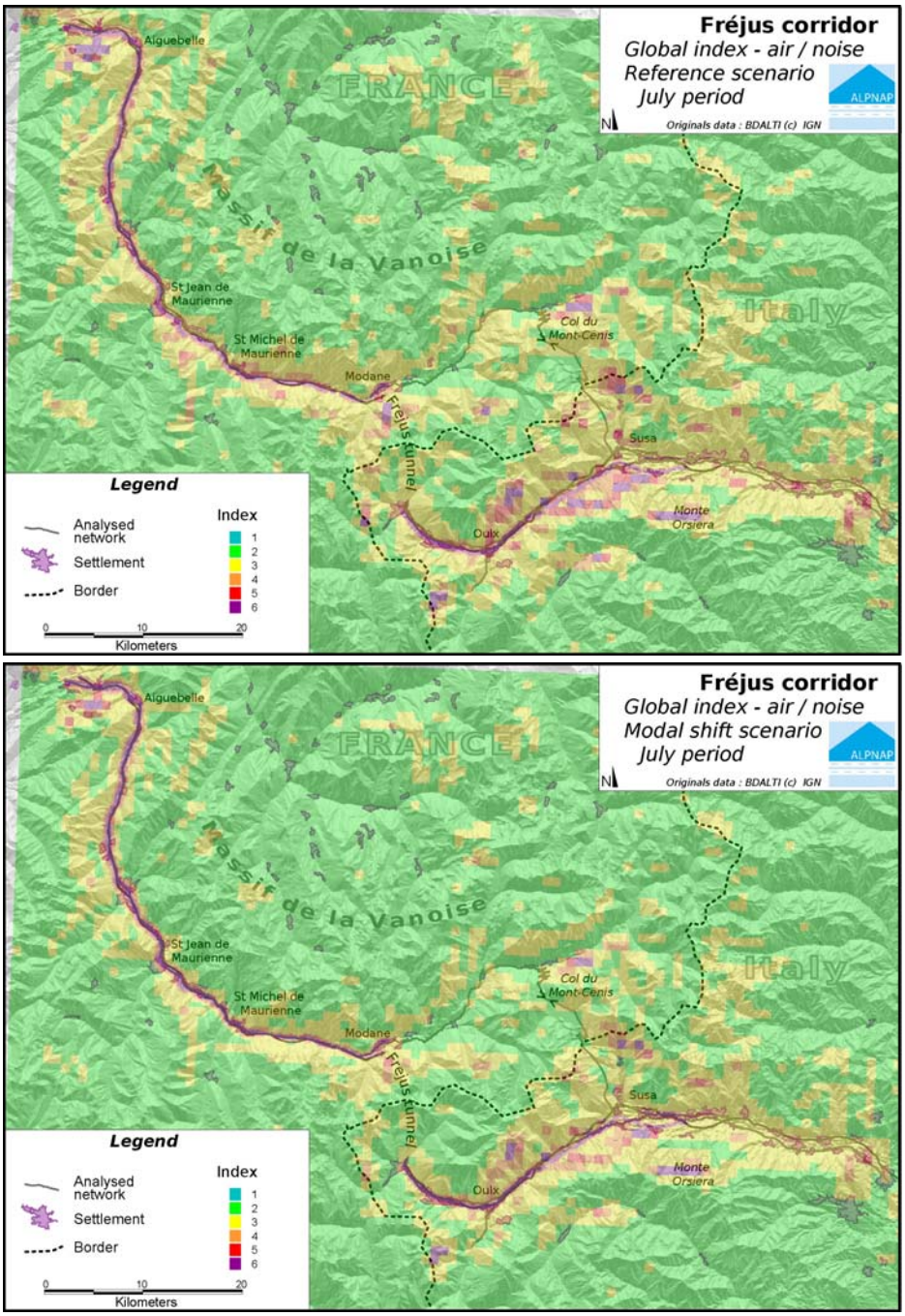

Fig. 7.164 Spatial representation of the Air and Noise Exposure Index (*EI*) computed over the Fréjus target area: July 2004 episode. Comparison between reference and modal shift scenarios

Fig. 7.164 gives a clear overview of the distribution of the combined air and noise exposure in the valleys. During the July episode, air pollution is more diffused all over the domain compared to noise energy only impacting the first three hundred meters around the transport infrastructures. The superposition of sub-indices *API* and *NPI* (Fig. 7.163 and Tab. 7.17) leads a common index which is governed by air pollution for the low and middle categories. The effect of the modal shift scenario is expressed by a shift of the index distribution towards the extreme values: air quality is improved whereas noise is significantly deteriorated for people living close to the railway infrastructure. This shift in distribution concerns about 4 % of the population (5850 inhabitants). The benefit of using the maximum values in the computations of the common index *EI* is to highlight the difference between scenario and the reference. It is however impossible to determine (without any spatial analysis) the portion of people exposed to both pollutions. However, using the weight-aggregation method can help to clarify this point.

Tab. 7.17 *API*, *NPI*, and *EI* (Max. function) and corresponding number of exposed people (and percentages) for both scenarios

	Air			**Noise**			**Air+Noise *EI* (Max. function)**		
Index	Reference	Modal Shift	Deviation	Reference	Modal Shift	Deviation	Reference	Modal Shift	Deviation
1	0 %	0 %	0.0 %	79.8 %	78.4 %	-1.5 %	0 %	0 %	0.0 %
2	45.4 %	49.8 %	+4.4 %	5.3 %	4.2 %	-1.2 %	45 %	49.1 %	+4.1 %
3	46.5 %	46.0 %	-0.5 %	4.0 %	4.0 %	0.0 %	38.2 %	34.6 %	-3.7 %
4	4.8 %	3.4 %	-1.4 %	3.1 %	3.2 %	+0.1 %	6.3 %	5.3 %	-1.0 %
5	3.3 %	0.7 %	-2.6 %	2.4 %	3.0 %	+0.6 %	5.1 %	3.7 %	-1.4 %
6	0 %	0 %	0.0 %	5.3 %	7.3 %	+2.0 %	5.3 %	7.3 %	+2.0 %

Computation of Exposure Index based on weight-aggregation method

Tab. 7.18 Exposure Index (average function) and corresponding percentage of exposed people for both scenarios.

EI Index (average)	**Reference**	**Modal Shift**
1	0 %	0
2	75.9 %	76.9 %
3	12.3 %	9.4 %
4	5.9 %	6.2 %
5	5.5 %	7.5 %
6	0.4 %	0

The main drawback of using the maximum of the sub-indices *API* and *NPI* to estimate a common air and noise exposure index *EI* is that non-dominant indices are masked by higher ones even if they are similar. Multi-exposure is therefore underestimated. Tab. 7.18 gives a valuation of the number of people exposed to the different *EI* categories when the average (weight value of 0.5, rounded to the nearest integer) of air and noise sub-indices is used. The interpretation of *EI*, and the meaning of the scale are now noticeably different from maximum function based procedure. Since, for instance, an index of 6 means that at least one of the sub-indices takes a value of 6 and the other one is at least 5. Comparing results for boths scenario shows that 0.4 % of the population (612 inhabitants) live under high levels of air pollution and noise pollution considering the reference scenario. Both approaches are probably complementary, but a lot of care and explanations must accompany the analysis in order to avoid misinterpretations.

To conclude, the global impact assessment methodology applied to the Fréjus target area, reveals to be an efficient tool for comparing transport scenario. Although no systematic sensitivity study was performed, the application shows that expected tendencies are corroborated. The graphical representation of indices helps to identify the areas that are simultaneously affected by air and

noise pollutions. The spatial integration, carried out by classifying populations according to categories of exposure provides a global view of the situation very useful when dealing with large scale domains.

A bottom-up/top-down application of this methodology is highly recommended: First, high advanced data are used to provide relevant aggregated information. This macroscopic point of view helps to compare scenarios. Secondly, disaggregated information helps refining the diagnostic and studying compensatory measures.

The methodology is still to be improved and should be tested on real scenario, but we hope it gives a good illustration of how complex data can be utilized to catch the environmental stakes of large geographic areas and transport policies.

8 Recommendations

8.1 Introduction

Environmental science is rapidly developing, bringing with it new knowledge about advanced observation tools and processes. These advancements allow us to more effectively monitor environmental strains. Sophisticated models allow us to predict the impact of human activities on these environments. Of course, scientific gains cannot be directly transferred into the practice, but need a phase of adaptation. This process, however, often takes several years (if not decades), if methods undergo time-consuming negotiations to become a state-of-the-art. Nevertheless, the process can be shortened substantially and advantages of up-to-date knowledge and science-based methods can be put into use before respective regulations are set into effect. Examples of benefits that could be immediately taken from available and validated science-based methods are listed below.

- Since standard methods are mainly based on simplifications, they do not account for the complexity of processes found in the Alpine space. Even if they provide sufficient accuracy under many conditions, they may not be reliable in special situations when and where natural processes are dominating that are beyond the validity range of these standards. Advanced methods may help to estimate errors which may be encountered by using standard methods.
- Advanced methods may also be applied to solve problems for which standard methods are not available. In these cases it is possible to apply the best method available to obtain the most reliable answer.
- Up-to-date science based methods can be also applied in cases when standard methods are prescribed, but an opening clause enables the use of more adapted methods where the standard is evidently not appropriate.

The following sections provide advice and recommendations on how to use actual, evaluated and validated scientific procedures and methods.

8.2 Base data

8.2.1 Gridded base data

Activities related to spatial data from different countries, and from different fields, are faced with problems of different spatial resolution in data sets from different data sources (e.g., elevation, land use, population, etc.). It would be desirable to achieve homogenisation of such data, and, as an intermediate step, the development of best practices for merging inhomogeneous data.

High-resolution base data are often available only on a commercial basis and at prices which exclude the usage for large areas, especially in scientific research, but also for applications such as environmental impact assessments. Given the fact that these data sets have been developed by public bodies and with public funds, ways of accessing them have to be created which will enable their full use. Access from one central distribution point or at least from one institution per country would be desirable.

8.2.2 Coordinate systems

For many applications, geographical information systems (GIS) are used, and spatial data are often stored and manipulated in specific map projections. Each country has its own national coordinate system(s). On the other hand, the meteorological and air pollution modelling community, as well as the World Meteorological Organisation, usually work with geographical coordinates (latitude and longitude). In order to facilitate data exchange, all data providers should be able to deliver their data sets in a single reference projection as well as in geographical coordinates. It is recommended that the reference projection should be the European standard, UTM WGS84.

As an immediate action, data transmitted in a map projection should always be accompanied by the full specification of the projection and other pertinent information, if possible, following the specifications of the European Environment Agency's "Metadata Standard for Geographic Information"[1].

8.2.3 Traffic flow data

There is an urgent need for harmonisation between different countries of the traffic flow data, the counting systems, and the vehicle categories systems used in emission modelling. Access to traffic flow data should be unbureaucratic and available close to real time. The latter point will allow the use of the data in short-term impact forecasts (nowcasting).

The advances in electronic traffic monitoring for tolling purposes should be made available for impact assessment. While, confidential data needs to be protected, it should be possible to make information available to researchers and environmental authorities on the numbers, gross weight and EURO emission class of heavy-duty vehicles using the new monitoring systems.

8.3 Emission data

8.3.1 Traffic models

Traffic models should be prepared for all critical regions (transit corridors). These models should allow traffic flow estimates for the whole traffic network, (not only motorways) as a function of time of day, week, month, and the occurrence of holidays. Such data are needed for realistic air pollution modelling. Additionally, it would be appropriate to have systems capable of using the hourly traffic counts on each day as input. For real-time applications (e.g., emission-controlled limits) such systems have to work in real time.

8.3.2 Emission inventories

For correct air pollution modelling, emission inventories need to have high spatial resolution in mountainous areas corresponding to the topographic structure. A resolution of 1 km is desirable for major Alpine valleys.

---

[1]See http://www.eionet.europa.eu/gis/geographicinformationstandards.html. These standards implement the ISO 19115 standards and also includes the reference coordinate systems adopted by EUREF (European subcommission of the International Association of Geodesy's Commission X on Global and Regional Geodetic Network, see http://www.euref-iag.net/).

A standard method is available for the classification of air pollution sources (namely CORINE, see **Chapter 2**). This classification system is usually considered in the emission inventories. This is important in order to enable replacing inventory emissions in a specific sector by more accurate ones from other sources. For example, inventory-based road traffic emissions should be replaced by those calculated from traffic flow data where the latter are available.

8.4 Measurements

8.4.1 Design of monitoring networks

Existing environmental monitoring networks are often incompatible with each other. This is the consequence of the functional responsibility which is split over many regional authorities in the Alps. Hence, a comparison of the environmental situation between adjacent regions is often not possible or at least complicated.

A coordination and possibly homogenisation of existing monitoring networks is necessary. Of course, the networks may serve different purposes which justify some of this diversity. Nevertheless, it is required to have a homogeneous distribution of basic meteorological and air quality data in the whole Alpine space. For example, given the scarcity of standard synoptic stations in the Italian and French Alps, it would be highly desirable to improve and harmonise the existing meteorological networks, with respect to the needs of reliable air pollution and noise assessments. Of particular relevance is the compliance with uniform standards regarding thee sensor quality and time-averaging and archiving strategies. The need for such actions may be illustrated by the fact that along the Brenner South corridor six different institutions collect data with strongly varying parameter acquisition strategies.

While certain meteorological data are exchanged internationally, and certain data are freely available for research in all countries, the density of these data is insufficient for regional-scale studies. The meteorological services of the Alpine countries, already having close relationships with each other from large field campaigns in the past as well as regional cooperation programmes such as the INTERREG Alpine Space Programme, should work towards an observation network which meets the needs of air pollution and noise issues over the whole Alpine area. Such a network should also include organisations beyond national meteorological services, it is should be harmonised, and it should be accessible across borders for authorities and scientists.

The monitoring networks for air pollution are not dense enough everywhere, and existing stations are not always suitable for monitoring the impact of motorways. Finding adequate monitoring sites is especially difficult for regions where the roads are along slopes or on viaducts. The representativeness of each station needs to be appropriately considered, allowing for the possible employment of different kinds of applications (model validation, health impact studies, etc.). If necessary, the degree of influence of the various sources (close or more distant) needs to be assessed in order to understand for what it can be considered representative.

8.4.2 Vertical profiles of meteorological variables

The vertical thermal structure of the atmosphere is critical for the assessment of air pollution and noise, and it is evident that it is quite variable between different valleys and basins, as well as adjacent plains. Therefore it is necessary to set up a sufficiently dense network of meteorological profile measurement systems. In order to achieve this, possible means are

- Radiosoundings (should of course be operated from the valley bottom, not from elevated sites, so that there data include the valley atmosphere) ,
- tethered balloons (can be equipped with a variety of appropriate instruments, need permits, not with strong winds)
- acoustic soundings (mini-sodar (up to about 200 m), sodar (up to about 500-1000m), deliver wind profiles and estimates of mixing height, possible annoyance of nearby people by noise has to be taken into account)
- Radio-acoustic sounding systems (RASS, deliver temperature profiles, possible annoyance of nearby people by noise has to be taken into account),
- Wind profilers (electro-magnetic, optical profilers for the lower few hundreds of metres above ground are presently under development, the first of these are commercially available),
- Ceilometers (estimates of mixing height),
- Slope profiles (slope profiles, e.g. along a funicular, are only useful if set up well and corrected on the base of comparison with soundings and expert knowledge),
- Temperature and accurate atmospheric pressure measurements at a valley site and a nearby mountain site (this is the cheapest option, but it also brings the least benefit).

8.4.3 Vertical profiles of air quality parameters

The vertical thermal structure of the atmosphere has also a severe influence on the vertical distribution of air pollutants, and it is evident that this distribution may be quite variable between different valleys and basins, as well as adjacent plains. Therefore it is necessary to set up a sufficiently dense network of air quality profile measurement systems. In order to achieve this, possible means are

- tethered balloons (can be equipped with a variety of appropriate instruments, need permits, not with strong winds),
- ultra-light aircraft for local-scale observations,
- aircraft with in-situ instruments and downward-looking Lidars for regional-scale observations,
- DOAS and FTIR along slanted paths from the valley floor to a slope site (path-averaged pollutant concentrations for paths up to several kilometres in length),
- Lidars for the measurement of vertical profiles of aerosol concentration and selected gases,
- Ceilometers (a simple Lidar, vertical profiles of aerosol concentrations),
- Slope profiles (slope profiles, e.g. along a funicular, are only useful if set up well and corrected on the base of comparison with soundings and expert knowledge),
- monitoring stations at a valley site and a nearby mountain site (this is the cheapest option, but it also brings the least benefit).

8.4.4 Supplemental measurements for specific purposes

Supplemental measurements should be carried out if suitable and representative base data with long-term availability from a network are not available at a site. Another motivation is the study of specific phenomena. It is important to have sufficiently long data series. Measurements for planning purposes should not be shorter than one year, or one season, if critical conditions are limited

to a specific season. Even then, it is mandatory to compare the measurement period with climatological records (10 to 30 years) and to use a nearby site to assess the long-term representativeness of the measurement period. In the case of unrepresentative conditions, measurements have to be extended, or a suitable statistical correction needs to be applied. Also for the interpretation of case studies, comparisons with longer-term conditions are necessary.

8.4.5 Technical recommendations

The quality of measurements strongly depends on many factors. Often compromises have to be found for logistic reasons (cost of the instrument, maintenance, available power supply, consent of property owners, etc.).

Site selection is a very critical parameter, and experienced experts should be involved. It is necessary that the sensor location is representative of the area for which information is sought. If the measurement should be representative of a larger area it is important that the sensors are not affected by local influences.

Sensors and data loggers should be of high quality (like used in networks of meteorological services, or research-grade) and comply at least with ISO 9060 and WMO standards (WMO, 1996).

Sensor calibrations should be performed and documented, corresponding to the characteristics of the sensor and the manufacturer's rules. Calibration is especially important for radiation and atmospheric trace gas sensors. Field intercomparisons can also be useful, especially if different types of instruments measuring the same parameter (wind, trace gas concentration, etc. are engaged in one network or field campaign. Calibration and/or intercomparisons before and after a field campaign help to ensure good performance.

The importance of data quality assurance and the amount of work for data preparation and evaluation is often underestimated. The consultation of external experts (not only technical but scientific) should be considered in the planning phase.

Meta data, such as site and sensor description, calibrations, accuracy and precision of data (especially for non-standard instruments), data acquisition, average and storing times, failures, maintenance activities etc., must be well documented and should be supplied together with the data.

For wind speed measurements ultrasonic anemometers are recommended instead of mechanical ones (cup anemometers), as they work well even under very low wind speeds as often encountered in Alpine valleys and basins, and are also less sensitive to malfunction under low temperatures. Heating is essential during the winter in any case.

Temperature and humidity sensors require effective radiation shields and should be ventilated.

8.5 Relationship between measurements and models

8.5.1 Applications

Models – simple ones or complex ones – are applied for several purposes with respect to noise and air pollution. Especially relevant purposes are:

- assessment of future scenarios and planned measures;
- assessment of the present situation with spatial coverage;

– assessment of planned or implemented measures; in this case, modelling is useful, if not necessary, to separate the influence of the measures from the influence of other factors, such as traffic flow or different meteorological situations;
– investigation of underlying mechanisms and relevant processes; in this case it is often convenient to apply the models not to a specific real situation, but to an idealised though realistic one. The results can be transferred to all similar situations and are not only valid for one situation.

In relationship to models, measurements are required, inter alia, for

– providing direct input to models, e. g., traffic data, wind speed and direction, stability, pollutant concentrations, etc.;
– providing indirect input to models, for example by being fed into operational weather models whose output is utilised as initial and boundary condition of specialised smaller-scale models;
– providing data for model testing, adaptation, and validation.

Measurements are also important independent of models, for example for

– investigation of phenomena occurring in the environment, e.g. specific wind systems and mixing layer heights;
– monitoring of the situation at some point or, in the case of remote sensing devices, in the profile, section, area etc. covered by the device; this is important especially for judging compliance with air quality regulations.

8.5.2 Specific recommendations

Unless a model (see Section 8.6 below) has been well validated under comparable conditions (similar topography, emissions, meteorological situation, input data availability, etc.), it is mandatory to compare the model output with measurements from some past episodes. This will allow for a critical assessment of the model performance, its possible shortcomings (in specific situations) and/or its other limitations. Results of such performance assessments have to be included in the presentation of results.[2] Even if a suitable validation has already been carried out, it can be quite useful to repeat such comparisons for the specific spatial and other context of a specific study.

Obtaining a spatial distribution from point measurements is never a trivial task. Procedures implemented (for example in GIS systems) can easily fail in complex terrain like the Alps, even if height dependence is included. Spatial patterns can be influenced by prevailing flow directions, sun and shadow, weather divides between valleys, etc. Producing gridded data from measurements always involves an appropriate interpolation and extrapolation model in the background, be it simple and statistical or more complex and possibly based on physical relationships. It has to be documented and justified. Even an isoline analysis of single measured parameter values in a map implies knowledge of the spatial distribution of the parameter that needs to be justified.

[2] More details are given later under “Model validation”.

8.6 Modelling

8.6.1 General considerations for model selection

Models can be used for a large variety of very different problems. The problems can be associated with different scales in space (local or regional) or time (short-term exceedance or long-term statistics) and different processes can be involved. Available models are often optimised to certain scales or processes. Therefore, it is necessary to select a model with special care.

The following questions should be borne in mind for the selection of a model or model system:

- What expertise is required for proper handling of the model?
- What is the required computer infrastructure, taking into account the necessary resolution?
- Can the model simulate the relevant physical processes?
- How can the quality of the model results be assessed?
- What is the expected reliability and accuracy of the model and does it meet the requirements?
- Which kind of input is needed to achieve the desired quality, and is this input available?
- Is the model state-of-the-art, well-tested, documented and developed by an active community?

8.6.2 Specific recommendations for model selection

8.6.2.1 Meteorological models

Prognostic models are preferable for the production of meteorological fields as input to transport and dispersion models in complex and inhomogeneous terrain. The technical recommendations given below (especially the minimum resolution) need to be considered.

Diagnostic models can be a profitable tool when a rich observed data set of both surface and upper-level wind data is available. This can be the case, for instance, in the context of field campaigns with surface stations and Sodars, tethered balloons, etc. Unfortunately, in the Alpine region usually not enough input data are available to ensure reliable model output.

Downscaling the output of a prognostic model using a diagnostic model may be a proper tool to reach very high spatial resolution – on the order of 100 m or less.

8.6.2.2 Dispersion, transport and chemistry models

Models which can only use the meteorological conditions at one point (i.e., Gaussian models and some Lagrangian particle models made for regulatory purposes as a replacement for the Gaussian models) are obviously limited to a range of at most several kilometres. Inside of valleys, they are suitable only as long as the Gaussian plume is not impacting the valley sidewalls, and the wind and turbulence field is approximately homogenous (which depends very much on the specific application). In practice this means that they can only be used in larger valleys with a rather flat floor and on distances on the order of the width of the valley floor or even less.

Models which assume stationary conditions (i.e., Gaussian models and some local-scale Lagrangian particle models) are confronted with the same limitation as any model with a very small (few kilometres) domain: they can only simulate the part of the ambient concentration that is caused by recent and nearby emissions. In general, this will only be a fraction of the total concentration. Unless this is all that is needed, more complex numerical models with full consideration of the variations in all three dimensions and in time are required.

The strength of Lagrangian particle dispersion models is that they can resolve well sharp gradients, including point and line sources. This is important, especially close to the sources. Their drawback is the limited ability to consider chemical transformations, and sometimes the computational cost. In these models, it is also easier to track separately emissions from specific sources. This is useful for process studies, inverse modelling and deriving emission control strategies.

Eulerian chemistry-transport models are well suited for simulations of larger domains (whole valley or region). For such purposes, they could be run at grid resolutions on the order of 1 km. Therefore, one cannot expect them to resolve realistically e.g. concentration gradients along the roads. On the other hand, their strength is the ability to include the contribution of more distant sources through nesting, and to simulate all relevant chemical reactions. For ozone and particulate matter, this is mandatory.

For all these models, appropriate and accurate meteorological and emission input data are a key to good performance.

In general, statistical models are nowadays considered only suitable for very short-range forecasting (few hours) and for statistical improvement of the output of deterministic models. In Alpine terrain, they are even more difficult to set up because of the complexity of influence factors. It needs to be considered that recent emissions are responsible only for a rather small fraction of the total variance of concentration, except for concentrations very close to a source and on short time scales.

8.6.2.3 Noise prediction models

The selection of the appropriate noise propagations models is mainly determined by the computational effort which is needed for the various applications, and the processes which are included in the different models. Applications span from specific problems in a defined propagation path to extended noise mapping. There are needs for the prediction of long-term (annual) mean values, as well as the assessment of maximum levels. Finally, the models can be used for optimisations, e.g. to find the routing of a planned road or rail connection with the minimum noise exposure, or optimal protection measures in the propagation path (e.g. noise barriers) in a given environment.

For the calculation of the long-term, large-scale average impact of traffic noise, the use of a ray model is the best compromise between accuracy and calculation time. The global effect of meteorological conditions on noise propagation may then be considered through a two-dimensional frequency distribution in categories based on direction and meteorological situation.

For specific boundary studies, such as the effect on noise propagation of small height protections, complex noise barriers, or viaduct geometry, it is advised to use an adapted numerical approach like the boundary element method. A 2D simulation is a good compromise in most cases. This method can be used to find optimal solutions for efficient noise protection installations.

For accurate prediction of the local effects of meteorological conditions on received noise, one may use a specific numerical code such as the Euler-type finite-difference time-domain model or the Parabolic Equation approach. Such models can be used in worst-case assessments to find (weather) conditions in which the violation of limits is likely for a given emission.

For incidences when a study is considering both, complex boundaries and fine meteorological scenarios, predictions maybe undertaken with a hybrid model, for instance the boundary element method, in the vicinity of the traffic noise source, and the parabolic equation, for long range propagation from the infrastructure.

Another point of interest is the prediction of the temporal evolution of the sound level for a moving source, e.g. a train. This can be achieved by a series of 2D calculations performed in successive vertical planes. Such calculations should contain data on the moving source and receiver. It may also be obtained by from a convolution product between the impulse response of the moving source and the temporal distribution of the source power level along the path.

8.6.3 Technical recommendations for prognostic numerical modelling

For simulations in the interior of Alpine valleys with a floor width of a few kilometres, prognostic numerical models need to be run at grid distances of 1 km (or less). Smaller valleys may require even smaller grid size. This condition needs to be fulfilled even if diagnostic modelling is added to downscale results. This is necessary because these diagnostic schemes can only adapt the wind to topography, but will not correct wrong results.

These models have to be run with a nesting approach and cover a sufficiently large domain to minimise boundary effects, while at the same time, capturing the region producing the flow.

Truly horizontal diffusion (sometimes called *z*-diffusion) has to be used in order to avoid artificial vertical mixing under stable conditions.

Further model features can improve the accuracy (though not yet being standard) in all models. They include:

- the upper boundary condition for dynamics should be the so-called radiative boundary condition, allowing wave energy to radiate through the model top;
- a coordinate system which damps the small-scale height variability of model layers more higher up in the atmosphere more strongly than the larger-scale variability;
- consideration of topographic effects on solar radiation (cosine effects on slopes and shadowing by surrounding terrain).

8.7 Evaluation methods

In order to allow the drawing of the desired conclusions, both measurement data and model results need to be evaluated, condensed, combined and presented. Established evaluation methods should be used and the state-of-the-art in science considered.

One should be aware that models, especially the more simple types of air pollution models, cannot be expected to yield very close agreement between measured and modelled values for each measurement site and hour. The more data are aggregated and corresponding statistical parameters are considered (e.g., the agreement of the cumulative frequency distributions for a whole year, or the annual mean values), the better the agreement will be. For values paired in space and time, it is already considered a very good agreement if most of the data are within a factor of two, and a factor of five is often still considered acceptable. This holds, however, only if bias and frequency distributions are also reasonably good. In particular, the following recommendations are given:

- Comprehensive air pollution and ambient noise assessment studies require a solid meteorological expertise. Otherwise it is not possible to associate causes and effects. In the Alps it is necessary to know about the possible interactions between the topography and the atmosphere because they are often dominating the transport conditions for air pollutants and the propagation condition for noise.

- For a reference on standard statistical scores for model evaluation see Mosca et al. (1998a, b). Though not used as much, the methods proposed by Taylor (2001) deserve consideration also for air pollution modelling and related applications.
- Directional data (e.g., wind direction) must not be analysed with standard statistical methods such as correlation coefficients. Evaluations need to be based on components such as east-west and north-south wind component. The identity of 0° and 360° has to be considered.
- Temperatures at different heights should be presented in the form of potential temperature because this makes it much easier to infer the stability.

8.8 Noise assessment and abatement in Alpine areas

8.8.1 Monitoring exposure

The application of different noise mapping software in ALPNAP has demonstrated that significant differences occur when the fraction of people highly annoyed by noise from different sources is estimated by linkage to survey data. The differences vary by type of built-up area and by noise intensity (L_{den}). Even for L_{den} > 70 dB(A), differences in the highly annoyed can reach 8 dB(A). For L_{den} < 55 dB(A) the differences are much larger (mainly in urban areas). Since some type of software performs better in urban, other in rural areas, or in predicting noise exposure on slopes, it is recommended to consider the strengths and weaknesses of the currently available software. Expert advice is also necessary, especially for the evaluation of action plans in the framework of the Environmental Noise Directive (END). Some software may not be able to detect the effects of actions taken in the course of fulfilling the requirements demanded by the END.

8.8.2 Evaluation of noise mapping software

The performance of noise mapping models should not only be tested in a model validation with respect to measured noise levels, it is much more necessary to estimate the sensitivity and robustness of the models with respect to the derived noise pollution indices and exposure-response function. Annoyance has proved to be the most sensitive indicator with respect to differences between different numerical noise propagation models.

8.8.3 A railway bonus in Alpine areas ?

A so-called “rail bonus”, typically 5 dB(A), is applied by law in several European countries with Alpine territory (Austria, France, Germany, Italy, Switzerland). The ALPNAP health study has revealed strong deviations from the standard rail annoyance curve for general rail annoyance in spite of serious noise abatement efforts during the last 10 years in the area of investigation. At levels above 70 dB(A), the rail is the dominant noise source, and the annoyance level (during the night) increased rather strongly at these high levels. The high share of freight trains during night was a key contributor to these higher noise levels. However, the direct propagation of noise to the residential areas on the valley slope, also contributed. Thus it is recommended to take a cautious approach in applying the “rail bonus” in Alpine areas without having adequate exposure effect information available.

8.8.4 Noise mitigation measures

Noise mitigation strategies in alpine valleys should focus on reductions in the vicinity of the source – as mitigation measures on the pathway to the receiver are much less effective through several processes acting against full effectiveness. It means that the effort should be put on two main actions: the reduction of noise emission at the source itself (speed limits, limitation in the number of heavy vehicles, reduction of rolling noise, etc.) and the optimisation of noise abatement due to close obstacles such as noise barriers or terrain relief (presence of berms, road or railways in cuttings, etc.). High-rising viaducts have also shown to be interesting noise abatement solutions.

The effect on annoyance of existing noise barriers for residential areas beyond 300 m distance was found to be rather poor to null for receivers located on a mountainous configuration (dwellings on a slope "above" road or railway track). The effectiveness was weaker for barriers along railways than for those along motorways. Therefore, it is recommended to account for this reduced effectiveness of noise barriers already in planning, using appropriate noise propagation model which is able to detect the reduced effectiveness and to invest more serious efforts in the evaluation of existing noise barriers as well as in the optimisation of complex ones (small height, crowned, etc.).

8.9 Health impact assessment

8.9.1 Instruments and procedures for health survey methods

Instruments used should also target lower level (less serious) indicators of health, such as quality of life and satisfaction providing information to track early signs of unsustainable development. These instruments should contain standard modules of evaluated pieces of questionnaires but also be supplemented by newly developed questions to target specific issues unique to the alpine areas being investigated and to their communities.

As the health risks involved with air or noise pollution are small compared to strong individual risk factors such as smoking, larger samples are required to detect these risks. The scattered pattern of residential areas (especially on the slopes in contrast to the valley bottom) often needs complex sampling schemes (more stages and stratification) to arrive at reasonably representative and meaningful samples.

8.9.2 Monitoring

Routinely collected health data (vital statistics, hospital admissions, special disease registries such as cancer and myocardial infarction, health insurance data) could be an inexpensive way to assess potential health effects of transportation in alpine areas. In practice, however, one is faced with several limitations. The requirements for data quality are high and standardised data exchange procedures should have been established. Unfortunately, most routinely collected health data are not yet organised in a way that facilitates an automated GIS based analysis.

Furthermore, the population size is, more than often than not, too small to obtain reliable statistical differences for health indicators related to severe illnesses (e.g. lung cancer or myocardial infarction) between subsets of areas of interest (e.g. health outcome prevalence within certain distances from traffic sources compared with background prevalence).

Improvements at this level of health information could be made, to some extent, through the establishment of doctor-based surveillance systems and easier access to standard collections of health and medication consumption data. In Scandinavia such a scheme has be already implemented. A

pilot study using medication data from a health-insurance data base demonstrated the potential for health monitoring, but did also uncover problems related to inhomogeneous and incomplete data bases (Rüdisser et al., 2007).

Data from various sources normally differ in many areas, such as data quality, spatial or temporal resolution, aggregation, geographic reference system, choice of attributes, classes and so forth. The integration and homogenisation of data from different sources is a critical requirement. Such work should be supported by public institutions wherever possible and help to define data and metadata standards, providing reference data like official address registers etc.

Given the existing limitations, repeated general health and quality of life (QoL) surveys are a recommendable method to gather standardised overall health information, particularly for the assessment of relative importance of traffic-related factors over time in alpine areas. Surveys by computer-assisted telephone interviewing are an economic means to gather broad health and QoL information. This type of information is also necessary and suitable to monitor the effects of action plans required by the European directives on air pollution and noise pollution.

Prerequisite for an effective and efficient health monitoring is a comprehensive, high quality and up-to-date database, including spatial and statistical data. These data should be organised within a Geographic Information System and must include data about topography (e.g. a digital elevation model DEM), infrastructure and housing, indicators of air pollution (PM10, NO_2) and noise (L_{den}, L_{night}) and general socio-demographic and health data. Then, the opportunity is opened to link and analyse aggregate and individual-level data. This option requires the definition of harmonised data access rules in the member states – particularly to protect privacy.

8.9.3 Risk assessment

Standard exposure effect curves available from literature should be handled with care, when undertaking impact assessment in sensitive areas. The specific conditions of air pollution and noise propagation in alpine valleys differ from those in urban and suburban areas from where most of the available standard data originate. While the use of air pollution effect data from similar regions may give reasonable effect estimates for the health burden (due to the “toxicology” model) it is strongly recommended not to use external exposure effect curves in risk assessments for noise (due to the underlying “stress” model). Previous studies (Lercher, 1998; BBT Public Health Study, priv.comm.) and the actual health study within ALPNAP provide strong evidence against such a use of standard data, namely deviating exposure effect curves for all traffic sources (rail, motorway, main road) with a high risk of underestimation of real health effects and costs.

8.9.4 Cumulative/combined effects

The limited space available for traffic structures in typical Alpine valleys leads to a high concentration of traffic tracks within small stretches of land designated as residential area. This concentration of traffic can lead to interaction between sources (e.g., road and rail) which is difficult to foresee. Combined effects result mainly from the interaction of road and rail traffic noise, or interactions between noise, air pollution and vibration (from different traffic sources). Interactions between traffic sources, prominent in narrow alpine valleys, may explain the deviation in exposure effect curves. Thus, an integrative approach in planning is required.

8.9.5 Integration and harmonisation of action plans for health issues

Action plans to reduce the burden of traffic on the population in alpine areas need to adopt an integrative strategy as proposed by WHO during the Ministerial Conference on Environment and Health (London 1999). This means to consider all the possible effects of the actions taken on air pollution, noise, vibration, injuries and potential stress effects (traffic jams, rerouting of traffic into residential areas etc.). It also includes the greater potential for cumulative and combined effects in sensitive areas. A specific concern is the isolated consideration of air pollution abatement measures (e.g. flexible speed limits instead of fixed ones) without considering the potential adverse effects on traffic flow, injuries, noise exposure and stress. A simple, reductionist approach will lead to distorted impact assessments and major problems in risk communication at the population level. Therefore, it is recommended to conduct integrated pre-tests (including all possible outcomes) in advance.

8.10 Transit traffic trading systems

"Cap-and-trade" systems have been proposed for limiting the burden due to transit traffic (at least its freight share) to sustainable levels.[3] In order to achieve this goal without too severe side effects, the cap needs to be determined by the immissions, not the emissions or vehicle numbers. The first system, for setting a variable speed limit on a transit motorway-depending on the air pollution situations has recently become operational in Tyrol.[4] Both measures involve the need for atmospheric transport and dispersion modelling, and the involvement of experts in these fields.

The level of complexity of the "cap" determination method mainly depends on the temporal scale of the target parameters. It is easier to find appropriate limits for the traffic if the aim is to limit the annual mean concentrations than if the measure is targeted towards half-hour means. If this path is to be pursued further, there is an obvious need for more science-based expertise.

8.11 Knowledge transfer and future scientific developments

Science is a continuous process and actual scientific developments can be a major progress with respect to former developments. However, present-day developments are likely to be replaced by even more improved developments in the future. The transfer of scientific knowledge into practice must be also a continuous process. Presently, it takes about 10 to 20 years until a new scientific development is transferred into a legal regulation. As a fist step in this knowledge transfer process new developments are applied in special cases where experiences are gained to better adapt the methods to practical needs. These adaptations are often organised in standardisation committees. Approved new standards are published for instance by ISO or national standardisation institutions.

---

[3] Alpentransitbörse. Abschätzung der Machbarkeit verschiedener Modelle einer Alpentransitbörse für den Schwerverkehr Forschungsauftrag Nummer VSS 2002/902 auf Antrag des Schweizerischen Verbandes der Strassen- und Verkehrsfachleute (VSS) Schlussbericht, 8. Dezember 2004. Online unter http://www.verkehr-schweiz.ch/imperia/md/content/strasse/15.pdf. Gobiet et al. (2006).

[4] Verordnung des Landeshauptmannes vom 6. November 2007, mit der auf der A 12 Inntal Autobahn zwischen der Gemeinde Unterperfuss und der Gemeinde Ebbs eine immissionsabhängige Reduktion der zulässigen Höchstgeschwindigkeit eingeführt wird. Landesgesetzblatt für Tirol 28 (2007).
http://www.tirol.gv.at/fileadmin/www.tirol.gv.at/themen/politik/landesgesetzblatt/downloads/2007/lgbl282007.pdf

These standards then define the “state-of-the-art” or a “best practice”. In a third step, standards or modifications of standards may become legally prescribed methods for well defined applications, e.g. in administrative approval procedures.

A typical example of such a transfer process is the Lagrangian air pollution model which was developed at universities and research centres with public funding in the early 80ies of the 20th century. Numerous validation studies and various applications to real cases led to many improvements in the computer codes. So, the accuracy and the numerical efficiency of this type of model could be significantly increased. In the 90ies of the 20th century the Lagrangian model became a national standard in Germany through a VDI guideline after a three-year process of further adaptations and validity tests. Eventually, in the year 2002 the Lagrangian air pollution dispersion model became part of the legal clean-air regulation “TA Luft” which in turn is an annex to the German federal immission control law.

This interminable transfer process can be accelerated by a close interaction between administrations and experts in consulting offices on the one side and scientists on the other side. The project ALPNAP and the present book may contribute to this process. The book describes the state of science-based methods of the first decade of the 21st century. It is hoped that these methods are successively transferred into practice to become new standards or even part of legal procedures in the next couple of years.

A mentioned above science does not stop and further developments are in the pipeline of future research programmes. In the following we present a short perspective of new developments that are planned to overcome the still existing deficiencies of the present-day methods.

The development of instruments for the measurement of meteorological and air quality parameters is continuing. New electronic chips allow a progressing miniaturisation of the instruments which e.g. enables their use mounted at ultra-light aircraft or tethered balloons. Likewise, this miniaturisation leads to a lower power consumption of the instruments. This latter development makes the long-term autonomous operation of these instruments away from electrical grids possible. New principles of measurement – especially in the field of remote sensing - are still under investigation.

Numerical modelling of atmospheric phenomena in Alpine areas is still a challenge, due to the large differences in scale. One would like to cover a major portion of the Alps with a model domain while achieving a resolution of approximately 1 km, and down to 10 m for certain purposes in local sub-domains. This has started to become feasible for research purposes and in simulations of a few days, but many applications would require simulations in real time, or/and for periods of one to several years and multiple scenarios. To bridge this gap, intermediate solutions combining e.g. statistical and numerical methods are sometimes applied. There is however, a huge area for improvements.

Most air pollution problems involve chemical transformations, but models which can not or not fully account for them still need to be used. Here, the situation is similar to meteorological models. Intermediate solutions should be further developed while at the same time computer power progress may be utilised to bring full chemistry simulations to more and more applications.

A special challenge for all kinds of models is to properly reproduce the strong tendency of air inside Alpine valleys and basins, especially in the cold season, to form stagnant cold-air pools. These situations are also among the most critical from an impact point of view!

Numerical models (codes) for application in Alpine terrain and with high resolution are under ongoing development. From an air pollution and noise point of view, numerical aspects and parameterisation of turbulence are most important.

Equally important, and becoming more and more demanding with higher resolutions, are appropriate input data for meteorological models such as gridded fields of albedo, soil properties, vegetation, snow cover, and soil moisture. Air pollution models require time-dependent values of anthropogenic (traffic, industry, residential) and biogenic (organic compounds from the vegetation) emissions on a spatial resolution, corresponding to the model grid. Developments in emission inventories need to keep pace with the trend of higher model resolution. More sophisticated models for the integration of different types of information relevant for emission fluxes (e.g., traffic flow data, detailed stack emission data for large point sources, and temperature-dependent area emissions from heating buildings) are also needed.

8 Recommendations

Abbreviations

AADT	annual average daily traffic
ABL	atmospheric boundary layer
ACI	Automobile Club d'Italia
ADT	average daily traffic
ADTV	average daily traffic volume
AFM	Autostrada Ferroviaria Modalohr (a piggy-back train system)
AGL	above ground level
Air-APS	L'Air de l'Ain et des Pays de Savoie (air quality survey in the French departments of Ain and Savoie)
ALADIN	ire Limitée Adaptation dynamique Développement InterNational (a NWP model)
AMV	annual mean value
APHEA	Air Pollution and Health - A European Approach (an EU project)
API	air pollution index
ARIA	ARIA Technologies (a French consulting company)
ARIANET	ARIANET s.r.l (an Italian environmental consulting company)
ARPA	Agenzia Regionale per la Protezione Ambientale (Italian regional environmental protection agencies)
ASFINAG	Autobahnen- und Schnellstraßen- Finanzierungs-Aktiengesellschaft (Austrian motorway operator)
ASL	above sea level
AWS	automatic weather station
BAU	business as usual (an emission scenario)
BBSG	Béton Bitumineux Semi-Grenu (semi-granular concrete asphalt)
BBT	Brenner Base Tunnel SE
BDTOPO	La Base de Données Topographiques (a geographical information data base)
BEG	Brenner Eisenbahn Gesellschaft mbH (an Austrian railway infrastructure company)
BEM	Boundary Element Model (a type of sound propagation model)
BIPM	Bureau International des Poids at Mesures (International Bureau of Weights and Measures)
BMA	British Medical Association
BOKU	Universität für Bodenkultur, Wien
BVOC	biological volatile organic compounds
CALGRID	California Photochemical Grid Model
CALINE	California Line Source Model
CALPUFF	California Puff Model
CAPI	computer assisted personal interviewing
CATI	computer assisted telephone interviewing
CET	Central European Time
CETE	Centre d’Etudes Techniques de l’Equipement
CFL	Courant–Friedrichs–Lewy (a numerical stability criterion)
CI	confidence interval
CLC	

Abbreviations

CNR	Consiglio Nazionale delle Ricerche (Italian research council)
COPD	chronic obstructive pulmonary disease
COPERT	an emission model
CORINNE	Coordinated Information on the European Environment
COST	Coopération européenne dans le domaine de la recherche scientifique et technique
CPU	central processing unit
CPX	Close-Proximity Method
CSTB	Centre Scientifique et Technique du Bâtiment
CVD	cordiovascular disease
DAC	dense asphalt concrete
DALY	disability-adjusted life year
dB	decibel
DEM	digital elevation model
DDE	Direction départementale de l'équipement
DG TREN	Directorate-General for Energy and Transport (of EC)
DIN	Deutsches Institut für Normung (German standardisation institute)
DJF	December, January, February
DLR	Deutsches Zentrum für Luft- und Raumfahrt e.V. (German Aerospace Centre)
DOAS	Differential Optical Absorption Spectroscopy
DTM	digital terrain model
DWD	Deutscher Wetterdienst (German Weather Service)
EB	Eurobarometer
EC	European Commission
ECE	Economic Commission for Europe
ECMWF	European Centre for Medium-Range Weather Forecasts
EEA	European Environment Agency
EF	ecological footprint
EHIA	environmental health impact assessment
EHIS	environmental health information system
EI	exposure index
EIA	Environmental Impact Assessment
EIONET	European Environment Information and Observation Network
EMEP	Co-operative Programme for Monitoring and Evaluation of the Long-Range Transmissions of Air Pollutants in Europe
EN	Standard of the European Committee for Standardisation
END	Environmental Noise Directive
EPA	Environmental Protection Agency (USA)
EPHT	Environmental Public Health Tracking
ERDF	European Regional Development Fund
ETA	mesoscale meteorological model by NCEP
EU	European Union
EUFAR	European Fleet for Airborne Research
FDTD	finite-difference time-domain

FFP	Fast Field Programme
FFT	Fast Fourier Transform
FP	European Research Framework Programme
FTIR	Fourier transform spectroscopy
FZK	Forschungszentrum Karlsruhe GmbH
GFS	Global Forecast System
GIS	Geographical Information System
GLOBEMI	automatisierte Bilanzierung von Verbrauchs-,
GPL	Verbrauchs-, Emissions- und Verkehrsdaten in größeren Gebieten (fuel consumption, emission and traffic data in larger areas)
GPS	Global Positioning System
GRAL	Graz Lagrangian Model - a Lagrangian dispersion model
HA	highly annoyed
HARMONOISE	Harmonized accurate and. reliable methods for the EU directive on. the as-sessment and management of. environmental noise (EU project)
HBEFA	Handbuch für Emissionsfaktoren (Handbook for Emission Factors)
HCN	Health Council of the Netherlands
HCR	high capacity rail line
HDV	heavy duty vehicle
HREQ	health-related environmental quality
HV	heavy vehicle
HYENA	Hypertension and Exposure to Noise near Airports, an EU-funded noise and health study
ICD	International Classification of Disease
IEC	International Electrotechnical Commission
IGN	Institut Geographique National (French national geographic institute)
IHD	ischemic heart disease
INEL	a French company for measurement equipment
INNAP	a EUFAR project studying the boundary layer structure in the Inn valley
INNOX	a EUFAR project studying the air pollution in the Inn valley
INSEE	Institut National de la Statistique
INTEC	Institut National de la Statistique et des Études Économiques (French institute on statis-tics an economical studies)
INTERREG	a community initiative of ERDF
IOP	intensive observation period
IPC	Index de la Pollution à Court terme (short term pollution index)
IPL	Index de la Pollution à Long terme (long term pollution index)
IRGA	Infrared Gas Analyzer
IRIS	Ilots Regroupés pour l'Information Statistique
ISAAC	International Study of Asthma and Allergies in Childhood
ISAC	Istituto di Scienze dell'Atmosfera e del Clima, Torino/Italy
ISBN	International Standard Book Number
ISO	International Organization for Standardization
JJA	June, July, August

KINDL	Questionnaire to obtain health related quality of life in children
LARES	Large Analysis and Review of European Housing and Health Status - a WHO study
LDV	light duty vehicle
LE	Linear Euler (a type of noise propagation models)
LfU	Bayerisches Landesamt für Umwelt (Bavarian environmental administration)
LIDAR	Light Detecting And Ranging
LV	light vehicle
MAM	March, April, May
MCCM	Mesoscale Chemistry Climate Model (developed at FZK IMK-IFU)
METAR	Meteorological Aviation Routine Weather Report
MI	myocardial infarction
MID	a GIS data format
MIF	a GIS data format
MISA	Metanalisi italiana degli studi sugli effetti a breve termine dell'inquinamento atmosferico (Italian study on short-term air pollution effects)
MITHRA	a French noise prediction model
MITHRA-SIG	software environment of MITHRA
MLH	mixing-layer height
MM5	Mesoscale Model Version 5 (by NCAR and PSU)
MONITRAF	Monitoring of Road-Traffic Related Effects and Common Measures (an INTERREG project)
MOS	model output statistics
MP	measurement point
MUI	Medizinische Universität Innsbruck
NCAR	National Center for Atmospheric Research (USA)
NCEP	National Centers for Environmental Prediction
NEAT	Neue Eisenbahn-Alpentransversale (new railway tunnels in Switzerland)
NEMO	Network Emsssion Model
NGI	Institut géographique national (France)
NMHC	non-methane hydrocarbonates
NMMAPS	National Morbidity, Mortality and Air Pollution Study (USA)
NMPB	Nouvelle Méthode de Prevision du Bruit (a French noise prediction tool)
NPI	noise pollution index
NWP	numerical weather prediction
OC	organic compounds
OECD	Organisation for Economic Co-operation and Development
OEHHA	Office of Environmental Health Hazard Assessment
OLEX	Ozone Lidar Experiment
ÖNORM	standard of the Austrian standardisation institute
OR	Odds ratio: a statistical approximation of the relative risk in cross-sectional or case-control studies
PAB	PKW mit Anhänger und Busse (passenger cars with trailer and busses)
PAC	porous asphalt concrete

PE	parabolic equation
PHEM	Passenger car and Heavy duty vehicle Emission Model
PM	particulate matter
POVA	pollution des vallées alpines (a French measurement campaign on air quality)
ppb	parts per billion
ppm	parts per million
PSR	pressure-state-response
PSU	Pennsylvania State University
QoL	quality of life
RAM	random access memory
RAMS	Regional Atmospheric Modeling System
RASS	Radio Acoustic Sounding System
RD	Réseau Départemental (French departemental road)
RFF	Réseau Ferré de France (French railway infrastructure operator)
RLS	Richtlinie für den Lärmschutz an Straßen (German standard on road noise)
RMS	RAMS-MIRS-SPRAY
RN	route nationale (French national road)
SAPALDIA	Swiss Study on Air Pollution and Lung Diseases in Adults
SCAN	Type of map produced by IGN
SCARPOL	Swiss Surveillance Program of Childhood Asthma and Allergies with respect to Air Pollution and Climate
SEA	Strategic Environmental Assessment
SFTRF	Société Française du Tunnel Routier du Fréjus (French operator of Frejus tunnel)
SIREDO	Système Informatisé de Recueil de Données (French computerised data collection system)
SITAF	Società Italiana per il Traforo Autostradale del Frejus SpA (Italien operator of Frejus tunnel)
SLZ	Sattel und Lastzüge; subcategory of heavy duty vehicle
SODAR	Sound Detection and Ranging
SON	September, October, November
SOP	special observation period
SRTM	Shuttle Radar Topography Mission
SS	strada statale (Italian state highway)
SWB	subjective well-being
SYNOP	surface synoptic observation
TA	target area
TEMP	Aerological Observations
TEN	Trans-European Networks
TGKK	Tiroler Gebietskrankenkasse (Tyrolean regional health insurance)
TGV	train à grande vitesse (French highspeed trains)
TKE	turbulent kinetic energy
TNO	Nederlandse Organisatie voor Toegepast Natuurwetenschappelijk Onderzoek (Dutch natural science research enterprise)
TSP	total suspended particles

Abbreviations

TU	Technical University
TVM	Threedimensional Vorticity Mode Model
U.S.	United States
UHF	ultrahigh frequency
UKMO	United Kingdom Meteorological Office
UN	United Nations
UNECE	United Nations Economic Commission for Europe
UNFCCC	United Nations Framework Convention on Climate Change
USA	Ultra Sonic Anemometer
USGS	US Geological Survey
UTC	Universal Time Coordinated
UTM	Universal Transverse Mercator (a map projection)
VDI	Verein Deutscher Ingenieure (German Engineering Association)
VOC	volatile organic compounds
VUV	vacuum ultraviolet
WGS	World Geodetic System
WHO	World Health Organisation
WMO	World Meteorological Organization
WRF	Weather Research and Forecasting Model
YOLL	years of life lost
ZAMG	Zentralanstalt für Meteorologie and Geodynamic (Austrian Weather Service)

References

Aballéa F., Defrance J., 2007: Multiple reflection phenomena under meteorological conditions using the PE method with a complementary Kirchhof approach. *Acta Acustica*, **93**, 22-30.

Abbey D.E., Nishino N., McDonnell W.F., Burchette R.J., Knutsen S.F., Beeson W.L., Yang J.X, 1999: Long-term inhalable particles and other air pollutants related to mortality in nonsmokers. *Am. J. Respir. Crit. Care Med*. **159**, 373-382.

Ajtay D., Weilenmann M., 2004: Direct dynamic instantaneous emission modeling WP 300 – Task 3321, Contributory report version 1.

Alessandrini S., Ferrero E., Trini Castelli S., Anfossi D., 2005: Influence of turbulence closures on the simulation of flow and dispersion in complex terrain. *Int. J. of Environment and Pollution*, **24**, 154-170

Allinger-Csollich E., 2006: From IG-Luft Maßnahmenbündel 2006: Verkehrstechnische Grundlagen zur Abschätzung der Emissionsentwicklung, Abt. Verkehrsplanung, Amt der Tiroler Landesregierung, August 2006.

Allwine K.J., Whiteman C.D., 1994: Single-station integral measures of atmospheric stagnation, recirculation and ventilation. *Atmos. Environ*., **28**, 713-721.

Almbauer R.A., 1995: A new nite volume discretisation for solving the Navier-Stokes equations. Numerical Methods in Laminar and Turbulent Flow, **9**. *Proceedings of the Ninth International Conference*, 286-295. ISBN 0-906674-86-7.

Almbauer R.A., Öttl D., Bacher M., and Sturm P.J., 2000: Simulation of the air quality during a field study for the city of Graz. *Atmos. Environ*., **34**, 4581-4594.

Alpine Convention, 2007: *Report on the State of the Alps - Alpine Signals: Transport and Mobility in the Alps*, Permanent Secretariat of the Alpine Convention.

Anderl M., Gangl M., Poupa S., Schodl B., 2006a: *Bundesländer Luftschadstoff-Inventur 199-2004. Regionalisierung der nationalen Emissionsdaten auf Grundlage von EU-Berichtspflichten, Datenstand 2006.* Umweltbundesamt, Wien.

Anderl M., Kampl E., Köther T., Muik B., Schodl B., Poupa S., Wappel D., 2006b: *Austrian's Annual Air Emission Inventory 1990-2005. Submission under National Emission Ceilings Directive 2001/81/EC.* Umweltbundesamt, Wien.

Anfossi D., Alessandrini S., Trini Castelli S., Ferrero E., Ött D., Degrazia G., 2006: Tracer dispersion simulation in low wind speed conditions with a new 2-D Langevin equation system. *Atmos. Environ.*, **40**, 7234-7245.

Anfossi D., Tinarelli G., Trini Castelli S., Ferrero E., Öttl D., Degrazia G., Mortarini L., 2007: Well mixed condition verification in windy and low wind speed conditions. *Int. Journal of Environment and Pollution,* in press.

Annest J. L., 1983: Trends in the blood lead levels of the U.S. population: The Second National Health and Nutrition Examination Survey (NHANES II) 1976-1980. In: Lead Versus Health (eds. Rutter, M, R. Jones), pp. 33-58. Wiley.

Anto J. M., Vermeire P., Vestbo J., and Sunyer J., 2001: Epidemiology of chronic obstructive pulmonary disease. *Eur.Respir.J*., **17**, 982-994.

Antonacci G. and Tubino M., 2005: An estimate of day-time turbulent diffusivity over complex terrain from standard weather data, *Theoretical and Applied Climatology*, **80**, 205-212.

ARE (Bundesamt für Raumentwicklung), 2005: Alpinfo 2004, Alpenquerender Güterverkehr auf Straße und Schiene.

Arya S. P., 1988: *Introduction to Micrometeorology*. Academic Press, 307 pp.

Aschauer H., Obleitner F., Vergeiner J. and Emeis S., 2007: Measurement and simulation of the energy and mass balance of snow at an Alpine valley site. Extended abstract for proceedings of ICAM-International Conference on Mountain meteorology, Chambery, 5.6.2007, 4pp.

References

Balfour J. L. and Kaplan G. A., 2002: Neighborhood Environment and Loss of Physical Function in Older Adults: Evidence from the Alameda County Study. *Am.J.Epidemiol.*, **155**, 507-515.

Barker S. M. and Tarnopolsky A., 1978: Assessing bias in surveys of symptoms attributed to noise. *J.Sound.Vib.*, **59**, 349-354.

Baulac M., Defrance J., Jean P., Minard F., 2006: Efficiency of low height noise protections in urban areas: Predictions and scale model measurements. *Acta Acustica*, **92**(4), 530-539.

Bayer-Oglesby L., Grize L., Gassner M., Takken-Sahli K., Sennhauser F. H., Neu U., Schindler C., and Braun-Fahrlander C., 2005: Decline of ambient air pollution levels and improved respiratory health in Swiss children. *Environ.Health Perspect.*, **113**, 1632-1637.

Becker K., Schulz C., Babisch W., Dürkop J., Roskamp E., Seiwert M., Szewzyk R., Ullrich D., and Seifert B., 2005: German environmental survey for children (GerES IV) 2003-2006. *Pollution Atmospherique*, 188, 475-479.

Benson P.E., 1979: CALINE3 - A versatile dispersion model for predicting air pollutant levels near highways and arterial street. Report No. FHWA/CA/TL-79/23

Benson P.E., 1992: A review of the development of the CALINE 3 and CALINE 4 models. *Atmos. Environ.*, **26B**(3): 379-390.

Berglund B., Lindvall T., Schwela D., 2000: Guidelines for community noise. WHO.

Bickel, P., S. Schmid, W. Krewitt, R. Friedrich (Eds.), 1997: External costs of transport in ExternE. JOULE III. IER, Germany Publishable Report. Contract JOS3-CT95-0004. http://externe.jrc.es/trans.pdf

Biggeri A., Bellini P., Terracici B., 2004: Metanalisi italiana degli studi sugli effetti a breve termine dell'inquinamento atmosferico—MISA 1996–2002. *Epidemiol Prev*, **28**,S1-S100.

Blokhintzev D., 1946: The propagation of sound in an inhomogeneous and moving medium. *J. Acoust. Soc. Am*, **18**, 329-334.

Bonnefoy X. R., Braubach M., Moissonnier B., Monolbaev K., and Röbbel N., 2003: Housing and health in Europe: Preliminary results of a Pan-European Study. *Am.J.Pub. Health*, **93**, 1563.

Bossard M., Feranec J., Otahel J., 2000: CORINE Land Cover Technical Guide – Addendum 2000. *Technical report* No 40. Copenhagen (EEA).

Botteldooren D., Lercher P., 2004: Soft-computing base analyses of the relationship between annoyance and coping with noise and odor. *J.Acoust.Soc.Am.*, **115**, 2974-2985.

Botteldooren D., Verkeyn A., 2003: Fuzzy models for accumulation of reported community noise annoyance from combined sources. *J.Acoust.Soc.Am.*, **112**, 1496-1508.

Botteldooren D., Verkeyn A., Lercher P., 2003: A fuzzy rule based framework for noise annoyance modeling. *J.Acoust.Soc.Am.*, **114**, 1487-1498.

Botteldooren, D., Verkeyn, A., De Baets, B., Lercher P., 2006: Fuzzy integrals as a tool for obtaining an indicator for quality of life fuzzy systems. ISBN: 0-7803-9488-07, 1065-1071. IEEE International Conference on Fuzzy Systems.

Boynton P. M. , Greenhalgh T., 2004: A hands on guide to questionnaire research part one: Selecting, designing, and developing your questionnaire. *BMJ*, **328**, 1312-1315.

Braun-Fahrlander C., Vuille J. C., Sennhauser F. H., Neu U., Kunzle T., Grize L., Gassner M., Minder C., Schindler C., Varonier H. S., Wuthrich B., 1997: Respiratory health and long-term exposure to air pollutants in Swiss schoolchildren. SCARPOL Team. Swiss Study on Childhood Allergy and Respiratory Symptoms with Respect to Air Pollution, Climate and Pollen. *Am.J.Respir.Crit.Care Med.*, **155**, 1042-1049.

Breugelmans O.R.P., Wiechen C.M.A.G. van, Kamp I. van, Heisterkamp S.H., Houthuijs J.M., 2005: Tussenrapportage Monitoring Gezondheidskundige Evaluatie Schiphol: Gezondheid en beleving van de omgevingskwaliteit in de regio Schiphol: 2002. Bilthoven: Rijksinstituut voor Volksgezondheid en Milieu, RIVM report 630100001.

Briggs G.A., 1973: Diffusion Estimation for Small Emissions, Paper No. 79, Atmospheric Turbulence and Diffusion Laboratory, NOAA. Paper No. 79.

British Medical Association, 1997: Road Transport and Health. BMA Professional Division Publications.

Brock, 2001: *Meteorological measurement systems*, Oxford University Press, 290pp.

Brody S. D., Zahran S., 2007: Commentary: Linking particulate matter and sulphur concentrations to air pollution annoyance: problems of measurement, scale and control. *Int.J.Epidemiol.*, **16**, 820-823.

Brosseaud Y., Anfosso-Lédée F., 2005: Review of existing low-noise pavement solutions in France. SILVIA Project Report. N°SILVIA-LCPC-011-01-WP4-310505.

Burris R. K., Canter L. W., 1997 : Cumulative impacts are not properly addressed in environmental assessments. *Environmental Impact Assessment Review*, **17**, 5-18.

Callan, R., 2003: *Neuronale Netze*. Pearson Studium.

Carlslaw D.C., 2005: Evidence of an increasing NO2/NOx emission ratio from road traffic emissions. *Atmos. Environ.*, **39**, 4793 - 4802.

Carter N. L., 1996: Transportation noise, sleep, and possible after-effects. *Environment International*, **22**, 105-116.

Carter W.P.L., 1990: A detailed mechanism for the gas -phase atmospheric reactions of organic compounds. *Atmos. Environ.*, **24A**, 481-518.

Carter W.P.L., 1996: Condensed Atmospheric Photooxidation Mechanisms for Isoprene. *Atmos. Environ*., **30**, 4275-4290.

Carter W.P.L., 2000: *Implementation of the SAPRC-99 Chemical Mechanism into the Model-3 Framework.* Report to the United States Environmental Protection Agency.

Carvalho J., Anfossi D., Trini Castelli S., Degrazia G.A., 2002: Application of a model system for the study of transport and diffusion in complex terrain to the TRACT experiment. *Atmos. Env.*, **36**, 1147-1161.

Cercl'Air, 2005: Swiss society of air protection officers: Recommandation Cercl'Air n°27: Indice de pollution de l'air –Report. 20p.

Cerveny V., Popov M.M., Psencik I., 1982: Computation of wave fields in homogeneous media. Gaussian beam approach. *Geophys. J. R. Astron. Soc*, **70**, 109-128.

Chemel C. and Chollet J.-P., 2006: Observations of the daytime boundary layer in deep Alpine valleys. *Boundary-Layer Meteorology*, **119**(2), 239-262.

Chen H., Cohen P., Kasen S., 2007: Cohort Differences in Self-Rated Health: Evidence from a Three-Decade, Community-Based, Longitudinal Study of Women. *Am.J.Epidemiol.*, **166**, 439-446.

Chevalier H., Jos F., Boichut D., et al.,1999 : Evaluation of severe insomnia in the general population: results of a European multinational Evaluation of severe insomnia in the general population. *J.Psychopharmacol*., **13**, S21-S24.

Chien C.F., Soroka W.W., 1980: A note on the calculation of sound propagation along an impedance surface. *J. Sound Vibration*, **69**(2), 340-343.

Ciccone G., Forestiere F., Agabiti N., Buggeri A., Bisanti L., Chellini E., Corbo G., Dell'Orco P., Dal Masso P., Volante T.F., Galassi C., Piffer S., Tenzoni E., Rusconi F., Sestini P., Viegi G., 1998: Road traffic and adverse respiratory effects in children. SIDRIA Collaborative Group. *Occupational and Environmental Medicine*, **55,** 771-778.

Ciskowski R.D., Brebbia C.A, 1994: Boundary Element Methods in Acoustics. Computational Mechanics Publications, Elsevier Applied Science, New York.

Clench-Aas J., Larssen S., Bartonova A., Aarnes M. J., Myhre K., Christensen C. C., et al., 1991: The health effects of traffic pollution as measured in the Valerenga area of Oslo.Norwegian Institute for Air Research. Contributions by A. Wagner, E. Ekhart and F. Defant. PNL-5141 / ASCOT-84-3. Pacific Northwest Laboratory, Richland, Washington, 121 pp

Cooper L. M., Sheate W. R., 2002: Cumulative effects assessment; A review of UK environmental impact statements. *Environmental Impact Assessment Review*, **22**, 415-439.

Cotton W.R., Pielke R.A., Walko R.L., Liston G.E., Tremback C.J., Jiang H., McAnnelly R.L., Harrington J.Y., Nicholls M.E., Carrio G.G., McFadden J.P., 2003: RAMS 2001: Current status and future directions. *Meteorology and Atmospheric Physics*, **82**, 5-29.

References

Council of the European Union, 1996: *Council Directive 96/62/EC of 27 September 1996 on ambient air quality assessment and management.*

COWI, 2006 : Estimation des potentialités du trafic fret à travers les Alpes - Cas spécifique de la nouvelle liaison ferroviaire transalpine France-Italie , Framework Contract TREN/CC/03-2005, report for EC, December 2006.

Dab W., Medina S., Quenel P., Le Moullec Y., Le Tertre A., Thelot B., Monteil C., Lameloise P., Pirard P., Momas I., Ferry R.A., Festy B., 1996: Short term respiratory health effects of ambient air pollution, Results of the APHEA project in Paris. *J. Epidemiol. Comm. Health*, **50** (Suppl 1), S42-S46.

Daniels M.J., Dominici F., Samet J.M., Zeger S.L., 2000: Estimating particulate matter - mortality dose-response curves and threshold levels: an analysis of daily time-series for the 20 largest US cities. *Am. J. Epidemiol*, **152,** 397-406.

Danninger E., 2005: Statuserhebung gemäß Immissionsschutzgesetz-Luft für NO_2 im Jahr 2003. Grenzwertüberschreitung des Luftschadstoffs Stickstoffdioxid an der Autobahn A1 in Enns-Kristein im Jahr 2003. Amt der Oberösterreichischen Landesregierung.

Defant F., 1949:. Zur Theorie der Hangwinde, nebst Bemerkungen zur Theorie der Berg- und Talwinde. *Archiv für Meteorologie, Geophysik und Bioklimatologie Serie A,* **1,** 421-450.

Defrance J., Gabillet Y., 1999: A new analytical method for the calculation of outdoor noise propagation. *Applied Acoustics*, **57**(2), 109-127.

Defrance J., Jean P., 2003: Integration of the efficiency of noise barrier caps in a 3D ray tracing method. Case of a T-shaped diffracting device. *Applied Acoustics*, **64**(8), 765-780.

Defrance J., Barrière N., Premat E., 2002: Sound propagation through forests with realistic meteorological conditions: theory and experiment. *10th International Symposium on Long Range Sound Propagation, Grenoble, France.*

Defrance J., Roland J., Perraudeau M., Baulac M., 2004: Characterisation, performance and conception of vented and absorptive road covers. *InterNoise'2004, Prague, Czech Republic*

Defrance J., Noordhoek I., Salomons E., Heimann D. et al., 2007: Outdoor sound propagation reference model developed in the European Harmonoise project. *Acta Acustica*, **93**(2), 213-227.

de Hollander A. E. M., Staatsen B. A. M., 2003: Health, environment and quality of life: an epidemiological perspective on urban development. *Landscape and Urban Planning*, **65** , 53-62.

de Hollander A. E. M., Melse J. M., Lebret E., Kramers P. G., 1999: An aggregate public health indicator to represent the impact of multiple environmental exposures. *Epidemiology*, **10**, 606-617.

Delany M.E., Bazley E.N., 1970: Acoustical properties of fibrous absorbent materials. *Applied Acoustics*, **3**, 105-116.

DELTA. 1995: Metrics for environmental noise in Europe. Danish comments on INRETS Report LEN 9420. AV 837/95. DELTA Acoustic & Vibration.

Demarest S., Gisle L., Van der Heyden J., 2007: Playing hard to get: Field substitutions in health surveys. *Int.J.Public Health*, **52**, 188-189.

Diener E., Suh E., 1997: Measuring quality of life: Economic, social and subjective indicators, *Soc.Indicators Res.*, **40**, 189-216.

Diener E., Emmons R. A., Larsen R. J., Griffin S., 1985: The Satisfaction with Life Scale. *Journal of Personality Assessment*, **49**, 71-75.

Diez-Roux A. V., 2005: Commentary: Estimating and understanding area health effects. *Int.J.Epidemiol.*, **34**, 284-285.

Di Napoli F.R., Deavenport R.L., 1980: Theoretical and numerical Green's function solution in a plane layered medium. *J. Acoust. Soc. Am.*, **67**, 92-105.

Di Nisi J., Muzet A., Ehrhart J., and Libert.J.P., 1990: Comparison of cardiovascular responses to noise during waking and sleeping in humans. *Sleep*, **13**, 108-120.

Dockery D. W., Pope A. C., Xu X., Splengler J. D., Ware J. H., Fay M. E., Ferris B.G. J., Speizer F. E., 1993: An association between air pollution and mortality in six U. S. cities. *N. Engl. J. Med.*, **329**, 1753–1759.

Dora C., 1999: A different route to health: implications of transport policies. *BMJ*, **1318**, 1686-1689.

Dora C., Racciopi F., 2003: Including health in transport policy agendas: the role of health impact assessment analyses and procedures in the European experience. *Bulletin of the World Health Organization*, **81**, 399-403.

Dosio A., Emeis S., Graziani G., Junkermann W., Levy A., 2001: Assessing the meteorological conditions of a deep Italian valley system by means of a measuring campaign and simulations with two models during a summer smog episode. *J. Atmosph. Environ.* **35**, 5441–5454.

Dreiseitl E., 1988: Slope and Free Air Temperature in the Inn Valley. *Meteorol. Atmos. Phys*,. **3**9, 25-41.

Dreiseitl E., et al., 1980: Windregimes an der Gabelung zweier Alpentäler. *Archiv für Meteorologie, Geophysik und Bioklimatologie Serie B,* **28**(3), 257.

Dudhia, J.,1993: A non-hydrostatic version of the Penn State-NCAR Mesoscale Model: validation tests and simulation of an Atlantic Cyclone and cold front. *Month. Wea. Rev.*, **121**, 1493-1513.

Duhamel D., 1996: Efficient calculation of the three-dimensional sound pressure field around a noise barrier. *J. Sound Vibration*, **197**, 547-571.

EC, 1985:. Council Directive 85/337/EEC of 27 June 1985 on the assessment of the effects of certain public and private projects on the environment.

EC, 1997: Council Directive 97/11/EC of 3 March 1997 amending Directive 85/337/EEC on the assessment of the effects of certain public and private projects on the environment.

EC, 2002: Position paper on dose response relationships between transportation noise and annoyance – EU's future noise policy, WG2 – Dose/Effect. 40P.

EC, 2007: Research for a quieter Europe 2020. An update. Brussels, European Commission.

EEA – European Environment Agency, 2005: *EMEP/CORINAIR Emission Inventory Guidebook – 2005.* Technical ReportNo. 30, Copenhagen. http://reports.eea.eu.int/EMEPCORINAIR4/en

EEA-ETC/TE, 2002. CORINE Land Cover update, I&CLC2000 project, Technical Guidelines.

Ellaway A., Macintyre S., and Bonnefoy X. R., 2005: Graffiti, greenery, and obesity in adults: secondary analysis of European cross sectional survey. *BMJ*, **331**, 611-612.

Elliott P., Cuzick J., English D., Stern R., 1996: Geographical and Environmental Studies. Methods for Small Area Studies. Oxford University Press.

Embleton T.F.W., 1996: Tutorial on sound propagation outdoors. J.Acoust.Soc.Am., 100, 31-48.

Emeis S., 2000: *Meteorologie in Stichworten. Hirt's Stichwortbücher.* Borntraeger, Stuttgart. 199 pp.

Emeis S., Türk M., 2004: Frequency distributions of the mixing height over an urban area from SODAR data. *Meteorol. Z.*, **13**, 361-367.

Emeis S., Schoenemeyer T., Richter K., Ruckdeschel W., 1997: Sensitivity of ozone production to VOC and NO_x emissions – a case study with a box model BAYROZON. *Meteor.Z.*, **6**, 60-72.

Emeis S., Jahn C., Münkel C., Münsterer C., Schäfer K., 2007: Multiple atmospheric layering and mixing-layer height in the Inn valley observed by remote sensing. *Meterol. Z.*, **16**, 415-424.

ENVIRON, 2006: User's Guide to the Comprehensive Air Quality Model with Extensions (CAMx), Version 4.40, ENVIRON International Corporation, Novato, CA

European Commission DG TREN, The SEA manual - A source-book on strategic environmental assessment of transport infrastructure plans and programmes, edited by ISIS with contributions from the BEACON project partners, 1999.

European Environmental Agency, 2002: Atmospheric Emission Inventory Guidebook, 3rd Edition.

European Parliament and the Council of the European Union, 2002: *Directive 2002/49/EC of the European Parliament and of the council of 25 June 2002 relating to the assessment and management of environmental noise.*

Evans G. W., 1994: The psychological costs of chronic exposure to ambient air pollution. In: The vulnerable brain and environmental risks, Vol. 3 (eds. R. L. Isaacson, K. F. Jensen), pp. 167-182. Plenum Press.

Evans G. W., Colome S. D., and Shearer D. F., 1988: Psychological reactions to air pollution. *Environ.Res*., **45**, 1-15.

References

Fast J.D., 2003: Forecasts of Valley Circulations Using the Terrain-Following and Step-Mountain Vertical Coordinates in the Meso-Eta. *Model. Wea. Forecasting*, **18**, 1192–1206.

Ferraro K. F., Su Y., 2000: Physician-evaluated and self-reported morbidity for predicting disability. Am.J.Pub. Health, **90**, 103-108.

Ferrero E., Trini Castelli S., Anfossi D., Finardi S., Di Lisi E., 2001: Study of different turbulence closure models simulating a neutral wind tunnel flow experiment. *Hybrid Methods in Engineering*, **3**(1), 11-23.

Ferrero E., Trini Castelli S., Anfossi D., 2003: Turbulence fields for atmospheric dispersion models in horizontally non-homogeneous conditions. *Atmos. Env*., **37**(17), 2305-2315.

Fidell S., 1999: Assessment of the effectiveness of aircraft noise regulation. Noise & Health 3, 17-25.

Fidell S. and Silvati L., 1991: An assessment of the effect of residential acoustic insulation on prevalence of annoyance in airport community. *J.Acoust.Soc.Am.*, **89**, 244-247.

Fields J. M., 1990: Policy-related goals for community response studies. In: Noise as a public health problem, Vol. 5 (eds. B. Berglund, T. Lindvall), pp. 115-134. Swedish Council of Building Research.

Fields J.M., 1993: Effect of personal and situational variables on noise annoyance in residential areas. *J.Acoust.Soc.Am.*, 93, 2753-2763.

Fields J.M., 1998: Reactions to environmental noise in an ambient noise context in residential areas. *J.Acoust.Soc.Am.*, **104**, 2245-2260.

Fields J.M., Ehrlich G.E., Zador P., 2000. Theory and design tools for studies of reactions to abrupt changes in noise exposure. Langley Research Center. Report No: NAS 1.26210280.

Fields J.M., De Jong R. G., Gjestland T., Flindell I. H., Job R. F. S., Kurra S., Lercher P., Vallet M., and Yano T. 2001. Standardized general-purpose noise reaction questions for community noise surveys: Research and a recommendation. *J.Sound.Vib.*, **242**, 641-679.

Filliger P., Puybonnieux-Texier V., Schneider J., 1999: Health Costs due to Road Traffic-related Air Pollution. An impact assessment project of Austria, France and Switzerland. PM10 Population Exposure - Technical Report on Air Pollution. Prepared for the WHO Ministerial Conference for Environment and Health, London, June 1999.

Flindell I., Stallen P. J. M., 1999: Non-acoustical factors in environmental noise. *Noise and Health*, **1(3)**, 11-16.

Flindell I., Witter I., 1999: Non-acoustical factors in noise management at heathrow airport. *Noise and Health*, **1(3)**, 27-44.

Forkel R., Knoche R., 2006: Regional climate change and its impact on photooxidant concentrations in southern Germany: Simulations with a coupled regional climate-chemistry model, *J. Geophys. Res.*, **111**, doi:10.1029/2005JD006748, 2006.

Forkel R., G. Smiatek F. Hernandez R. Iniestra B. Rappenglück R., Steinbrecher, 2004: Numerical simulations of ozone level scenarios for Mexico City, 84th AMS Annual Meeting (6th Conference on Atmospheric Chemistry: Air Quality in Megacities), Seattle, Wa. 11-15 January 2004, Combined Preprint CD, contribution P1.2 (4pp.), http://ams.confex.com/ams/pdfpapers/70640.pdf.

Forsberg B., Stjernberg N., Wall S., 1997: People can detect poor air quality well below guideline concentrations: a prevalence study of annoyance reactions and air pollution from traffic. *Occup.Environ.Med*., **54**, 44-48.

Friedrich R., B. Wickert, P. Blank, S. Emeis, W. Engewald, D. Hassel, H. Hoffmann, H. Michael, A. Obermeier, K. Schäfer, T. Schmitz, A. Sedlmaier, M. Stockhause, J. Theloke, F.-J. Weber, 2002: Development of Emission Models and Improvement of Emission Data for Germany. *J. Atmos. Chem.*, **42**, 179-206.

Gabillet Y., Van Maercke D., 1995: Outdoor noise propagation in urban areas: principles and use of the MITHRA software. *Euronoise. Lyon, France*

Galobardes B., 2002: Key steps in planning survey. *Int.J.Public Health*, **47**, 349-351.

Garcia J., Colosio J., 2002: *Air-quality indices*. Les Presses de l'Ecoles des Mines Paris. 112p.

Gehrig, R., Hill, M., Buchmann, B., Imhof, D., Weingartner, E., Baltensperger, U., Purghart, B. G., Bürgisser, G., Dolecek, L., Evequoz, R., Hauser-Strozzi, E., Infanger, K., Jenk, H., Porchet, A., Sommer, H.,

Sprenger, P., Stauffer, J., and Vaucher, C., 2003: "Verifikation von PM10-Emissionsfaktoren des Strassenverkehrs.", PSI, EMPA, BUWAL, Schweiz.

Gehrig, R., Hill, M., Lienemann, P., Zwicky, N. B., Bukowiecki, N., Weingartner, E., Baltensperger, U., Buchmann, B., 2007: Contribution of railway traffic to local PM10 concentrations in Switzerland, *Atmos. Environ.*, **41**, 923-933.

Geiger H., Barnes, I., Benjan, I, Benter, T., Splitter M., 2003: The tropospheric degradation of isoprene: an updated module for the regional chemistry mechanism. *Atmos. Env.*, **37**, 1503-1519.

Gery M.W., G.Z. Whitten, J.P. Killus, and M.C. Dodge, 1989: A Photochemical Kinetics Mechanism for Urban and Regional Scale Computer Modelling. J. Geophys. Res. 94, 12925-12956.

Gilbert K.E., White M.J., 1989: Application of the parabolic equation to sound propagation in a refracting atmosphere. *J. Acoust. Soc. Am.*, **85**, 630-637.

Gilliam R.C., Hogrefe C., Rao S.T., 2006: New methods for evaluating meteorological models used in air quality applications, *Atmos. Env.*, **40**, 5073-5086.

Gobiet W. et al., 2006: Emissionsgesteuerter Verkehrüber die Alpen - Alp-EmiV. Schwerpunkt Güterverkehr. Anlagen-rechtliche Innovationen und Emissionsrechtehandel zur Steuerung des Verkehrs in ökologisch sensiblen Räumen. Endbe-richt. Graz. ISBN-10 3-7001-3778-8, ISBN-13 978-3-7001-3778-8 doi: 10.1553/alp-emiv, http://epub.oeaw.ac.at/alp-emiv

Goldberg P., Guéguen A., Schmaus A., Nakache J.-P., Goldberg M., 2001: Longitudinal study of associations between perceived health status and self reported diseases in the French Gazel cohort. *J.Epidemiol.Community Health*, **55**, 233-238.

Golder, D., 1972: Relations among stability parameters in the surface layer. *Boundary-Layer Meteor.*, **3**, 47-58.

Green D. M., Fidell S., 1991: Variability in the criterion for the reporting annoyance in community noise surveys. *J.Acoust.Soc.Am.*, **89**, 234-243.

Grell G., Dudhia J. and Stauffer D., 1994: A Description of the Fifth-Generation Penn State/NCAR Mesoscale Model (MM5), NCAR/TN-398+STR

Grell G., Emeis S., Stockwell W.R., Schoenemeyer T., Forkel R., Michalakes J., Knoche R., Seidl W., 2000: Application of a multiscale, coupled MM5/Chemistry Model to the complex terrain of the VOTALP Valley Campaign, *Atmospheric Environ.*, **34**, 1435-1453.

Griefahn B., 2007: Noise and sleep. In: Noise and its effects (eds. L. Luxon, D. Prasher), pp. 567-587. Wiley.

Grießer, E., 2003: Quantitative Simulation des NOx-Konzentrationsverlaufes während der Belastungsepisode im November/Dezember 1999. Diploma thesis. University of Innsbruck, 79 pp.

Groß G., 1992: Results of supercomputer simulations of meteorological mesoscale phenomena. *Fluid Dynamics Research*, **10**, 483-498.

Guski R., 1999: Personal and social variables as co-determinants of noise annoyance. *Noise and Health*, **3**, 45-56.

Haas E., Forkel R., Suppan P., 2007: Application and Intercomparison of the RADM2 and RACM Chemistry Mechanism including a new Isoprene Degradation Scheme within the Regional Meteorology-Chemistry-Model MCCM, *Int. J. Environment and Pollution*, in press.

Hajak G., Rodenbeck A., Voderholzer U., et al., 2001: Doxepin in the treatment of primary insomnia: a placebo-controlled, double-blind, polysomnographic study. *J.Clin.Psychiatry*, **62**, 453-463.

Halpern, D., 1995: Mental health and the built environment. More than bricks and mortar?, Taylor & Francis, London.

Hangartner M., 1987: Evaluation of annoyance caused by motor traffic. In: Environmental annoyance (ed. H. Koelega), pp. 363-370. Elsevier.

Hanna S.R., Chang J.C., 1992: Representativeness of wind measurements on a mesoscale grid with station separations of 312 m to 10 km, *Journal of Boundary-Layer Meteorology*, **60(4)**, 309-324

References

Hanna S. R., Strimaitis D.G., Chang J.C., 1991: Hazard response modeling uncertainty (a quantitative method). Vol. 2, Evaluation of commonly used hazardous gas dispersion models. Sigma Research Corporation for AFESC, Tyndall AFB, FL, and API, Report Nos. 4545, 4546, and 4547, 338 pp

Hanna S. R., Yang R., Moses Kang, 2001: Evaluations of Mesoscale Model Predictions of Near-Surface Winds, Stabilities and Mixing Depths, *J. App. Meteor*., **40**, 1095-1104.

Hargreave F., Parameswaran K., 2005: Asthma, COPD and bronchitis are just components of airway disease. *Eur. Respir. J.*, **28**, 264-267.

Harnisch F., Gohm A., Fix A., Schnitzhofer R., Hansel A., Neiniger B., 2007: Spatial distribution of aerosols in the Inn Valley atmosphere during wintertime. Submitted to *Met. Atmos. Phys*.

Hatfield, J. and Job, RFS. Examination of perceived air pollution as a moderator of reaction to aircraft noise. 2004. Prag, Internoise.

Hausberger S., 1997: Globale Modellbildung für Emissions- und Verbrauchsszenarien im Verkehrssektor. Mitteilungen des Institutes für Verbrennungskraftmaschinen und Thermodynamik der TU-Graz.

Hausberger S., 2002: Update of the Emission Functions for Heavy Duty Vehicles in the Handbook Emission Factors for Road Traffic; Institute for Internal Combustion Engines and Thermodynamics; Graz.

Hausberger S., 2003: Simulation of Real World Vehicle Exhaust Emissions; VKM-THD Mitteilungen; Heft/Volume 82; Verlag der Technischen Universität Graz; ISBN 3-901351-74-4; Graz.

Hausberger S., 2006: Statistical projection of the fleet structure of heavy commercial vehicles on the A12 until 2012, Institute for Internal Combustion Engines and Thermodynamics, by order of the Tyrolean Provincial Government office.

Hausberger, S. and Rexeis, M., 2004: Emission behaviour of modern heavy duty vehicles in real world driving. *IJEP*, **22**, No. 3, 2004.

HBEFA, 2004: Handbuch für Emissionsfaktoren des Strassenverkehrs (handbook of emission factors for road traffic). Umweltbundesamt Berlin, Bundesamt für Umwelt, Wald und Landschaft Bern, Infras AG, Bern (published on CD-ROM).

HCN, 2004: Effects of noise on sleep and health. Publication no. 2004/14. The Hague, Health Council of the Netherlands.

Heimann D., 2006: Sound propagation in a nocturnal slope-wind layer – a numerical model study. *Acta Acustica united with Acustica*, **92**, 362-369.

Heimann D., Groß G., 1999: Coupled simulation of meteorological parameters and sound level in a narrow valley. *Applied Acoustics*, **56**, 73-100.

Heimann D., Karle R., 2006: A Linearized Euler Finite-Difference Time-Domain Sound Propagation Model with Terrain-Following Coordinates. *J.Acoust.Soc.Am.*, **119**, 3813-3823.

Heimann D., Bakermans M., Defrance J., Kühner D., 2007: Vertical sound speed profiles determined from meteorological measurements near the ground. *Acta Acustica*, **93**, 228-240.

Henne S., M. Furger, S. Nyeki, M. Steinbacher, B. Neininger, S. F. J. de Wekker, J. Dommen, N. Spichtinger, A. Stohl, A. S. H. Prévôt, 2004: Quantification of topographic venting of boundary layer air to the free troposphere. *Atmos. Chem. Phys*., 4, 497-509.

Herd J. A. 1991. Cardiovascular response to stress. Physiological Reviews 71, 305-330.

Hesstvedt E., Isaksen I.S.A., Hovey O., 1978: Ozone generation over rural areas. *Environmental Science and Technology*, **12**, 1279-1284.

Holland W. W. and Reid D. D., 1979: Health effects of particulate pollution: reappraising the evidence. *Am.J.Epidemiol.*, **110**, 525-659.

Holtslag A.A.M., van Ulden A.P., 1983: A simple scheme for daytime estimates of the surface fluxes from routine weather data, *J. Clim. App. Meteor.*, **22**, 517-529

Hossein J. L., Shapiro C. M., 2002: The prevalence, cost implications and management of sleep disorders: An overview. *Sleep and Breathing*, **6**, 85-102.

Howarth H. V. C., Griffin M. J., 1991: The annoyance caused by simultaneous noise and vibration. J.Acoust.Soc.Am., **89**, 2317-2323.

Idler E. L., Benyamini Y., 1997: Self-rated health and mortality: A review of twenty-seven community studies. *J.Health Soc.Behav.*, **38**, 21-37.

Idler E. L., Kasl S., 1995: Self-ratings of health: Do they also predict change in functional ability? J. of *Gerontology: Social Sciences*, **50B**, S344-S353.

IGC-CGPC, 2006: Rapport d'enquête sur l'évaluation de l'autoroute ferroviaire alpine. Ministère des Transports de l'Equipement du Tourisme et de la Mer. 46P.

International Organisation for Standardization, 1993: *Acoustics – attenuation of sound during propagation outdoors – Part 1: Calculation of the absorption of sound by the atmosphere*. ISO 9613-1.

International Organisation for Standardization, 1999: *Acoustics – attenuation of sound during propagation outdoors – Part 2: General methods of calculation*. ISO 9613-2.

Jacquemin B., Sunyer J., Forsberg B., Götschi T., Bayer-Oglesby L., Ackermann-Liebrich U., de Marco R., Heinrich J., Jarvis D., Toren K., Künzli N., 2007: Annoyance due to air pollution in Europe. *Int.J.Epidemiol.*,**16**, 809-820.

Jarup L., Dudley M., Babisch W., Houthuijs D., Swart W., Pershagen G., Bluhm G., Katsouyanni K., Velonakis M., Cadum E., and Vigna-Taglianti F., 2005: Hypertension and exposure to noise near airports (HYENA): Study design and noise exposure assessment. *Environ. Health Perspect.*, **113**, 1478.

Jazcilevich A.D., Garcia A.R., Ruiz-Suarez L.G., 2003: A study of air flow patterns affecting pollutant concentrations in the Central Region of Mexico, *Atmos. Environ.*, **37**, 183-193.

Jean P., Defrance J., Gabillet Y., 1999: The importance of source type on the assessment of noise barriers. *J. Sound Vibration*, **226**(2), 201-216.

Job R.F.S., 1988: Community response to noise: A review of factors influencing the relationship between noise exposure and reaction. *J.Acoust.Soc.Am.*, **83**, 991-1001.

Job R.F. S., 1991: Impact and potential use of attitude and other modifying variables in reducing community reaction to noise. *Transportation Research Record*, 109-115.

Job R.F. S., Hatfield J., 2001a: The impact of soundscape, enviroscape, and psychscape on reaction to noise: Implications for evaluation and regulation of noise effects. *Noise Control Engineering Journal*, **49**, 120-124.

Job, R.F.S., Hatfield, J., 2001b: Responses to noise from combined sources and regulation against background noise levels. Proc. Internoise 2001, 1801-1806.

Jurriens A. A., Griefahn B., Kumar A., Vallet M., Wilkinson R.T., 1983: An essay in European research collaboration: Common results from the project on traf.c noise and sleep in the home. In G. Rossi (Ed.), Noise as a public health problem. proceedings of the 4th international congress turin, Vol. 2 (pp. 929–937). Milano, Italy: Edizioni Techniche a cura del centro ricerche e studi amplifon.

Kabuto M., Kageyama T., 1994: Nighttime road traffic noise and sleep quality. 2, 104-106. Tokyo, The Institute of Noise Control Engeneering Japan and the Acoustical Society of Japan.

Kageyama T., Kabuto M., Nitta H., et al., 1997: Population study on risk factors for insomnia among adult Japanese women: a possible effect of road traffic volume. *Sleep*, **20**, 963-971.

Kaimal J.C., Finnigan J.J., 1994: *Atmospheric Boundary Layer Flows*. Oxford University Press.

Kaiser A., Petz E., Cuhalev I., 2005: Ermittlung der Gesamtbelastung durch Luftschadstoffe im Kurzzeitmittel anhand von Zeitreihen der Vor- und Zusatzbelastung; Vergleich mit statistischen Methoden. Das zur Berechnung von Zeitreihen der Zusatzbelastung adaptierte ÖNORM M 9440 Modell ONGAUSSplus. Österr. Beiträge zu Meteorologie und Geophysik (ISSN 1016-6254), Heft 35.

Karakatsani A., Andreadaki S., Katsouyanni K., et al., 2003: Air pollution in relation to manifestations of chronic pulmonary disease: a nested case-control study in Athens, Greece. *Eur.Respir.J.*, **18**, 45-53.

Katsouyanni K., Zmirou D., Spix C., Sunyer J., Schouten J.P., Ponka A., Anderson H.R., Le Moullec Y., Wojtyniak B., Vigotti M.A., Bacharova L., 1995: Short-term effects of air pollution on health: a European approach using epidemiological time-series data. *Eur Respir J*, **8**, 1030-1038.

References

Katsouyanni K., Touloumi G., Spix C., Schwartz J., Balducci F., Medina S., Rossi G., Wojtyniak B., Sunyer J., Bacharova L., Schouten J.P., Ponka A., Anderson H.R., 1997: Short term effects of ambient sulphur dioxide and particulate matter on mortality in 12 European cities: results from time series data from the APHEA project. *BMJ*, **314**, 1658-1663.

Katsouyanni K., Touloumi G., Samoli E., Cryparis A., Le Tertre A., Monopolis Y., Rossi G., Zmirou D., Ballester F., Boumghar A., Anderson H.R., Wojtyniak B., Paldy A., Braunstein R., Pekkanen J., Schindler C., Schwartz J., 2001: Confounding and effect modification in the short-term effects of ambient particles on total mortality: results from 29 European cities within the APHEA-2 project. *Epidemiology*, **12**, 521-531.

Keller J. B., 1962: Geometrical theory of diffraction. *Journal of the Optical Society of America*, **52**(2), 116-130.

Kim, D., Stockwell W.R., 2007: An online coupled meteorological and air quality modeling study of the effect of complex terrain on the regional transport and transformation of air pollutants over the Western United States, *Atmospheric Environment*, **41**, 2319-2334.

Klæboe R., 1998: The combined effects of road traffic- implications for environmental guidelines. In: Noise as a Public Health Problem. Eds. N. L. Carter, R. F. S. Job, *Noise Effects*, **1**, 264-267.

Klæboe, R., 2000: Analysing the impacts of combined environmental effects - can structural equation models (sem) be of benefit? Société Française d'Acoustique. Nice, Internoise 2000.

Klæboe R., 2007: Are adverse impacts of neighbourhood noisy areas the flip side of quiet area benefits? *Appl. Acoustics*, **68**, 557-575.

Klæboe R., Kolbenstvedt M., Clench-Aas J., and Bartonova A., 2000: Oslo traffic study - part 1: an integrated approach to assess the combined effects of noise and air pollution on annoyance. *Atmos. Environ.*, **34**, 4727-4736.

Klæboe R., Turunen-Rise I. H., Harvik L., and Madshus C., 2003: Vibration in dwellings from road and rail traffic -- Part II: exposure-effect relationships based on ordinal logit and logistic regression models. *Appl. Acoustics*, *64*, 89-109.

Klæboe R., Engelien E., and Steinnes M., 2006: Context sensitive noise impact mapping. *Appl. Acoustics*, **67**, 620-642.

Klinger M., Voigtländer M., Anke K., Sähn E., 2006: *PM10-Prognosemodell.* Fraunhofer IVI, Im Auftrag des Landesamtes für Umwelt und Geologie, Dresden.

Klug, W., G. Graziani, G. Grippa, D. Pierce, and C. Tassone, 1992: Evaluation of Long Range Atmospheric Transport Models Using Environmental Radioactivity Data from the Chernobyl Accident: The ATMES Report. Elsevier Applied Science, London, 366 pp.

Korn E. L., Graubard B. I., 1999: Analysis of health surveys. Wiley.

Kouyoumjian R., Pathak. P., 1974: A uniform geometrical theory of diffraction for an edge in a perfectly conducting surface. *IEEE*, **62**, 1448-1461.

Kripke G.F., Garfinkel L., Wingard D. L., et al., 2002: Mortality associated with sleep duration and insomnia. *Arch.Gen.Psychiatry*, **99**, 131-136.

Krüger B.C., 2004: Aktionsplan für Sofortmaßnahmen gemäß § 15 Ozon-Gesetz - Meteorologisch chemische Modellrechnungen -. Endbericht, Auftraggeber: Magistrat der Stadt Wien, Amt der niederösterreichischen Landesregierung, Amt der burgenländischen Landesregierung.

Krüger B.C., Baumann-Stanzer K., Langer M., Hirtl M., 2005: A New Air Quality Model System for Austria. In: European Geosciences Union: EGU General Assembly 2005, 24.-29. April 2005, Wien, 7, 6284; ISSN 1029-7006.

Kryter K.D., 1990: Aircraft noise and social factors in psychiatric hospital admission rates: a re-examination of some data. *Psychol. Med*., **20**, 395-411.

Künzli N., Kaiser R., Medina S., Oberfeld G., Hoark F., 1999: Health Costs due to Road Traffic-related Air Pollution. An impact assessment project of Austria, France and Switzerland - Air pollution Attributable cases - Technical Report epidemiology. Prepared for the WHO Ministerial Conference for Environment and Health, London, June 1999

Künzli N, Kaiser R, Medina S, et al., 2000: Public-health impact of outdoor and traffic-related air pollution: a European assessment. *Lancet*, **356**, 795-801.

Kuroiwa N., Xin P., Suzuki S., et al., 2002: Habituation of sleep to road traffic noise observed not by polygraphy but by perception. *J.Sound.Vib.*, **250**, 101-106.

Kurze U.J., Anderson G.S., 1971: Sound attenuation by barriers. *Applied Acoustics*, **4**, 35-53.

Lambert J., 2002: Caractérisation, mesures et descripteurs acoustiques de la gêne due au bruit routier. *Revue Générale des Routes et des Aérodromes*, (803 - Dossier bruit du trafic routier), 17-21.

Langdon J., 1987: Some residual problems in noise nuisance: A brief review. In: Environmental annoyance: Characterisation, measurement and control. (ed. H. S. Koelega), pp. 321-329. Elsevier.

Langdon F.J., Scholes, W.E., 1968: The Traffic Noise Index: A Method of Controlling Noise Nuisance, Building Research Station Current Papers 38168, April 1968, pp. 2-3.

Larssen S., Sluyter R., Helmis C., 1999: Criteria for EUROAIRNET - The EEA Air Quality Monitoring and Information Network. Technical Report No. 12 (EEA).

Leclercq L., Lelong J., 2001: Dynamic evaluation of urban traffic noise (pdf). In ICA International Commission for Acoustics: 17th ICA - International Congress of Acoustics, Roma, Italy, 2-7 September, 2001.

Lee X., Massman W., Law B. (Eds), 2004: *Handbook of micrometeorology: a guide for surface flux measurement and analysis*, Kluwer Academic Publ.

Legret M., Pagotto C., 1999: Evaluation of Pollutant Loadings in the Runoff Waters from a Major Rural Highway. *The Science of the Total Environment*, **235**, 143-150.

Lekander M., Elofsson S., Neve I.-M., Hansson L.-O., Unden A.-L., 2004: Self-rated health is related to levels of circulating cytokines. *Psychosom.Med.*, **66**, 559-563.

Leonardi G. S., Houthuijs D., Nikiforov B., Volf J., Rudnai P., Zejda J., Gurzau E., Fabianova E., Fletcher T., and Brunekreef B., 2002: Respiratory symptoms, bronchitis and asthma in children of Central and Eastern Europe. *Eur. Respir. J.*, **20**, 890-898.

Lepore J. S., Evans G. W., 1996: Coping with multiple stressors in the environment. In: Handbook of coping. Theory, research, applications (eds. M. Zeidner, N. S. Endler), pp. 350-377. Wiley & Sons.

Lercher P., 1992: Auswirkungen des Straßenverkehrs auf Lebensqualität und Gesundheit: Transitstudie - Sozialmedizinischer Teilbericht. Amt der Tiroler Landesregierung.

Lercher P., 1996: Environmental noise and health: an integrated research perspective. Environment International 22, 117-128.

Lercher P., 1998: Deviant dose-response curves for traffic noise in "sensitive areas" In: The New Zealand Acoustical Society Inc. (Ed.), Inter Noise 98. The New Zealand Acoustical Society Inc.

Lercher P., 2003: Which health outcomes should be measured in health related environmental quality of life studies? *Landscape and Urban Planning*, **65**, 63-72.

Lercher P., 2007a: Environmental noise: A contextual public health perspective. In: Noise and its effects. (eds. L. Luxon, D. Prasher), pp. 345-377. Wiley.

Lercher P. 2007b: In Kephalopoulos S. (organiser), Schwela D., Koistinen K., Paviotti M., Kotzias D.(eds). Proceedings of the International Workshop on "Combined Environmental Exposure: Noise, Air Pollution, Chemicals" organised by the JRC/IHC/PCE on 15-16 January 2007, Ispra (Italy). Luxembourg: Office for Official Publications of the European Communities, EUR 22883 EN, ISBN 978-92-79-06542-2, ISSN 1018-5593.

Lercher, P., Botteldooren, D., 2006: General and/or local assessment of the impact of transportation noise in environmental health impact studies ? CD-ROM edition. Tampere, European Acoustics Association. Euronoise 2006.

Lercher P., Schulte-Fortkamp B., 2003: The relevance of soundscape research to the assessment of noise annoy ance at the community level. In: de Jong R.G., Houtgast T., Franssen E., Hofman W. (Eds). Proceedings of the 8th International Congress on Noise as a Public Health Problem, Rotterdam, July, 2003, Foundation ICBEN: Schiedam, Netherlands: pp 225- 231 (also on CD-ROM)

References

Lercher P., Schmitzberger R., Kofler W.,1995: Perceived traffic air pollution, associated behavior and health in an alpine area. *Sci.Total.Environ.*, **169**, 71-74.

Lercher P., Brauchle, G., Widmann, U., 1999: The interaction of landscape and soundscape in the Alpine area of the Tyrol: an annoyance perspective. Cuschieri, J., Glegg, S., and Yong, Y. Proceedings of Internoise. Ft. Lauderdale, INCE. pp. 1347-1350. INCE.

Lindström B., 1992: Quality of life: a model for evaluating Health for All. Conceptual and policy implications. *Soz. Präventivmed.*, **37**, 301-306.

Mackenbach J.P., Simon J.G., Looman C.W., Joung I.M., 2002: Self-assessed health and mortality: Could psychosocial factors explain the association? *Int.J.Epidemiol.*, **31**, 1162-1168.

Maddox G.L., Douglas E.B., 1973: Self-assessment of health: A longitudinal study of elderly subjects. *J.Health Social Behavior*, **14**, 87-93.

Maekawa Z., 1968: Noise reduction by screens. *Applied Acoustics*, **1**, 157-173.

Marquis-Favre C., Premat E., Aubree, D. Vallet M., 2005: Noise and its effects – A review on qualitative aspects of sound. Part I and II: Notions and acoustic ratings. *Acta Acustica*, **91(4)**, 613-625.

Maschke C., Ising H., Hecht K., 1997: Schlaf - nächtlicher Verkehrslärm - Streß - Gesundheit: Grundlagen und aktuelle Forschungsergebnisse. Teil II: aktuelle Forschungsergebnisse. Bundesgesundheitsblatt 97, 86-95.

Maynard R. L., 2007: Acceptable risk of environmental air pollution. *Int.J.Hyg.Environ.Health*, **204**, 203-206.

McCarthy M., Biddulph J. P., Utley M., Ferguson J., Gallivan S., 2002: A health impact assessment model for environmental changes attributable to development projects. *J.Epidemiol.Community Health*, **56**, 611-616.

McGeehin M. H., Qualters J. R., Niskar A. S., 2004: Mini-monograph: National Environmental Public Health Tracking Program: Bridging the information gap. *Environ. Health Perspect.*, **112**, 1409-1413.

Meier-Ewert H. K., Ridker P. M., Rifai N., et al., 2004: Effect of sleep loss on C-reactive protein, an inflammatory marker of cardiovascular risk. *JACC*, **43**, 678-683.

Meloni T., Krüger H., 1990: Wahrnehmung und Empfindung von kombinierten Belastungen durch Lärm und Vibration. *Z.Lärmbekämpf.*, **37**, 170-175.

Meyer T., Schäfer I., Matthis C., Kohlmann T., Mittag O., 2006: Missing data due to a "checklist misconception-effect". *Int.J.Public Health*, 51, 34-42.

Miedema, H.M.E., 2004a: Self reported sleep disturbance caused by aircraft noise. Delft, TNO.

Miedema H.M.E., 2004b: Relationship between exposure to multiple noise sources and noise annoyance. *J.Acoust.Soc.Am.*, **116**, 949-957.

Miedema H.M., Oudshoorn C. G., 2001: Annoyance from transportation noise: relationships with exposure metrics DNL and DENL and their confidence intervals. *Environ. Health Perspect.*, **109**, 409-416.

Miedema H.M., Vos H., 1998 : Exposure-response relationships for transportation noise. *J.Acoust.Soc.Am.*, **104**, 3432-3445.

Miedema H.M., Vos H., 1999 : Demographic and attitudinal factors that modify annoyance from transportation noise. *J.Acoust.Soc.Am.*, **105**, 3336-3344.

Miedema H.M.E., Vos H., 2003 : Noise sensitivity and reactions to noise and other environmental conditions. *J.Acoust.Soc.Am.*, **113**, 1492-1504.

Miedema H.M.E., Vos H., 2004 : Noise annoyance from stationary sources: Relationships with exposure metric day-evening-night level (DENL) and their confidence intervals. *J.Acoust.Soc.Am.*, **116**, 334-343.

Miedema H.M.E., Fields J. M., Vos H., 2005: Effect of season and meteorological conditions on community noise annoyance. *J.Acoust.Soc.Am.*, **117**, 2853-2865.

Miedema H.M.E., Oudshoorn C.G.M., 2001: Annoyance from Transportation Noise: Relationships with Exposure Metrics. *Environmental Health Perspectives*, **109 (4)**, 409-416.

MISA, 2004: Metanalisi italiana degli studi sugli effetti a breve termine dell'inquinamento atmosferico 1996-2002, *Epidemiologia & Prevenzione*, Anno 28 (4-5), luglio-ottobre, supplemento.

Möhler U., Liepert M., Schuemer R., Griefahn B., 2000: Differences between railway and road traffic noise. *J.Sound.Vib.*, **231**, 831-864.

Morgenstern V., Zutavern A., Cyrys J., Brockow I., Gehring U., Koletzko S., Bauer C.P., Reinhardt D., Wichmann H.E., Heinrich J., 2007: Respiratory health and individual estimated exposure to traffic-related air pollutants in a cohort of young children. *Occup.Environ.Med.*, **64**, 8-16.

Mosca S., Bianconi R., Bellasio R., Graziani G., Klug W., 1998a: ATMES II, Evaluation of long-range dispersion models using data of the 1st ETEX release. EUR 17756 EN, Office for Official Publications of the European Communities, L-2985 Luxembourg, 459 pp. + app.

Mosca S., Graziani G., Klug W., Bellasio R., Bianconi R., 1998b: A statistical method-ology for the evaluation of long-range atmospheric dispersion models: an application to the ETEX exercise. *Atmos. Environ.*, **32**, 4307-4327.

Mossey J.M. , Shapiro E., 1982: Self-rated health: A predictor of mortality among the elderly. *Am.J.Pub. Health*, **72**, 800-808.

Münkel, C., Emeis S., Müller W.J., Schäfer K., 2004: Aerosol concentration measurements with a lidar ceilometer: results of a one year measurement campaign. SPIE 10th Intern. Symp. Remote Sensing, 8.-12.9.2003, Barcelona (Conf. 5235 paper 64). In: Remote Sensing of Clouds and the Atmosphere VIII.

Muzet, A., Ehrhart, J., 1980: Habituation of heart rate and finger pulse resonses to noiseduring sleep. In Noise as a Public Health Problem (ed. J. V. Tobias), pp. 401-404. ASHA report no. 10, Rockville, Maryland.

Natale P., Anfossi D., Cassardo C., 1999: Analysis of an anomalous case of high air pollution concentration in Turin after a foehn event. *Int. J. Environment and Pollution*, **11**, 147-164

Nickus, U., Vergeiner I., 1984: The thermal structure of the Inn Valley atmosphere. *Arch. Meteor. Geophys. Bioklim.*, **A33**, 199- 215.

Niemann H., Maschke C., Hecht K., 2005: Lärmbedingte Belästigung und Erkrankungsrisiko – Ergebnisse des paneuropäischen Lares-Survey. *Bundesgesundheitsblatt-Gesundheitsforschung-Gesundheitsschutz*, **48**, 315-328.

Nieuwstadt F.T.M., 1981. The steady state height and resistance laws of the nocturnal boundary layer: theory compared with Cabauw observations. *Boundary-Layer Met.*, **20**, 3 - 17.

Nijs L., Wapenaar C.P.A., 1990: The influence of wind and temperature gradients on sound propagation, calculated with the two-way wave equation. *J. Acoust. Soc. Am.*, **87**, 1987-1998.

Nilsson M. E., 2001: Perception of traffic sounds in combination. *Archives of the Center for Sensory Research*, **6**, 1-117.

NNGL, 2007: Nighttime noise guidelines. Final report. WHO-Europe. Geneva: 2007, in press.

Ntziachristos L., Samaras Z., 2001: COPERT III – Computer Programme to calculate Emissions from Road Transport – Methodology and Emission Factors.

NUA, 2005: Immissionsmessungen im Umfeld der Deponie Ahrental, Gemeinde Innsbruck (Stickstoffdioxid und Staubdeposition) im Zeitraum 16.3.2004 – 15.3.2005. Niederösterreichische Umweltanalytik GmbH, Maria Enzersdorf 2005.

OECD, 1993: OECD Core set of indicators for environmental performance review. Environment Monograph N°83. Report., 39p.

OECD, 2002: Aggregated environmental indices review of aggregation methodologies in use. Report. 43p.

OECD, 2006: Environmentally sustainable transportation guidelines. Paris.

OEHHA, California Environmental Protection Agency, 2003: The Air Toxics Hot Spots Program Guidance Manual for Preparation of Health Risk Assessments.

Oglesby L., Kunzli N., Monn C., Schindler C, Ackermann-Liebrich U., Leuenberger P., 2000: Validity of annoyance scores for estimation of long-term air pollution exposure in epidemiological studies. *Am.J.Epidemiol.*, **152**, 75-83.

Ohayon M. M., Partinen M., 2002: Insomnia and global sleep dissatisfaction in Finland. *J. Sleep Res.*, **11**, 339-346.

References

Öhrström E., 1997: Effects of exposure to railway noise--a comparison between areas with and without vibration. *J.Sound.Vib.*, **205**, 555-560.

Öhrström E., Skanberg A.-B., 1996: A field survey on effects of exposure to noise and vibration from railway traffic, part I: Annoyance and activity disturbance effects. *J.Sound.Vib.*, **193**, 39-47.

Öhrström E., Barregård L., Andersson E., Skånberg A., Svensson H., Ängerheim P., 2007. Annoyance due to single and combined sound exposure from railway and road traffic. *J.Acoust.Soc.Am.*, **122**, 2642-2652.

Oke T.R., 2004: Initial guidance to obtain representative meteorological observations at urban sites[R]. WMO/TD No.1250. Geneva, Switzerland.World Meteorological Organization

Oppenheim A. N., 1992: Questionnaire design, interviewing and attitude measurement. Continuum.

Ota A., Yokoshima S., Kamitani J., Tamura A., 2006: A study on evaluation methods of combined traffic noises, Part 2: Community response to road traffic and conventional railway noises. Internoise 2006.

Öttl D., 2000: Weiterentwicklung, Validierung und Anwendung eines Mesoskaligen Modells. Dissertation, Institute for Geography at Graz University, p. 155.

Öttl D., Almbauer R., Sturm P. J., 2001: A new method to estimate diffusion in low wind, stable conditions. *Journal of Applied Meteorology*, **40**, 259-268.

Öttl D., Sturm P.J., Bacher M., Pretterhofer G., Almbauer R.A., 2002: A simple model for the dispersion of pollutants from a road tunnel portal. *Atmos. Environ.*, **36**, 2943-2953.

Öttl D., Sturm P.J., Pretterhofer G., Bacher M., Rodler J., Almbauer R.A., 2003a: Lagrangian dispersion modeling of vehicular emissions from a highway in complex terrain. *J. of the Air and Waste Management Association*, **53**, 1233-1240.

Öttl D., Almbauer R.A., Sturm P.J., Pretterhofer G., 2003b: Dispersion modelling of air pollution caused by road traffic using a Markov Chain - Monte Carlo model. *Stochastic Environmental Research and Risk Assessment*, **17**, 58-75.

Öttl D., Goulart A., Degrazia G., Anfossi D., 2005: A new hypothesis on meandering atmospheric flows in low wind speed conditions. *Atmos. Environ.*, **39**, 1739 - 1748.

Öttl D., Sturm P., Anfossi D., Trini Castelli S., Lercher P., Tinarelli G., Pittini T., 2007: Lagrangian particle model simulation to assess air quality along the Brenner transit corridor through the Alps; *Air Pollution Modelling and its Applications XVIII*; Developments in Environmental Science, **6**, 689-697, Elsevier.

Pacione M., 2003: Urban Environmental Quality - A Social Geographical Perspective. *Landscape und Urban Planning*, **65**, 19-31.

Passchier-Vermeer W., 1998: Vibrations in the environment. Factors related to vibration perception and annoyance. TNO.

Passchier-Vermeer W., Zeichart K., 1998: Vibrations in the living environment. Relationships between vibration annoyance and vibration metrics. TNO.

Patel S. R., Ayas N. T., Malhotra, M.R., et al., 2004: A prospective study of sleep duration and mortality risk in women. *Sleep*, **27**, 440-444.

Pattenden S., Hoek G., Braun-Fahrlander C., Forastiere F., Kosheleva A., Neuberger M., Fletcher T., 2006: NO_2 and children's respiratory symptoms in the PATY study. *Occup.Environ. Med.*, **63**, 828-835.

Paulsen R., Kastka J., 1995: Effects of combined noise and vibration on annoyance. *J.Sound.Vib.*, **181**, 295-314.

Pfeffer U., Beier R., Zangt T., 2006: Measurements of nitrogen dioxid with diffusive samplers at traffic-related sites in North Rhine-Westphalia (Germany), Landesumweltamt Nordrhein-Westfalen, Essen. Gefahrenstoffe – Reinhaltung der Luft 66 (2006), Nr. 1/2, p38-44.

Physick W. , Trini Castelli S., 2005: Lagrangian Particle Models. Link with meteorological models. Section 11.2.5. in *Air Quality Modelling. Theories, Computational Methods and Available Databases and Software*, *vol II – Advanced Topics*, Zannetti P. Ed., 116-118.

Pielke R.A., Cotton W.R., Walko R.L., Tremback C.J., Lyons W.A., Grasso L.D., Nicholls M.E., Moran M.D., Wesley D.A., Lee T.J., Copeland J.H., 1992: A Comprehensive Meteorological Modeling System –RAMS. *Meteorology and Atmospheric Physics*, **49**, 69-91.

Pope, C.A., Thun M.J., Namboodiri M.M., Dockery D.W., Evans J.S., Speizer F.E., Heath C.W., 1995: Particulate Air Pollution as a Predictor of Mortality in a Prospective Study of U.S. Adults. *American Journal of Respiratory and Critical Care Medicine*, **151**, 669-674.

Pope C.A. III, Burnett R.T., Thun M.J., Calle E.E., Krewski D., Ito K., Thurston G.D., 2002: Lung cancer, cardiopulmonary mortality, and long-term exposure to fine particulate air pollution. *JAMA*, **287**, 1132-1141.

Potthoff P., Eller M., 2007: Survey mit Fragebogen: Vor- und Nachteile verschiedener Erhebungsverfahren. *Zeitschrift für Gesundheitswissenschaften*, **8**, 100-105.

Prandtl L., 1952: *Essentials of fluid dynamics*. Hafner Publishing, New York.

Pruppers M. J. M., Janssen M. P. M., Ale B. M. J., 1998: Accumulation of environmental risks to human health: geographical differences in the Netherlands. *J.Hazardous Mat.*, **61**, 187-196.

Raymond K., Coates A., 2001: Guidance on EIA – Screening, ERM - Environmental Resources Management, Office for official publications of the European Communities, Luxembourg, 2001.

Reilly J. J., Armstrong A. R., Dorosty A. R., et al., 2005: Early life risk factors for obesity in childhood: cohort study. *BMJ*, **330**, 1357.

Reisin T., Altaratz Stollar O., Trini Castelli S., 2007: Numerical simulations of microscale urban flow using the RAMS model; *Air Pollution Modelling and its Applications XVIII*; *Developments in Environmental Science*, **6**, 31-43.

Rexeis M., Hausberger S., 2005: Calculation of Vehicle Emissions in Road Networks with the model "NEMO"; Transport and Airpollution Conference; ISBN: 3-902465-16-6, Graz.

Ritz B., Tager I., Balmes J., 2005: Can lessons from public health disease surveillance be applied to environmental public health tracking? *Environ. Health Perspect*., **113**, 243-249.

Robe F. R., Scire J.S., 1998: Combining Mesoscale Prognostic and Diagnostic Wind Models: A Practical Approach for Air Quality Applications in Complex Terrain, 10th Joint Conf. on Air Poll. Met., Phoenix, Arizona, American Meteorological Society.

Rogerson R. J., 1995: Environmental and health-related quality of life: conceptual and methodological similarities. *Soc.Sci.Med.*, **10**, 1373-1383.

Rosen T., Olsen J., 2006: Invited Commentary: The Art of Making Questionnaires Better. *Am.J.Epidemiol.*, **164**, 1145-1149.

Rüdisser J., Lercher P., Heller A., 2007: Adressbasierte Analyse von Gesundheitsdaten - eine Medikationsstudie im Nordtiroler Wipptal., *GIS-Zeitschrift für Geoinformatik*, 5-11.

Sachs L., 1992: Angewandte Statistik. Springer-Verlag, Berlin, 846 pp.

Salomons E.M., 2001: *Computational atmospheric acoustics*, Kluwer Academic Publishers, Dordrecht

Salomons E.M., Blumrich R., Heimann D., 2002: Eulerian time-domain model for sound propagation over a finite-impedance ground surface. Comparison with frequency-domain models. *Acta Acustica united with Acustica*, **88**, 483-492.

Samet J.M., Dominici F., Curriero F.C., Coursac I., Zeger S.L., 2000: Fine particulate air pollution and mortality in 20 U.S. cities, 1987 – 1994. *N. Engl. J. Med.*, **343**, 1742-1749.

Sapsford R., 1999: Survey research. Sage.

Sato T., 1988: The effect of vibration on annoyance of noise: A survey on traffic noise and vibration in Sapporo. In: Noise as a public health problem, Vol. 3 (eds. B. Berglund, U. Berglund, J. Karlsson, Th. Lindvall), pp. 259-264. Swedish Council for Building Research.

Sato T., 1994: Path analyses of the effect of vibration on road traffic and railway noise annoyance. 2, 923-928. Yokohama, Internoise 94. Noise-quantity and quality.

Schäfer, K., Emeis S., Rauch A., Münkel C., Vogt S., 2004: Determination of mixing-layer heights from ceilometer data. In: Remote Sensing of Clouds and the Atmosphere IX, Klaus Schäfer, Adolfo Comeron, Michel Carleer, Richard H. Picard, Nicolas Sifakis (eds.), Proceedings SPIE, Bellingham, WA, USA, Vol. 5571, 248-259.

References

Schell B., Ackermann I.J., Hass H., Binkowski F.S., Ebel, A., 2001: Modeling the formation of secondary organic aerosol within a comprehensive air quality model system. *Journal of Geophysical Research*, **106**, 28275-28293.

Schicker I., Seibert P., 2007: Simulation of the meteorological conditions during a winter smog episode in the Inn Valley. Submitted to *Meteor. Atmos. Phys.*

Schikowski T., Sugiri D., Ranft U., Gehring U., Heinrich J., Wichmann H.E., Kramer U., 2005: Long-term air pollution exposure and living close to busy roads are associated with COPD in women. *Respiratory Research*, **6**, 152.

Schilling L. M., Kozak K., Lundahl K., Dellavalle R. P., 2006: Inaccessible Novel Questionnaires in Published Medical Research: Hidden Methods, Hidden Costs. *Am.J.Epidemiol*., **164**, 1141-1144.

Schnitzhofer R., Norman M., Dunkl J., Wisthaler A., Griesser E., Vergeiner J., Harnisch F., Gohm A., Obleitner F., Fitz A., Neiniger B., Hansel A., 2007: A multimethodical approach towards quantifying spatial Air-Pollution distribution in an Alpine valley. Submitted to *Atmospheric Chemistry and Physics*.

Schomer P., 2005: Assessing multi-source noise environments with an "equally annoying"' exposure summation model. *J.Acoust.Soc.Am.*, **117**, 2591.

Schomer P. D., Suzuki Y., Saito F., 2001: Evaluation of loudness-level weightings for assessing the annoyance of environmental noise. *J.Acoust.Soc.Am.*, **110**, 2390-2397.

Schreiber H., Gundert-Remy U., Jung T., et al., 2007: Aktionsprogramm Umwelt und Gesundheit (APUG). Umsetzung der Querschnittsmaßnahmen. *Bundesgesundheitsbl - Gesundheitsforsch – Gesundheitsschutz*, **44**, 1180-1187.

Schulte-Fortkamp B., Dubois D., 2006: Preface: Recent advances in soundscape research. *Acta Acoustica united with Acoustica*, **92**, V-VIII.

Schulte-Fortkamp B., Weber R., Ronnebaum T., Doennges T., 1996: Literaturstudie zur Gesamtgeräuschbewertung. Oldenburg, Universität Oldenburg.

Schuman L.L., Shire J.S., 1980: Buoyant line and Point Source (BLP) Dispersion Model User's Guide. Document P-7304B. Enviromental Research and Technology, Inc, Concord, MA. (NTIS PB 81-164642)

Schwela D., Kephalopoulos S., Prasher D., 2005: Confounding or aggravating factors in noise-induced health effects: air pollutants and other stressors. *Noise and Health*, **7**, 41-50.

Scire J.S., Robe F.R., Fernau M.E., Yamartino R.J., 1999: A User's Guide for the CALMET Meteorological Model, Earth Tech Inc.

Scire J.S., Strimaitis D.G., Yamartino R.J., 2000: A User's Guide for the CALPUFF Dispersion Model, Earth Tech Inc.

Seibert P., 1996: In Kromp-Kolb H., Kröger H., Seibert P., Stohl A., Wotawa G. (1998): Report of IMP: Vertical ozone transports in the Alps (VOTALP). *Final report to the European Union, Contract Nr. ENV4 CT95 0025*.) (http://www.boku.ac.at/imp/envmet/alpine_vert_exchg.html)

Seibert P., Beyrich F., Gryning S. E., Joffre S., Rasmussen A., Tercier P., 2000: Review and intercomparsion of operational methods for the determination of the mixing height.. *Atmos. Environ.*, **34**, 1001-1027.

Seifert B., Becker K., Hoffmann K., Krause C., Schulz C., 2000: German Environmental Survey 1990/92 (GerES II): A representative population study. *J.Exp.Anal.Environ.Epidemiology*, **10**, 103-114.

Seinfeld J.H., 1975: Air Pollution – Physical and Chemical fundamentals. McGraw Hill

Sen A.K., 1999: Commodities and capabilities. Oxford University Press, New Delhi.

Shigeta H., Shigeta M., Nakazawa A., Nakamura N., Yoshikawa T., 2001: Lifestyle, obesity, and insulin resistance. *Diabetes Care*, **24**, 608.

Singh M., Drake L., Roehrs T., Hudgel D. W., Roth T., 2005: The association between obesity and short sleep duration: a population- based study. *J.Clin.Sleep Med.*, **15**, 357-363.

Singh-Manoux A., Marmot M. G., Adler N. E., 2005: Does Subjective Social Status Predict Health and Change in Health Status Better Than Objective Status? *Psychosom.Med.*, **6**7, 855-861.

Singh-Manoux A., Guéguen A., Martikainen P., Ferrie J., Marmot M., Shipley M. 2007. Self-rated health and mortality: Short- and long-term associations in the Whitehall II study. *Psychosom. Med.*, **69**, 138-143.

Smith G. D., Ebrahim S., 2004: Mendelian randomization: prospects, potentials, and limitations. *Int.J.Epidemiol.*, **33**, 30-42.

Sommer H., Seethaler R., Chanel O., Herry M., Masson S., Vergnaud J.C., 1999: Health Costs due to Road Traffic-related Air Pollution. An impact assessment project of Austria, France and Switzerland. WHO - Regional Office For Europe, Berne.

Sozzi R., Georgiadis T., Valentini M., 2002: Introduzione alla turbolenza atmosferica, Pitagora Ed., Italy, pp. 525.

Spangl W., Schütz Ch., Krismer A., 2006: Räumliche Verteilung der Stickstoffdioxid-Konzentration an zwei Profilen in Tirol, Umwelt Bundesamt, Wien, REP-0019, Wien, 37pp.Strangeways, I., 2003: *Measuring the natural environment*, 2nd edition, Cambridge University Press.

Spiegel K., Leproult R., van Kauter E., 1999: Impact of sleep debt on metabolic and endocrine function. *Lancet*, **354**, 1435-1439.

Staatsen B., Knol A., 2007: EBD Estimation - Annoyance. In: WHO-Europe. Quantifying burden of disease from environmental noise: Second technical meeting report. Copenhagen: 2007, Denmark: pp 47-59.

Stallen P. J. M., 1999: A theoretical framework for environmental noise annoyance. *Noise and Health*, **3**, 69-79.

Stansfeld S. A., 1992: Noise, noise sensitivity and psychiatric disorder: Epidemiological and psychological studies. *Psychol.Med. Monograph Supplement*, **22**, Cambridge University Press: Cambridge.

Stansfeld S. A., Matheson M. P., 2003: Noise pollution: non-auditory effects on health. *British Medical Bulletin*, **68**, 243-257.

Stansfeld S. A., Haines M. M., Burr M., Berry B., Lercher P., 2000: A Review of Environmental Noise and Mental Health. *Noise and Health*, **2**, 1-8.

Staples S. L., 1996: Human response to environmental noise. Psychological research and public policy. *Am.Psychol.*, **51**, 143-150.

Staples S. L., 1997: Public policy and environmental noise: modeling exposure or understanding effects. *Am.J.Pub.Health*, **87**, 2063-2067.

Steinacker R., 1984: Area-height distribution of a valley and its relation to the valley wind. *Beitr. Phys. Atmosph.* **57**(1): 64-71.

Steinacker R., 1987: Orographie und Fronten. *Wetter und Leben*, **39**, 65-70.

Stockwell W., Middelton P., Chang J., 1990: The Second Generation Regional Acid Deposition Model – chemical Mechanism for Regional Air Quality Modeling. *J. Geophys. Res.*, **95**, 16343-18367.

Stockwell W., Kirchner F, Kuhn M., Seefeld S., 1997: A new mechanism for regional atmospheric chemistry modeling. *J. Geophys. Res.*, **102**, 847-879.

Strawbridge W. J., 1999: Self-rated health and mortality over three decades: Results from a time-dependent covariate analysis. *Research on Aging*, **21**, 402-416.

Stull R., 1988: An Introduction to Boundary Layer Meteorology. Kluwer Academic Publishers, 666 pp.

Sunyer J., 2001: Urban air pollution and chronic obstructive pulmonary disease: a review. *Eur. Respir. J.*, **17**, 1024-1033.

Sunyer J., Jarvis D., Gotschi T., et al., 2006 : Chronic bronchitis and urban air pollution in an international study. *Occup.Environ.Med.*, **63**, 836-843.

Suppan P., Schädler G., 2004: The impact of highway emissions on ozone and nitrogen oxide levels during specific meteorological conditions, *Sci. Tot. Environ.*, **334-335**, 215-222.

Sutherland L.C., Daigle G.A., 1997: Atmospheric sound propagation. In: Crocker M.J. (Ed.): *Encyclopedia of Acoustics*, John Wiley & Sons, Inc., New York.

Tamakoshi A., Ohno J., 2004: Self-reported sleep duration as a predictor of all-cause mortality: Results from the JACC study, *Japan. Sleep*, **27**, 51-54.

Taylor K.E., 2001: Summarizing multiple aspects of model performance in a single diagram. *J.Geophys.Res.*, **106(D7)**, 7183-7192.

References

Taylor A.W., Dal Grande E., Gill T., 2006: Beware the pittfalls of ill-placed questions - revisiting questionnaire ordering. *Int.J.Public Health*, **51**, 43-44.

Tinarelli G., Anfossi D., Brusasca G., Ferrero E., Giostra U., Morselli M.G., Moussafir J., Tampieri F., Trombetti F., 1994a: Lagrangian particle simulation of tracer dispersion in the lee of a schematic two-dimensional hill. *J. Appl. Meteor.*, **33**(6), 744-756

Tinarelli G., Brusasca G., Morselli M.G., 1994b: Il modello lagrangiano a particelle SPRAY. Descrizione generale e validazioni. *ENEL Report* E1/94/10/MI

Tinarelli G., Anfossi D., Bider M., Ferrero E., Trini Castelli S., 2000: A new high performance version of the Lagrangian particle dispersion model SPRAY, some case studies. *Air Pollution Modeling and its Application XIII*, Gryning S.E. and Batchvarova E. Eds, 499-507.

TOI, 1991: Traffic and the environment: Summary report. Oslo, Transport Economics Institute.

Trini Castelli S., 2000: MIRS: a turbulence parameterisation model interfacing RAMS and SPRAY in a transport and diffusion modelling system, *Rap. Int. ICGF/C.N.R.* No 412/2000, 34 pp.

Trini Castelli S., Anfossi D., 1997: Intercomparison of 3-D turbulence parametrizations as input to 3-D dispersion Lagrangian particle models in complex terrain, *Il Nuovo Cimento*, **20C**(3), 287-313.

Trini Castelli S., Ferrero E., Anfossi D., Ying R., 1999: Comparison of turbulence closure models over a schematic valley in a neutral boundary layer. *Proceedings of the 13th Symposium on Boundary Layers and Turbulence* - 79th AMS Annual Meeting - Dallas, Texas (USA), 10-15 January 1999, 601-604.

Trini Castelli S., Ferrero E., Anfossi D., 2001: Turbulence closure in neutral boundary layer over complex terrain. *Boundary-Layer Meteor.*, **100**, 405-419.

Trini Castelli S., Anfossi D., Ferrero E., 2003: Evaluation of the environmental impact of two different heating scenarios in urban area. *Int. J. Environment and Pollution*, **20**, 207-217.

Trini Castelli S., Ferrero E., Anfossi D., Ohba R., 2005: Turbulence closure models and their application in RAMS. *Environmental Fluid Mechanics*, **5**, 169-192.

Trini Castelli S., Hara T., Ohba R., Tremback C.J.Y, 2006: Validation studies of turbulence closure schemes for high resolutions in mesoscale meteorological models, *Atmos. Env.*, **40**, 2510-2523.

Uhrner U., von Löwis S., Vehkamäki H., Wehner B., Bräsel S., Hermann M., Stratmann F., Kulmala M., Wiedensohler A., 2007: Dilution and Aerosol Dynamics within a Diesel Car Exhaust Plume – CFD Simulations of On-road Conditions. *Atmos. Environ.*, **41**, 7440-7461.

Uliasz M., 1993: The atmospheric mesoscale dispersion modeling system. *J. Appl. Meteor.*, **32**(1), 139-149.

Valent F., Brusaferro S., and Barbone F., 2001: A Case-Crossover Study of Sleep and Childhood Injury. *Pediatrics*, **107**, e23 (http://www.pediatrics.org/cgi/content/full/107/2/e23).

Vallet M., Gagneux J. M., Blanchet V., et al., 1983 : Long term sleep disturbance due to traffic noise. *J.Sound.Vib.*, **90**, 173-191.

van Kamp I., Leidelmeijer K., Marsman G., de Hollander A., 2003: Urban environmental quality and human well-being Towards a conceptual framework and demarcation of concepts; a literature study. *Landscape and Urban Planning*, **985**, 1–14.

van Kempen E., Staatsen B. A. M., van Kamp I., 2005: Selection and evaluation of exposure-effect-relationships for health impact assessmant in the field of noise and health. RIVM report 630400001/2005. Bilthoven, Rijksinstituut voor Volksgezondheid en Milieu.

van Kempen E., Van Kamp I., Fischer P., Davies H., Houthuijs D., Stellato R., Clark C., Stansfeld S., 2006: Noise exposure and children's blood pressure and heart rate: the RANCH project. *Occup.Environ. Med.*, **63**, 632-639.

van Maercke D., Defrance J., 2007: Development of an analytical model for outdoor sound propagation within the Harmonoise project. *Acta Acustica*, **93**(2), 201-212.

van Renterghem T., Botteldooren D., 2007: Prediction-step staggered-in-time FDTD: An efficient numerical scheme to solve the linearised equations of fluid dynamics in outdoor sound propagation. *Applied Acoustics*, **68**, 201-216.

Veenhoven R., 1999: Quality-of-life in individualistic society: a comparison of 43 nations in early 1990s. *Soc. Indicators Res.*, **48**, 157–186.

Venkatram A., 1980: Estimating the Monin_Obukhov length in the stable boundary layer for dispersion calculations. Boundary-Layer Meteor., **19**, 481-485.

Vergeiner, I., 1982: An energetics theory of slope winds. *Meteor. Atmos. Phys*., **19,** 189-191.

Vergeiner I., Dreiseitl E., 1987: Valley winds and slope winds - Observations and elementary thoughts. *Meteorology and Atmospheric Physics*, **36**(1-4), 264.

Vergeiner, I., E. Dreiseitl, et al., 1978: Inversionslangen in Innsbruck. *Wetter und Leben* **30**: 69-86.

Verkeyn A., Botteldooren D., 2002: The effect of land-use variables in a fuzzy rule based model for noise annoyance. Dearborn USA, Internoise 2002.

Vestreng V., Breivik K., Adams M., Wagener A., Goodwin J., Rozovskkaya O., Pacyna J.M., 2005: Inventory Review 2005, Emission Data reported to LRTAP Convention and NEC Directive, Initial review of HMs and POPs, Technical report MSC-W 1/2005, ISSN 0804-2446

Visschedijk A.H.J., Denier van der Gon H.A.C., 2005: *Gridded European anthropogenic emission data for NO_x, SO_2, NMVOC, NH_3, CO, PM10, PM2.5 and CH_4 for the year 2000*, TNO B&O-A Rapport 2005/106, 2nd version November

Vos J., 1992: Annoyance caused by simultaneous impulse, road-traffic, and aircraft sounds: A quantitative model. *J.Acoust.Soc.Am*., **91**, 3330-3345.

Wakefield J. C., Elliott P., 1999: Issues in the statistical analysis of small-area health data. *Statist. Med*., **18**, 2377-2399.

Walko R.L., Tremback C.J., Bell M.J., 2001: Hybrid Particle And Concentration Transport Model Version 1.2.0 User's Walko, R., and C. Tremback, 2002: The Adaptive Aperture (ADAP) Coordinate. *5th RAMS Workshop and Related Applications*, Santorini, Greece, 29 September - 3 October 2002.

Wanner H. U., Wehrli B., Nemecek J., Turrian V., 1977: Die Belästigung der Anwohner verkehrsreicher Strassen durch Lärm und Luftverunreinigungen. *Sozial- und Praeventivmedizin*, **22**, 108-115.

Weiland S. K., Björksten B., Brunekreef B., Cookson W. O., von Mutius E., Strachan D. P., 2004: Phase II of the International Study of Asthma and Allergies in Childhood (ISAAC II): rationale and methods. *Eur. Respir. J.*, 24, 406-412.

Whiteman C.D., 1982: Breakup of temperature inversions in deep mountain valleys: Part i. Observations. *J. Appl. Meteor*., **21**, 270-289.

Whiteman C.D., 1990: Observations of thermally developed wind systems in mountainous terrain, Amer. Meteor. Soc., Boston, MA, chapter 2 in Atmospheric processes over complex terrain, W. Blumen Ed., Meteorological Monographs, no. 45., 5-42.

Whiteman C. D., 2000: *Mountain Meteorology, Fundamentals and Applications*, Oxford University Press.

Whiteman C. D., Dreiseitl E., 1984: Alpine Meteorology. Translations of Classic Contributions by Wagner, A., Ekhart, E., Defant, F. PNL-5141/ASCOT-84-3, Pacific Northwest Laboratory, Richmond, WA, 121 pp.

Whiteman C.D., Hubbe J.M., ShawW. J., 2000: Evaluation of an inexpensive temperatude datalogger for meteorological applications. *J. Atmos. Ocean. Tech.*, **17**, 76–81.

Whiteman C.D., Eisenbach S., Pospicihal B., Steinacker R., 2004: Comparison of vertical soundings and sidewall air temperature measurements in a small alpine basin. *J. Appl. Meteorol.*, **43**, 1635–1647.

WHO, 2001. World Health Report 2001: Mental Health – New Understanding, New Hope. Geneva 2001

WHO, 2004: *Development of Environment and Health Indicators for European Union Countries: Results of a Pilot Study*, WHO Working Group

WHO, 2005: Health Effects of Transport Related Air Pollution, World Health Organization, edited by Michal Krzyzanowski, Birgit Kuna-Dibbert and Jürgen Schneider, ISBN 92-890-1373-7

WHO Europe, 2004a. Declaration: 4th Ministerial Conference on Environment and Health, Budapest, Hungary, 23–25 June 2004. Copenhagen: WHO, 2004. (http://www.euro.who.int/document/e83335.pdf, accessed October 2007).

WHO Europe, 2004b. Environmental Health Indicators for Europe. A Pilot indicator based report. Geneva: World Health Organisation, 2004.

References

WHO Europe, 2007. Quantifying burden of disease from environmental noise: Second technical meeting report. Copenhagen: 2007, Denmark.

Wilcox A. J., 1999: The quest for better questionnaires. *Am.J.Epidemiol*., **150**, 1261-1263.

Wilks D.S., 1995: *Statistical Methods in the Atmospheric Sciences*, Academic, New York, 277-281.

Wilks D.S., 2006: Statistical Methods in the Atmospheric Sciences, *Elsevier*.

Wilson D.K., Ostashev V.E., Collier S.L., Symons N.P., Aldridge D.F. David H., Marlin D.H., 2007: Time-domain calculations of sound interactions with outdoor ground surfaces. *Applied Acoustics*, **68**, 173-200.

WMO, 1996: Guide to meteorological instruments and methods of observation, 6th edition, WMO n. 8, Geneva

WMO, 2000: Temperature measurements, some considerations for the intercomparison of radiation screens (J. P. van der Meulen). Papers presented at the WMO Technical Conference on Meteorological and Environmental Instruments and Methods of Observation (TECO-2000), Instruments and Observing Methods Report No. 74, WMO/TD-No. 1028, Geneva.

Wolf-Maier K., Cooper R. S., Banegas J. R., Giampaoli S., Hense H. W., Joffres M., Kastarinen M., Poulter N., Primatesta P., Rodriguez-Artalejo F., Stegmayr B., Thamm M., Tuomilehto J., Vanuzzo D., Vescio F., 2003: Hypertension Prevalence and Blood Pressure Levels in 6 European Countries, Canada, and the United States. *JAMA*, **289**, 2363-2369.

Wordley J., Walters S., Ayres J.G., 1997: Short term variations in hospital admissions and mortality and particulate air pollution. *Occup. Environ. Med*., **54**, 108-116.

Wotawa G., Seibert P., Kromp-Kolb H., Hirschberg M., 2000: Verkehrsbedingte Stickoxid-Belastung im Inntal: Einfluss meteorologischer und topographischer Faktoren. Endbericht zum Projekt Nr. 6983 "Analyse der Schadstoffbelastung im Inntal" des Jubiläumsfonds der Österreichischen Nationalbank. Institut für Meteorologie und Physik, Universität für Bodenkultur Wien Oktober 2000, 28 pp. http://www.boku.ac.at/imp/envmet/Inntal-Bericht.pdf

Yamartino R.J., Scire J.S., Hanna S.R., Carmichael G.R., Chang Y.S., 1989a: CALGRID: A mesoscale photochemical model − I. Model formulation.

Yamartino R.J., Scire J.S., Carmichael G.R., Chang Y.S., 1989b: CALGRID: A mesoscale photochemical model − II. User's Guide.

Yamartino R.J., Scire J.S., Carmichael G.R., Chang Y.S., 1992: The CALGRID mesoscale photochemical model−I. Model formulation. *Atmos. Environ.*, **26A**, 1493-1512.

Yano T., Morihara T., Sato T., 2005: Community response to Shinkansen noise and vibration: a survey in areas along the Sanyo Shinkansen Line. Budapest, Forum Acusticum.

Yano T., Sato T., Morihara T., 2006: Impact of vibration on railway and road traffic noise annoyance. Honolulu, Internoise 2006.

Yokoshima S., Tamura A., 2005: Combined annoyance due to the Shinkansen railway noise and vibration. 2, 923-928. 2005. Rio de Janeiro, Internoise 2005. Noise-quantity and quality.

Yokoshima S., Tamura A., 2006: Interactive effects between Shinkansen railway noise and vibration on annoyance. Honolulu, Internoise 2006.

Zallinger M., Le Anh T., Hausberger S., 2005: Improving an instantaneous emission model for passenger cars; Conf. Transport and Air Pollution, Graz.

Zammit G. K., Weiner J., Damato N., et al., 1999: Quality of life in people with insomnia. *Sleep*, **22**, 379-385.

Zängl G., 2002a: Stratified flow over a mountain with a gap. Linear theory and numerical simulations. *Quarterly Journal of Royal Meteorological Society*, **128**, 927-949.

Zängl G., 2002b: An improved method for computing horizontal diffusion in a sigma-coordinate model and its application to simulations over mountainous topography. *Mon. Wea. Rev.*, **130**, 1423-1432.

Zängl G., 2003a: A generalized sigma coordinate system for the MM5. *Mon. Wea. Rev*., **131**, 2875-2884.

Zängl G., 2003b: A reexamination of the valley wind system in the Alpine Inn Valley with numerical simulations. *Meteorol. Atmos. Phys*., **87**, 241-256

Zannetti P., 1986: Critical survey of mathematical models of atmospheric pollution transport and deposition. Vol. I, Main Report. JRC Report AV-FR-85/525

Zannetti P., 1993: Air Pollution Modeling, Theories, Computational Methods and Available Software;,Computation Mechanics Publications Southampton Boston ; VNR New York, ISBN 1-85312-100-2.

Zeichart K., 1998: Kombinatorische Wirkungen von Bahnlärm und Bahnerschütterungen. *Z. Lärmbekämpf.*, **45**, 7-16.

Zemp E., Elsasser S., Schindler C., et al., 1999: Long-term ambient air pollution and respiratory symptoms in adults (SAPALDIA study). *Am.J.Respir.Crit.Care Med.*, **159**, 1257-1266.

Zhang M., Kang J., 2007: Towards the evaluation, description, and creation of soundscapes in urban open spaces. Environment and Planning B: *Planning and Design*, **34**, 68-86.

Zwikker C., Kosten C.W., 1949: *Sound absorbing material.* Elsevier, New York.

This project has received European Regional Development Funding through the INTERREG IIIB Community Initiative

Interreg III B

“Air Pollution, Traffic Noise and Related Health Effects in the Alpine Space” is a guide for governmental administrations and consulters who deal with the environmental impact of traffic in and through the Alps and its management. The book summarises main results of the Interreg IIIB Alpine Space project ALPNAP (2005 – 2007). It provides information about the state-of-the-art of science-based methods to monitor and model air pollution and noise emissions in complex terrain. With these methods meteorological fields, the dispersion of air pollutants and the propagation of noise are observed and computed; and air quality and noise levels are assessed. Different types of methods are described and their respective advantages and shortcomings are discussed.

Especially, this book relates air pollution and noise to human health effects. It presents methods to assess the effects of transport related environmental exposures on health and well-being. The application of all these methods is demonstrated in a comprehensive chapter focussing on selected target areas: the Fréjus corridor, the Brenner corridor between Verona and Bolzano/Bozen and near Schwaz in Tyrol. This volume concludes with recommendations how the outlined methods can be utilised for the benefit of the Alpine environment.

The ALPNAP project consortium:

ISBN 978-88-8443-207-0 (electronic version)